Clicking polyelectrolytes to form a crosslinked hydrogel; their use for surface modification, electrospinning and preparation of nanoparticles

Von der Fakultät für Mathematik, Informatik und Naturwissenschaften

der RWTH Aachen University zur Erlangung des akademischen Grades eines

Doktors der Naturwissenschaften genehmigte Dissertation

vorgelegt von

Master of Science

Miran Yu

aus Nonsan, Südkorea

Berichter: Universitätsprofessor Dr. rer. nat. Martin Möller

Universitätsprofessor Dr. rer. nat. Alexander Böker

Tag der mündlichen Prüfung: 18. Februar 2011

시작과 끝을 함께 한

사랑하는 나의 가족을 위해

TABLE OF CONTENTS

LIST OF ABBREVIATIONS

AAS	atomic absorption spectroscopy
AFM	atomic force microscopy
AOX	absorbable organic chlorides
$AgNO_3$	silver nitrate
B. sub	*Bacillus subtilis*
Cryo	cryogenics
$CDOD_4$	methanol
DDS	drug delivery system
D_2O	deuterium oxide, heavy water
E. coli	*Escherichia coli*
EDX	energy disperive X-ray
FE SEM	field emission scanning electron microscopy
FTIR	fourier transform infrared
G′	elastic moduli
G″	viscous moduli
h	hour(s)
HCl	hydrogen chloride
H_2O	water
IGAsorp	isothermal gravimetric analyzer
LBL	layer-by-layer
LD_{50}	lethal dose
LDH	lactate dehydrogenase
MEOH	methanol
M_w	weight average molecular weight
$NaBH_4$	sodium borohydride
$NaC_6O_7H_5$	sodium citrate
NaOH	sodium hydroxide
NBF	4-chlor-7-nitrobenzofurazon
nm	nanometer
NMR	nuclear magnetic resonance
NVF	*N*-vinylformamide
O_2	oxygen
PAE	poly(amideamine-epichlorohydrin)

PECs	polyelectrolyte complex
PEI	poly(ethylene imine)
ppm	part per million
PVAm	poly(vinylamine)
R_h	hydrodynamic radius
SEM	scanning electron microscopy
SFM	scanning force microscopy
TEM	transmission electron microscope
Tg	glass transition temperature
TGA	thermogravimetric Analysis
TMS	tetramethylsilane
Triton® X-100	octylphenoldecaethylenglycolether
UV	ultraviolet
W/O	water in oil
XPS	X-ray photoelectron spectroscopy
°C	degree Celsius
µm	micrometer

SUMMARY

This thesis presents the preparation and characterization of ultra-thin hydrogel films, ultra-thin hydrogel nanofibers and silver nanoparticles functionalized nanogels based on crosslinked polymers. The crosslinking was performed by "click" chemistry applying the well-known azetidinium-amine coupling reaction. Hydrogel properties, such as water swelling behavior, metal chelating ability, antimicrobial activity and cell toxicity, have been investigated in detail.

This new type of hydrogel particles offers tunable material properties from macrostructure to nanostructure. Furthermore, this approach offers the great opportunity to design functional hybrid hydrogels by incorporation of inorganic nanoparticles, e.g. silver nanoparticles.

The polymer used in for the new approach is the commercially available poly(vinylamine) (PVAm), which is a weak cationic polyelectrolyte bearing primary amine group among the polymer backbone. PVAm is a useful material for coupling other molecules or chelating metal ions due to the nucleophilic character of primary amines. Poly(amideamine-epichlorohydrin) (PAE) is a reactive polymer resin and a weak cationic polyelectrolyte, which has a four-membered 3-hydroxy-azetidinium ring among the polymer backbone.

The developed PVAm/PAE hydrogels could be successfully applied to a wide range of applications ranging from surface modification of silicon oxide surface and wool fibers, to electrospinning from aqueous gelating solution or to the fabrication of polymeric nanoparticles as an antimicrobial coating on fabrics.

In summary, the developed PVAm/PAE hydrogels are a promising platform for various applications. The systems can be easily modified to fulfill different tasks. The systems can be easily adjusted to a specific application. To this respect, PVAm/PAE hydrogels will be applied to surface coating of materials for further textile as well as biomedical applications.

Zusammenfassung

In dieser Arbeit wird die Synthese und Charakterisierung von neuartigen ultra dünnen Hydrogelfilmen, Hydrogelnanofaser, Nanogelpartikeln und Silbernanopartikel-Nanogel Hybridsystemen beschrieben. Die verschiedenen Nanogelsysteme basieren auf quervernetzten Polymeren. Die Vernetzung wurde durch die Verwendung der Azetidinium-Amine Reaktion auf einfache Weise realisiert. Im weiteren wurden die Hydrogele auf ihr Schwellverhalten, chelatierenden und biologische Eigenschaften hin untersucht und optimiert.

Die neuartigen Hydrogelpartikel bieten auf Grund ihrer Funktionalisierbarkeit die großartige Möglichkeit die Partikeleigenschaften auf makro- und mikroskopischer Ebene gezielt zu steuern. Ebenso ermöglicht die einfache Funktionalisierbarkeit die Synthese von Hydridsystemen aus Nanogelen und anorganischen Silbernanopartikeln.

Die neuartigen Hydrogelpartikel basieren zum einen auf dem kommerziell erhältlichen schwachen kationischen Elektrolyt, Polyvinylamin (PVAm). Auf Grund seiner primären Aminfunktionen kann es ohne weiteres zur Funkfionalisierung oder Chelatisierung von Metalionen genutzt werden. Zum anderen wurde Poly(amideamine-epichlorohydrin) (PAE) verwendet. Hierbei handelt es sich um ein reaktives Polymer und schwaches kationisches Polyelektrolyt. Die am Polymer gebundene 3-Hydroxy-azetidiniumringe können zur einfachen Anbindung von Nukleophilen, wie Aminen, genutzt werden.

Auf Grund dieser Tatsachen konnten die entwickelten Hydrogele in einer Vielzahl von Bereichen, wie zur Oberflächenmodifikation von Silizium oder Wolle, zur Erzeugung von Nanofasern mittels Elektrospinnen oder zur Erzeugung antimikrobiotischer Oberflächen, eingesetzt werden.

Zusammenfassend lässt sich festhalten, das die im Rahmen dieser Arbeit entwickelten Hydrogele eine vielversprechende Plattform für verschiedene Anwendungen bilden, da sich die PVAm/PAE Systeme auf Grund ihrer einfachen Funktionalisierbarkeit auf viele Anforderungen optimieren lassen.

CHAPTER 1

INTRODUCTION

1.1 POLY(VINYLAMINE)/POLY(AMIDEAMINE EPICHLOROHYDRIN) HYDROGELS

Poly(vinylamine) (PVAm) is a weak cationic polyelectrolyte containing one primary amine group per repeating unit. PVAm is synthesized by an indirect method. The first approach for the synthesis of linear PVAm is based on the polymerization of a precursor monomer, *N*-vinylformamide (NVF), which can be polymerized using free-radical initiators as was first reported by Kurtz *et al.* in 1969.[1] The precursor can be easily hydrolysed under acidic or basic conditions yielding PVAm.[2-3] The second approach to make PVAm is based on the Hoffmann rearrangement of polyacrylamides.[4] However, the most practical route for preparing PVAm is the polymerization and hydrolysis of NVF. This method can be applied for the synthesis of high molecular weight polymers up to a molecular weight of 340.000 g/mol. Scheme 1 shows the synthetical pathway to PVAm based polymers, including homopolymerization, copolymerization and hydrolysis of PNVF.

As mentioned above, PVAm bears reactivity primary amine groups providing a general platform for modification and functionalization. The amine of PVAm can react with acids, epoxides, isocyanates, aldehydes, anhydrides, lactones, acid chlorides, carbon dioxide, Michael acceptors and chelate metal cations as shown in Scheme 2.[5] PVAm·HCl is soluble in water, *N*,*N*-dimethylformadmid, ethylene glycol and alcohol/water mixtures and has a T_g of 45 °C as well as an amorphous character. In addtion, the number of primary amine groups is directly related to the molecular weight of the polymer and therefore the overall functionality can be easily adjusted by the degree of polymerization.

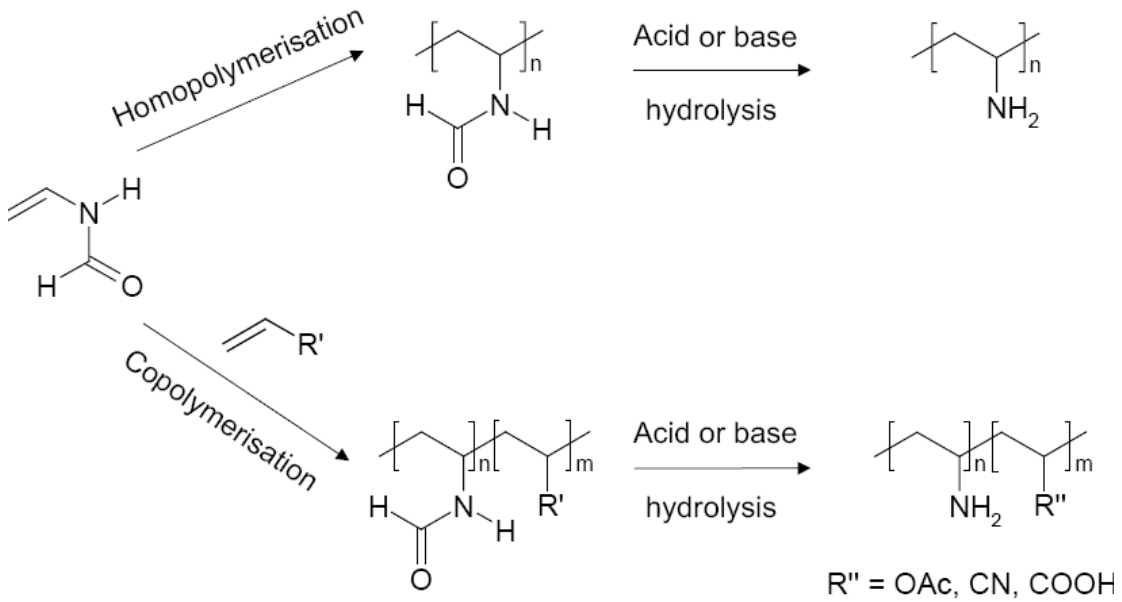

Scheme 1. Homo- and copolymers based on PVAm from NVF monomer

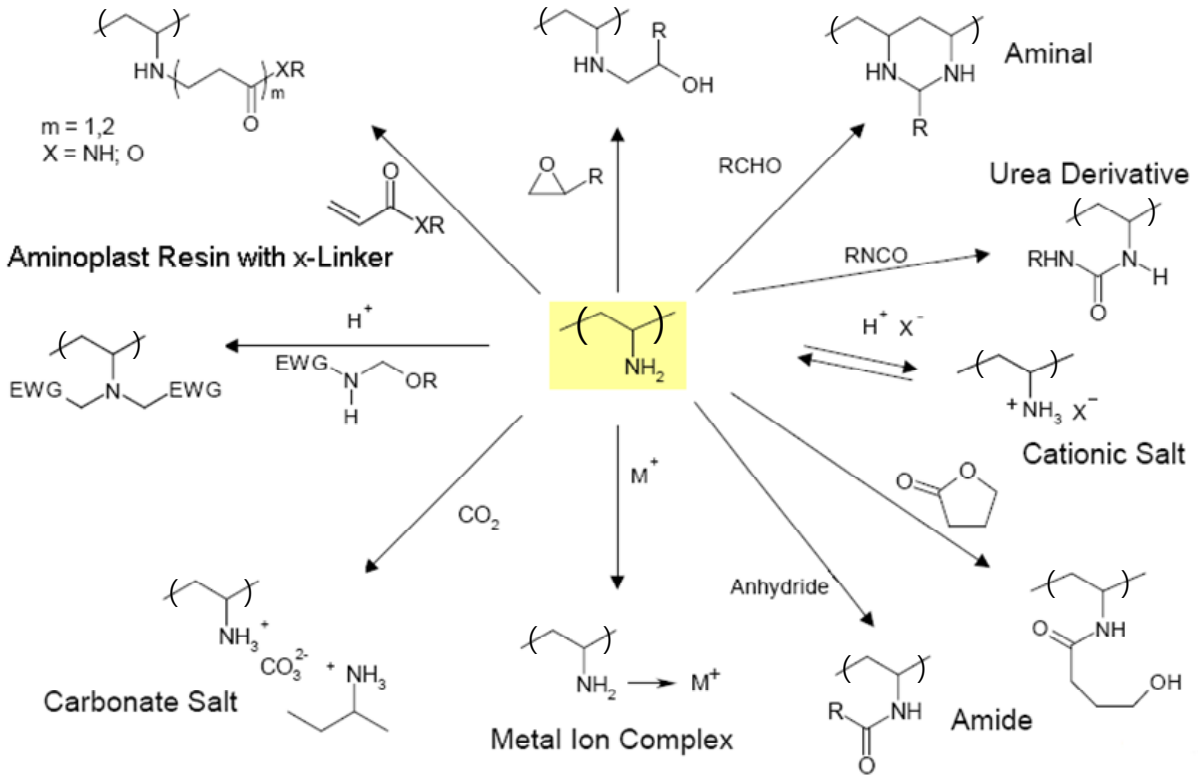

Scheme 2. A brief overview about the possible modifications of PVAm.[5]

Poly(amideamine epichlorohydrin) (PAE) is a reactive water-soluble resin, which has been developed and commercialized at the end of the 1950s. The polymer itself bears reactive four-membered 3-hydroxy-azetidinium groups on the polyamideamine backbone. In the commercial product an azetidinium content of 70-80 % is common.[6]

Because of the reactivity of the PVAm primary amine groups among the polymer backbone, the blends with poly(amideamine epichlorohydrin) (PAE) result in a crosslinked hydrogel by means of a ring-opening coupling reaction at room temperature. In this thesis, the blends of PVAm/PAE have been investigated in respect to the potential properties for various applications as shown in Figure 1. Therefore, PVAm/PAE hydrogels are extremely valuable materials and promising candidates for various applications in the field of surface modification, electrospinning and micro/nanogels.

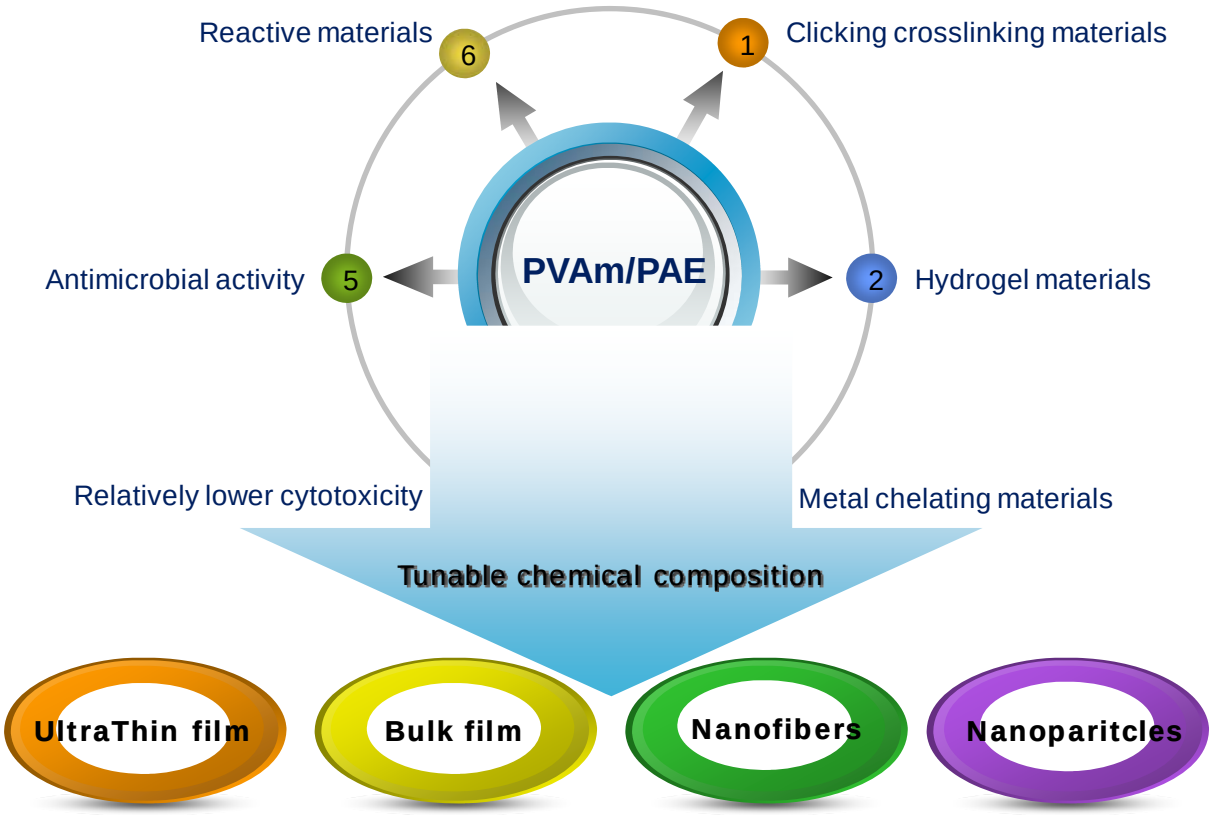

Figure 1. Schematic presentation of properties and potential applications of crosslinked PVAm/PAE hydrogels.

1.2 SURFACE MODIFICATION

The modification of surfaces is an important approach to obtain interfaces with special properties tailored for various applications.[7-9] The most often applied techniques for changing surface characteristics are based on modifying the surface properties by physical treatments, e.g. flame and plasma treatments, and chemical treatments such as direct coating with functional polymers.[10-11]

Whenever a polymer is adsorbed at an interface, a large number of the monomer segments of the polymer chain will be simultaneously in contact with the substrate. At the interface of polymer and substrate, the configuration of the adsorbed polymer chains is determined by the entropy of the polymer chain as well as the enthalpy of the polymer-substrate interaction. As a result of all combined factors, the adsorbed chain configuration includes loops, tails, and trains as shown in Figure 2.[11] The adsorption of polyelectrolyte has been intensively studied towards absorption behavior onto various kinds of solid material i.e. colloidal inorganic oxides, cellulose fibers, glass fibers and flat surfaces, due to their dual character as highly charged electrolyte and flexible chain molecule. They are widely used in various fields of textile coatings, biomaterials, biochemistry, electronics and catalyst technology.

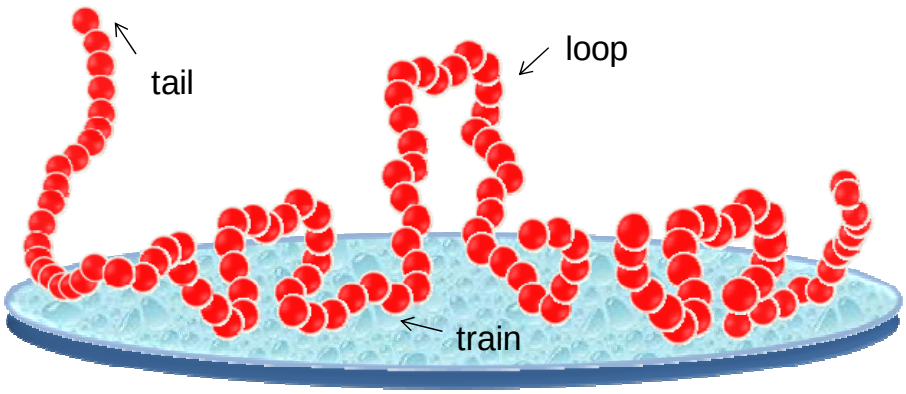

Figure 2. Schematic representation of model conformations of an adsorbed polymer chain on surface: relative portion of loop, train and tail.

1.3 AQUEOUS ELECTROSPINNING

Electrospining is a process for producing the polymer fibers at diameter of micro/nanometer scale.[12] The earliest patent of electrospinning machinary was presented by Cooley[13] and Morton[14] in 1902. The development of commercial electrospinning equipment was described by Formhals[15] in a sequence of patents in 1934. A schematic image of an electrospinning apparatus is shown in Figure 3. There are generally three components involved in the process of electrospinning: a high voltage supplier, a capillary tube with a syringe and a metal collector. In the process itself, a high voltage is applied generating an electrically charged jet of polymer solution. The charged polymer drop at the tip of syringe formes a Taylor cone.[16] Above a critical voltage, the droplet is ejected and whipping towards the targeted metal collector while the solvent evaporates. Finally, the polymer jet is collected as nanofibers.

Various polymers from natural and synthetic origin have been used for electrsospinning.[17-18] In addition, some inorganic materials[19-21] such as metal particles and carbon nanotube[22-23] have been electrospun as the hybrid nanofibers webs for various applications. The increasing demands for nanofibers is evidenced by the increasing number of publications on special electrospun materials offering distinctive properties in many fields of chemical and biological applications. In recent years, electrospining was extensively used for the generation of fibers based on synthetic polymers such as PLA[24], PLGA[25], PVA[26] and PEO[27] and biopolymers such as silk fibroin[28], collagen[29], chitin and chitosan[30] for biomedical applications.

Environmentally friendly production conditions are required for both polymer synthesis as well as polymer processing especially when focusing on biomedical applications. To this respect, a straightforward process without additional disposal of hazardous organic solvents is mandatory. Electrospinning at DWI mainly focuses on avoiding organic solvents during fibers generation (i) by means of melt-electrospinning processes[31] or (ii) by using water as a polymer solvent.[32] Aqueous electrospinning offers obvious advantages for biological and

biomedical applications such as multifunctional membranes,[48] tissue engineering,[49, 50] wound dressing,[51] drug delivery,[52, 53] artificial organs,[54] and vascular grafts.[55, 56]

However, the nanofibers from aqueous solution are hydrated in contact with moisture or water. Thus, the generated nanofibers need to be stabilized before they can be used in aqueous biomedical applications. In current thesis stabilizing the nanofibers is studied based on covalent crosslinking of PVAm and PAE. The high specific surface area and small pore size of electrospun nanofibers make them interesting candidates for various applications.

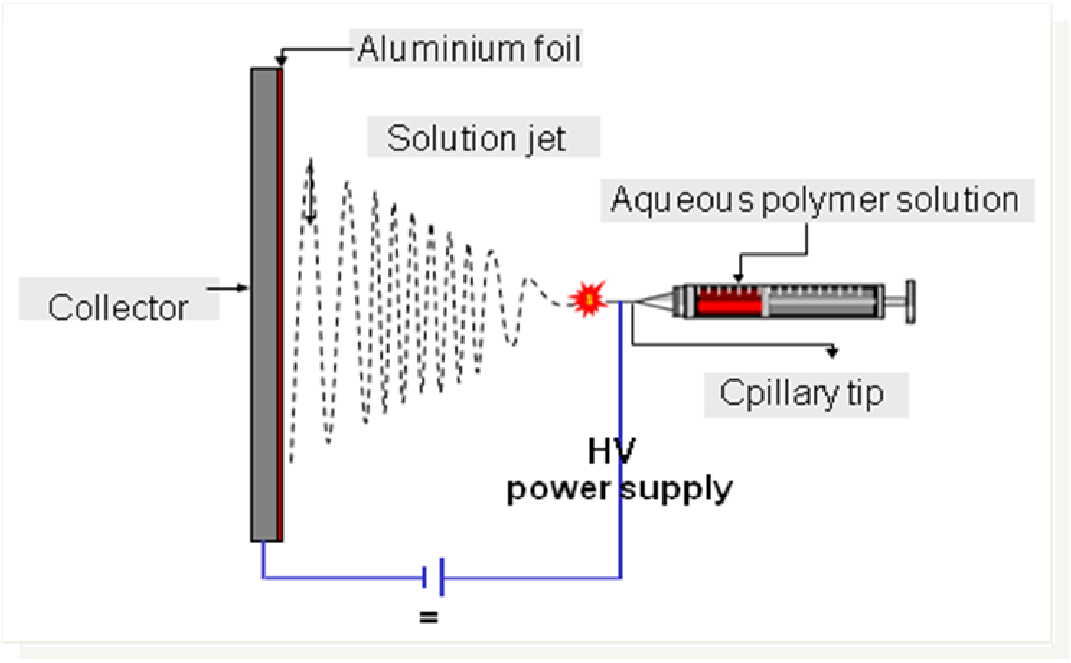

Figure 3. Schematic image of the electrospinning process from aqueous solution.

1.4 POLYMERIC MICRO/NANOGELS

Polymeric micro/nanogels are crosslinked particles that swell in a good solvent.[33-35] The size of the swollen particles is generally in the range from 1 nm to 10 μm. The term microgel was first introduced by Baker in 1949.[37] Staudinger and Husemann prepared microgel particles based on divinylbenzoate (DVB) in a good solvent at high dilution.[36]

In recent years, a large amount of work has been performed on the synthesis and characterization of new micro/nanogel systems for various application. The broad applications of microgel arise from their stimulus-responsive swelling behavior. The formation of microgels can be dependent on various parameters, such as pH, temperature, ionic strength of the surrounding medium and external electromagnetic field.[38] Pelton and Chibante prepared poly(NIPAM) microgel particles having temperature-sensitive properties.[39] Thermosensitive microgel may open the road to a new class of injectable biomaterials due to their spontaneous gelation at the body temperature or specifically in regions with enhanced temperature, e.g. inflammated sites.[40] In addtion, the functionalization of a poly(NIPAM) microgel with acrylic acid (AA) offers an additional response to pH and ionic strength of the surrounding.[41] The development and design of new microgels is accelerated by the rapid growth of biomaterials research. In particular, microgels are expected to enrich the pool of drug delivery system (DDS). Besides polymer-protein conjugates, polymer-drug conjugates, micelles, capsules and vesicles, microgels may offer unique avantages in transport of biomolecules, e.g. proteins or oligonucleotides.[42,43]

Micro/nanogels are usually prepared by emulsion polymerization, precipitation polymerization or inverse (mini) emulsion polymerization. The water-in-oil (W/O) emulsion method takes place in two steps: i) emulsification of water droplets of water soluble polymers in continuous oil phase with oil-soluble surfactants and ii) crosslinking of polymer particles with a water-soluble crosslinker.[33] Figure 4 illustrates the preparation of microgel particles containing drug.[33] The colloidal polymeric particles are sterically stablilized and show a high

degree of hydration. On the other hand, the aqueous homogeneous gelation method can be used for the preparation of hydrogel polymeric particles in water. An example involves the preparation of chitosan microspheres entrapping complexes of HBV, DNA and PEI. This method can take place as a one step process in water.[44] The advantage of this aqueous method is the simple purification and the lack of organic solvents. The well-known class of polyelectrolyte complexes (PECs) are formed when oppositely charged aqueous polyelectrolytes solutions such as polycation/polyanion come together.[45] The swelling behavior is sensitive to chemical properties such as pH and ionic strength of the applied solution. An increasing polycation/polyanion ratio results in more compact aggregates.

Micro/nanogels can be expected to be excellent intelligent carriers for targeted delivery of compounds such as inogranic particles, drugs or biomacromolecules. Pich *et. al* have presented hybrid microgels functionalized with silver nanoparitcles based on poly(vinylcaprolactam-*co*-(acetoacetoxyethyl methacrylate)).[46] Magnetic nanoparticles could also be prepared using PVAm nanoparticles from the absorption of iron ions .[47]

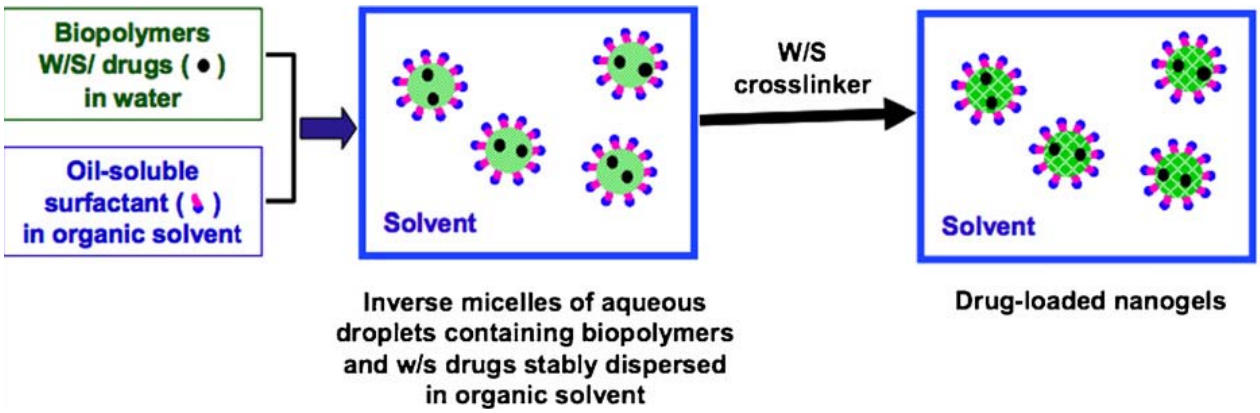

Figure 4. Schematic overview of the fabrication of reverse micelles for the preparation of drug loaded nanogels.[33]

1.5 CONTENT OF THIS THESIS

The objective of this thesis is the preparation and the characterization of crosslinked hydrogel by azetidinium-amine coupling reactions. The hydrogels consist of a polyamine poly(vinylamine) (PVAm) or poly(ethyleneimine) and poly(amideamine epichlorohydrin) (PAE) and were investigated for surface modification, electrospinning, and synthesis of polymeric nanoparticles.

CHAPTER 2 presents the preparation of a stable ultrathin hydrogel film on an oxygen plasma treated silicon oxide surface and characterization by atomic force microscopy (AFM) and ellipsometry to determine the layer thickness, stability and swelling behavior.

CHAPTER 3 describes the azetidinium-amine coupling reaction on oxygen plasma treated silicon oxide surface and evaluates its potential for antimicrobial coatings.

CHAPTER 4 presents the formation of a ultra thin PVAm/PAE hydrogel coating on corona treated wool tops for improving the shrinkproofing.

CHAPTER 5 reports electrospinning of PVAm and its blend with gelatine-hydrolysates from aqueous PVAm solution.

CHAPTER 6 demonstrates the preparation of water stable PVAm nanofiber webs by azetidinium-amine coupling reaction. In addition, the rheological properties of PVAm and PAE are based on the blend ratio and the results are correlated to the electrospinning ability of the solution.

CHAPTER 7 deals with the fabrication of hydrogel nanofibers incorporating nanosilver and the evaluation of their antimicrobial activities for gram-positive bacteria (*Bacillus subtilis*) and gram-negative bacteria (*Escherichia coli*).

CHAPTER 8 reports the synthesis of hydro-nanogels with/witout silver nanoparticles in a one pot reaction in aqueous media.

CHAPTER 9 demonstrates the potential of the hydro-nanogels with/without silver particles developted in chapter 8 for antimicrobial surface modification of cotton and polyester.

1.6 REFERENCES

[1] Kurtz, P.; Disselnkoetter, *German Patents* 1 228 246 and1 224 304, **1965**, to Bayer.

[2] Badesso, R. J.; Nordquist, A. F.; Pinsch-midt, R. U.; Sagl, D. J. *Adv Chem Ser* **1996**, 248, 490.

[3] Pinschmidt, R.K.; Renz, W. L.; Caroll, W.E.; Yacouth, K.; Drescher, J.; Nordquist, A. F.; Chen, N. *J Macromol Sci Pure Appl Chem A* **1997**, 34, 1885.

[4] Tanaka, H. *J Polym Sci Polym Chem Ed* **1979**, 17, 1239.

[5] Pinschmidt, R. K.; Sagl, D. J. *Encyclopedia* **1997**.

[6] Obokata, T.; Yanagisawa, M.; Isogai, A. *J. Appl. Poly. Sci.* **2005,** 97, 2249.

[7] Myers, D. *Surfaces, interfaces and colloids.* 2nd ed.; Wiley Interscience: New York **1999**.

[8] Sperling, L. H. *Introduction to Physical Polymer Science* 3rd ed.; Wiley Interscience: New Yoork **2001**.

[9] Fleer, G. J.; Cohen Stuart, M. A.; Scheutjens, J. M. H. M.; Cosgrove, T.; Vincent, B. *Polymer at Interfaces* Eds.; Chapman & Hall: London, **1993**.

[10] Garbassi, F.; Occhiello, E. *Polymeric Mat.Encyclopedia* **1996**

[11] Garbassi, F.; Morran, M.; Occhiello, E. *in Polymer surface from Physics to Technology*; John Wiley&Sons: New York **1994**.

[12] Subbiah, T.; Bhat, G. S.; Tock, R. W.; Parameswaran, S.; Ramkumar, S. S. *J Appl. Polym. Sci.* **2005**, 96, 557.

[13] Cooley, J.F. *US patent* **1902**, 692,631.

[14] Morton, W.J. *US patent* **1902**, 0,705,691.

[15] Formhals, A. *US patent* **1934**, 1,975,504.

[16] Taylor, B. *Proc. Roy. Soc.* London A **1969**, 313, 453.

[17] Subbiah, T.; Bhat, G. S.; Tock, R. W.; Parameswaran, S.; Ramkumar, S. S. *J Appl. Polym. Sci.* **2005**, 96, 557.

[18] Greiner, A.; Wendorff, J. H. *Angew. Chem. Int. Ed.* **2007**, 46, 5670.

[19] Shao, C.; Kim, H.; Gong, J.; Lee, D. *Nanotechnology* **2002**, 13, 635.

[20] Xu, P.; Han, X.; Wang. C.; Zhang, B.; Wang, X.; Wang, H. *Macromol. Rapid Commun.* **2008**, 29, 1392.

[21] Wang, C.; Yan, E.; Huang, Z.; Zhao, Q.; Xin. Y. *Macromol. Rapid Commun.* **2007**, 28, 205.

[22] McCann, J. T.; Lim, B.; Ostermann, R.; Rycenga, M.; Marquez, M.; Xia, Y. *Nano Lett.* **2007**, 7, 2470.

[23] Moya, S. E.; Ilie, A.; Bnedall, J. S.; Hernandez-Lopez, J. L.; Ruiz-Garcia, J.; Huck, W. T. S. *Macromol. Chem. Phys.* **2007**, 208, 603

[24] You, Y.; Min, B. M.; Lee, S. J.; Lee, T. S.; Park, W. H. *J. Appl. Polym. Sci.* **2005**, 95, 5158.

[25] Jiang, H.; Fang, D.; Hsiao, B. S.; Chu, B.; Chen, C.; *Biomacromolecules* **2004**, 5, 326.

[26] Yao, L.; Haas, T. W.; Elie, A. G.; Simpson, D. G.; Bowlin, G. L.; Wnek, G. E. *Chem. Mater.* **2003**, 15, 1860.

[27] Fong, H.; Chun, I.; Reneker, D. H. *Polymer* **1999**, 40, 4585.

[28] Min, B. M.; Lee, G.; Kim, S. H.; Nam, Y. S.; Lee, T. S.; Park, W. H. *Biomaterials* **2004**, 25, 1289.

[29] Matthews, J. A.; Wnek, G. E.; Simpson, D. G.; Bowlin, G. L.; *Biomacromolecules* **2002**, 3, 232.

[30] Geng, X.; Kwon, O. H.; Jang, H. *Biomaterials* **2005**, 26, 5427.

[31] Dalton, P. D.; Klinkhammer, K.; Salber, J.; Klee, D.; Moeller, M. *Biomacromolecules* **2006**, 7, 686.

[32] Voigt, W.; Thomas, H.; Heine, E.; Möller, M. *"Textiles for Sustainable Development"* Anandjiwala, R.; Hunter, L.; Kozlowski, R.; Zaikov, G. (Eds.), Nova Publishers, New York IV **2007**, 373.

[33] Oh, J. K.; Drumright, R.; Siegwart, D. J.; Matyjaszewski, K. *Prog. Polym. Sci.* **2008**, 33, 448.

[34] Saundersa, B. R.; Vincent, B. *Adv. Colloid Interface Sci.* **1999**, 80, 1.

[35] Antonietti, M. *Angew. Chem. Int. Ed.* **1988**, 27, 1743.

[36] Staudinger, H.; Husemann, E. *Ber* **1935**, 68, 1618.

[37] Baker, W.O. *Ind. Eng. Chem.* **1949**, 41. 511.

[38] Das, M.; Zhang, H.; Kumacheva, E. *Annu. Rev. Mater. Res.* **2006**, 36, 117

[39] Pelton, R. H.; Chibante, P. *Colloids Surf.* **1986**, 120, 247.

[40] Yu, L.; Ding, J. *Chem. Soc. Rev.* **2008**, 37, 1473.

[41] Snowden, M. J.; Chowdhry, B. Z.; Vicent, B.; Morris, GE. *J. Chem. Soc. Faraday Trans.* **1996**, 92, 5013.

[42] Saunders, B. R.; Laajam, N.; Daly, E.; Teow, S.; Hu, X.; Stepto, R. *Adv. Colloid Interface Sci.* **2009**, 147-148, 251.

[43] Kabanov, A. V.; Vinogradov, S. V. *Angew. Chem. Int. Ed.* **2009**, 48, 5418.

[44] Zhou, X.; Liu, B.; Yu, X.; Zha, X.; Zhang, X.; Chen, Y. *J Control Release* **2007**, 121, 200.

[45] Koetz, J.; Kosmella, S. *Polyelectrolytes and Nanoparticles* : Springer, Berlin **2007**.

[46] Pich, A.; Karak, A.; Lu, Y.; Ghosh, A. K.; Adler, H. J. P. *Macromol. Rapid Commun.* **2006**, 27, 344.

[47] Mohammadi, Z.; Cole, A.; Berkland, C. J. *J. Phys. Chem.* **2009**, 1113, 7652.

[48] Ma, Z. W.; Kotaki, M.; Ramakrishna, S. *J. Membrane Sci.* **2005**, 265, 115.

[49] Schindler, M.; Ahmed, I.; Kamal, J.; Nur-E-Kamal, A.; Grafe, T. H.; Chung, H. Y.; Meiners, S. *Biomaterials* **2005**, 26, 5624.

[50] Ma, Z. W.; Kotaki, M.; Inai, R.; Ramakrishna, S. *Tissue Engineering* **2005**, 11, 101.

[51] Kyong, S.; Lim, J.; Lee, G. *Biomaterials* **2006**, 27, 1452.

[52] Katti, D. S.; Robinson, K. W.; Ko, F.K.; Laurencin, C. T. *J. Biomed. Mater. Res. Part B-Appl. Biomaterials* **2004**, 70B, 286.

[53] Prabaharan, M.; Reis, R. L.; Mano, J. F. *Drug Delivery* **2005**, 12, 41.

[54] Zilla, P.; Greisler, H. *Tissue Engineering: Vascular Prosthetic Grafts.* Austin, Texas: R.G. Landes Company, **1999**.

[55] Miller, D. C.; Webster, T. J.; Haberstroh, K. M. *Expert Rev. Med. Devices* **2004**, 1, 259.

[56] Stitzel, J.; Liu, L.; Komura, M.; Berry, J.; Soker, S.; Lim, G.; Van Dyke, M.; Czerw, R.; Yoo, J. J.; Atala, A. *Biomaterials* **2006**, 27, 1088.

CHAPTER 2

CROSSLINKED SELF-ASSEMBLED POLY(VINYLAMINE) (PVAM) /POLY(AMIDEAMINE-EPICHLOROHYDRIN) (PAE) HYDROGEL FILMS FOR SILICON OXIDE SURFACE MODIFICATION [M1]

ABSTRACT

In this work the fabrication of poly(vinylamine) (PVAm) / poly(amideamine-epichlorohydrin) (PAE) ultrathin films on plasma treated silicon oxide surface (primer concept) and the effect of various processing parameters such as polymer concentration, pH and polyamine structure are described. The primer-concept surface modification is a simple and versatile for modification of silicon oxide surfaces with polyamines. The process starts with the generation of negative surface charges on the silicon oxide surfaces by oxygen-plasma treatment. Subsequently, thin films are prepared by dip-coating of PVAm and PAE from aqueous solution. The resulting self-assembled films are stabilized by a spontaneous ring-opening crosslinking reaction between PVAm and PAE. Ellipsometry was used to determine the thickness of the thin films of PVAm and crosslinked PVAm/PAE. The layer thicknesses are directly related to the concentration and molecular weight of PVAm. The atomic composition of the surface was determined by X-ray photoelectron spectroscopy (XPS). Furthermore, the influence of the coating on the surface topology as well as the swelling behaviour and the stability of the hydrogel coatings were investigated by atomic force microscopy (AFM) and ellipsometry. The results demonstrate that a stable ultrathin hydrogel film was prepared by the simple primer surface modification concept. This approach is believed to be applicable to a wide variety of surfaces.

2.1 INTRODUCTION

In recent years, many different surface modification techniques have been developed and applied to modify solid surfaces. The traditional means of forming an organic monolayer is termed Langmuir-Blodgett (LB) and was developed in the late 1930s.[1] The LB technique is based on the adsorption of organic molecules on interfaces leading to the formation of films. In addition, the introduction of the electrostatic layer-by-layer (LBL) techniques by Decher et al. has earned great attention for the fabrication of multilayer thin films.[2,3] Thin films of defined composition and uniform thickness in the nano-scale range can be produced by alternatively dipping the substrate into aqueous solutions of oppositely charged polyelectrolytes. A large variety of charged materials, including polyions, liquid crystal molecules, fluorescence dyes, organic/inorganic particles, proteins, viruses, and enzymes have been incorporated into multilayer assemblies using LBL technique.[4-6] The primary substrate materials used in self-assembly LBL techniques are mainly based on silicon surfaces such as silicon wafer, glass, and quartz due to specific grafting properties of Si surface. The thin organic films opened new gate for chemical and physical modified silicon oxide surfaces.

However, the structure and stability of LBL film is strongly dependent on the chosen polyelectrolytes and adsorption conditions which can be varying with the pH and ionic strength of dipping solution.[7,8] To enhance the stability of multilayer films, the use of photoreactive polyanions with azido groups grafted to poly(acrylic acid) for fabricating LBL self assembly films has induced cross-linking by UV irradiation.[9]

Polyelectrolytes have been widely used in a number of important applications, for example as additives for colloidal stability and to control adhesive properties of surfaces. Several papers have discussed the adsorption behavior of poly(vinylamine) (PVAm) polyelectrolytes onto silica surfaces[13-16] and cellulose fibers.[17-19] PVAm is a well known cationic polyelectrolyte containing primary amine groups and it is commercially available under the name Lupamin, in various molecular weights.[39] PVAm cannot be synthesized directly from vinylamine, but, it

is produced by acid or base hydrolysis of poly(vinylformamide) (PVFA) as shown in Scheme 1.[10-12] PVAm is a useful material for coupling other molecules or chelating metal ions due to the nucleophilic character of the primary amines. A wide range of applications of PVAm are reported in the paper-making and processing area,[10,11] waste water treatment,[20] as vectors for in vitro gene delivery[21] and superabsorbent materials.[22] In addition, PVAm is a potential cationic polyelectrolyte candidate for functionalization of silica surfaces in aqueous solution.[13,14] Poly(amideamine-epichlorohydrin) (PAE) is a reactive polymer resin and a weak cationic polyelectrolyte, which is commercially available (Scheme 1). The first stage of the synthesis of PAE is the polycondensation reaction of diethylene triamine with adipic acid. In the second stage, the polymer is reacted with epichlorohydrin, resulting in the formation of the four-membered 3-hydroxy-azetidinium ring as well as cross-links increasing the molecular weight of the material.[23-25] The final polymer is a weak cationic polyelectrolyte, which is water soluble and mainly used to enhance wet strength cellulose during paper making process.[26,27] The reactive PAE polymer is used in various applications, such as adhesives, coating, and thermo setting resins.[28,29] The azetidinium ring is known to react with necleophiles resulting in ring-opening, which we have exploited to form cross-linked networks with PVAm. Couty *et al.* have screened the nucleophilic opening of azetidinium ions by C-nucleophiles and studied in detail the regioselectivity of the nucleophilic opening of substituted azetidinium ions bearing the functional group such as amines, azide anions and acetate anions.[30,31] The advantage of this system is the possibility to functionalize PVAm by chemical modification. The primary amine groups have a high chemical potential for subsequent derivatization to control the surface properties. Serizawa *et al.* studied the fabrication of ultrathin hydrogel films by LBL techniques with sequential chemical reactions of poly(vinylamine-co-N-vinylformamide) and poly(acrylic acid).[32] Another approach to prepare stable multilayer films was reported based on poly(vinylamine-co-N-vinylformamide) with various amounts of vinylamine and poly(sodium styrenesulfonate).[33]

Here, we report the preparation of a thin cross-linked PVAm/PAE hydrogel film on negatively charged plasma treated silicon oxide surface. In Chapter 3, we reported this novel approach to enhance the stability of films by exploiting the chemical reaction of primary amine groups and azetidinium ions. In Chapter 2, detailed investigations on the effect of processing parameters on the film thickness, homogeneity, atomic content, and wetting behaviors of the hydrogel films on the substrate are reported. In addition, thickness changes of PVAm/PAE films before and after immersing in sodium hydroxide (NaOH) with a pH of 13 are discussed to evaluate the stability of the thin films. Furthermore, the swelling behavior of crosslinked PVAm/PAE hydrogel films in aqueous solution was determined by AFM measurements.

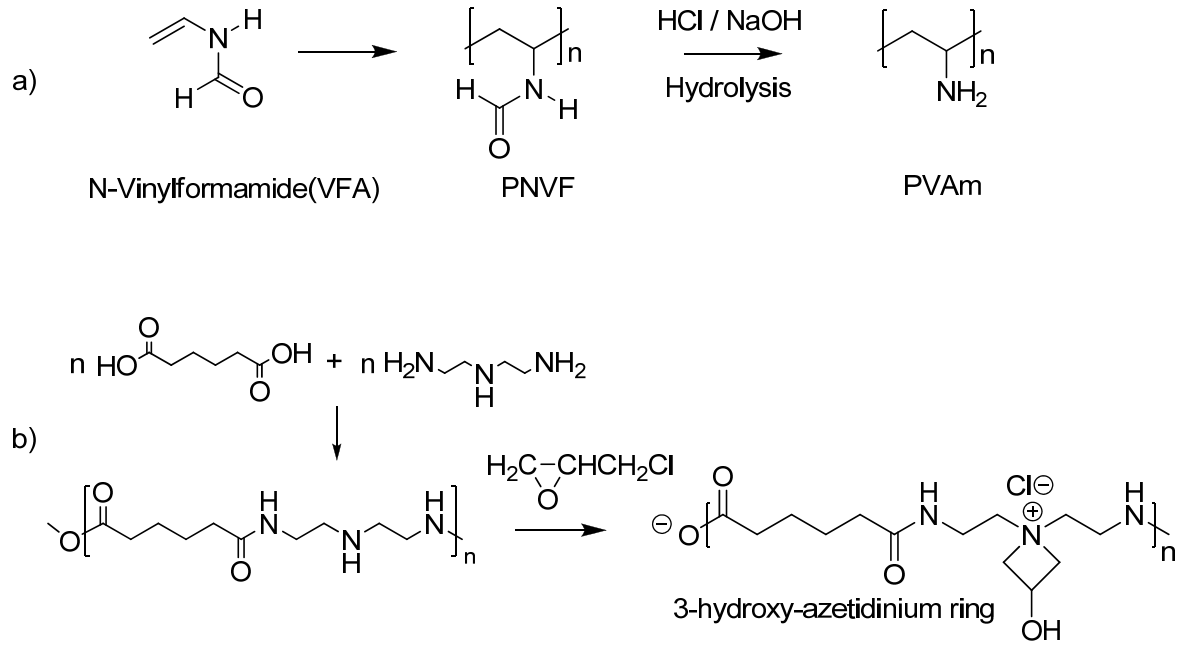

Scheme 1. Industrial preparation method of the commercially available polyelectrolytes a) poly (vinylamine) (PVAm)[10] and b) polyamideamine-epichlorohydrin (PAE).[25]

2.2 EXPERIMENTAL PART

Materials and Methods

The cationic poly(vinylamine) polyelectrolyte (PVAm; Lupamin 9095) was kindly provided by BASF AG, Ludwigshafen. The polymer was obtained from the hydrolysis of poly (*N*-vinylformamide) with molecular weight of 340.000 g/mol. The polymer was purified by membrane filtration and dialysis before ultra thin film fabrication was performed. Hyperbranched polyethyleneimine (PEI), with a weight average molecular weight of 25.000 g/mol, was obtained from Aldrich and was used as received. Polyamideamine-epichlorohydrin (PAE) (12.5 wt% aqueous solution) was purchased from SI group and has weight average molecular weight of 269.000 g/mol which were measured by static light scattering. Propylamine (99%) was received from Fluka. Ultrapure water was used as the solvent for all experiments (Milli-Q, 18.2MΩ). Silicon wafers with a diameter of 3" and a thickness of 380 μm, oriented 1.0.0 (CrysTec, Germany), were used as the substrate. The silicon wafers were cut with a RV-diamond cutter and substrates were sonicated in isopropanol for 10 min and then washed with Milli-Q water. Oxygen plasma activation was carried out in a self-designed installation, AK300 from Roth & Rau (Germany), which allowed freedom in selecting the process parameters. The plasma treatment was performed using the following parameters: microwave power 500W, working pressure 0.25 mbar, O^2 gas flow 50 ft^3/min, and 60 s treatment time. The freshly surface-activated silicon substrates were used within 1 h for the adsorption experiments. Films were generated with a dip coater on the plasma oxidised silicon surface.

The model reactions of primary amines with azetidinium groups, were studied by ^{1}H NMR spectroscopy. Before the experiment, H_2O from the aqueous PAE solution was substituted stepwise with D_2O by vacuum distillation to avoid self-crosslinking. The resulting D_2O PAE solution was reacted with propylamine in a round-bottom flask with a mechanical stirrer. ^{1}H NMR spectra of PAE and before and after the reaction with propylamine were recorded on a

Bruker DPX-300 FT-NMR spectrometer at 300 MHz. D_2O and $CDOD_4$ were used as solvent and tetramethylsilane (TMS) served as an internal standard.

Ultra thin film fabrication

To fabricate the ultra thin films, freshly oxidised silicon substrates were subsequently dipped into aqueous PVAm/PAE solutions in a series of dipping concentrations (1mM, 10mM, 100mM PVAm/0.1 wt% PAE) with varying dipping pH (3, 6.5, 9) and polyamine structure (linear PVAm, branched PEI). Afterwards the substrate was rinsed with ultrapure water two times to remove excess polymer. After the adsorption of the first layer, the substrates were dipped into a diluted PAE solution for the adsorption of the second layer and then washed in ultrapure water. The resulting films were stored in an ambient atmosphere for fabricating crosslinked PVAm modified silicon substrates and were cleaned with nitrogen gas before further examination.

Surface characterization

Ellipsometry was performed with an OMT instruments using VisuEl software version 3.4.1 (Optische Messtechnik GmbH) at the angle of incidence of 70 º and a spectral method in the wavelength range from 460 to 870 nm. In order to measure ultrathin layers the azimuthal angle was maintained at 15 º. The resulting thickness is the average of at least 5 measurements from different areas of the silicon oxide surface. Sessile drop contact angle measurements were carried out by G402 with DSAII (drop shape analyzer) software (Krüss). Average contact angles are presented from 10 independent sessile drop measurements. XPS analysis of polymer coated silicon oxide surface was performed on an Ultra AxisTM Spectrometer from Kratos analytical (UK). The elements on the substrate were excited with monoenergetic Aluminium K1,2 irradiation with an energy of 1486.6 eV and a power of 150 W. The analysed sample area was 600 x 800 μm² with an information depth of around 10 nm.

The surface topology of absorbed thin polymer films was accomplished using an atomic force microscopy (Nanoscope III). The tapping mode imaging was performed with standard silicon cantilevers (Nano world, NCH-W point probe). The force constant and resonant frequency was reported by the manufacturer as 42 N/m and 320 kHz respectively. Furthermore, the stability tests of PVAm/PAE films were conducted by immersing 24 hours into 0.1 M NaOH solution followed by measuring the thickness by Ellipsometry.

2.3 RESULTS AND DISCUSSION

The adsorption of polyelectrolytes onto various types of solid materials, for example inorganic oxide particles, flat solid surfaces or cellulose fibers, has been studied extensively. In this work we describe detailed investigation on a new approach for the fabrication of ultrathin films of poly(vinylamine) /poly(amideamine-epichlorohydrin) on silicon oxide surfaces resulting in stable hydrogel layers on negatively charged surfaces as we recently communicated. The activated negatively charged silicon oxide surface was generated by an oxygen plasma treatment. Subsequently, commercially available PVAm (Lupamin 9095; M_w 340.000 g/mol) was absorbed on the negatively charged silicon oxide surfaces by electrostatic interactions. This first step is well known in the LBL process to build multilayer structure.[32,33] The resulting PVAm coating contains free amino group which might be used for the further reaction with poly(amideamine-epichlorohydrin) yielding a stable crosslinked hydrogel (see Scheme 2).

Polymers containing azetidinium side groups allow crosslinking by ring-opening reaction with nucleophilic compounds, e.g. primary amines. To demonstrate the reactivity of the azetidinium ions, the ring-opening reaction of the azetidinium group was first investigated in a model reaction with n-propylamine at 25 ºC for 30 minutes (Scheme 2). Importantly, in the ^{1}H NMR spectra a quantitative conversion of the azetidinium group (disappearance of peak a)

was observed after reaction with excess of n-proplylamine (Figure 1). In addition, new peaks appeared (b and c in Figure 1) indicating the attachment of n-propylamine to PAE. These data demonstrate the high reactivity of the azetidinium groups to primary amines indicating that effective cross-linking might be achieved by reaction of PVAm with PAE.

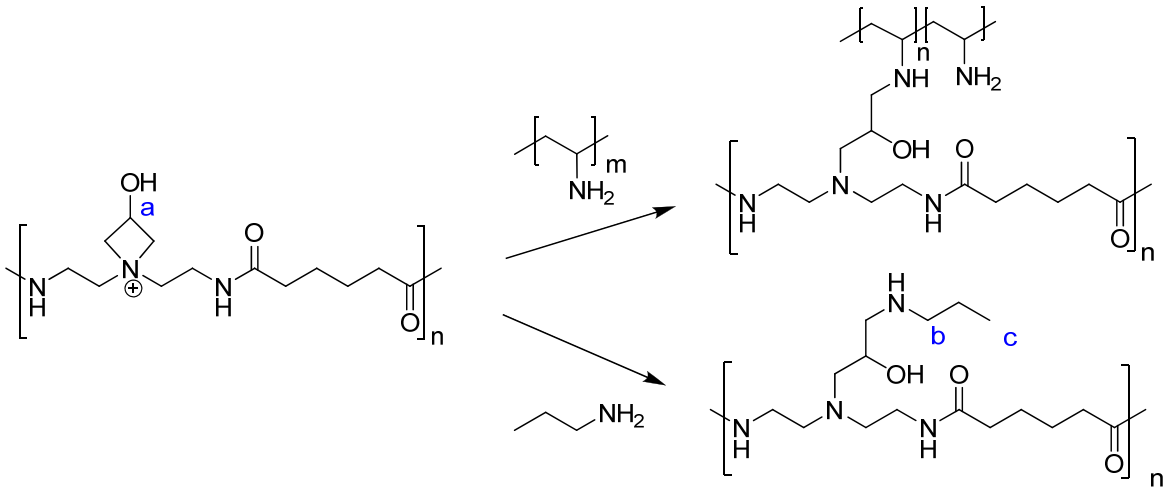

Scheme 2. Schematic representation of the ring-opening reaction of PAE with PVAm and propylamine

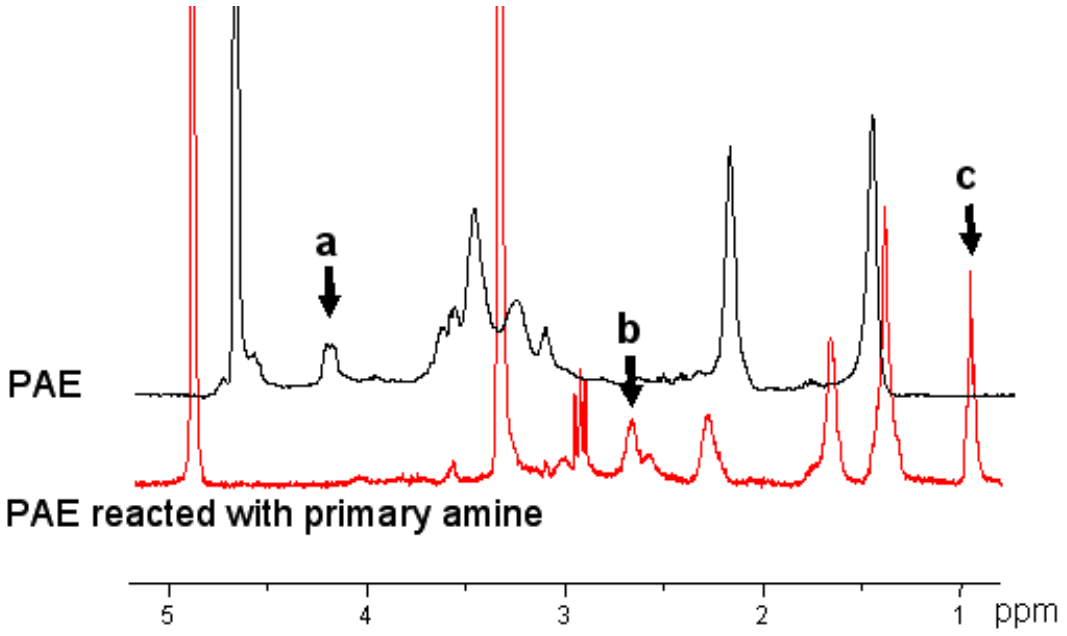

Figure 1. ^{1}H NMR spectra of (a) PAE in D_2O and(b) PAE after reaction with n-propylamine for 30 minutes at 25 ºC measured in methanol-d4.

Molecular weights of commercial PAE were determined by the static light scattering (SLS) measurement using the aqueous condition of 0.1M NaCl and pH 2 to remove the polyelectrolyte effects, where their dn/dc values of 0.1471. Figure 2 shows the Zimm plot to estimate the molecular weight of PAE. The average molecular weight is 269.000 g/mol, the second virial coefficient, A_2 is 6.14×10^{-5} mol · ml/ g · g and radius of gyration R_g is 77 nm were calculated from the concentration and angular dependency of excess Rayleigh ratio by mean of Berry approximation. The molecular weights of PAE were reported in the range from 6,700 to 230.000 g/mol.[25]

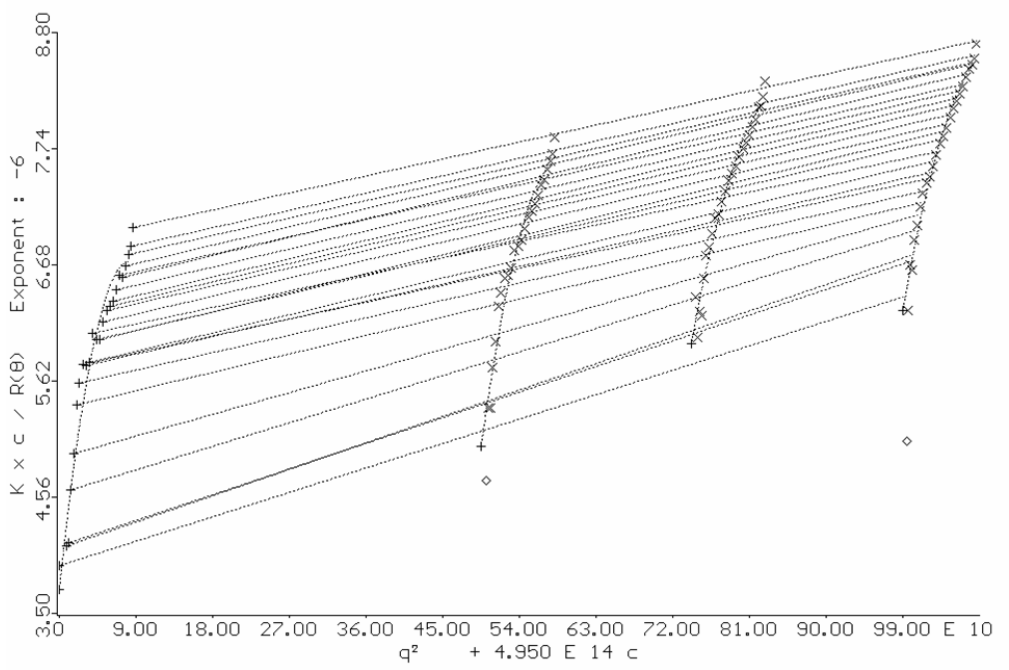

Figure 2. Berry plot of poly(amideamine-epichlorohydrin) (PAE) determined by static light scattering in aqueous medium (0.1M NaCl, pH 2, 25 ºC): c = 0.10 mg/ml, c = 0.50 mg/ml, c = 0.75 mg/ml and c = 1.00 mg/ml, reflective idex (dn/dc) = 0.1471

To investigate whether the adsorbed polyamine can be crosslinked for stabilization, the modified silicon surface was post-treated with a reactive PAE. Atomic force microscopy (AFM) was used to study the surface structure of the primer coating with PVAm and the topology of film formed after treatment with reactive PAE. AFM images of the polyelectrolytes adsorbed on the plasma oxidized silicon surface demonstrated that a very smooth film is formed of PVAm on the plasma treated silicon surface (Figure 3 a). In contrast, the monolayer structure of PAE (Figure 3 b) was uneven and the formation of separated islands was observed. This effect is likely due to partial self-crosslinking of reactive PAE resulting in larger more globular PAE particles. Interestingly, the surface of the formed film after the reaction of the adsorbed PVAm with PAE (0.1 wt% in water, 10 ml), is smoother than a PAE film on the surface itself (see Figure 3 c) indicating the interaction between PVAm and PAE.

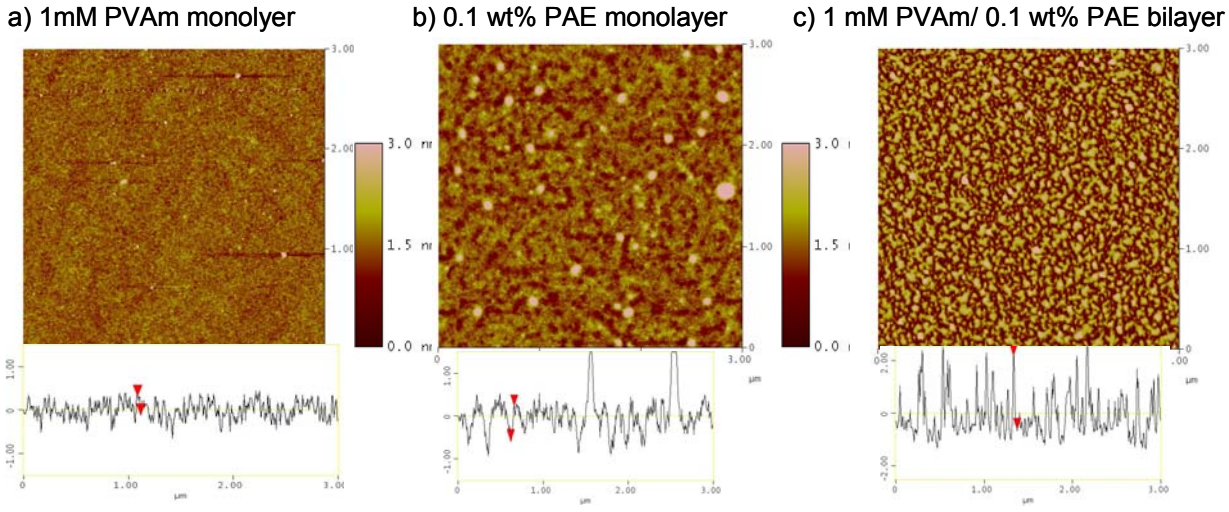

Figure 3. AFM tapping mode images and height profiles of PVAm (Mw 340.000 g/mol) (a) and PAE (Mw 269.000 g/mol) (b) as well as combined PVAm/PAE (c) ultra thin films: scan size is 3×3 μm^2 and z-range is 3 nm for all images.

XPS analysis was carried out to determine the chemical composition of the oxidized silicon surface with the different monolayer. The comparison of the chemical composition of the oxidized plasma and control silicon surface (Table 1) clearly shows that the oxygen plasma treatment leads to higher oxygen and reduced carbon content of the surface. Thus, the oxygen plasma leads to an oxidation as well as decontamination of the surface. After dip-coating of the oxidized silicon surface with PVAm and PVAm/PAE, an increase in nitrogen concentration and decrease in silicon concentration was detected respectively, due to surface coating with polymers. The atomic composition can be determined using the N 1s content, which results only from the adsorbed polyelectrolyte layer. The N:C and N:Si atomic ratios can be taken as measure for the amount of adsorbed polyelectrolyte. Table 1 shows that the PVAm/PAE system has higher N:C (0.25) and N:Si (0.24) atomic ratio ensuring the film formation and demonstrating the presence of more polymer on the surface compared to both the PAE and PVAm coatings. The thickness of the coatings formed on the oxidized plasma silicon surfaces was investigated by ellipsometry. As shown in Table 1 the thickness of the water film on the oxidized wafer surface is 2.53 nm and the thickness of the PVAm film on the oxidized wafer surface is 3.15 nm. The PVAm/PAE coating revealed a thickness of 3.65 nm due to the adsorption of PAE suggesting that the reactive azetidinium groups formed crosslinks with free amino groups on the surface of the PVAm layer.

Table 1. XPS atomic concentration with N/C relative amount of nitrogen, thickness of films determined by Ellipsometry and AFM, contact angle data for the control, the oxygen plasma treated, the individual PVAm (1 mM, Mw 340.000 g/mol), PAE (0.1 wt%, Mw 269.000 g/mol) and combined PVAm/PAE (1 mM/0.1 wt%) ultra thin films.

coated sample on silicon wafer	Surface composition (%)				N:C	N:Si	Ellipsometry (coated) thickness (nm)	AFM roughness (nm)	Contact angle (°)
	C1s Σ	O1s Σ	N1s Σ	Si2p Σ					
Control	22,08	31,85	0,00	45,76	0,00	0,00	3,1 ± 0,15		61 ± 1,5
O_2-Plasma	9,31	36,37	0,00	50,24	0,00	0,00	2,53 ± 0,05		29 ± 2,3
O_2-Plasma / PVAm	34,37	29,42	3,60	31,89	0,1047	0,1129	3,15 ± 0,02 (0,62)	0,429 ± 0,04	45 ± 0,5
O_2-Plasma / PAE	17,36	34,11	2,15	45,14	0,1238	0,0476	3,68 ± 0,83 (1,15)	0,809 ± 0,36	52 ± 3,9
O_2-Plasma /PVAm/PAE	28,54	32,17	7,27	30,50	0,2547	0,2384	3,65 ± 0,2 (1,12)	2,805 ± 0,59	37 ± 1,2

More detailed studies were performed on the effect of PVAm concentration in the dip-coating solution on the formation of crosslinked PVAm/PAE films (see Figure 4) revealing a strong influence of concentration on film thickness. The thickness of both the PVAm and PVAm/PAE coatings rapidly increased from 2.5 nm to 3.7 nm with increasing concentration (1 mM – 50 mM) followed by saturation up to 500 mM. The saturation thickness is most likely caused by full coverage of the anionic surface with cationic polymer. The slight increase in thickness of the PVAm/PAE film compared to PVAm can be related to the surface composition by the N:C content, which is a direct measure for the amount of adsorbed polymer. These results demonstrate that we can simply adjust the layer thickness by increasing the dipping solution concentration.

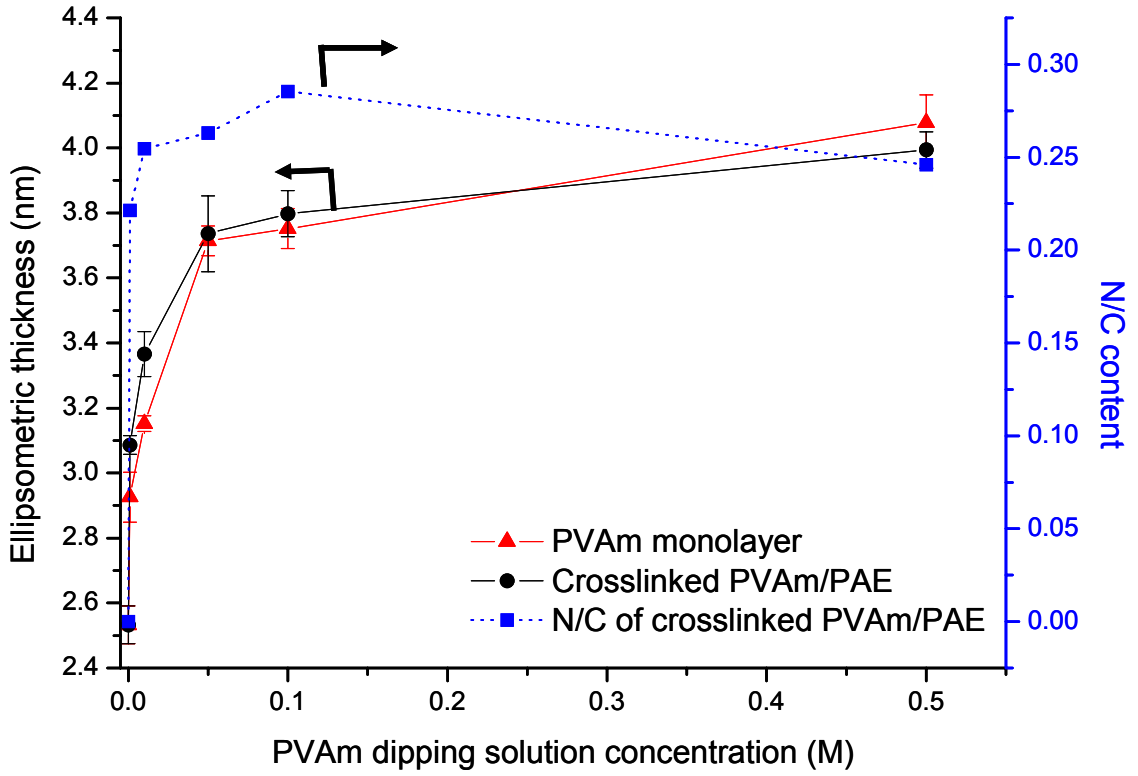

Figure 4. Ellipsometric thickness of PVAm monolayer and crosslinked PVAm/PAE (0.1 wt%, Mw 269.000 g/mol) films on plasma treated silicon wafer as function of PVAm concentration (1 mM -500 mM, Mw 340.000 g/mol) and the N/C relative amount of nitrogen determined by XPS analysis.

Furthermore, concentration related changes in topography of PVAm and PVAm/PAE coatings were investigated by tapping mode AFM (see Figure 5). The thickness of the PVAm and PVAm/PAE increases with increasing PVAm concentration, which is in good agreement with the ellipsometric measurements. The PVAm samples show smooth films at all concentrations with only a slight increase of roughness with concentration. Surprisingly, both the roughness and surface structure of the PVAm/PAE bilayer depend much stronger on the concentration of PVAm (see Figure 5). Apparently, the PVAm structure is amplified by crosslinking and attachment of PAE.

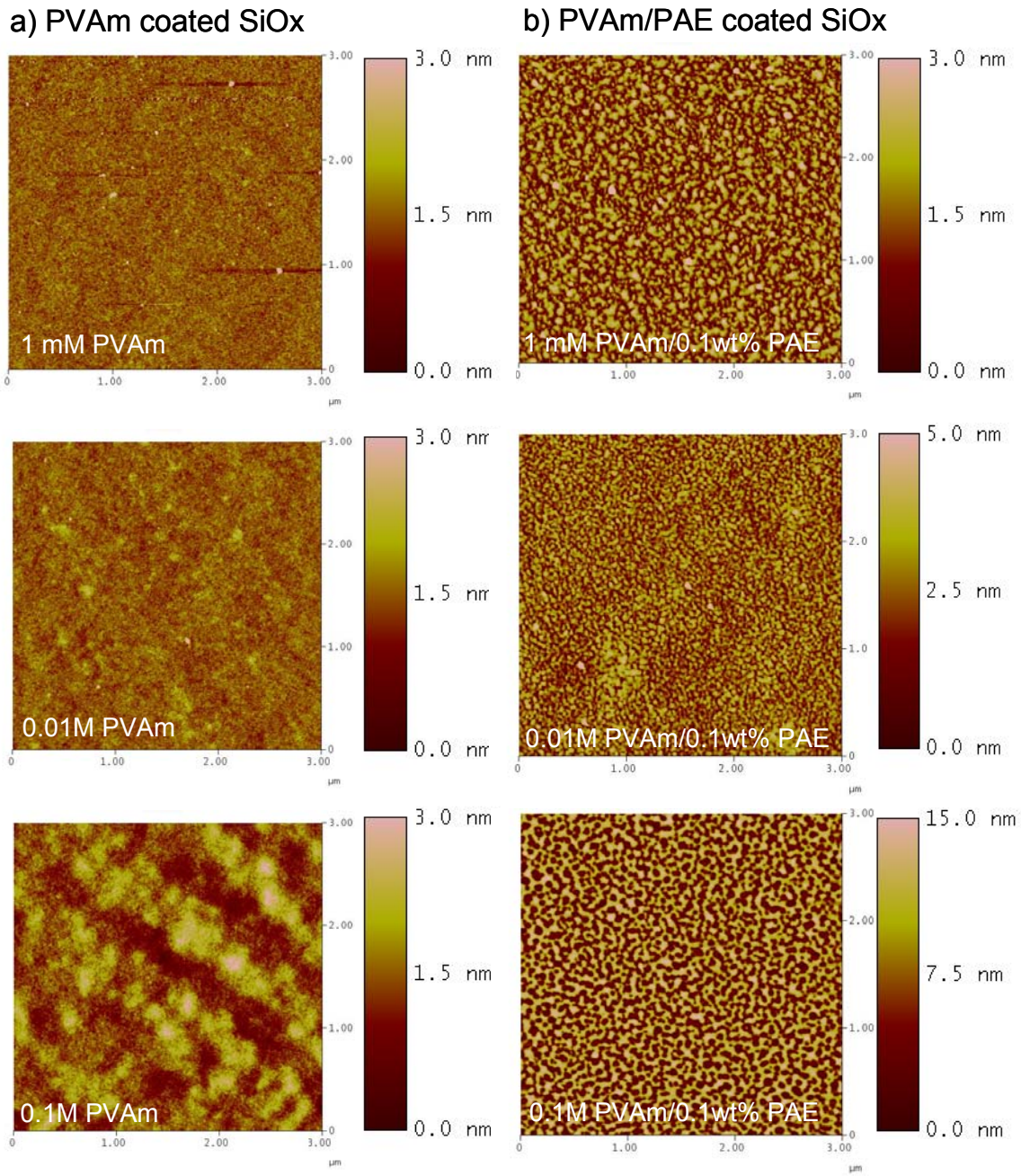

Figure 5. AFM tapping mode images of a) PVAm (Mw 340.000 g/mol) monolayer and b) PVAm (Mw 340.000 g/mol) /PAE (Mw 269.000 g/mol) thin films with varying PVAm dipping solution concentration (scan size is 3×3 μm^2) .

In addition, In addition to varying the PVAm concentration, we investigated the PVAm and PVAm/PAE hydrogel formation on plasma treated silicon oxide as function of the pH and polyamine structure (Figure 6). Ellipsometry was used to determine the adsorbed hydrogel layer thicknesses. When a polyelectrolyte adsorbs on oppositely charged surfaces, the adsorption is based on electrostatic interactions which depend on the nature of the ionic groups, the pH of dipping solution and ionic strength. The degree of protonation of PVAm is strongly pH dependent[34] and it has been demonstrated that he surface tension of PVAm films is also pH dependent showing a transition from higher to lower surface tension upon increasing the pH due to neutralization of the amine groups.[35] Figure 6 a) shows the influence of the pH value of the PVAm dipping solution on the layer thickness of adsorbed PVAm and PVAm/PAE revealing a thicker PVAm layer at higher pH values. This observation can can be ascribed to the higher charge density at lower pH resulting in more stiff and stretched polymer chains resulting in a lower amount of adsorbed polyelectrolyte.[36] Since the layer thickness is mostly governed by the PVAm adsorption, a similar trend is observed for the PVAm/PAE layers, i.e. thicker layers at higher pH values, whereby slightly thicker films are obtained compared to PVAM due to PAE adsorption.

The influence of polyamine structure on the adsorption behavior on the plasma oxidized silicon surface was examined by comparison of linear PVAm and branched PEI, whereby it is anticipated that the branched PEI is more bulky and cannot spread out onto the surface resulting in a thicker layer compared to PVAm. In general, an even more complicated adsorption behavior is observed for highly branched polyelectrolytes compared to the linear analogues.[37,38] In the current study, the adsorbed layer thickness between linear and branched polyamines is evaluated by ellipsometry revealing that branched PEI results in a thicker deposited layer on the plasma oxidized silicon surface than linear PVAm, even though the molecular weight of PVAm (340.000 g/mol) is ten times higher than the molecular weight of the branched PEI (25.000 g/mol). Linear PVAm has only primary amine groups whereas

branched PEI has a ratio of 25:50:25 of primary: secondary: tertiary amine. Both polyamines are charged in aqueous solution resulting in pH 9-10 for PVAm and pH 10-11 for branched PEI. The thicker adsorption layer with branched PEI can be related to the higher charge density and the shape of this branched polyamine, which is more bulky and rigid than the linear type. Again an addition increase in layer thickness is obtained for PVAm/PAE compared to PVAm due to PAE adsorption.

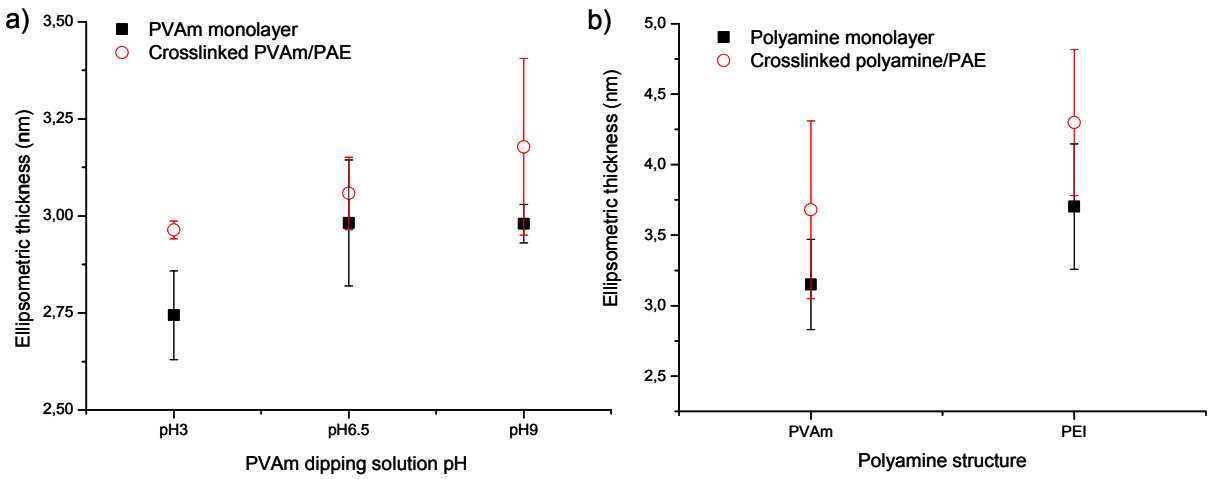

Figure 6. Film layers thickness influence of a) PVAm dipping solution pH 3, 6.5, 9 and d) linear and branched structure determined by ellipsometry measurement. All samples prepared with 10 mM PVAm (340.000 g/mol) and 0.1 wt% PAE.

Furthermore, the swelling behavior of the PVAm/PAE film was investigated by AFM analysis before (dry surface) and after (wet surface) exposure to water (Figure 7). The AFM images clearly show that the PVAm/PAE layer is swollen although the surface roughness did not significantly increase. Swelling of the hydrogel film proves the successful crosslinking between PVAm and the azetidinium groups of PAE since without crosslinks the film would have been dissolved in water.

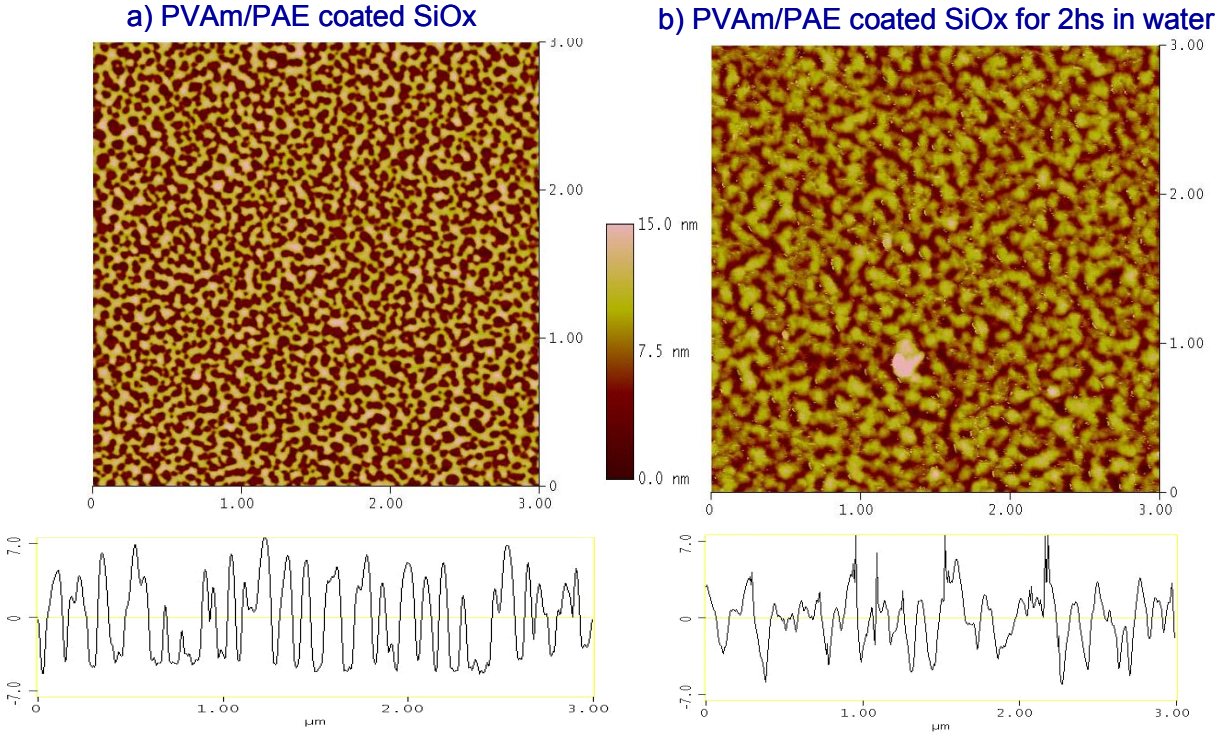

Figure 7. AFM images showing swelling behavior of 10mM PVAm (Mw 340.000 g/mol)/ 0.1 wt% PAE (Mw 269.000 g/mol) ultra thin hydrogel films on plasma oxidized silicon surface a) before and b) after exposition to water for 24 hours: scan size is 3×3 μm^2 and z-range is 15 nm for all images.

The effect of crosslinking density of the hydrogel network on the swelling behavior was investigated by ellipsometry of coatings prepared with various PVAm/PAE dipping concentrations (Figure 8 and table 2). The initial film thickness (drying thickness) was normalized by subtraction of the control silicon wafer thickness of 2.53 nm and the swelling thickness was calculated by the simple equation given in Table 2. The swelling behaviors of ultrathin hydrogel film were found to be in the range from 83% to 450%, indicating the fabrication of an ultrathin hydrogel. In general, it is observed that higher PAE concentrations lead to reduced swelling abilities, which can be ascribed to the higher crosslinking density. Thus, the physical properties of the PVAm/PAE hydrogels can be controlled by the crosslinking density. A closer look at Figure 8 reveals that the thickness of the dry films steadily increases with higher PAE concentration while the thickness of the swollen films are more scattered explaining the scatter in the calculated swelling ratios. In addition, the hydrogels prepared at 0.1 M PVAm concentration are thicker and reveal slightly more absolute swelling compared to the hydrogels prepared at 0.01 M PVAm as might be expected form the large amount of material that is adsorbed to the surface.

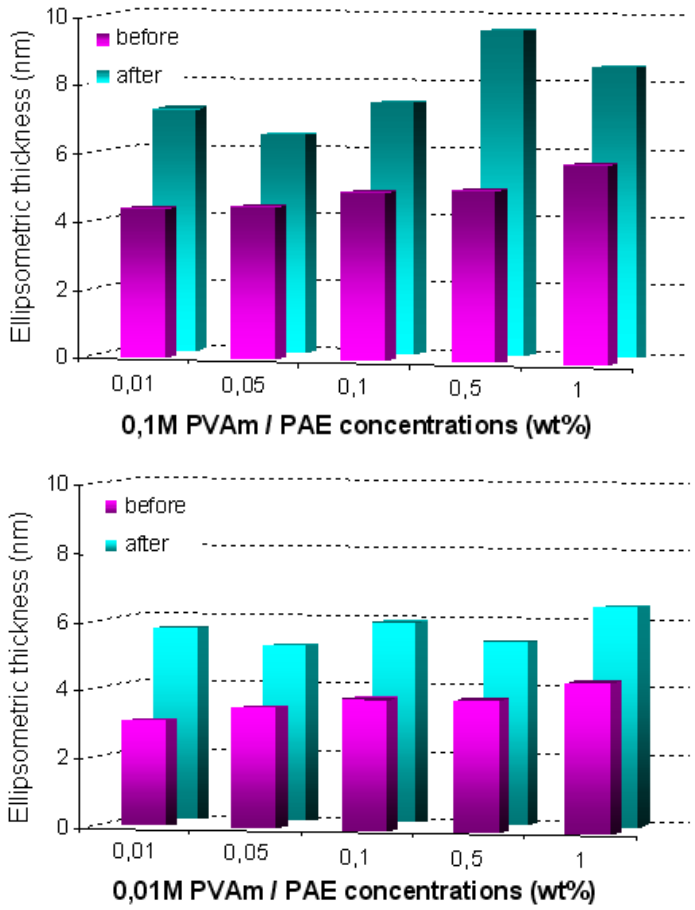

Figure 8. Thickness changes of PVAm/PAE ultra thin hydrogel films on plasma oxidized silicon surface before and after dipping in mili-Q water for 24 hours as function of the PVAm and PAE concentrations. Thicknesses are determined by ellipsometry.

Table 2. Relative swelling percentage of ultra thin hydrogel films calculated from the normalized thickness before and after exposure to water.

PVAm/PAE	Relative swelling percentage calculated from ellipsometry data (%) [a]				
Conc. PAE (wt%)	0.01	0.05	0.1	0.5	1
0.1M PVAm	149 %	100 %	103 %	181 %	83 %
0.01M PVAm	445 %	167 %	163 %	117 %	109 %

[a] Normalized samples thicknesses were obtained by subtraction of the average thickness of the silicon substrates (2.53 nm) determined by ellipsometry apply. The relative swelling percentage was calculated using the following equation:
((swelling thickness-drying thickness)/drying thickness) × 100.

The stability of the covalently crosslinked PVAm/PAE films is evaluated by washing with aqueous 0.1 M NaOH for 24 hours. The NaOH solution deprotonates the PVAm causing dissociation of the electrostatically assembled films.[9] The thicknesses of adsorbed PVAm, PAE and crosslinked PVAm/PAE films were determined by ellipsometry before and after exposure to the NaOH solution. Figure 9 demonstrates that the electrostatically adsorbed monolayers of PVAm and PAE are almost completely removed from the plasma treated silicon oxide surface after exposure to the NaOH solution. In contrast, the crosslinked PVAm/PAE films increased in thickness after exposure to the aqueous NaOH due to swelling clearly demonstrating the stability of the crosslinked films.

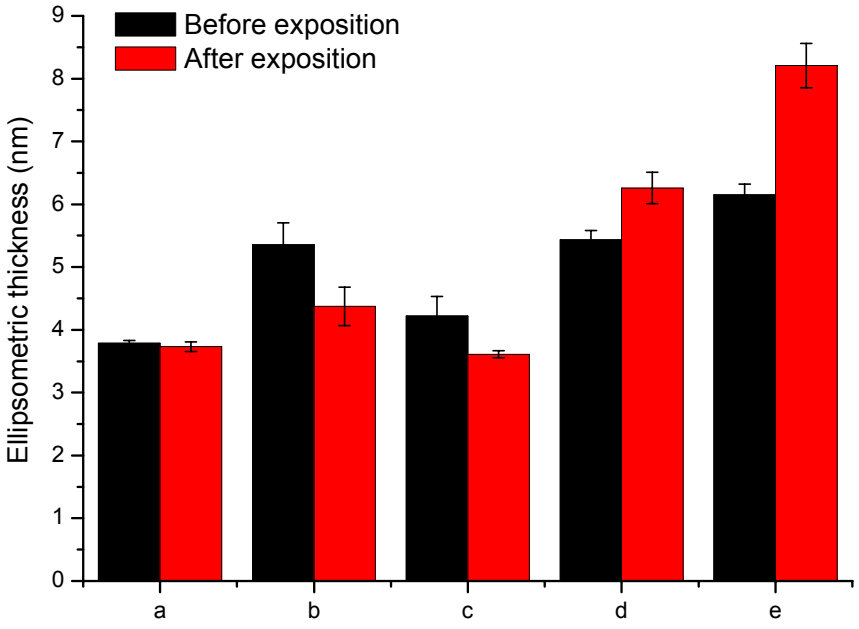

Figure 9. Films thickness changes of a) control silicon wafer, b) PVAm (50 mM; Mw 340.000 g/mol), c) PAE (0.1 wt%; Mw 269.000 g/mol), d) PVAm (50 mM; Mw 340.000 g/mol)/PAE (0.1 wt%; Mw 269.000 g/mol), and e) PVAm (100 mM; Mw 340.000 g/mol)/PAE (0.1 wt%; Mw 269.000 g/mol) thin hydrogel films on plasma oxidized silicon surface before and after exposition to 0.1M NaOH for 24 hours.

2.4 CONCLUSIONS

In summary, self-assembly of ultrathin crosslinked polyelectrolyte hydrogel films by primer concept surface modification were fabricated on oxygen plasma treated silicon oxide surfaces. The film formation occurred via the adsorption of PVAm in aqueous solution on the negatively charged surface followed by crosslinking with PAE based on the reaction of azitidinium groups with the amine. The adsorption of cationic PVAm is the initial factor to build up an ultrathin reactive film while PAE is responsible for crosslinking of the primary amine groups of PVAm. The presence of both PVAm/PAE on the silicon surfaces was confirmed by the nitrogen content is determined by XPS. In addition, we have shown that polymer concentration, PVAm solution pH and polyamine structure can be used to control the PVAm and PVAm/PAE film thicknesses, which increased with increasing PVAm concentration, higher pH and the use of a more bulky branched PEI polyamine. The adsorbed PVAm/PAE coatings were swellable in water, indirectly proving the formation of a crosslinked hydrogel film. Increasing the crosslinking density by increasing the PAE concentration leads to decreased swelling of the films. In addition, the formation of stable crosslinked PVAm/PAE films was demonstrated by exposure to an aqueous NaOH solution. All together, we demonstrated that this simple plasma treatment followed by dipcoating method can be applied for the generation of stable ultrathin hydrogel films on silicon substrates. Further functionalization reactions of the excess of PVAm primary amine groups are currently under investigation. Furthermore, the presented methodology is expected to be applicable to a range of other surfaces as well.

2.5 REFERENCES

M1 Reproduced with permission from Yu, M.; Hoogenboom, R.; Thomas, H.; Moeller, M. *manuscript in preparation.*

[1] Roberts, G. *Langmuir-Blodgett Films*, Plenum: New York, 1990.

[2] Decher,G.; Hong, J. D; Schmitt, J. *Thin Solid Films* **1992**, 210/211, 831.

[3] Decher,G. *Science* **1997**, 277, 1232.

[4] Tanga, Z.; Donohoea, S. T.; Robinsonb, J. M.; Chiarellia, P. A. *Polymer* **2005,** 46, 9043.

[5] DeLongcham, D.; Hammond, P.T. *Adv. Mater.* **2001**, 13, 1455

[6] Anzai, J.; Hoshi, T.; Nakamura, N.; *Langmuir* **2000,** 16, 6306

[7] Kharlampieva, E.; Sukhishvili, S. A.; *Langmuir* **2003,** 19, 1235

[8] Harris, J. J.; Bruening, M. L.; *Langmuir* **2000,** 16, 2006

[9] Wu, G.; Shi, F.; Wang, Z.; Liu, Z.; Zhang, X.; *Langmuir* **2009,** 25, 2949

[10] Diflavio, J. Bertoia,R. ; Pelton, R.; Leduc, M. *13th Fundamental research symposium*, Cambridge, **2005** 1293.

[11] Kobayashi, S.; Suh,KD.; Shirokura, Y. *Macromolecules* **1989**, 22, 2363.

[12] Gu,L.; Zhu, S.; Hrymark, *N. J. Applied Polymer Sci* **2002**, 86, 3412.

[13] Voigt, I.; Simon, F.; Jacobasch, H. J.; Spange, S. *Colloid Polym.Sci*. **2000**, 278, 48.

[14] Voigt, I.; Esthel, K.; Simon, F.; Spange, S. *Langmuir* **2001**, 17,3080.

[15] Roth,I.; Simon, F.; Bellmann,C.; Seifert, A.; Spange, S. *Chem.Mater.* **2006**, 18, 4730.

[16] Poptoshev, E.; Rutland, M.W.; Clasesson, P.M. *Langmuir* **1999**, 15, 7789.

[17] Ceffroy, C.; Labeau, M.P.; Wong, K.; Cabane, B.; Cohen Stuart, M.A. *Colloids Surface A: Physicochem. Eng. Aspects* **2000**, 172, 47.

[18] Shulga, A.; Widmaier, J.; Pefferkorn, Emile.; Champ, S.; Auweter, H. *J. Colloid Interface Sci.* **2003**, 258, 219.

[19] Shulga, A.; Widmaier, J.; Pefferkorn, Emile.; Champ, S.; Auweter, H. *J. Colloid Interface Sci.* **2003**, 258, 228.

[20] Burkert, H.; Brunnmueller, F.; Beyer, K.; Kroener, M.; Mueller, H. *U.S. Pat.* **1984**, 4,444,667, BASF.

[21] Monech, D.; Hartmann, H.; Buechner, K. *U.S. Pat.* **1993**, 5,225,088, BASF.

[22] Wolfert, M.A.; Dash, P.R.; Nazarova, O.; Oupicky, D.; Seymour, L.W.; Smart, S.; Strohalm, J.; Ulbrich, K. *Bioconjugate Chem.* **1999**, 10, 993.

[23] Monech, D.; Hartmann, H.; Buechner, K. U.S. Pat. 5,225,088(1993, to BASF).

[24] Obokata, T.; Isogai, A. *J. Appl. Polym. Sci.* **2004**, 92, 1847.

[25] Obokata, T.; Yanagisawa M.; Isogai, A. *J. Appl. Polym. Sci.* **2005**, 97, 2249.

[26] Obokata, T.; Isogai, A. *Colloids Surfaces A: Physicochem. Eng. Aspects* **2007**, 302,525.

[27] Feng, X.; Pelton, R. *Macromolecules* **2007**, 40, 1624.

[28] Bogaert, Y.; Goethals, E.; Schacht, E. *Makromol. Chem.* **1981**, 182, 2687.

[29] Laguerre, M.; Boyer, C.; Leger, J.; Carpy, A. *Can. J. Chem.* **1989**, 67, 1514.

[30] Couty, F.; David, O.; Drouillat, B. *Tetrahedron Lett.* **2007**, 48, 1027.

[31] Couty, F.; David, O.; Drouillat, B. *Tetrahedron Lett.* **2007**, 48, 9180.

[32] Serizawa, T.; Yamamoto, K.; Akashi, M. *Langmuir* **1999**, 15 4682.

[33] Serizawa, T.; Nakashima, Y.; Akashi, M. *Macromolecules* **2003**, 36, 2072.

[34] Katchalsky, A.; Mazur, J.; Spitnik, P.; *J. Polyer sci.*, **1957**, 23, 513

[35] Hong, J.; Pelton, R.; *Collod Polym. Sci.*, **2002**, 280, 203

[36] Bucatariu, F.; Simon, F.; Spange, S.; Schwarz, S.; Dragan, S.; *Macromol.Symp.* **2004**, 210, 219

[37] Mészáros, R.; Thompson, L.; Bos, M.; Groot, P.; *Langmuir*, **2002**, 18, 6164

[38] Oulanti, O.; Pefferkorn, E.; Champ, S.; Auweter, H.; *J. Colloid Interface Sci.* **2005**, 291, 105

[39] http://www.veredlungschemikalien.basf.de/ev-wcms-in/internet/de_DE/portal/show content_df/content/EV/EV5/ products/wsp/lupasol_lupamin

CHAPTER 3

AZETIDINIUM-AMINE COUPLING AS "CLICK" METHOD FOR THE PREPARATION OF ATHIN HYDROGEL FILMS ON SILICON OXIDE [M2]

ABSTRACT

This communication reports a simple preparation of ultrathin hydrogel films cross-linked by azetidinium-amine coupling on plasma treated silicon oxide surface using layer-by-layer (LBL) self assembly method. The swelling behavior and antimicrobial activity against gram positive (*Bacillus subtilis*) bacteria are discussed as potential applications.

3.1 INTRODUCTION

The use of polyelectrolytes for surface and interface modification of colloidal inorganic oxides,[1,2] cellulose[3] and solid substrates[3-11] is of growing interest in many different applications on analytical,[1,2] material[2] and biochemistry,[3] as well as in electronics.[4,5] Simple and representative routes for modifying surface characteristics are based on changing the surface properties, e.g. by flame and plasma treatments or direct coating with functional prepolymers.[10,11] To impart physical contact between hydrophobic substrates and polar coatings, a pre-treatment of the surface on chemical (RCA procedure) or physical basis (flame or plasma treatment) is required.

In chapter 3, we describe a new procedure for simple surface modification, which includes plasma treatment followed by the application of an ultra thin coating on the pre-treated surface. In this respect the primer-concept has been developed yielding an amino

functionalized monolayer on a silicon wafer.[12,13] However, a major challenge is the use of adsorbed polyamine as a stable coating instead of covalently attached aminopropyl alkoxysilane, which is the standard procedure for the fabrication of amino functionalized surfaces.[14-17] Primary amine groups of a high molecular weight poly(vinylamine) (PVAm) behave as a "primer" molecule providing an anchor to the surface and a reactive point for further surface functionalizations. The adsorption is driven by the electrostatic interactions of the negatively charged surface with the positively charged poly(vinylamine). This step is well established for fabrication of multilayer thin films. Various applications have been reported,[34-37] which are based on immobilization of different molecules such as enzymes,[42] organic dyes,[43] inorganic particles[1,2,21] and heavy metal particles.[44] To reproducibly fabricate a smooth PVAm monolayer, we have adapted a versatile and simple layer-by-layer (LBL) assembly by dip coating.[18,19] The electrostatic and/or hydrogen bonding interactions drive the adsorption of PVAm on plasma oxidized silicon wafer.[20] A Soxhlet extraction test was reported to test the stability of PVAm layer on negatively charged silica particles, whereby the PVAm layer was partially removed.[21] Therefore, crosslinking on the PVAm layer has been recommended to enhance the stability of the polyelectrolyte layer.

Click chemistry, as introduced by Sharpless in 2001, refers to versatile reactions that are, e.g., highly efficient, wide in scope and can be performed under ambient atmosphere, preferably in water.[22,23] As such, the use of click chemistry flourished in recent years in a wide variety of research fields including bioconjugation as well as polymer and material science.[24,25] The advantages of click chemistry were also applied for the stabilization of ultrathin coatings. [26-28]

In the current chapter, we report the stabilization of a PVAm coating on silicon oxide by a novel type of click reaction, namely azetidinium ring-opening by reaction with amines. Therefore, we reacted the PVAm primer film with poly(amideamine-epichlorohydrin) (PAE) that contains a large number of reactive hydroxyl-azetidinium groups[29-33] allowing efficient crosslinking with PVAm (Scheme 1). The hydroxyazetidinium is stable in water and only

reacts when it is brought into contact with the PVAm film. Therefore, we believe that this reaction has the potential to be developed into a metal free click reaction,[46,47] although the scope and selectivity have to be evaluated in further detail. Besides the synthesis of ultrathin PVAm-PAE hydrogel layers on silicon oxide, we also report the swelling behavior of the resulting films, demonstrate the antimicrobial activity of the resulting cationic hydrogel and illustrate the presence of reactive amine groups on the surface, which might be used for further functionalization.

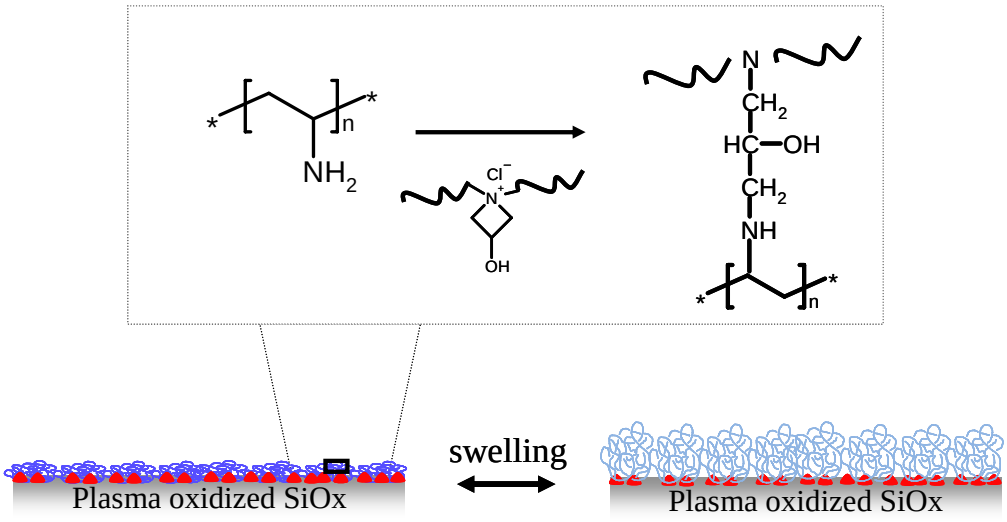

Scheme 1. Schematic representation of the fabrication of crosslinked PVAm/PAE on a plasma oxidized silicon oxide surface by ring-opening of azetidinium ions with PVAm as well as swelling of the resulting ultrathin hydrogel layer

3.2 EXPERIMENTAL PART

Ultra thin hydrogel film fabrication

The silicon substrates were cleaned by ultrasonication in isopropyl alcohol and mili-Q water for 10 min and activated by O_2 plasma treatment (500 W, 0.25 mbar, 50 ft^3/min, 60 s). After activation, the substrates were immediately coated with primer PVAm (Mw 350.000 g/mol, BASF AG, Ludwigshafen) in various concentrations by dip coating for 5 min. The primer coated substrates were rinsed intensively in Mili-Q water to remove excess primer. Subsequent cross-linking was performed by dipping for 5 min in a PAE solution. Crosslinked PVAm/PAE silicon wafers were washed in Mili-Q water. These freshly prepared films were stored in ambient condition and cleaning with nitrogen gas before further characterization.

Surface characterization

Layer thicknesses were determined by Ellipsometry (OMT instruments with VisuEl software) at an incidence angle of 70 º and a spectral method in the wavelength range from 460 to 870 nm. In order to measure ultrathin layers, the azimuthal angle was 15 º. All measured thicknesses were determined 5 times from different areas of the silicon wafer. The chemical surface composition of the ultrathin hydrogel films was measured by XPS at room temperature using a Ultra AxisTM Spectrometer from Kratos analytical (UK). The elements on the silicon wafer were excited with monoenergetic Aluminium K1, 2 irradiation with an energy of 1486.6 eV and a power source of 150 W. Surface topology was obtained by atomic force microscopy (AFM) under ambient conditions using a Nanoscope III (Digital instruments) operating in the tapping mode at a resonance frequency of about 370 kHz. Silicon cantilevers (Nano world, NCH-W point probe) with a spring constant between 25 and 100 N/m and resonance frequency in the range of 320-493 kHz were used.

Antimicrobial activity of the ultrathin films was performed by Schütteltest (shake test) with Gram-positive bacteria *Bacillus subtilis* (*B.sub*) (DSMZ 347). The ultrathin hydrogel coated

silicon substrates were sterilized at 120 ºC for 30 min and treated with 15 µL of a diluted suspension of *B.sub* in nutrient solution. After exposure, the coated silicon substrates were incubated in a climate chamber at 25 ºC and 90 % relative humidity for 3 hours. Schütteltest was carried out by shaking the incubated substrates with 1 ml nutrient solution at 20 ºC and 150 rpm for 30 min. Suspensions were extracted every 30 min and transferred into a 96 well plate and the optical density was measured at 612 nm and 37 ºC by using a microplate reader/incubator (GENIOS PRO, Tecan) and photometer Cary 100 (VARIAN). The bacteria growth curve was obtained by optical density. Fluorescence microscopy with 4-chloro-7-nitrobenzofurazon (NBF) as fluorescence dye was used to estimate relatively detection of amino-groups on the PVAm/PAE modified silicon surface. The amino functionalized silicon wafers were immersed into a solution of 0.02 g of NBF in 10 ml ethanol for 10 min. After rinsing intensively with ethanol, the wafers were dried with nitrogen stream. Then the fluorescence dye reacted samples were stored in a dark container before examining the fluorescence microscopy. The measurement was performed with Axioplan Zeiss at an absorption maximum of 495 nm and an emission maximum of 519 nm.

3.3 RESULTS AND DISCUSSION

The crosslinked hydrogel film was prepared by plasma treatment of the silicon oxide followed by dip coating into aqueous solutions of PVAm (0.01M) and PAE (0.1 wt%). X-ray photoelectron spectroscopy (XPS) was used to study the thin film formation. Figure 2 illustrates the chemical surface composition by the presence of Si 2s, Si 2p, C 1s, O 1s, and N 1s peaks in the XPS spectra. Oxygen plasma treatment of the silicon surface induces an oxidation process, which generates an oxide layer and thus, a negatively charged surface. Figure 2(b) shows an increase in intensity of the O 1s peak compared to the untreated surface demonstrating successful oxidation of the surface. In addition, the intensity of C 1s the peak decreases, which might be related to decontamination of the surface. The plasma treated silicon wafer was immediately modified with PVAm by dip coating followed by rinsing and dip coating in a PAE solution for crosslinking. For the PVAm modified substrate an increase in C 1s intensity and the appearance of a N 1s signal was observed by XPS proving the presence of PVAm on the surface. Furthermore, a high resolution spectrum is collected in the emission energy range of C atoms to differentiate between the chemical bonding of C-C, C-H, C-O, and C-N. The collected data ensure that the O_2 etching increases the C-O emission peak (see Figure 1(b)). After surface functionalization with PVAm, a C-N signal (c) appears in the spectrum indicating the presence of the primary amine moieties of PVAm on the plasma oxidized silicon surface. Finally, after crosslinking with the reactive PAE polymer, the intensity of the N 1s peak in XPS and the C-O in the high resolution spectrum (see Figure 1(d)) revealed even higher intensity than the PVAm functionalized silicon surface indicating the presence of PAE on the surface.

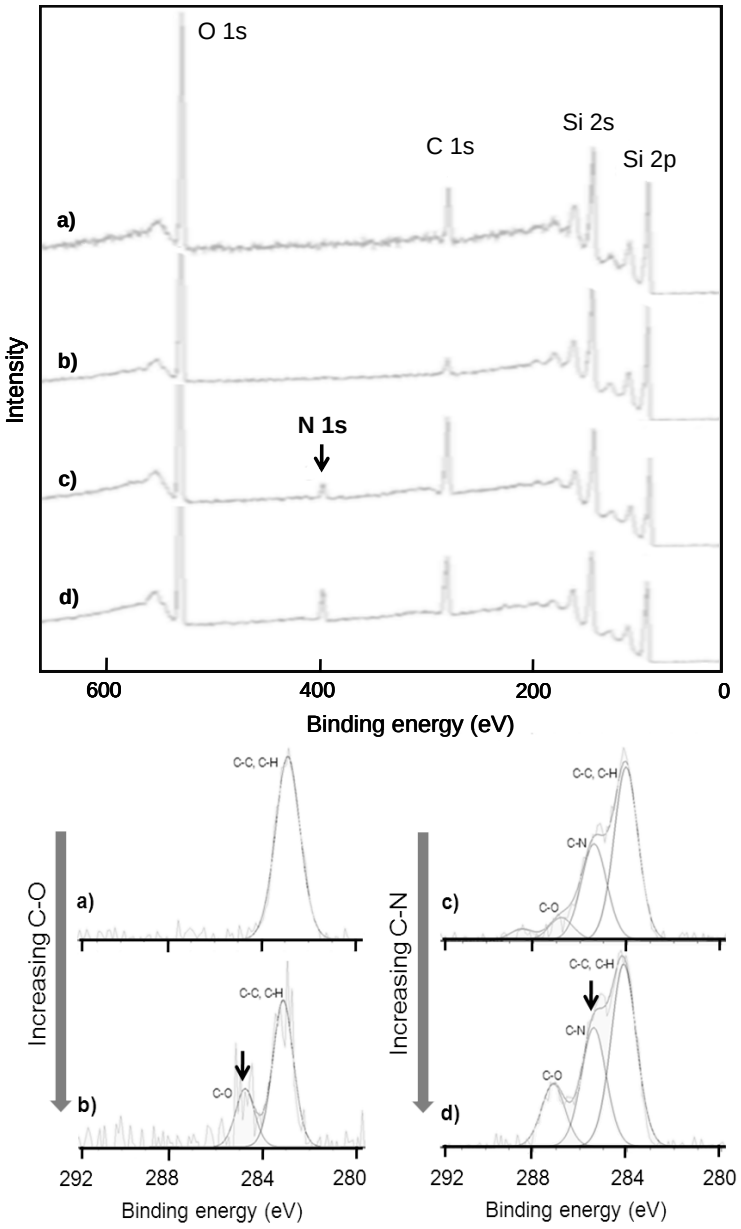

Figure 1. XPS spectra and high-resolution carbon scans for (a) control silicon oxide surface, (b) O2 plasma activated silicon oxide surface, (c) silicon oxide surface with PVAm (0.01M) and (d) silicon oxide surface sequentially modified with PVAm (0.01M) and PAE (0.1 wt%).

The thickness of the assembled ultrathin films was evaluated by ellipsometry measurements. The concentration of both the PVAm and PAE dip coating solutions was varied to fabricate films of different thickness. Figure 2 shows the increase in films thickness with increasing of both PVAm and PAE concentration. In general, increasing the concentration of PAE results in thicker hydrogel layers as expected. Strikingly, the observed trend with increasing

concentration of PVAm is not affected by the PAE concentration indicating that the initial PVAm absorption directs the formation of the crosslinked films. When increasing the PVAm concentration from 0 to 10 mmol, the thickness of the hydrogel layers linearly increases demonstrating a higher surface coverage. Further increasing the PVAm concentration to 50 mmol does not result in an increase in hydrogel thickness indicating full surface coverage. The thicker hydrogel layers obtained at 100 mmol PVAm might be due to further PVAm adsorption by intermolecular amine interactions driven by the higher concentration.

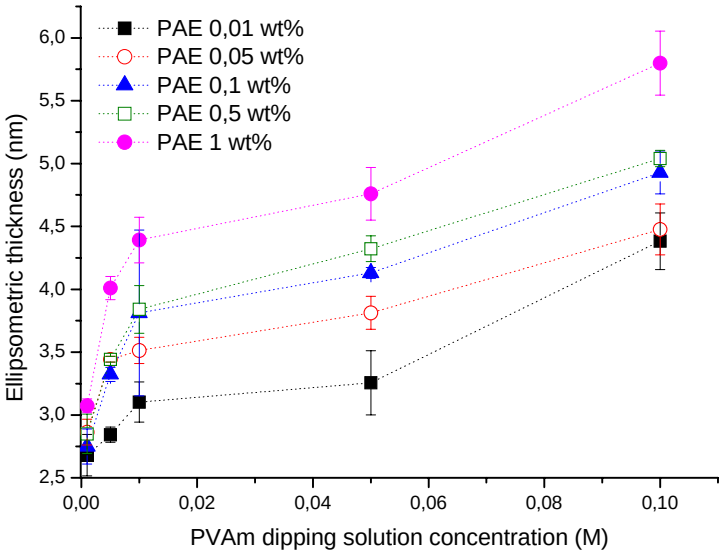

Figure 2. Ellipsometric thickness of PVAm/PAE ultrathin films on plasma oxidized silicon surface depends on dipping solution concentrations

Even though all previously discussed results demonstrated the formation of a thin hydrogel layer on the plasma etched silicon oxide, they did not prove efficient crosslinking by the azetidinium-amine click reaction since the formation of a hydrogel layer might also be due to only adsorption. To unambiguously prove efficient crosslinking, the swelling behavior was investigated since non-crosslinked films would dissolve during the swelling experiments.

The thickness of the films before and after swelling was measured by ellipsometry and the topology was monitored by atomic force microscopy (AFM). Both ellipsometry and AFM

clearly revealed swelling of the films in water proving efficient crosslinking by the azetidinium-amine clicking reaction (Figure 3). The AFM images of the dry ultrathin films show the presence of hydrogel domains that expand in all directions upon absorption of water. The higher concentration of PVAm (0.1M) during dip coating resulted in the formation of larger hydrogel domains as well as a more continuous hydrogel layer compared to 0.01M PVAm (Figure 3)

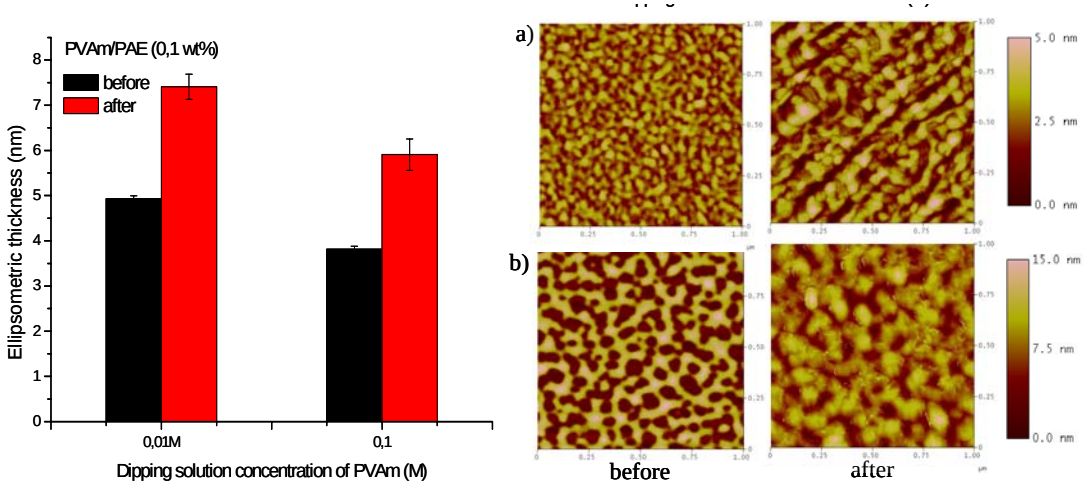

Figure 3. Swelling behavior of PVAm/PAE ultra thin hydrogel films on plasma oxidized silicon oxide surface before and after dipping in mili-Q water for 24 hours in dependence on the crosslinking amount of PVAm and PAE determined by ellipsometry measurement and tapping mode AFM topographies of drying and swelling stautes of hydrogel films: scan size is 1×1 μm^2 and z-ranges are 5 nm for (a) 0.01 M PVAm/ 0.1 wt% PAE and 15nm for (b) 0.1 M PVAm/0.1 wt% PAE.

Ellipsometry demonstrated that the dry hydrogel formed with higher PVAm concentration (0.1 M) is thicker than the film prepared with lower concentration (0.01 M PVAm). However, the absolute increase in thickness upon swelling is similar for both films, namely ~ 2 nm, which is most likely due to a similar crosslinking density since the concentration of PAE was constant.

As potential application of the reported hydrogel surface modification, antimicrobial tests were performed with Gram-positive bacteria *Bacillus subtilis* (*B.sub*). The physico-chemical principles by which antimicrobial peptides adhere to the cell envelope of bacteria to destroy its integrity can be mimicked by the use of amphiphilic cationic macro-molecules[39,40] As such, hydrophobically modified PEI and PVAm as well as cationically charged surfaces are known to kill bacteria.[41,45] Antimicrobial activity of our coating system is thus anticipated based on the partially positively charged free primary groups ($-NH_3^+$) that did not react with azetidinium groups. In addition, tertiary amine groups are formed by the ring-opening reaction between azetidinium and amines, which are easily protonated and might exhibit antimicrobial activity too. Therefore, we have investigated the gram positive antibacterial activity of the PVAm/PAE hydrogels (see Figure 4). The growth of bacteria was observed by measuring optical density at 612 nm for 20 hours. The hydrogel films indeed showed antimicrobial activity by inhibiting bacteria growth for 650 min in contrast to the control and amine coated silicon wafers that inhibit growth of 200 minutes. The improved antimicrobial activity of the cross-linked coating compared to the PVAm might be due to dissolution of the PVAm coating or due to the presence of the tertiary amine groups. The antimicrobial activity of the coatings might be enhanced activity by chemical modification of the primary amine groups in future work.

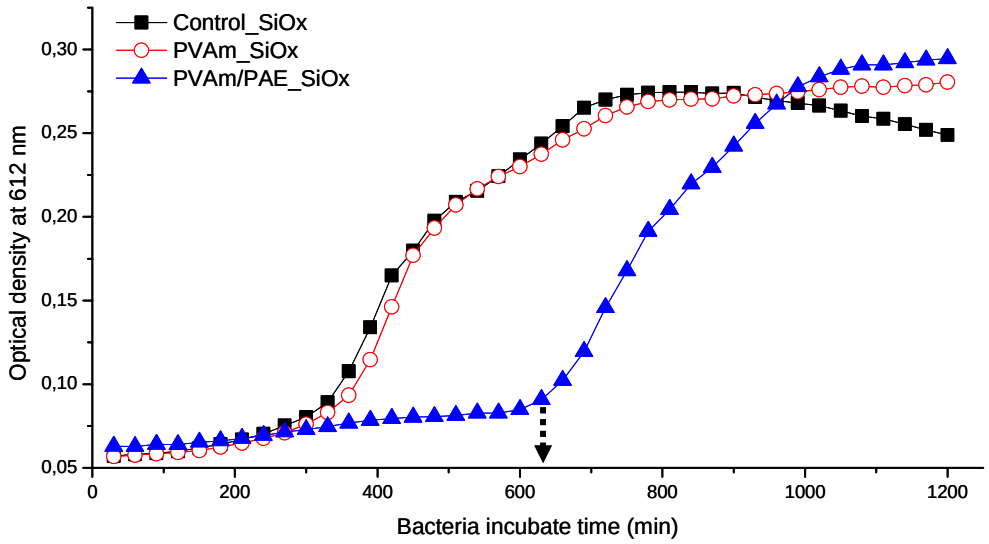

Figure 4. Antimicrobial activity of hydrogel ultrathin 10mM PVAm/0.1 wt%PAE modified silicon oxide surface compared to unmodified and PVAm modified silicon oxide surface recorded on bacteria growth.

After the antimicrobial tests, the hydrogel films were analyzed by AFM measurements to monitor topological changes (Figure 5). The measurements confirmed the stability of the PVAm/PAE hydrogel layer since it was similar to the swellon hydrogel depicted in Figure 3. In contrast, no hydrogel layer was left for the uncrosslinked PVAm layer explaining its lower antimicrobial activity.

Other potential applications of the developed PVAm/PAE crosslinked hydrogel layers are based on further functionalization of the amine groups. To demonstrate the reactivity of the remaining amine groups, the hydrogel was reacted with the fluorescent dye 4-chloro-7-nitrobenzofurazan (NBF), which reacts with primary and secondary amines. The presence of reactive amino groups on the silicon surface is demonstrated by the qualitative increase in fluorescence intensity as shown in Figure 6.

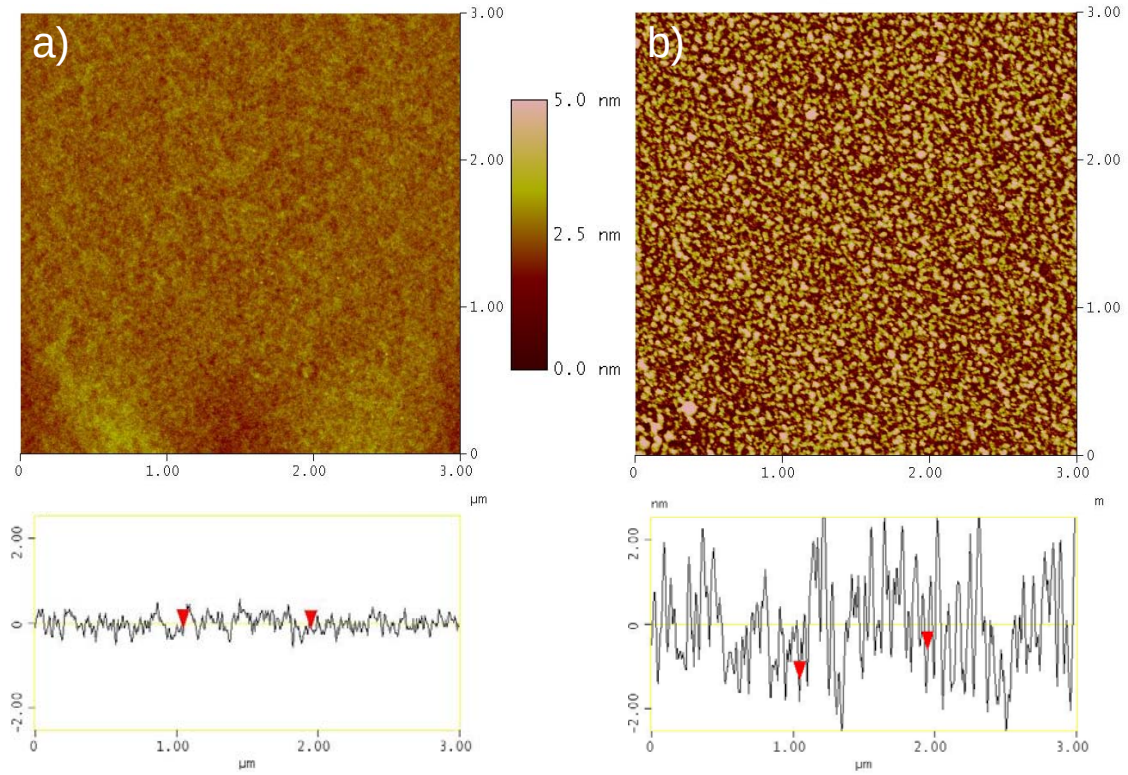

Figure 5. AFM images of a) PVAm monolayer and b) PVAm/PAE ultrathin hydrogel ultrathin film after antimicrobial measurement which is incubated in buffer solution for 24 hours: scan size is 3×3 µm^2 and the z-range is 5 nm.

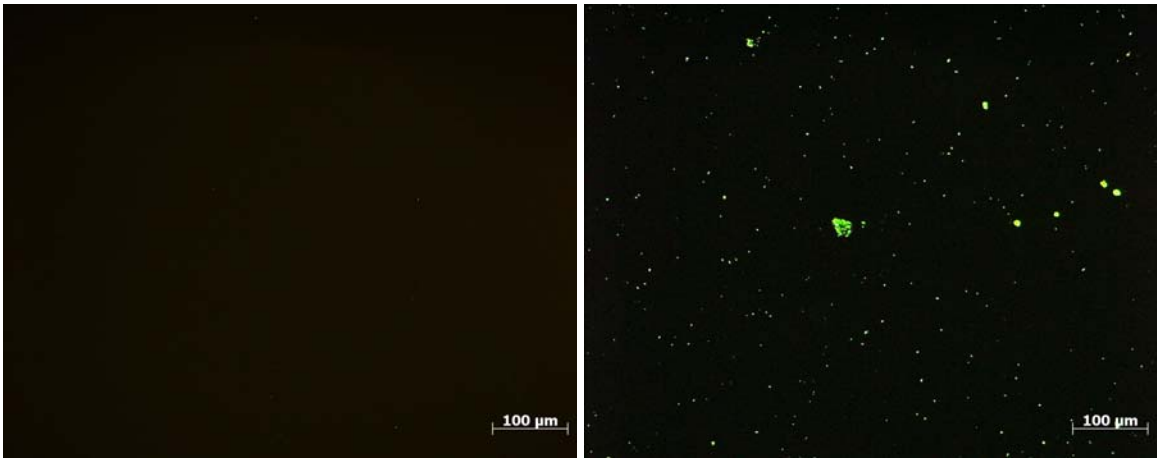

(a) (b)

Figure 6. Amino groups detection with NBF fluorescence dye labeled a) control silicon wafer and b) PVAm/PAE ultrathin hydrogel silicon wafer monitored with fluorescence microscopy

3.4 CONCLUSIONS

In conclusion, we have demonstrated a novel method (primer concept) for the construction of stable cross-linked thin hydrogel films on oxide surfaces. A LBL assembly process was used to fabricate ultrathin films of PVAm/PAE on a plasma oxidized silicon wafer. Crosslinking of the amino groups of polyvinylamine with azetidinium ions of PAE, which can be regarded as a metal free click reaction. As such, the primary amine containing hydrogels were successfully prepared by the use of low cost commercially available materials yielding a stable crosslinked material in a simple, fast and reliable process. The atomic composition of modified silicon wafers during the modification was investigated by XPS analysis, ensuring thin film formation. The swelling behavior of ultrathin hydrogel films revealing efficient crosslinking of PVAm/PAE was determined by ellipsometry. The changes in surface topology during the swelling process were successfully monitored by AFM. Moreover we have shown the potential of our thin films as antimicrobial material and we demonstrated the presence of primary amine groups for further functionalization. Further research efforts to develop antibacterial coatings based on modified PVAm/PAE hydrogel coatings, are ongoing in our laboratory.

3.5 REFERENCES

M2 Reproduced with permission from Yu, M.; Hoogenboom, R.; Thomas, H.; Moeller, M. *manuscript in preparation.*

[1] Voigt, I.; Simon, F.; Komber, H.; Jacobasch, H.-J.; Spange, S. *Colloid Interface Sci.* **2000**, 278, 48.

[2] Voigt, I.; Simon, F.; Estel, K.; Spange, S. *Langmuir* **2001**, 17, 3080.

[3] Diflavio, J.; Bertoia, R.; Pelton, R.; Leduc, M. *13th Fundamental research symposium*, Cambridge, **2005** 1293.

[4] Decher, G.; Maclennan, J.; Reibel, J.; Sohling, U. *Adv. Mater.* **1991**, 3, 617.

[5] Decher, G.; Lvov, Y.; Schmitt, J.*Thin Solid Films* **1994**, 244, 772.

[6] Reska, A.; Gasteier, P.; Schulter, P.; Moeller, M.; Offenhäusser, A; Groll, J. *Adv. Mater.* **2008**, 9999, 1.

[7] Wei, Z.; Wang, C.; Zhu, C.; Zhou, C.; Xu, B.; Bai, C. *Surface Sci.* **2000**, 459, 401.

[8] Song, X.; Zhai, J.; Wang, Y.; Jiang, L. *J. Colloid Interface Sci.* **2006**, 298, 267.

[9] Gao, J.; Chan-Park, B. *Surface Coatings Tech.* **2005**, 194, 244.

[10] Garbassi, F.; Occhiello, E. *Polymeric Mat.Encyclopedia* **1996**, 1.

[11] Garbassi, F.; Morran, M.; Occhiello, E. in *Polymer surface from Physics to Technology*, John Wiley& Sons, New York, **1994**.

[12] Goel, V.; Beginn, U.; Mourran, A.; Moeller, M. *Macromolecules* **2008**, 41, 8187.

[13] Calvet, J.; Grafahrend, D.; Klee, D.; M. Moeller, *J Mater Sci: Mater Med* **2008**, 19, 1631

[14] Kurth, D.G.; Bein, T. *Langmuir* **1993**, 9, 2965.

[15] Kurth, D.G.; Bein, T. *Langmuir* **1995**, 11, 2965.

[16] Vaidya, A.A.; Norton, M.L. *Langmuir* **2004**, 20, 11100.

[17] Heiney, P.A.; Grüneberg, K.; Fang, J.; Dulcey, C.; Shashidhar, R. *Langmuir* **2000**, 16,2651.

[18] Decher, G. *Science* **1997**, 277, 1232.

[19] Decher, G.; Hong, J.; Schmitt, J. D. *J. Macrol. Chem. Macromol. Symp.***1991**, 46, 321.

[20] Rubner, M.F.; Stockton, W.B. *Macromolecules* **1997**, 30, 2717.

[21] Bucatariu, F.; Simon, F.; Spange, S.; Schwarz, S.; Drgan, S. *Macromol. Symp.* **2004**, 210, 219.

[22] Kolb, H. C.; Finn M. G.; Sharpless, K. B. *Angwe. Chem. Int. Ed.***2001**, 40, 2004.

[23] Kolb, H. C.; Sharpless, K. B. *Drug Discovery Today* **2003**, 8, 1128.

[24] Buck, M. E.; Zhang, J.; Lynn, D. M. *Adv. Mater* **2007**, 19, 3951.

[25] Devaraj, N.K.; Miller, G.P.; Ebina, W.; Kakaradov, B.; Collaman, J.P.; Kool, E.T.; Chidsey, C.E.D. *J. Am. Chem. Soc.* **2005**, 127, 8600.

[26] Such, G.K.; Quinn, J.F.; Quinn, A.; Tjipto, E.; Caruso, F. *J. Am. Chem. Soc.* **2006**, 128, 9318.

[27] Tsai, H. A.; Moschou, E.A.; Daunert, S.; Madou, M.; Kulinsky, L. *Adv. Mater* **2009**, 21, 656.

[28] Lee, B.K.; Lee, H.Y.; Kim, P.; Suh, K.Y.; Seo, J.H.; Cha, H.J.; Kawai, T. *small* **2008**, 4, 342.

[29] Couty, F.; David, O.; Drouillat, B. *Tetrahedron Lett.***200**7, 48, 1027.

[30] Couty, F.; David, Drouillat, O. B. *Tetrahedron Lett.***200**7, 48, 9180.

[31] Obokata, T.; Isogai, A. *J. Appl. Polym. Sci.***2004**, 92, 1847.

[32] Obokata, T.; Yanagisawa, M. *J. Appl. Polym. Sci.* **2005**, 97, 2249.

[33] Obokata, T.; Isogai, A. *Colloids Surfaces A: Physicochem. Eng. Aspects* **2007**, 302,525.

[34] Serizawa, T.; Yamamoto, K.; Akashi, M. *Lanmuir* **1999**, 15, 4682.

[35] Yamamoto, K.; Serizawa, T; Muraoka,Y.; Akashi, M. *Macromoleules* **2001**, 34, 8014.

[36] Serizawa, T.; Kawanishi, N.; Akashi, M. *Macromoleules* **2003**, 36, 1967.

[37] Serizawa, T.; Wang, Z.; Tateishi, T.; Akashi, M. *Polymer J.* **2004**, 36, 54.

[38] Barbucci, R.; Magnani, A.; Consumi, M. *Macromolecules* **2000**, 33,7475

[39] Pasquier, N.; Keul, H.; Heine, E.; Moeller, M. *Biomacromolecules* **2007**, 8, 2874.

[40] Pasquier, N.; Keul, H.; Heine, E.; Moeller, M. *Macromol. Biosci.***2008**, 8, 903.

[41] Haldar, J.; An, D.; Cienfuegos, L.; Chen, J.; Klibanov, A. *Proc. Natl. Acad. Sci.* **2006**, 103, 17667.

[42] Anderson, N. J.; Blesing, N.V.; Bolto, B. A.; Jackson, M. B. *React. Polym.* **1987**, 7, 47.

[43] Serizawa, T.; Matsukuma, D.; Akashi, M. *Langmuir* **2005**, 21, 7739.

[44] Mohammadi, Z.; Cole, A.; Berkland, C. J. *J. Phys. Chem. C* **2009**, 1113, 7652.

[45] Westman, E.; Ek, M.; Enarsson, L.; Wågberg, L. *Biomacomolecules* **2009**, 10, 1478.

[46] Lutz, J. F. *Angew. Chem. Int. Ed.* **2008**, 47, 2182.

[47] Becer, C. R.; Hoogenboom,R.; Schubert, U. S. *Angew. Chem. Int. Ed.* **2009**, 48, 4900.

CHAPTER 4

ULTRATHIN HYDROGEL COATING TO ENHANE SHRNKIPROOFING OF PLASMA TREATED WOOL [M3]

ABSTRACT

The combination of plasma treatment and hydrogel coating is introduced as a new concept for shrinkproofing of wool top. The effects of plasma and polymer coating on the felting properties of wool tops were investigated. Pre-treatment of wool tops was performed to introduce anionic and hydrophilic groups by surface oxidation. Subsequently, ultrathin hydrogel films could be easily prepared by dip-coating with poly(vinylamine) (PVAm) and poly(amideamine epichlorohydrin) (PAE) from aqueous solution. The resulting self-assembled films are cross-linked by reaction between the azetidinium groups of PAE with the amine groups of polyamines resulting in a stable cross-linked hydrogel layer on the plasma treated fiber surface. It is demonstrated that this treatment provides excellent adhesion between hydrogel films and wool, which leads to enhanced shrinkproofing. To estimate the thickness of the deposited hydrogel film thickness on fiber surface, the thickness of a similar hydrogel (PVAm/PAE) prepared on oxygen plasma treated silicon oxide as a model surface was determined by ellipsometry. The thickness of the layer is correlated with the concentration and molecular weight of PVAm. The chemical composition of the surfaces was characterized by X-ray photoelectron spectroscopy (XPS). Furthermore, the moisture sorption of hydrogel coated wool was investigated by Isothermal Gravimetric Analysis (IGAsorp) demonstrating the enhanced swelling ability of hydrogel coated wool fibers. The morphology

of the hydrogel coated wool top was determined by scanning electron microscopy (SEM) revealing the deposition of an ultrathin hydrogel layer on the plasma treated fiber surface.

4.1 INTRODUCTION

A wool fiber has a complex histological structure and chemical composition i) an outer layer of cuticle cells, that represent about 10 % of weight of the fiber, consisting of three layers (epicuticle, exocuticle, and endocuticle) and ii) an inner layer of cortical cells that correspond to about 90 % of mass of the fiber and is based on the ortho- and the para cotex.[1-4] The hydrophobic nature and scale structure of the wool fiber surface is responsible for the felting behavior of wool.[1-5] The hydrophobicity of the wool fiber results from the fatty acid layer (predominantly 18-methyleicosanoic acid) covalently fixed to the surface of the cuticle cells.[5,6] The unique scale structure of wool comprises asymmetric edges pointing towards the tip and root of the fiber. This induces a defferential friction effect in the with- and against-scale direction being responsible for an unidirectional fiber movement towards the tip of the fiber during agitation in water. This results in an entanglement of the individual fibers, the felting of wool. (Figure 1, left)

The mechanism of wool shrinkproofing is complicated and not fully understood so that practical improvements of industrial processes and scientific theory are not always consistent.1 Mostly, the prevention of felting is accomplished by destroying and/or masking of the scale structure. (Figure 1, right). For conventional shrinkproofing of wool on top stage, the wool fibers are pre-treated with chlorine and subsequently reacted with Hercosett resin (poly(amideamine epichlorohydrin) (PAE)), the so called Chlorine-Hercosett process.[7-10] However, the severe disadvantage of this process is the resulting effluent load with absorbable organic chlorides (AOX), which discharges are restricted by legislation. To reduce the overall

effluent load with AOX environmentally friendlier (chlorine-free) processes have been developed.[11-30]

Alternatives to substitute the chlorination stage are low temperature plasma[15-23, 40-41] and enzyme treatments[24-27] as well as the application of polymers.[28-30] It is well-established that low temperature plasmas at reduced or atmospheric pressure oxidize the cystine (sulfur) to cysteic acid and the outermost hydrophobic lipid layer. Thus, the plasma-induced oxidation of wool introduces anionic charges into the surface thus providing a hydrophilic character to the fiber.[15, 17] An enzymatic pretreatment with proteases also imparts hydrophilicity, due to digesting proteins into amino acids and smaller peptides.[25] Especially the combination of processes that enhance fiber hydrophilicity and coating with natural polymers, as chitosan or collagen, resulted in effective reduction of wool felting.[28,31-32] The most effective treatment was obtained by the application of polyurethane-prepolymers. However except the polyurethane-finishing of plasma-treated wool top all other alternative procedures do not meet the shrinkproofing level of a Chlorine-Hercosett treated wool.

Importantly, Makinson *et al.* proposed a mechanism for the anti-felting properties of the Chlorine-Hercosett treatment. Apart from the effect of chlorination the Hercosett film on the fibre surface was supposed to increase the shrinkproofing effect. This was related to a masking of the cuticle scales which was supposed to be most effective in water due to the swelling of the Hercosett film.[33-34, 36]

Therefore, we have investigated the formation of a stable cross-linked hydrogel films for improving the shrinkproofing effect of plasma treated wool fibers. In this work, we have developed a finishing procedure for plasma treated top at atmospheric conditions based on the application of a thin hydrogel film covalently cross-linked by the reaction of primary amino groups in poly(vinylamine) (PVAm) with the azetidinium ions of poly(amideamine-epichlorohydrin) (PAE). The thickness and swelling behavior of PVAm/PAE model films on silicon oxide surface was previously reported demonstrating the feasibility of this approach.[39]

The chemical composition of PVAm/PAE hydrogel coated wool was determined by X-ray photoelectron spectroscopy (XPS). In addition, we evaluated the felting density by Aachen felting test (IWTO-20-69) and the moisture adsorption and swelling behaviour by isothermal gravimetric analysis. Furthermore, scanning electron microscopy (SEM) was performed to investigate the morphology of the hydrogel coated wool fibers.

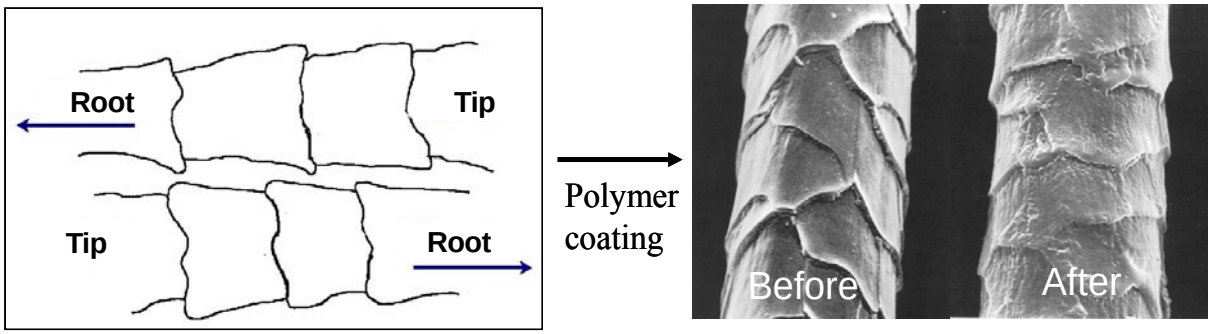

Figure 1. Illustration of the different direction of the structure of wool, which induces friction and entanglement of fibers resulting in the dense felt formation (left) and deposition of a coating to reduce the differential friction effect resulting in producing shrink-resistant wool.

4.2 EXPERIMENTAL PART

Materials

Wool top with a fiber thickness of 23 µm was obtained from Richter FA, Stadteppendorf. Poly(vinylamine) (PVAm) was kindly provided by BASF. PVAm is based on ~90% hydrolyzed poly(*N*-vinylformamide) with a molecular weight of 340.000 g/mol (Lupamin 9095). Commercially available polyamideamine-epichlorohydrin (PAE) (RIBAMID® C4948T, SI group) was purchased and has average molecular weight of 269.000 g/mol. Distilled water was used as the solvent for all experiments.

Low temperature plasma treatment of wool

Atmospheric low temperature plasma treatment of wool was carried out by Richter FA. The plasma treatment was performed using Richter-specific conditions.

Ultra thin coating on the plasma treated wool

Solutions of PVAm and PAE were prepared from 0.5 wt% and adjusted pH value. Plasma pre-treated wool tops were dipped into PVAm aqueous polymer solution (0.5 wt%, pH 6) followed by dipping into a PAE aqueous solution (0.5 wt%, pH 9) in water. Furthermore, prereacted of PVAm/PAE was applied to modify wool fiber surface. Finishing of the wool was performed by dipping in demineralised water and padding with 2 rolled padder machine. Between the different dipping stages, extensive washing was performed to remove excess ion polymer. The resulting samples were cured at 100 °C for 10 min and then were dried at 50°C for 4 hours in an oven. The dried wool samples were kept at the standard conditions (relative humidity 65 % , temperature 20 °C)

Characterization of hydrogel coated wool

The chemical composition of the hydrogel films on the plasma treated wool was measured by X-ray photoelectron spectroscopy (XPS) at room temperature using an Ultra Axis^{TM} Spectrometer from Kratos analytical (UK). The elements of the wool fiber surface were excited with monoenergetic Aluminium K1,2 irradiation with an energy of 1486.6 eV and a power source of 150 W. The water sorption behavior of the hydrogel coated wool fibers was measured with Isothermal Gravimetric Analysis (IGAsorp, HIDEN ISOCHEMA) as function of the relative humidity between 0 % and 95 %. Before the absorption measurement, the samples were conditioned in the chamber at 25 ºC and 0 % RH.

The shrink-resistant properties of untreated and hydrogel treated samples was performed according to IWTO 20-69 test method (Aachen felting test). One gram of loose ball formed

wool was shaken for 60 min with 50 ml of a pH 7 buffer solution in a standard container on a shaking machine with three dimensional movements. The loose ball was transformed into a dense felting ball. In order to obtain the felting density, the diameter of the felting ball before and after the process was measured. For each sample of wool the average felting density of 2 balls was determined.

4-chloro-7-nitrobenzofurazan (NBF) as reactive fluorescence dye was used to demonstrate the presence of reactive amino-groups on the PVAm/PAE modified wool surface by Fluorescence microscopy. The amino functionalized wool fibers were immersed into a solution of 0.02g of NBF in10ml ethanol for 10 min and then the samples were rinsed intensively with ethanol. The measurement was performed with an Axioplan Zeiss confocal microscope at an absorption maximum of 495 nm and an emission maximum of 519 nm. The images were processed with Axiovison software.

The morphology of the hydrogel coated wool fibers was investigated by scanning electron microscopy (SEM, Carl Zeiss, S 360) and field-emission scanning electron microscopy (FE-SEM, S-4800, HITACHI).

4.3 Results and Discussion

To develop a concept for hydrogel coating of plasma treated wool, we have adapted the hydrogel thin film formation process previously applied for hydrogel modification of silicon oxide surfaces.[39] Extension of this concept to wool fibers is schematically depicted in Figure 2: the wool fibers are first oxidized by plasma treatment at atmospheric conditions and the PVAm will be directly applied by dipcoating on the anionically charged wool fiber surface by electrostatic interaction between positively charged PVAm and negatively charged wool. Subsequently, the crosslinking reaction of amine modified wool fibers will be carried out by dipping into aqueous PAE solution. The reaction of the primary amino groups of PVAm and azetidinium ions of PAE using dip-coating method results in the formation of an ultra thin hydrogel layer on the plasma treated wool fibers. Plasma treatment is used to oxidize the fiber surface similar to the chlorination process. This treatment of wool results in an increase in hydrophilicity ensuring good wetting of the surface being essential for continuous film formation.

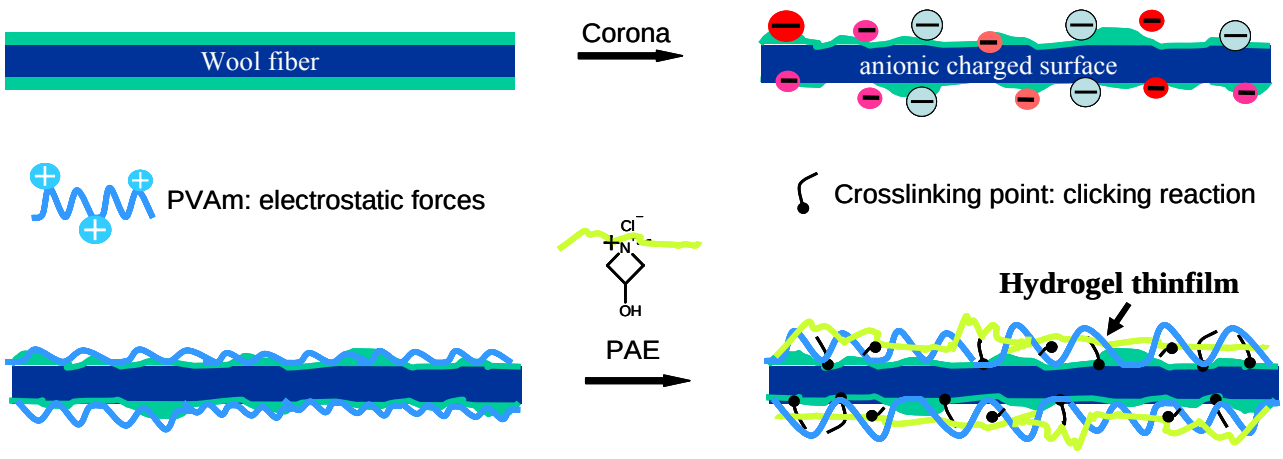

Figure 2. Schematic representation of the fabrication of crosslinked hydrogel ultrathin films on the wool fibers by reaction of primary amine groups from poly(vinylamine)(PVAm) and azetidinium groups from poly(amideamine-epichlorohydrin)(PAE).

The chemical composition of the surfaces of plasma, PVAm and PVAm/PAE treated wool fibers surface were investigated by X-ray photoelectron spectroscopy (XPS), as shown in Table 1. As expected, the PVAm/PAE modified wool surface shows an increased carbon and nitrogen content. This can be related to the presence of nitrogen containing polymers as coating on the wool surface clearly demonstrating that indeed the polymers were coated onto the wool fibers. Furthermore, the thicknesses of polymers coating were estimated from model hydrogels on silicon oxide surfaces. We have observed that the thicknesses of PVAm and PVAm/PAE were 0.62 nm and 1.12 nm.[39] Therefore, we have assumed that similar ultrathin films of PVAm/PAE were deposited on the wool surface.

Table 1. Relative amounts of carbon, oxygen, sulfur and nitrogen of PVAm (0.5 %, Mw 340.000 g/mol) and PVAm/PAE (0.25 %, Mw 269.000 g/mol) on the plasma treated wool samples as determined by XPS corelated to the thickness of model films on silicon oxide determined by ellipsometry.[39]

coated sample on wool top	Surface atomic composition (%)				Model surface thickness of modified silicon wafer (nm)
	carbon	oxygen	sulfur	nitrogen	
plasma	80.66	13.62	0.61	2.01	2,53 ± 0,05
plasma / PVAm	80.56	13.29	0.51	2.67	3,15 ± 0,02 (**0,62**)
plasma /PVAm/PAE	83.75	11.28	0.46	3.39	3,65 ± 0,2 (**1,12**)

Behavior of hydrogel modified wool fibers was tested according to the Aachen felting test as shown in Figure 3. The felting density of plasma treated wool compared to the control remarkably decreased from 0.152 (Figure 3 and 4 (a)) to 0.072 g/cm^3 (Figure 3 and 4 (b)) which might be ascribed to the presence of ionic groups that repel each other. PVAm (0.5 wt%, pH 6) treated wool results a felting density (Figure 3 and 4 (c)) which shows better

shrinkproofing behavior than PAE (0.5 wt%, pH 9) monolayer treated wool (Figure 3 and 4 (d)). Moreover, the results of the PVAm (0.5 wt%, pH 6) / PAE (0.5 wt%, pH 9) coated wool fibers demonstrate that the ultra coating is capable of further enhancing anti-felting properties in wool top. It is evident that the deposition of a hydrogel from PVAm/PAE applied in two steps shows more pronounced effect on the felting behavior of plasma oxidized wool surface (Figure 3 and 4 (e)). The blend of PVAm and PAE was applied onto plasma treated wool and results in a similar shrinkproofing level (Figure 3 and 4 (f)) indicating the efficiency of the treatment. The previous work on PVAm/PAE hydrogel coating of the silicon oxide has proved the different swelling behavior by applying different crosslinking density, thus, the hydrogel film is able to absorb a larger amount of water when the crosslinking density is lower.[39] As a result of the increased swelling of the films, the shrinkproofing is more effective for smaller PAE concentration.[40] For the Chlorine-Hercosett process, it was reported that the polymer coating must have at least a film thickness of 0.5 μm for effective shrinkproofing and the resin layer swells nearly five times in water.[33, 34] In present work, we have achieved effective shrinkproofing of wool fibers with ultrathin hydrogel films of 1.2 nm thickness and a swelling degree of up to 450% as determined for a model hydrogel coating on plasma treated silicon oxide.[39] This is obviously shown a significant improvement of the felting behavior of plasma treated wool top. In Figure 4, a picture of the resulting felting balls shows the different diameters after Aachen felting test. This picture clearly demonstrates the strong influence of the PVAm/PAE treatment on the feling behavior of wool.

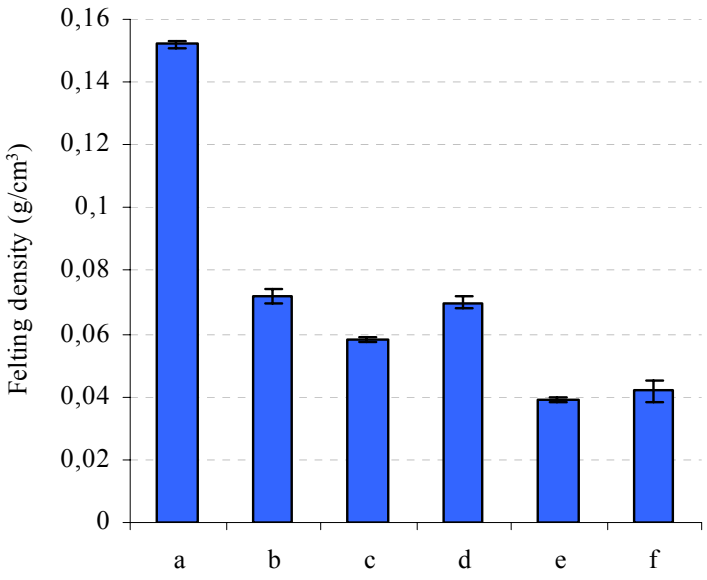

Figure 3. Felting density of the different treatments (a) control, (b) plasma treated, (c) plasma-PVAm (0.5 wt%, pH 6) treated, (d) plasma-PAE (0.5 wt%, pH 9) treated, (e) plasma-(PVAm-PAE) treated and (f) plasma-(PVAm+PAE) treated wool determined according to IWTO 20-69.

Figure 4. Picture of the resulting felting balls (a) control, (b) plasma treated, (c) plasma-PVAm (0.5 wt%, pH 6) treated, (d) plasma-PAE (0.5 wt%, pH 9) treated, (e) plasma-(PVAm-PAE) treated and (f) plasma-(PVAm+PAE) treated wool samples after testing aacording to IWTO 20-69.

With the plasma-induced surface oxidation and the subseqent deposition of a hydrogel layer on the fiber surface chnges in the water uptake by the fibers were expected. Therefore, the moisture absorption behavior of modified wool samples were measured at a given relative humidity (RH) and temperature by IGAsorp. The amount of water absorption depends on the relative humidity of the air, temperature, and history of the fibers.[35] The sorption and desorption curves of wool fibers show a hysteresis (Figure 5 (a)). Chemical and physical modification of wool may change its sorption behavior. The main effect of chemical treatment, which cleaves disulfide and pepide bonds, is an increase in the equilibrium water content (e.w.c.) at high relative humidity.[2] When the relative humidity reaches 95%, the e.w.c. of the control, Chlorine-PAE and plasma-hydrogel treated samples show different values and hysteresis between adsorption and desorption. The plasma-hydrogel coated wool achieved the highest e.w.c. (23%) compared to the control (16%) and Chlorine-PAE (21%). At high relative humidity, the e.w.c. of the hydrogel coated fibers increases. The kinetics of moisture uptake revealed a the shorter time for the polymer coated wool to reach the e.w.c. at a relative humidity of 95 % as shown in Figure 5 (b). The control wool requires 1123 min at 95% while the plasma-hydrogel treated sample needs only 575 min at 95%. The moisture diffusion speeds of control and polymer coated wool showed clearly differences as indicated by the slope of the moisture uptake: for the control wool 0.016, the chlorine-PAE treated wool 0,039 and the plasma-hydrogel treated wool 0,049. The hydrogel coated wool fibers absorb moisture 3.1 times faster than the control sample. Therefore, the hydrogel layer supports the fast diffusion of water molecules to the wool fiber and improves the shrinkproofing of wool fiber due to the presence of a swollen polymer layer.

The presence of free amino groups for potential further modification of the PVAm/PAE coated wool was investigated by selective labeling with a fluorescence dye to PVAm/PAE. The non-fluorescent 4-chloro-7-nitrobenzofurazan (NBF) reacts with primary and secondary amines resulting in formation of luorescent amino-7-nitrobenzofurazan. The fluorescence

images shown in Figure 6 (b) indicate an increasing fluorescence intensity for the hydrogel coated wool compared to control wool surface after treatment with NBF. This result clearly demonstrates that the plasma treated fiber surface was successfully modified by hydrogel which still contains amino groups that can be used for further functionalization.

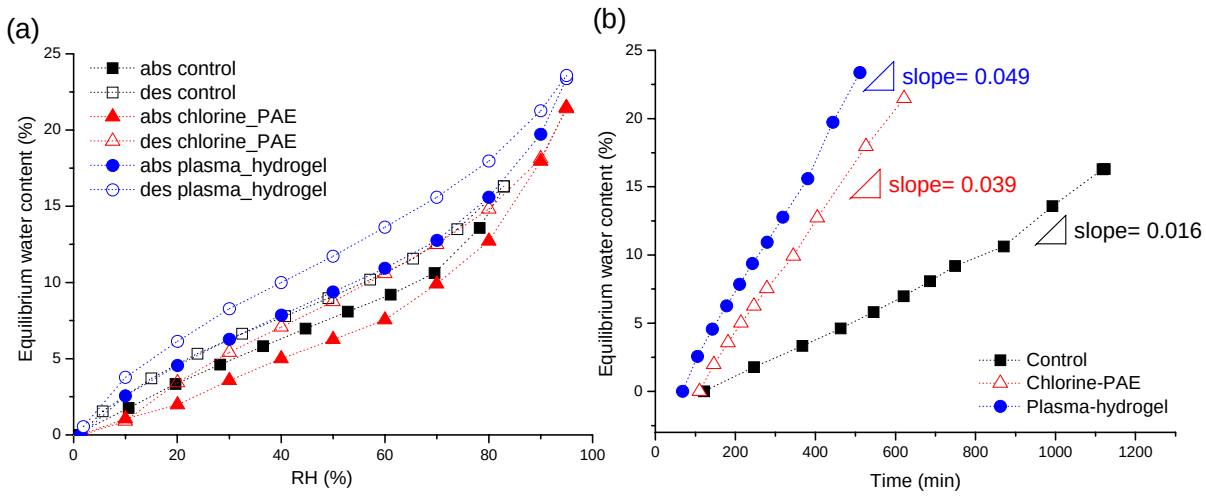

Figure 5. The equilibrium water content (a) and the kinetic of moisture absorbance (b) of control, chlorine-PAE and plasma-hydrogel (PVAm/PAE) modified wool tops monitoring by IGAsorp measurement.

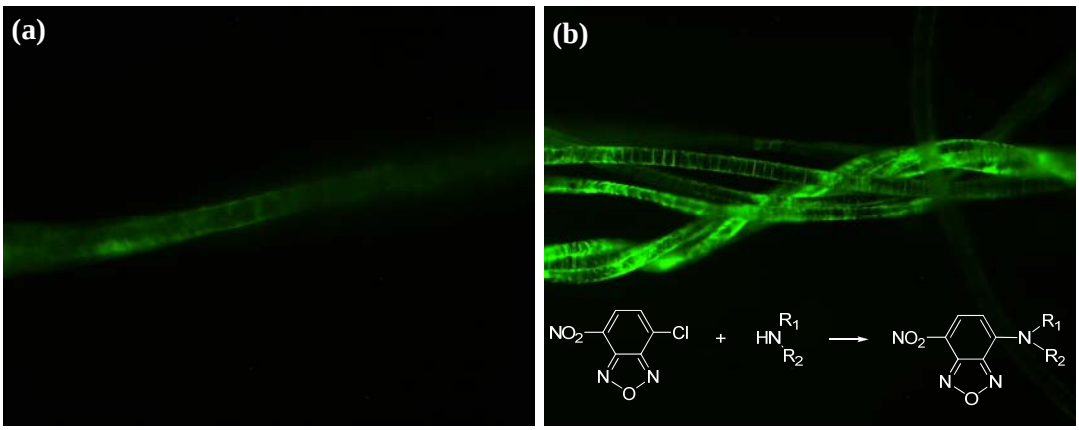

Figure 6. Fluorescence micrographs of NBF labeling of a) control wool and b) PVAm/PAE treated wool indicating the presence of reactive amino groups.

Scanning electron micrographs of the wool fibers are depicted in Figure 7 revealing the typical scale structure of wool consisting of flattened overlapping cells. After the plasma treatment, the wool surface is not significantly changed. This also counts upon treatment with PVAm or PVA/PAE, which might be expected for the ultrathin hydrogel coating with 1.2 nm thickness. As such, it can be concluded the topography of the fiber surface is not noticably changed by the different treatement stages.

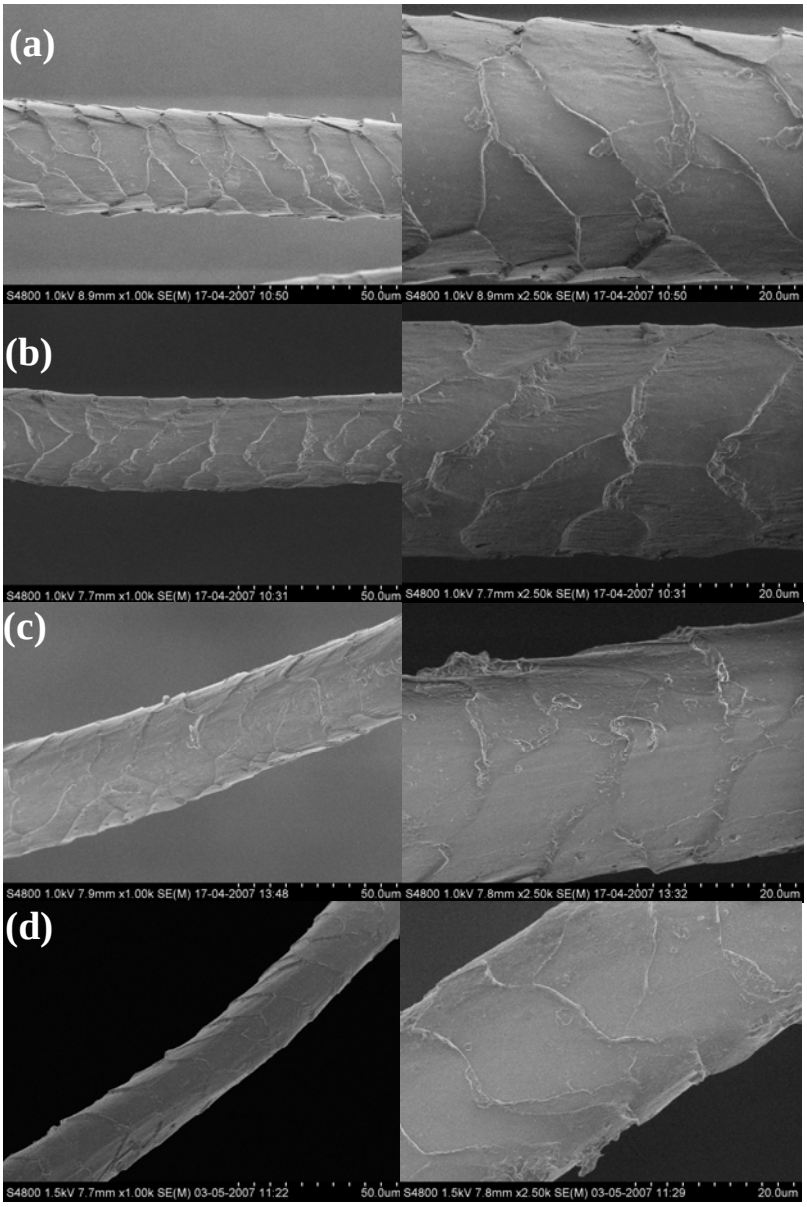

Figure 7. SEM images of PVAm and PAE coating on plasma treated wool. (a) control, (b) plasma treated, (c) PVAm (0.5 wt%, Mw 340.000 g/mol) and (d) PVAm (0.5 wt%, Mw 340.000 g/mol) / PAE (0.25 wt%, Mw 269.000 g/mol).

4.4 CONCLUSIONS

We have developed a new process for shrinkproofing of wool by hydrogel coating. Combination of plasma treatment and the deposition of a crosslinked ultrathin hydrogel layer by dipcoating successfully enhanced the felting resistance of wool. Polycationically charged poly(vinylamine) (PVAm) and poly(amidoamine-epichlorohydrin) (PAE) formed an ultra thin hydrogel film on the plasma treated wool fibers, which was prepared by step-wised polymer deposition and was cross-linked by chemical reaction of the primary amine groups of PVAm and azetidinium groups of PAE. The changes in chemical composition of modified wool were confirmed by XPS revealing increased nitrogen content of the wool surface. Importantly, the hydrophilic hydrogel layer on wool surfaces provided good shrinkproofing by high swellability of the ultra thin film, which ensures that fibers have no direct contact during washing and thus, reduces the differential frictional effect. Furthermore, the results of fluorescence dye labeling of primary and secondary amino groups indicates the presence of reactive amino groups within the hydrogel layer. This opens up the possibility of further modification of the polymer layer, e.g. for imparting further functionalities.

4.5 REFERENCES

M3 Reproduced with permission from Yu, M.; Hoogenboom, R.; Thomas, H.; Moeller, M. *manuscript in preparation.*

[1] Makinson, K. R. *Shrinkproofing of wool*, Marcel Dekker INC.: New York, **1979**.

[2] Maclaren, J. A.; Milligan, B. *Wool science: the chemical reactivity of the wool fibre,* Science Press: Australia, **1981**.

[3] Roper, K.; Föhles, J.; Peters, D.; Zahn, H. *Textile Research J.* **1984**, 54, 139.

[4] Roper, K.; Föhles, J.; Peters, D.; Zahn, H. *Textile Research J.* **1984**, 54, 262.

[5] Canal, C.; Erra, P.; Molina, R.; Bertrán, E. *Textile Research J.* **2007**, 77, 559.

[6] Dai, X. J.; Elms, F. M.; Gorge, G. A. *J. Appl. Polym. Sci.* **2001**, 80, 1461

[7] Holt, R. R. *J. Soc. Dyers Col.* **1975,** 38, 39

[8] Asquith, R. S.; Gardner, K. L.; Mcgarel, W. S.; Otterburn, M. S. *J. Appl. Polym. Sci.* **1978**, 22, 3267.

[9] Guise, G. B.; Smith, G. C. *J. Appl. Polym. Sci.* **1985**, 30, 4099.

[10] Guise, G. B.; Smith, G. C. *J. Chromatography* **1982**, 235, 365.

[11] De la Maza, A.; Parra, J. L.; Leal, J. S.; Comelles, F. *Textile Research J.* **1989**, 59, 173.

[12] De la Maza, A.; Parra, J. L.; Leal, J. S.; Comelles, F. *Textile Research J.* **1989**, 59, 687.

[13] De la Maza, A.; Parra, J. L.; Manich, A. M.; De Castellar, M. D. *Textile Research J.* **1990**, 60, 709.

[14] Cardamone, J. M.; Yao, J.; Nuñez, A. *Textile Research J.* **2004**, 74, 555.

[15] Höcker, H. *Pure Appl. Chem.* **2002**, 74, 423.

[16] Thomas, H.; Merten, Th,; Monser, V.; Höcker, H. *Proc. 10th Int. Wool Text. Res. Conf. Aachen (D)*, **2000**, PL-3.

[17] Thomas, H. *Plasma modification of wool*, *in Plasma Technologies for Textiles* **2007**, 228.

[18] Osenberg, F.; Theirich, D.; Decker, A.; Engemann, J. *Surface Coating Tech.* **1999**, 99, 808.

[19] Kan, C. W.; Yuen, C. W. M. *Textile Research J.* **2006**, 76, 309.

[20] Sun, D.; Stylios, G.K. *J. Mater. Proc. Tech.* **2006**, 173, 172.

[21] Biniaś, D.; Wlochowicz, A. Biniaś, W. *Fibres Textiles in Eastern Europe* **2004**, 12, 58.

[22] Vohrer, U.; Müller, Oehr, C. *Surface Coating Technol.* **1998**, 98, 1128.

[23] Thomas, H.; J. Herrling,; Rakowski, W.; Höcker, H. *DWI reports* **1992**, 111, 315.

[24] Kulik, C. PhD Thesis, RWTH Aachen, **2008**.

[25] Das, T.; Ramaswamy, G. N. *Textile Research J.* **2006**, 76, 126.

[26] Silva, C. J.S.M.; Prabaharan, M.; Gübitz, G.; Cavaco-Paulo, A. *Enzyme Microbial Tech.* **2005**, 36, 917.

[27] Cardamone, J. M.; Phillips, J. G. *Textile Research J.* **2007**, 77, 277.

[28] Erra, P.; Molina, R.; Jocic, D.; Julia, M. R.; Cuesta, A.; Tascon, J.M.D. *Textile Research J.* **1999**, 69, 811.

[29] Pascual, E.; Julia, M. R. *J. Biotechnol.* **2001**, 89, 289.

[30] Lim, S. H.; Hudson, S. M. *J. Mol. Sci. Part C- Polym. Rev.* **2003**, C43, 223.

[31] Hesse, A.; Thomas, H. Höcker, H. *Textile Research J.* **1995**, 65, 355.

[32] Hesse, A.; Thomas, H. Höcker, H. *Textile Research J.* **1995**, 65, 371.

[33] Makinson, K. R.; Lead, J. A. *Textile Research J.* **1973**, 43, 669.

[34] Tester, D. H.; Makinson, K. R. *Textile Research J.* **1983**, 53, 415.

[35] Popescu, C.; Höcker, H. *Chem. Soc. Rev.* **2007**, 36, 1282.

[36] Wakelyn, P. J. *Textile Research J.* **1972**, 42, 67.

[37] Makinson, K. R. *Textile Research J.* **1974**, 44, 187.

[38] Cook, J. R.; Rivett, D. E. *Textile Research J.* **1981**, 51, 596.

[39] Yu, M.; Hoogenboom, R.; Thomas, H.; Moller, M. *manuscript in preparation*.

[40] Thomas, H.; Moeller, Plasm- und UV-aktivierte chemische modifizierung von Faseroberflächen am Beispiel Wollle, in Final report of the IGF project No. 15118, August **2009**.

[41] Jansen, B.; Kümmeler, F.; Thomas, H.; Müller, H-B. *Proc. 10th Int. Wool Text. Res. Con. Aachen (D)*, **2000**, PL-6.

CHAPTER 5

AQUEOUS ELECTROSPINNING AND STABILISATION OF PVAM (POLYVINYLAMINE) BASED ULTRATHIN NANOFIBERS [M4]

ABSTRACT

Aqueous electrospinning of poly(vinylamine) (PVAm) and blend with Gelita® gelatine-hydrolysates thereof is reported resulting in the formation of nanofibers. The water soluble cationic polyelectrolyte, PVAm was electrospun from various concentrations and the results were related to the rheological viscosity of the electrospinning solutions. Nanofibers were prepared with different spinning conditions such as electrical potential, TCD (tip-collector distance) and spinning solution flow rate. In addition, salt addition to the aqueous electrospinning polymeric solution was investigated on spinning ability, which was related to the rheological viscosity as well as screening of electrostatic repulsive forces along the PVAm backbone. Also, we have studied electrospinning of PVAm/ Gelita® gelatine-hydrolysates for improving the biocompatability. The average diameters of the unmodified PVAm nanofibers were in the range 60–130 nm and PVAm/Gelita® gelatine-hydrolysates nanofibers were ~200 nm. The polyelectrolyte PVAm nanofibers were water soluble and could be stabilized by post-crosslinking with 4,4'-diisocyanate diphenyl methane and glutaraldehyde vapour. Stablization of the nanofibers of PVAm and its blend was demonstrated by exposure to Mili-Q water for 24 hours. The ultrathin PVAm nanofibers still contain primary amine group for further functionalization.

5.1 INTRODUCTION

Polyelectrolyes are highly charged polymers, which can be divided into polyanions, polycations, and polyampholytes. The unique properties of polyelectrolytes in aqueous media are governed by various intrinsic parameters, e.g. nature of ionic group, ionic strength, molecular weight and extrinsic parameters, e.g. pH of medium, ionic strength of the medium, added salt, temperature. Polyelectrolytes have been explored for a variety of applications, e.g., medicine, paper-making processes including paper coating, water treatment, mineral separation, paint and food industries, cosmetics and pharmacy as well as drug delivery, antimicrobial agents, chemical and biological protective clothing, and biomimetic actuators. [1-5] More specifically, the cationic polyelectrolyte polyvinylamine (PVAm) has recently become commercially available and is an attractive platform for the preparation of stimuli responsive materials. Based on its chemical structure, PVAm has an outstanding potential reactivity to ionic strength and pH, because of the presence of primary amino-groups attached to the hydrocarbon main chain (Scheme. 1). Amine functional polymers and the copolymers have been widely used in applications, because amines can act as bases, nucleophiles, ligands for metals and electron transfer agents. This highly interesting reactivity of primary amine groups can be useful for further functionalization. PVAm applications include catalysis, [14,15] metal chelation,[16] biomedical research,[17] paper-making[18-20] and fixed-site-carrier membranes for the facilitated transport of CO_2.[21,22] 50 years ago, the synthesis of PVAm was introduced[6] and various approaches to synthesize PVAm have been developed.[7-13] The vinyl amine monomer cannot be directly polymerized so that PVAm has to be prepared by modification of suitable precursor polymers. The two most common methods are Hoffmann rearrangements from polyacrylamide[7-10] and acid-base hydrolysis of poly(vinyl formamide) (PVFA) (scheme 1).[11-13]

The technique of electrospinning has been developed and applied to generate nano-scaled fibers from natural and synthetic organic and inorganic polymers for various applications.[23-28] It has been demonstrated that electrospun nanowebs have a high specific surface area, low density and high porosity with small pore size, which opens up new application fields including filtration materials, separation membranes, medical uses and nano composites. In general, the electrospinning setup requires three basic components; a high voltage power, a syringe and grounded or oppositely charged collector. The high voltage provides an electrically charged jet of the polymer solution which is stretched and whipped onto the collector. During this spinning process, the solvent evaporates and solidified nano-scale fibers are collected onto the target as a nonwoven. The nanofiber morphology, including fiber diameters and homogeneity of the fiber webs, is influenced by parameters of the electrospinning process including voltage power, TCD, flow rate, needle diameter as well as the polymer solution (polymer concentration, viscosity, polymer, solvent, surface tension, ionic strength, pH value). The polymer electrospinning process is generally performed with organic solvents due to good solubility and high volatility. However, these solvents are mostly toxic and their use should be preferably omitted. Therefore, we have concentrated on avoiding organic solvents and using water as a solvent for electrospinning.[29-34] Aqueous electrospinning is an environmentally friendly process resulting in nontoxic fibers for potential medical and biological applications. Some publications reported electrospinning of common water-soluble polymers such as PEO, PVA, poly(acrylic acid) (PAA), polyacrylamide, polyelectrolytes, polyvinylpyrrolidone (PVP), and hydroxypropylcellulose (HPC).[23] Nevertheless, the electrospinning of PVAm from aqueous solutions has not been reported to the best of our knowledge. PVAm nanofibers are important as potential material for technical applications as well biomedical applications.

In the present paper, the generation of water stable PVAm ultrathin nanofibers by electrospinning from aqueous solution followed by post-crosslinking procedures is reported

for the first time. The PVAm nanofiber spinnability is investigated as function of the polymer concentration and salt addition. In addition, the shear viscosity of PVAm with varying concentration and salt addition in water is correlated to the spinning ability. We have also studied electrospinning of PVAm/ Gelita® gelatine-hydrolysates having biocompatibility to permit as potential tissue engineering. Furthermore, post cross-linking of PVAm nanofibers with 4,4'-diisocyanate diphenyl methane and glutaraldehyde vapor is discussed to render the fibrous membranes water-insoluble.

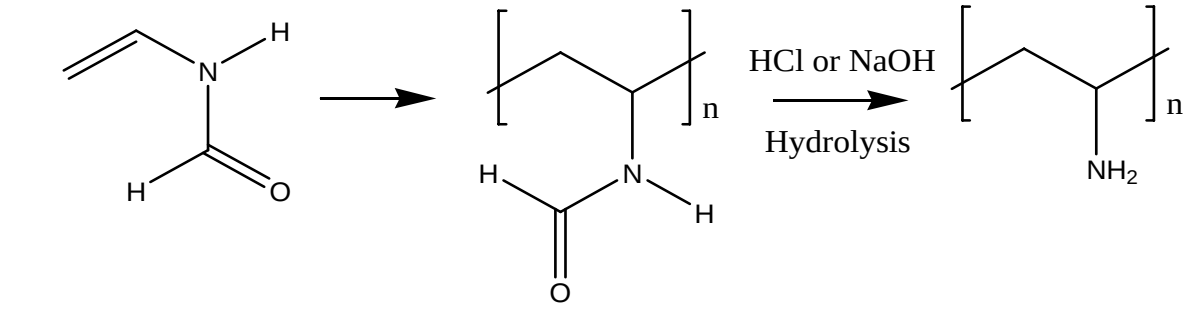

N-Vinylformamide(VFA) PNVF PVAm

Scheme 1. Simple synthesis of poly(vinylamine)(PVAm) from acid and base hydrolysis of poly(N-vinyl-formamide)(PNVF).[6]

5.2 EXPERIMENTAL PART

Materials

Poly(vinylamine) (PVAm; Lupamin 9095) was kindly provided by BASF. The polymer was obtained by ~ 90% hydrolysis of poly (*N*-vinylformamide) with a molecular weight of 340.000 g/mol and was purified with membrane filtration and dialysis before use. Gelita® gelatine-hydrolysates with molecular weight of 9,000- 130,000 g/mol were received from Gelita. Triton-X 100, 4,4'-diisocyanate diphenyl methane and glutaraldehyde solution were purchased from Merck. All reagents were of analytical grade and used as received.

Electrospinning of PVAm and its blend

Electrospinning was carried out using aqueous polymer solutions with various concentrations. Pure PVAm and PVAm/ Gelita® gelatine-hydrolysates (2:1, 1:1, 1:2) were dissolved in deionised water with 3 drops of surfactant Triton® X-100 (0.2 wt%) in order to reduce the surface tension of polymer solution and to fabricate homogeneous and uniform nanofibers. The spinning solutions were filled in the 3ml syringe, which was mounted in a syringe pump (Pilot A2, Fresenius Fial Infusion Technology) and used to provide a constant flow rate (0.5 ml/h). The positive source of a high voltage power supply (KNH34 / P2A, Eltex) in the range of 17.5 kV to 30 kV (typically 20 kV) was connected to the ID 0.8 mm syringe needle. The nanofibers were collected on a grounded aluminum target attached to the steel mesh screen and the distance from tip to collector was fixed at 20 cm.

Post croslinking of PVAm nanofibers

The post crosslinking reactions of pure PVAm have carried out using 4, 4'-diisocyante diphenyl methane as a coupling agent. The coupling agent was dissolved in acetone (0.01 wt%). Glutaraldehyde is commonly used as a crosslinking agent for collagen based

biomaterial. Furthermore, the crosslinking of nanofibres was performed by placing in a sealed beaker filled with 25 wt% glutaraldehyde vapour.

Characterization

The surface tension of the solution was measured by Wilhelmy-Plate method, i.e., the force that is needed to overcome the resistance of the liquid was measured when a platinum plate with known wetted length is immersed. Rheological viscosity was determined at room temperature by a stress controlled rheometer (Rheometrics) equipped with cone and plate geometry of 0.1 radian and of 25 mm diameter and the gap was 0.111 mm. The measurement was carried out with steady stress sweep in order to obtain zero shear viscosity. The morphology of the nanofibers were examined using scanning electron microscopy (SEM, Carl Zeiss, S 360) and field-emission scanning electron microscopy (FE-SEM, S-4800, HITACHI) and the diameters were measured from 50 arbitrary selected samples by Image J software.

5.3 RESULTS AND DISCUSSION

Preparation of PVAm-nanofibers

Poly(vinylamine) (PVAm) Poly(vinylamine) (PVAm) is a commercially available cationic polyelectrolyte which has charged ammonium groups in water and the technical grade product contains a certain unspecified amount of salt. Adding salt during electrospinning has been reported to significantly decrease the nanofiber diameter and increase the homogeneity the electrospun mats.[28] The salt can play a role as a counter ion near protonated amino groups and screening electrostatic charge repulsion occurs. To reduce the salt amount from PVAm (Lupamin 9095), ultra membrane filtration was performed by BASF who kindly supplied a low salt PVAm 5.5 wt% aqueous solution from BASF. Aqueous polymeric systems, towards environmentally friendly electrospinning, commonly have high surface tension and low volatility compared to organic solvents complicating the electrospinning process. The surface tension of PVAm aqueous solutions is pH dependent; 56 mN/m at pH 10 and 71.5 mN/m at pH 3.5. This transition of surface tension reflects the dissociation behavior of the amine groups.[35] However, adding a small amount of non-ionic surfactant can be used to generate homogeneous and uniform nanofibers by reducing the surface tension from 59 mN/m (without surfactant) to 31 mN/m (with surfactant). Therefore, aqueous polymer solutions were prepared with surfactant (0.01 wt% Triton-X 100) in all PVAm spinning solutions in this work, leading to a simple method for generating polyvinylamine (PVAm) nanofibers by electrospinning.

Figure 1 shows the zero shear viscosity dependence on the PVAm concentration and the SEM images of PVAm nanofibers prepared from different concentrations ranging from 3.5wt% to 9.5wt%. The electrospinning setup was operated at 20 kV voltage power, 20 cm TCD and a flow rate of 0.5 ml/h at seven different concentrations. As many researchers have already mentioned,[23-26] the concentration or solution viscosity has a direct influence on electrospun

fiber diameter and morphology. In general, when the polymer solution concentration increases, the entanglement density in solution is increased leading to more uniform and thicker fibers. Thus, figure 1 shows a transition for the electrospun morphologies from droplets to bead mixed fibers to uniform fibers. The steady rheological measurement revealed increasing shear viscosity when the PVAm concentration increases as well as remarkable shear thinning behavior typical for polyelectrolytes (Figure 1(a)). The zero shear viscosity significantly increased in the PVAm concentration range from 8.5 – 9.5 wt% (Figure 1(b)). The SEM images of PVAm electrospun fibers depict mostly beads at the lower concentration of 4.5 wt%, but extremely thin fibers were also generated (Figure 1 (c)). The morphologies of the nanofibers prepared from 5.5 wt% to 6.5 wt% PVAm concentration demonstrated that uniform nanofibers started to be formed. Above 6.5 wt% PVAm concentration electrospinning results in the formation of well defined uniform nanofibers. The average diameters of PVAm nanofiber prepared from different concentrations are 68.7 ± 24 nm at 4.5 wt%, 60.1 ± 21 nm at 5.5 wt%, 178.3 ± 32 nm at 6.5 wt%, 172.8 ± 34 nm at 7.5 wt%, 185.9± 35 nm at 8.5 wt% and 283.5 ± 67 nm at 9.5 wt%. From 8.5 wt% to 9.5 wt% polymer concentration, the average diameter increases about 100 nm and the zero shear viscosity significantly rises.

Even though well-defined PVAm nanofibers were successfully prepared by aqueous electrospining, the resulting PVAm nanofibers are instable in water and even in contact with humid air. The SEM image of PVAm nanofibers prepared from 6.5 wt% reveals swollen structures indicating the hygrosopic nature of PVAm. Due to the water solubility of PVAm, the generated nanofiber webs had to be stored in a desiccator with Argon atmosphere. Therefore, it is necessary to develop water stable PVAm nanofibers for further applications.

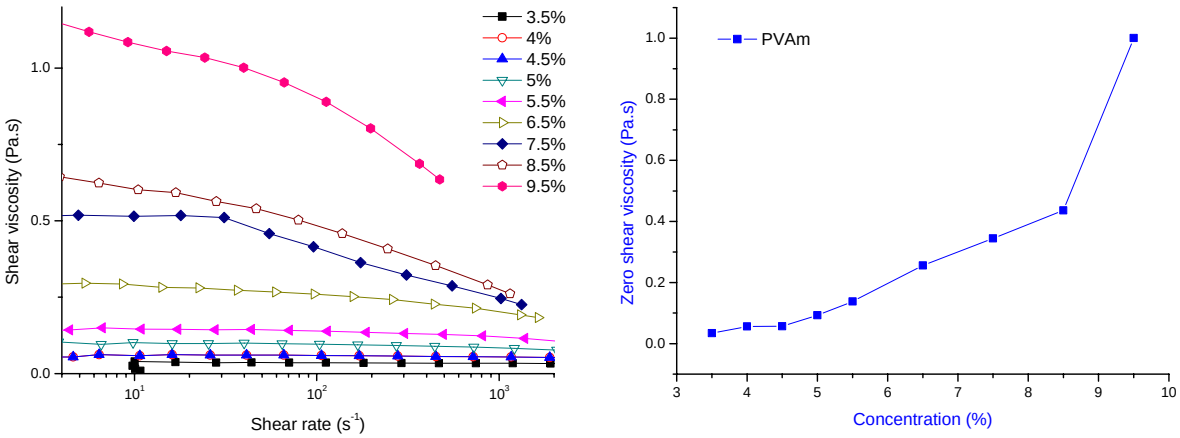

(a) (b)

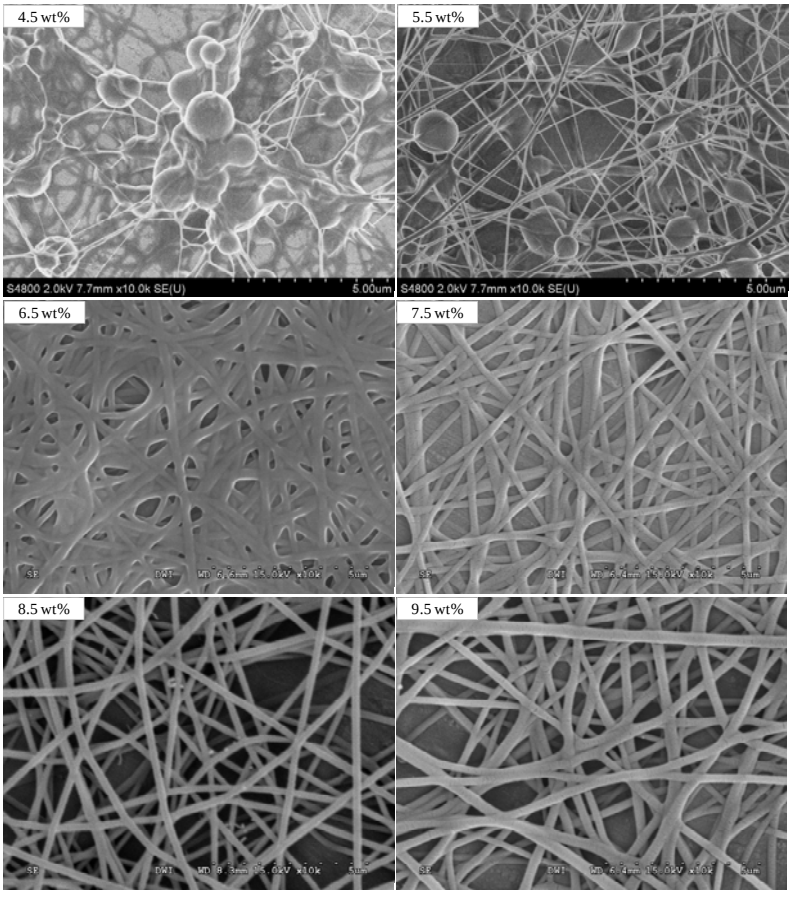

(c)

Figure 1. Rheolgocial viscosity (a) and its zero shear viscosity (b) dependence on the PVAm concentration and SEM morphologies of PVAm nanofibers (c) in various concentrations from 4.5 wt% to 9.5 wt%.

Many parameters can influence the formation of nanofibers through aqueous electrospinning. Figure 2 demonstrates the influence of the process parameters such as voltage, feeding rate

and TCD in 7.5 wt% PVAm aqueous solution. Lower applied voltage 17.5 kV shows the narrower size distribution than higher applied voltage 30 kV due to jet stability. Regarding to spinnability, higher potential power is more effective since more fluid is jetted compared to lower potential power. The diagram presents the effect not only the applied voltage but also variation of TCD and flow rate. The polymer jet diameter is related to the flow rate, electro field strength and the surface tension. Lower flow rate results in a smaller amount of polymer solution. So, slower polymer solution feeds contributes to faster water evaporation as well smaller fiber diameters. The distance from tip to collector is also playing role to evaporate water during electrospinning process. Larger TCD distance results in thinner nanofibers size. The feeding rate at 0.5ml/h and TCD at 20 cm represent the optimal electrospinning condition to produce the thin nanofibers on wide applied voltage. The thinnest diameter and most uniform morphology were generated at the condition 20 kV, 20 cm, 0.5 ml/h shown in Figure 2.

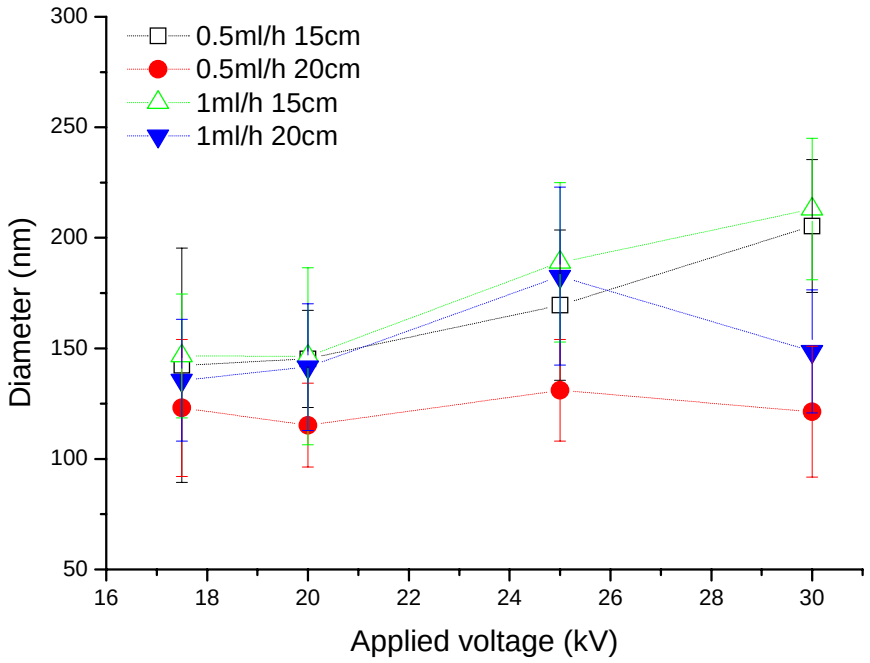

Figure 2. Average diameters of the 7.5wt% PVAm nanofibers depend on the spinning conditions (a) electrical potential (17.5kV – 30kV) (b) TCD (15cm, 20cm) (c) flow rate of aqueous spinning solution (0.5ml, 1ml).

The addition of NaCl to polymer aqueous solution changes polymer solution conductivity. Increasing ionic strength leads to higher net charge density of the electrospinning jet which is increasing the charge repulsion in the spinning jet.[23,36] Figure 3 shows the effect of salt addition on the zero shear viscosity for 5.5 wt% PVAm aqueous solution and the obtained electrospun morphologies. It should be noted that the ultra membrane filtered 5.5 wt% polymer stock solution still holds a little amount of salt in solution. Nonetheless, the added salt amount was 0 – 50 wt% of PVAm. Addition of NaCl to the polymer solution decreased the zero shear viscosity up to 10 wt% while between 10 wt% and 50 wt% NaCl the zero shear viscosity increased. SEM images in figure 3 depict that the nanofiber morphology depends on the rheological viscosity. The lowest zero shear viscosity demonstrates more bead like morphology and higher zero shear viscosity results in more fiber like morphology. The average diameter of the fibers was evaluated by image analysis software and we found that the diameter was thinner when more salt was added. The average diameters of the nanofibers prepared with 0 wt% to 50 wt% salt were 98.1 ± 57, 89.3 ± 39, 79.1 ± 37, 77. 4 ± 26, and 63.4 ± 20 nm. The increase in charge density and the charge repulsion in the electrospinning jet lead to the generation of thinner fibers.[36]

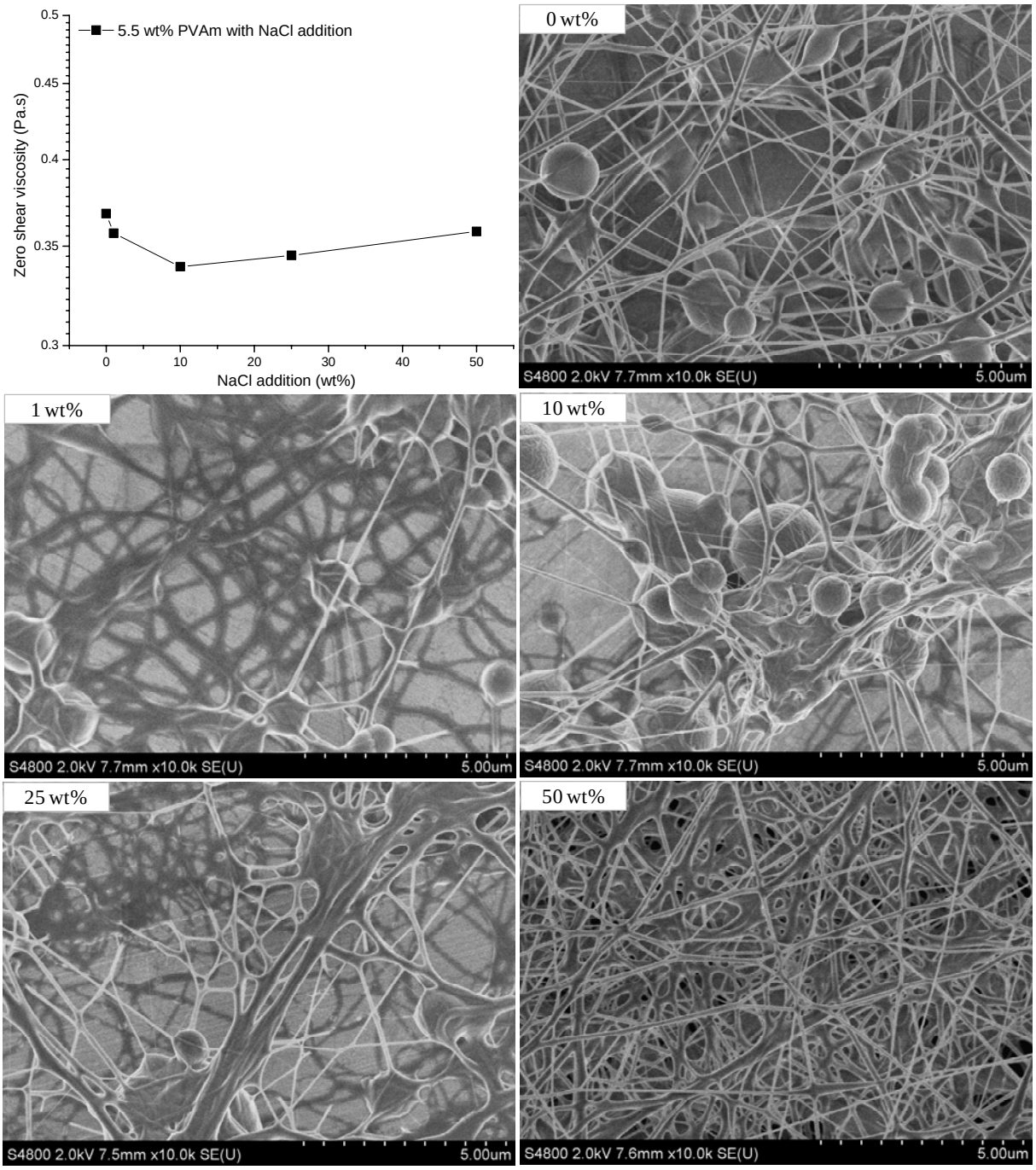

Figure 3. Zero shear viscosity dependence on the salt addition in 5.5wt% PVAm nanofibres and SEM morphologies of PVAm in various salt additions from 0 to 50 wt% of PVAm amount.

Besides electrospinnign of the ultramembrane filtered PVAm, direct electrospinning (17.5 kV, 20 cm, and 0.5 ml/h) of the technical grade Lupamin 9095 PVAm was investigated resulting in a homogeneous nanofiber web (Figure 4). The technical product holds 21.5 wt% solids in solution and it contains about 47 wt% amount of salt relative to PVAm. The nanofiber diameter was 90 ± 15 nm and the size distribution is remarkably uniform. The salt effect leads to the smaller size of nanofibers and more homogenous electrospun webs as we also found by addition of salt to ultramembrane filtered PVAm.

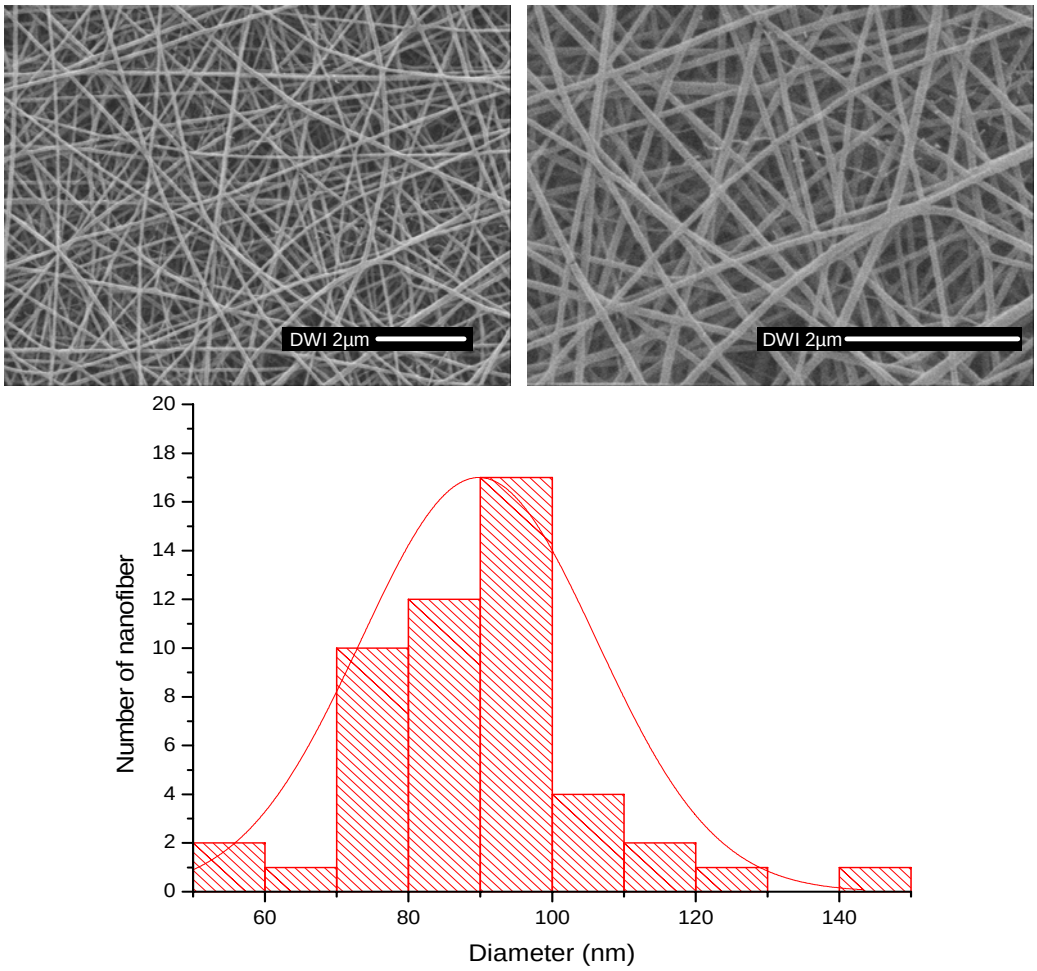

Figure 4. SEM-images of PVAm nanofibres from technical product Lupamin 9095 (without ultra membrane filtration, certain amount of salts) and its diameter distribution at the eletrospinning condition (17.5 kV, 15 cm, 0.5 ml/h).

Post crosslinking of PVAm nanofibers for water stabilization

Investigation of water stability on the PVAm nanofibers revealed immediate hydration in contact to water due to PVAm water solubility. Therefore subsequent functionalization reaction is required to stabilize the fibers. The accessible amino groups of PVAm were post crosslinked with commercially available 4,4'-diisocyanate diphenyl methane, which includes two isocyanate groups. Voigt *et al.* have studied this crosslinking reaction by solid state ^{13}C cross-polarized magic-angle spinning (CPM-AS) NMR spectroscopy and XPS measurements.[4] Crosslinking was performed by dipping the nanofiber web in a an acetone solution of the crosslinker for 10 min. Afterwards, the crosslinked PVAm nanofibers were immersed in Milli Q water for 24 hours in ambient condition. Figure 5 shows the SEM images of the crosslinked PVAm nanofibers before (a) and after (b) immersion in water. However the morphology of figure 5 (b) shows that, even though the nanofibers are stabilized, partial merging of fibers did occur. This might be due to insufficient crosslinking due to a too slow crosslinking reaction or due to partial salvation of the fibers when immersed in acetone.

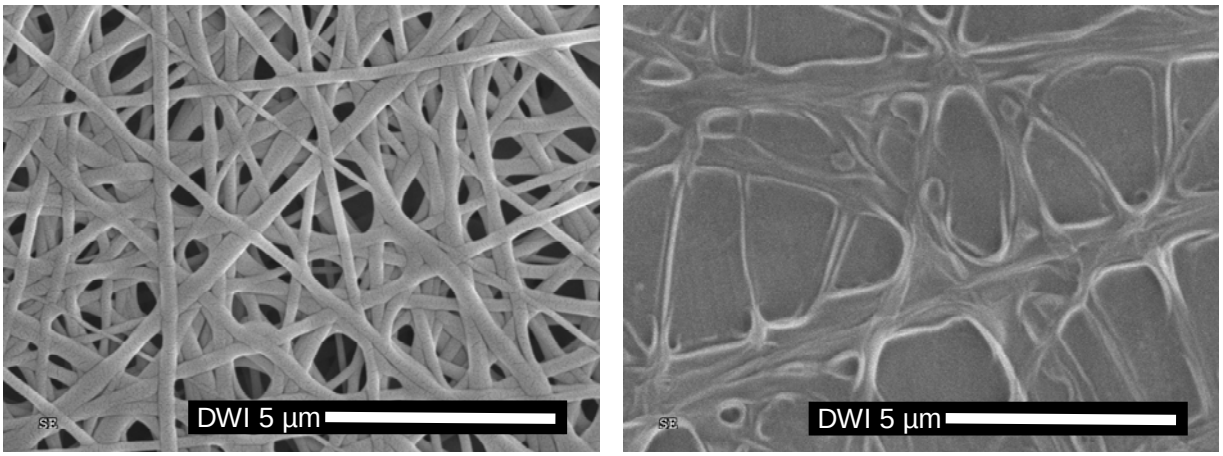

(a) (b)

Figure 5. SEM images of post crosslinking PVAm nanofibers with 4,4'-diisocyante diphenyl methane (a) and post crosslinking nanofibres after exposition in water for 24 hours (b)

Therefore, we subsequently investigated the most well-known post crosslinking agent, glutaraldehyde, (GA) for collagen-based biomaterials.[37] Condensation of a collagen amine group with the aldehyde groups of GA results in crosslinking. Post crosslinking of the PVAm fibers was performed by vapor exposition from a 25 wt% glutaraldehyde (GA) solution in a sealed beaker for 10 min. The stability of the crosslinked fibers was subsequently tested by incubating the samples in water for 24 hours. The morphologies of GA crosslinked PVAm nanofibers before (Figure 6(a)) and after (Figure 6(b)) exposure to Milli Q water (Figure 6(b)) reveal fully crosslinked stable PVAm nanofibers. After water stability test, GA post crosslinking PVAm nanofibers are swollen, but still individual and uniform fibers are observed indicating that they are stable in water.

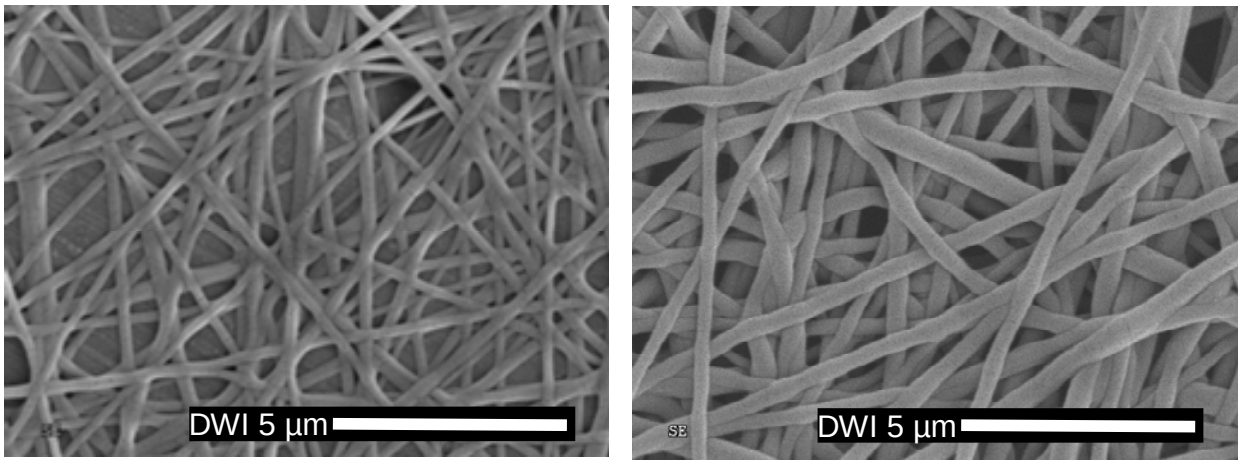

(a) (b)

Figure 6. SEM images of post crosslinking PVAm nanofibers with glutaraldehyde vapor (a) and the post crosslinking nanofibres after exposition in water for 24 hours (b).

Electrospinning of PVAm/Gelita® gelatine-hydrolysates

Besides electrospinning of pure PVAm, we were interested to develop a biocompatible nanofibers composed PVAm and Gelita® gelatine-hydrolysates. Successful co-electrospinning of PVAm and gelatine requires a good solubility in the water for aqueous electrospinning. Thus, Gelita® gelatine-hydrolysates were used as co-spinning aqueous solution. Figure 7 shows the SEM images of PVAm/Gelita® gelatine-hydrolysates clearly indicating successful electrospinning from aqueous polymer solution under different blend ratio and voltage. Average diameters with PVAm: Gelita® gelatine-hydrolysates of 2:1, 1:1, and 1:2 are 160 nm, 210 nm, and 380 nm. Increase of amount of Gelita® gelatine-hydrolysates results increase of the diameter of resulting fibers. The applied voltages were slight influence on fiber diameter. Nanofibers based on PVAm/Gelita® gelatine-hydrolysates may be interesting candidates for tissue engineering, wound dressing, and drug delivery systems due to water based electrospinning and biocompatibility of gelatine.

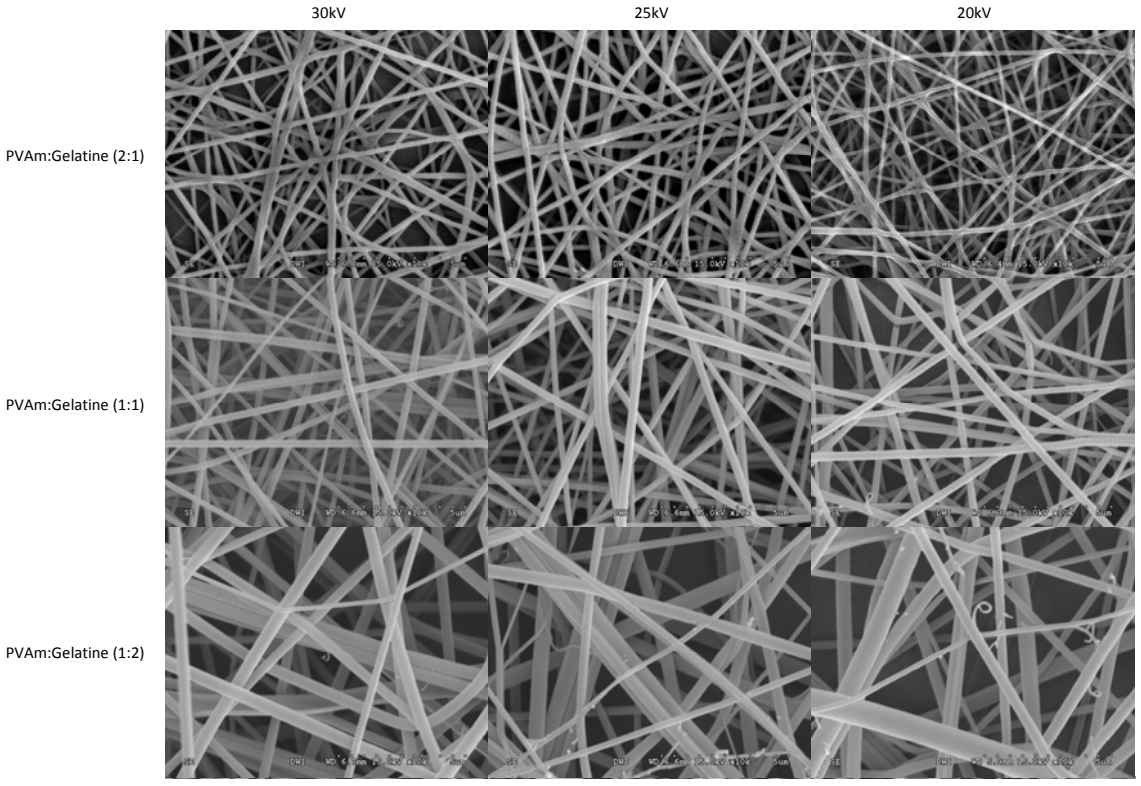

Figure 7. SEM images of PVAm/Gelita® gelatine-hydrolysates nanofiber (2:1, 1:1, 1:2) at the electrospinning condition 30-20 kV, 20 cm, and 0.5 ml/h.

5.4 CONCLUSIONS

Electrospinning is a useful platform to generate homogeneous nanofiber webs for a wide range of applications. In the present work, PVAm nanofibers were successfully prepared and the morphology of the resulting fibers could be controlled by the process parameters and was related to the zero shear viscosity of the spinning solution. Furthermore, the addition of salt to the spinning solution resulted in the formation of thinner fibers. Since the prepared PVAm nanofibers readily dissolve in water, various crosslinking methods were evaluated to stabilize the structures. The water stabilization of PVAm nanofibers was successfully performed by simple post crosslinking with 0.01 wt% 4, 4'-diisocyanate diphenyl methane in acetone and glutaraldehyde vapor. In addition, electrospinning of PVAm with Gelita® gelatine-hydrolysates was prepared nanofibers making them interesting in field of biomedical application.

All together, we have demonstrated an environmentally friendly aqueous electrospinning process as well as post-crosslinking methodologies, which will serve as basis for the use of PVAm nanofibers in a range of applications. The remaining PVAm amino groups in the nanofibers can be used for postmodification reactions, which will be of interest for various potential applications for, e.g., protective clothing, antimicrobial materials as well as catalysts.

5.5 REFERENCES

M4 Reproduced with permission from Yu, M.; Bozukov, M.; Hoogenboom, R.; Thomas, H.; Moeller, M. *manuscript in preparation.*

[1] Loucheux, C.; Francois, J. *The polymeric materials encyclopedia* **1996**.

[2] Koetz, J.; Kosmella, S. *Polyelectrolytes and Nanoparticles* Springer **2007**.

[3] Decher, G. *Science* **1997,** 277, 1232.

[4] Voigt, I.; Simon, F.; Komber, H.; Jacobasch, H. J.; Spange, S. *Colloid Interface Sci.* **2000**, 278, 48.

[5] Li, X.; Pelton, R. *Ind. Eng. Chem. Res.* 2005, 44, 7398.

[6] Weisgerber, C. A. *USP2* **1955**, 721, 150.

[7] Achari, A. E.; Coqueret, X.; Lablache-Combier, A.; Loucheux, C: *Makromol. Chem*. **1993**, 194, 1879.

[8] Tanaka, H. *J. Polym. Sic. Part B* **1978**, 16, 87.

[9] Schiller, A. M.; Suen, T. J. *Ind. Eng. Chem.* **1956**, 48, 2132.

[10] Tanaka, H. *J. Polym. Sci. Polym. Chem. Ed.* **1979**, 17, 1239.

[11] Pinschmidt, R. K.; Renz, W. L.; Caroll, W. E.; Yacouth, K.; Drescher, J.; Nordquist, A. F.; Chen, N. *J. Macromol. Sci. Pure. App. Chem. A* **1997**, 34, 1885.

[12] Badesso, R. J.; Nordquist, A. F.; Pinschmidt, R. U.; Sagl, D. J. *Adv Chem. Ser*.**1996**, 248, 489.

[13] Kurtz, P.; Disselnkoetter, H. *Liebigs Ann. Chem.* **1972**, 764, 69.

[14] Prabhakaran, P. V.; Venkatachalam, S.; Ninan, K. N. *Eur. Polym. J.* **1999**, 35, 1743.

[15] Martel, B.; Leckchiri, Y.; Pollet, A.; Morcellet, M. *Eur. Polym. J.* **1995**, 31, 1083.

[16] Kobayashi, S.; Suh, K. D.; Shirokura, Y. *Macromolecules* **1989**, 22, 2363.

[17] Qiu, Y.; Zhang, T.; Ruegsegge, M.; Marchant, R. E. *Macromolecules* **1998**, 31, 165.

[18] Wu, Z. H.; Chen, S. P.; Tanaka, H. *J. Appl. Polym. Sci*. **1997**, 65, 2159.

[19] Kanie, O.; Tanaka, H.; Mayumi, A.; Kitaoka, T.; Wariishi, H. *J. Appl. Polym. Sci.* **2005**, 96, 861.

[20] Espy, H. H. *Tappi J.* **1966**, 70, 129.

[21] Kim, T.; Li, B.; Hägg, M. *J. polym. sci. Part B. Polym. physics* **2004**, 42, 4326.

[22] Hägg, M.; Lindbråthenlnd, A. *Eng. Chem. Res.* **2005**, 44, 7668.

[23] Greine, A.; Wendorff, J. H. *Angew. Chem. Int. Ed.* **2007**, 46, 567.

[24] Huang, Z. M.; Zhangb, Y. Z.; Kotakic, M.; Ramakrishnab, S. *Comp. Sci & Tech.* **2003**, 63, 2223.

[25] Teo, W. E.; Ramakrishna, S. *Nanotechnology* **2006**, 17, R89.

[26] Shin, M. K.; Kim, S. K.; Lee, H.; Kim, S. I.; Kim, S. J. *Nanotechnology* **2008**, 19 195304.

[27] Thomas, H.; Heine, E.; Wollseifen, R.; Cimpeanu, C.; Moeller, M. *Int. Nonwovens J.* **2005**, 25, 1600.

[28] Voigt, W.; Thomas, H.; Heine, E.; Moeller, M.; Electrospinning and stabilization of Poly(vinylalcohol) nanofibre webs with antimicrobial activity in Textiles for Sustainable Development *Nova publishers NY* **2007**.

[29] Du, J.; Hsieh, Y. *Nanotechnology* **2008**, 19, 125707.

[30] Li, L.; Hsieh, Y. *Polymer* **2005**, 46**,** 5133.

[31] Song, J. H.; Kim, H. E.; Kim, H. W. *J. Mater. Sci.: Mater. Med.* **2007**, 19, 95.

[32] Zhang, S.; Huang, Y.; Yang, X.; Mei, F.; Ma, Q.; Chen, G.; Ryu, S.; Deng, X. J. *Biomed. Mat. Res. Part A*, **2009**, 90A, 67.

[33] Mincheva, R.; Manolava, N.; Paneva, D.; Rashkov, I. *J Bioact. Compati. Poly.* **2005**, 20 419.

[34] Nagarajan, R.; Drew, C.; Mello, C. M. *J. Phy. Chem. C Lett.* **2007**, 111, 16105.

[35] Hong, J.; Pel ton, R. *Colloid Polym. Sci.* **2002**, 280, 203.

[36] Mckee, M. G.; Hunley, M. T.; Layman, J. M.; Long, T. E. *Macromolecules* **2005**, 39, 575.

[37] Oldedaminko, L. H. H.; Dijkstra, P. J.; Vanluyn, M. J. A.; Van Wachem, P. B.; Nieuwenhuis, P.; Feijen, J. *J. Mat. Sci.: Mat. In Med.* **1995**, 6, 460.

CHAPTER 6

POLYELECTROLYTE CROSSLINKED HYDROGEL NANOFIBERS BY AZETIDINIUM-AMINE CLICK REACTION FROM AQUEOUS GELATING SOLUTION [M5]

ABSTRACT

The preparation of water stable PVAm nanofibers by a novel type of click reaction, namely ring-opening of azetidinium group of PAE by reaction with amines of PVAm is reported. In particular, this work reports the gelation time of aqueous PVAm/PAE solutions to determine the available time for electrospinning of hydrogel nanofibers. Rheological measurements revealed that electrospinning should be performed within 10 hours after mixing the PVAm/PAE in order to obtain homogenous nanofiber webs. More interestingly, the nanofibers have a narrowly distributed average diameter of 160 nm and behave as a superabsorbent fibrous hydrogel when exposed to water. The moisture sorption of hydrogel nanofibers was investigated by isothermal gravimetric analysis. The PVAm/PAE hydrogel films showed up to 25 times swelling upon exposure to water. The swelling degree can be controlled by the PVAm/PAE ratio as well as the pH of the solution. In addition, the isotherm shows 250 % moisture uptake relative to the dry weight of the nanofibers at a relative humidity of 95 %. The vapor absorption and swelling behavior of the nanofibers can be controlled by the blending ratio of the reacting components.

6.1 INTRODUCTION

In recent years, remarkable efforts have been dedicated in various areas of chemistry to click chemistry, which represents nearly perfect chemical reactions.[1] Click chemistry was defined by Sharpless *et al.* in 2001 as "a modular approach that uses only the most practical and reliable chemical transformations."[2] Since the introduction of click chemistry, a number of different click chemistry methods have been reported based on e.g. nucleophilic ring opening reaction, thiol additions to carbon-carbon multiple bonds, and cycloaddition reactions.[3-7] Nucleophilic ring opening reaction, especially of strained heterocyclic electrophiles such as epoxides, aziridines, cyclic sulphate, cyclic sulfamidates, aziridinium ion and episulfonium ions, might also be considered as click reactions if they are modular and are insensitive to water. Fascinating candidate for nucleophilic ring opening click reaction is azetidinium ions.[8-11] These strained nitrogen heterocycles are stable in the presence of water, but can react with nucleophiles such as amines, azide anions and acetate anions. In this study, a weak cationic polyelectrolyte containing reactive azetidinium ions is used, namely poly(amideamine-epichlorohydrin) (PAE), which is commercially available as Hercosett resin.[12-15] The azetidine side groups allow modification or crosslinking by reaction with nucleophiles. PAE has been used as wet strength additive for paper making, thermo setting resins, and wool shrinkproofing coating.[16-17]

Electrospinning is a suitable and simple technique to generate nano-scaled fibers exhibiting a high surface-area-to-weight ratio, high porosity and small pore size making them interesting for e.g. filtration, catalysis, protective clothes, drug delivery and wound dressing. By applying a high voltage to the syringe tip, the aqueous gelating solution charges to form a Taylor cone and the spinning jet undergoes a whipping motion to transport electrospun nanofibers on a collector (Scheme 1). Viscoelastic behavior and the concentration of the polymer solution play an important role in generating bead free fibers, which is related to polymer chain entanglements.[18-21] In previous research to generate water stable poly(vinylamine) (PVAm)

nanofibers by aqueous electrospinning, we have demonstrated PVAm modification and post crosslinking by photo irradiation and chemical reaction to obtain water-stable nanofibers.[22] In addition, we reported the optimized spinning conditions for PVAm and adapted these conditions in this present work.

Hydrogels are three-dimensional hydrophilic polymeric networks absorbing a substantial amount of water. PVAm is an excellent candidate for superabsorbent gels, and is widely used in sanitary and hygienic goods, thickening agents, and water-retaining materials.[23-33] In particular, hydrogel nanofibers can be attractive materials for tissue engineering due to their three-dimensional structure and capability of retaining water or biological fluids.

In this paper, we report the preparation of water stable PVAm/PAE nanofibers by aqueous electrospinning and investigate the steady and dynamic rheological properties of aqueous gelating polymer solutions. In Figure 1, it is shown that the primary amine groups from PVAm can undergo electrophilic addition making them suitable for ring opening reaction of azetidinium ions, i. e. a click crosslinking reaction. Based on the click reaction of the primary amine groups with azetidinium ions, the polymer solution will form a gel based on covalent crosslinking. Moreover, water swelling behavior and moisture uptake of a model PVAm/PAE monolithic films and PVAm/PAE hydrogel nanofibers are reported. Various ratios of PVAm/PAE nanofibers were prepared and evaluated the swelling behavior as well as the effect of pH.

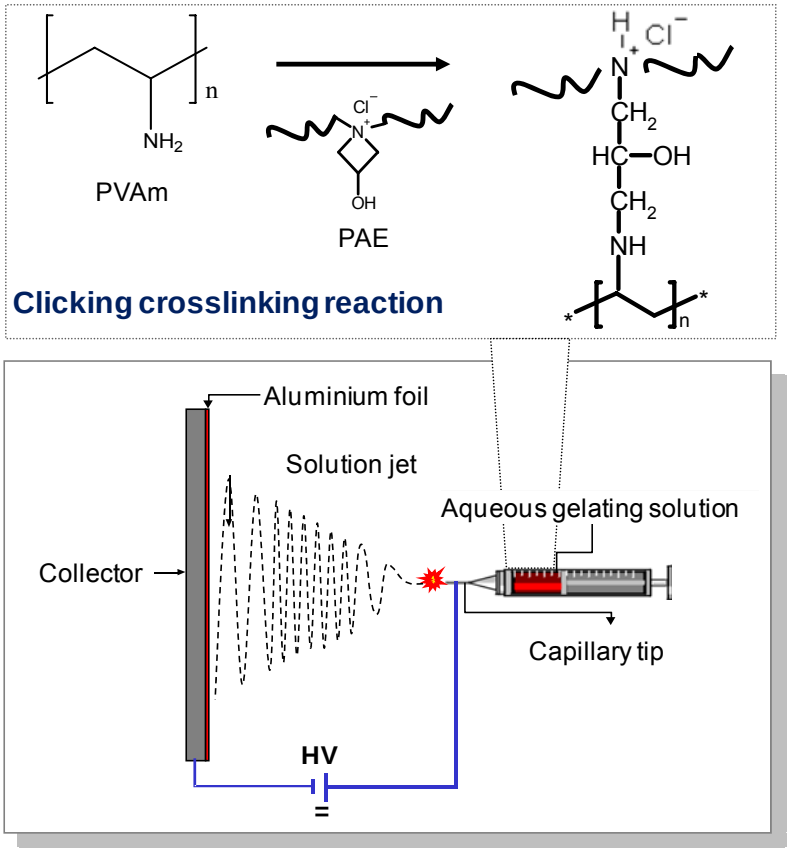

Scheme 1. Schematic representation of electrospinning process with a high voltage supply, aluminum foil collector and a syringe filled with aqueous gelating polyelectrolyte solution of PAE and PVAm.

6.2 Experimental Part

Materials

The cationic polyelectrolyte poly(vinylamine) (PVAm), Lupamin 9095 was kindly provided by BASF AG, Ludwigshafen. Poly(amideamine-epichlorohydrin) (PAE) was purchased from SI group. The polymer has an average molecular weight of 269.000 g/mol and was obtained as 12.5 wt% polymer solution in water. These cationic polyelectrolytes PVAm and PAE were used as received. The nonionic surfactant Triton X-100 was purchased from Aldrich and consists of a hydrophilic oligoethylene oxide group and a hydrocarbon lipophilic group.

Electrospinning setup

A schematic diagram of the environmental friendly electrospinning process based on an aqueous gelating solution is shown in Scheme 1. There are basically three components for the spinning process; a high voltage supply, a capillary tip filled with polymer solution, and a metal collecting screen. Technical PVAm has been successful used to generate nanofibers from a 21.5 wt% concentration using an applied voltage 20 kV, tip to collector distance of 20 cm and a feeding rate of 0.5 ml/h in our previous work.[22] The preparation of spinning blends was performed by mixing 21.5 wt% PVAm and 12.5 wt% PAE in different volume ratios (10/1, 7/1, 5/1, 3/1, 1/1). Triton X-100 (0.01 wt%) was added and mechanical stirring was performed for 30 min before electrospinning. The concentrations and initial zero shear viscosity of all solution are summarized in Table 1.

Table 1. Overview of the concentration and zero shear viscosity of spinning solutions of the resulting nanofiber and the average diameter using 20 kV, 20 cm, and 0.5 ml/h

Sample	PVAm/PAE (ml)	Concentration (wt%)	PAE/PVAm (w/w%)	Zero shear viscosity (Pa.s)	Average diameter (nm)	Diameter after water exposition (nm)
1	3	22	0/100	1.479	105 ± 80	soluble
2	10/1	21	6/94	1.053	160 ± 10	140 ± 40
3	7/1	20.4	8/92	0.771	160 ± 90	150 ± 10
4	5/1	20	11/89	0.703	160 ± 20	170 ± 30
5	3/1	19	19/81	0.514	160 ± 70	170 ± 40
6	1/1	17	57/43	0.181	170 ± 30	160 ± 50
7	3	13	100/0	0.092	beads	beads

Rheological characterization

The reactive 3-hydroxy-azetidinium rings of PAE act as a crosslinker resulting in PVAm/PAE aqueous gelation. The rheological measurements were performed in a stress-controlled

rheometer equipped with cone and plate geometry at room temperature. To measure zero shear viscosity, the measurement was carried out with steady shear sweeps. Furthermore, dynamic time sweeps were conducted to determine the elastic (G′) and viscous moduli (G″) in a stress controlled rheometer using plate and plate geometry at 25 ºC. The dynamic rheological experiment was performed for 24 hours using time sweep to determine the gelation time. Furthermore, each 6 hours a frequency sweep was measured to determine the viscoelastic properties of the aqueous gelating polymer solutions.

Water absorption measurement

The swelling behaviors of the monolithic films and nanofiber webs were studied in time. The dried samples were immersed into distilled water for 24 hours at room temperature. Then the water present at the swollen sample surface was carefully removed with paper and the water saturated hydrogel fims and nanofibres were weighed. The swelling percent was calculated as follows:

$$\text{Swelling capacity (\%)} = (W_2\text{-}W_1) / W_1 \times 100 \qquad (1)$$

W_1: Initial (dry) weight W_2: Swollen (wet) weight

An Isothermal gravimetric analyzer (IGAsorp) was used to monitor the precise weight add and loss of ultrathin nanofiber webs by increasing and decreasing relative humidity from 0 to 95 % in step of 10 % at 25 ºC.

Chacterization of nanofiber webs and hydrogel films

The morphology of the nanofibres was observed using scanning electron microscopy (SEM, Carl Zeiss, S 360) and field-emission scanning electron microscopy (FE-SEM, S-4800, HITACHI). Average diameter of nanofibers was calculated with 50 times measurement by Image J software. The ^{13}C solid-state NMR spectra were recorded on a Bruker DPX 500

spectrometer using a 3.2 mm MAS probe operating at 500 MHz and 700 MHz, respectively. The spinning rate was 3 kHz. The samples were prepared the cylinder type of hydrogels at the different blends ratio of 1:1, 5:1 and 10:1. The spectra were referenced using the CH signal of adamantane ($^{13}C_{10}H_{16}$) at 38.6 ppm. The experiments were performed with pulse duration of 5 μs, a contact time of 1 ms, and a recycle delay of 2 s. Fourier Transform Infrared (FT-IR) spectra were obtained with a Biorad FTS 6000 spectrometer. Thermogravimetric analysis (TGA) was performed on a Netzsch TG 209 C under nitrogen using heating rate 5 ºC min^{-1}. The PVAm and the crosslinked PVAm/PAE were determined the changes in weight in relation to change in temperature from 25 ºC to 1000 ºC. Cryo field-emission scanning electron microscopy (Cryo FE-SEM) was performed using HITACHI S-4800 instrument in a cryo-chamber with the cryo-transfer system Alto 2500 (GATAN). The hydrogels in bulk were quickly frozen in liquid nitrogen. The frozen hydrogels was placed in cryo chamber and was fractured on cross-section by equipping knife. The samples were sublimated at -90 ºC for 10 min to remove the water. To avoid the artefact, the microscope images were observed inner-structure of frozen nanogels and waere measured below -120 ºC.

6.3 RESULTS AND DISCUSSION

Solution rheology and estimation of gel point

The gelation of PVAm/PAE in aqueous solution is investigated in time to determine the gelation time. This is an important parameter for subsequent electrospinning to avoid clogging of the system due to cross-linking. The rheological behavior of gel point is accomplished by using multiple waveform rheology where the crosslinking progress is monitored of different frequencies and reaction time.

$$\gamma(t) = \Sigma\gamma i \sin\omega i(t) \qquad (2)$$

in which γ is the applied strain and ω is the frequency . This method applied a multiwave osciallatory strain and the resulting stress is measured. The gel point is estimated by measuring G′, G″ in the time scale of chemical gelation under simultaneous multiwave frequency sweep. In this rheological study, the gel point and crosslinking kinetics were analyzed by a dynamic time sweep for the mixtures of PVAm/PAE with various volume ratios (10/1, 5/1, 1/1). When polymer chains are crosslinked, the viscosity is increasing with reaction time under a small amplitude oscillatory shear as shown in Figure 1 (a). As the complex viscosity starts to increase quickly, the gel point is approaching. For the PVAm/PAE blend 5:1 the sol to gel transition occurs after ~11 hrs while for the 10:1 ratio it occurs after ~13.8 hrs. The slower gelation can be ascribed to the lower fraction of PAE resulting in slower cross-linking. Surprisingly, the 1:1 blend with the highest amount of PAE does not show a clear increase of complex viscosity and, thus, no gel point can be determined. However, the determination of gel point from complex viscosity plots only provides a rough estimation. Tung and co-workers have introduced the determination of gel point by the crossover point of the elastic modulus (G′) and viscous modulus (G″) curves in time.[34] Since for the electrospinning process of PVAm/PAE blends the gelation time is crucial, the

crossover point of G′ and G″ was determined with frequency of 1 rad/s and a strain of 5% (Figure 1 (b)). The crossover points of 5:1 and 10:1 blends are ~14.1 hrs and ~15.5 hrs, respectively, which is in agreement with the values obtained from the complex viscosity. It is also evident that the PVAm/PAE 1:1 blend has no crossover point indicating that the sol-gel transition has not occurred yet within the investigated time. The absence of a gel point for the 1:1 blend with the highest amount of PAE is most likely due to the formation of a two-phase system consisting of a densely cross-linked phase with high polymer concentration and a low polymer concentration aqueous phase. As a result, only parts of the system gel and the elastic modulus will only slowly increase. Nonetheless, after longer times the formation of a complete crosslinked gel was observed.

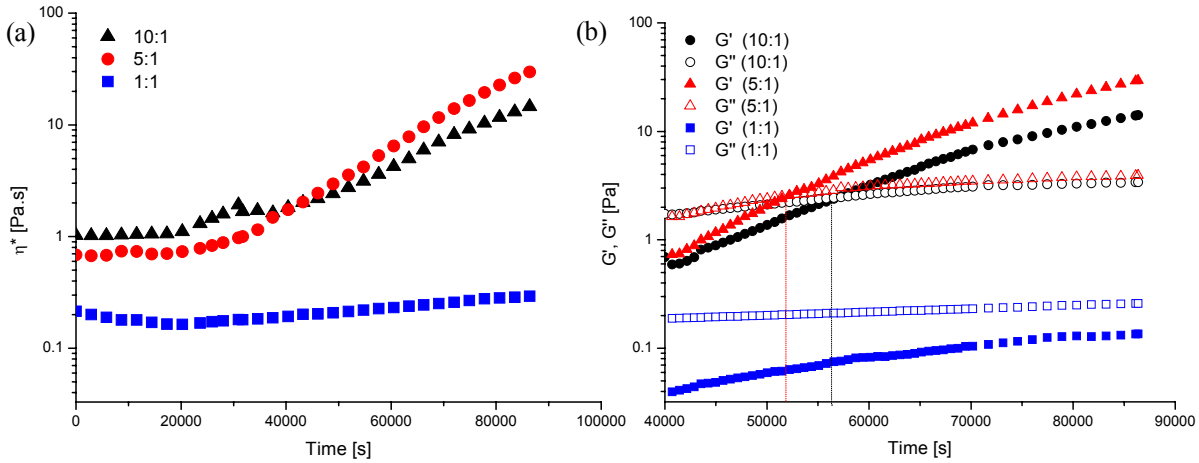

Figure 1. Complex viscosity (a), elastic modulus (G′) and viscous modulus (G″) curves (b) as a function of time at ω = 1 rad/s, shown for different ratios of PVAm/PAE (10/1, 5/1, 1/1).

Figure 2 illustrates the effect of PVAm/PAE ratio on the steady shear viscosity. Before gelation, the plot confirms that all solutions reveal shear thinning behavior like a non-Newtonian fluid and the viscosity decreases non-linearly with respect to increasing shear rate.

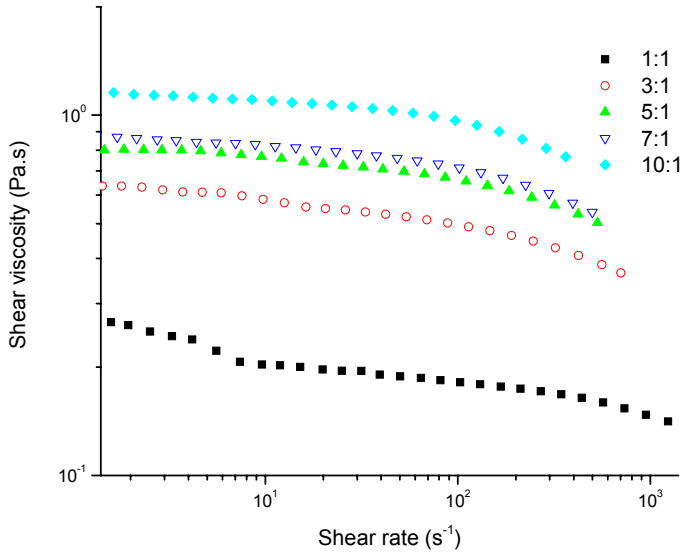

Figure 2. Comparison of steady shear viscosity dependence on PVAm/PAE blend ratio before gelation (10/1, 7/1, 5/1, 3/1, 1/).

The elastic modulus (G′) and viscous modulus (G″) were measured at a wide range of frequencies ranging from 1 to 100 rad/s for the PVAm/PAE ratio of 5:1 after 0h, 12h, and 18h (Figure 3). The plots clearly reveal the gelation and show representative behavior for a sol phase (a), a soft gel (b) and a hard gel (c) transition. The generalized Maxwell model is used to analyze dynamic oscillatory measurements, by fitting G' and G" with a unique relaxation strength (G_i) and relaxation time (λ_i) under low frequency ($\lim_{\omega \to 0}$):[41]

$$G'(\omega) = \sum_i G_i \frac{\omega^2 \lambda_i^2}{1+\omega^2 \lambda_i^2} \quad , \quad G''(\omega) = \sum_i G_i \frac{\omega \lambda_i}{1+\omega^2 \lambda_i^2} \qquad (3)$$

Below the gel point, the sol phase shows a viscoelastic liquid behavior obeying the Maxwell model where G" has a slope of 0.97 and G' has a slope of 1.6 as observed in Figure 3 (a). At the gel point, parallel lines of G' and G" are found with a viscoelastic exponent of 0.73 indicative for the formation of a critical gel[42] and, thus, the gel time can be roughly estimated to be around 12 hours (Figure 3 (b)). Figure 3 (c) shows the hard gel phase with G' > G" and a flat slope of G'.[43] Note that the fluid-like behavior of the hard gel (c) only occurs at higher frequencies. As such, the G' frequency sweep shows the chemical gelation kinetics, i.e. G'

increases in magnitude as the crosslinking progresses and G' becomes almost independent of frequency indicating hard gel conditions with increasing reaction time.

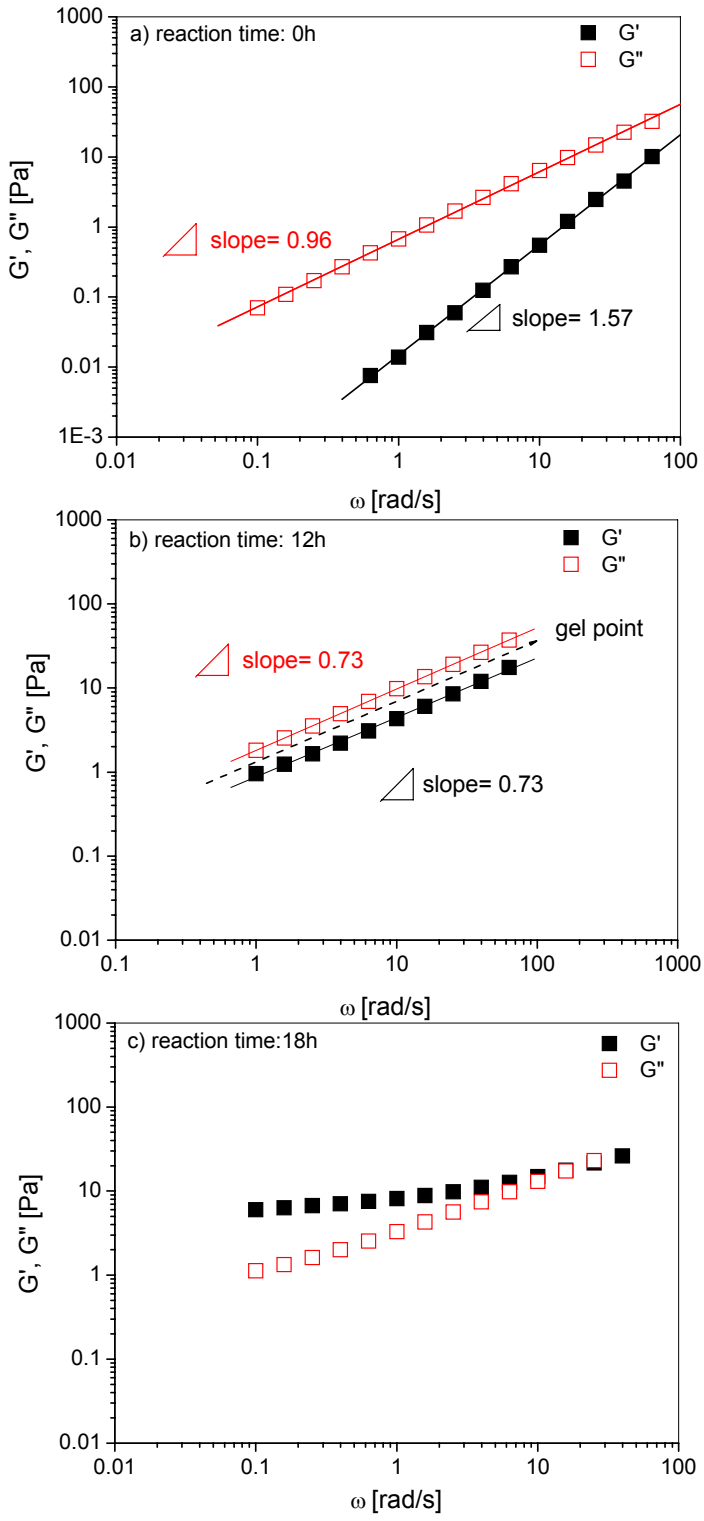

Figure 3. Dynamic frequency sweep of the elastic modulus (G′) and viscous modulus (G″) of a 5:1 PVAm/PAE blend after 0h (a), 12h (b) and 18h (c) reaction time.

Electrospinning of gelating polyelectrolyte solutions

The previously optimized conditions for electrospinning of aqueous PVAm solutions, 20kV, feeding speed of 0.5 ml/h and the tip to collector distance of 20 cm,[22] are used for spinning of PVAm/PAE solutions in this work as well. To reduce the surface tension of spinning solution, 0.1 wt% Triton X-100 is added as a non ionic surfactant. The "click" reaction of azetidinium ions with the primary amine will result in crosslinking of the electrospun nanofibers stabilizing them in water. The crosslinking will proceed faster in the electrospun fibers compared to the previously discussed solutions due to evaporation of the water and, thus, increasing concentration. Recently, Mckee *et al.* have reported that the electrospinning fiber formation is strongly affection by the polymer concentration and solution rheology. Increasing concentration results in less defects and more effective fiber formation.[35-37] In order to generate uniform fibers, the polymer concentration of the solutions should exceed the entanglement concentration at which polymer chains are overlapping to form topologically constrained chain motion.[38] On the other hand, Yu *et al.* have demonstrated that the elasticity of the polymer solution is more important for electrospinning jet stability than the number of entanglements.[39] However, during electrospinning of PVAm/PAE solutions, the viscosity will increase due to crosslinking making it difficult to predict the spinnability of the solutions. Nonetheless, it was observed that all the different compositions of PVAm/PAE can form nanofibers even though the zero shear viscosity is very different. Therefore, Figure 4 depicts SEM-images of the polyelectrolyte crosslinked nanofibers with different composition from 10/1 to 1/1 at low and high magnifications. The PVAm/PAE nanofibrous webs appear very homogenous. The average diameter of the fibers is listed in Table 1 and no noteworthy difference in fiber diameter is observed with varying PVAm/PAE ratio. However, the diameter of pure PVAm is 105 nm and PAE could not be spun while the mean diameter of the blends is 160 nm indicating that the crosslinking causes expansion of the fibers. Interestingly, the zero viscosity of PVAm (1.479 Pa.s) is higher than for the PVAm/PAE blends as shown in

Table 1 meaning that the zero shear viscosity does not directly correlate to the obtained fiber diameters. Instead the increasing elastic modulus and shear shear viscosity may be the reason that thicker fibers are obtained for the blends compared to pure PVAm. In summary, very homogenous polyelectrolyte crosslinked nanofiber webs could be prepared by an environmentally friendly aqueous electrospinning process based on PVAm and PAE. In order to demonstrate the stability of the nanofibers in water, they were immersed in distilled water for 24 hours. Figure 4 clearly shows that the crosslinked PVAm/PAE nanofibers, without any post treatment, retain the fibrous shape indirectly demonstrating that they were effectively crosslinked by the azetidinium-amine “click” reaction. However, the shape of nanofibers after dipping in water is partially deformed but the fibers still keep the fibrous morphology as expected. The diameter and topology of water exposed nanofibers is slightly increased by water swelling and drying.

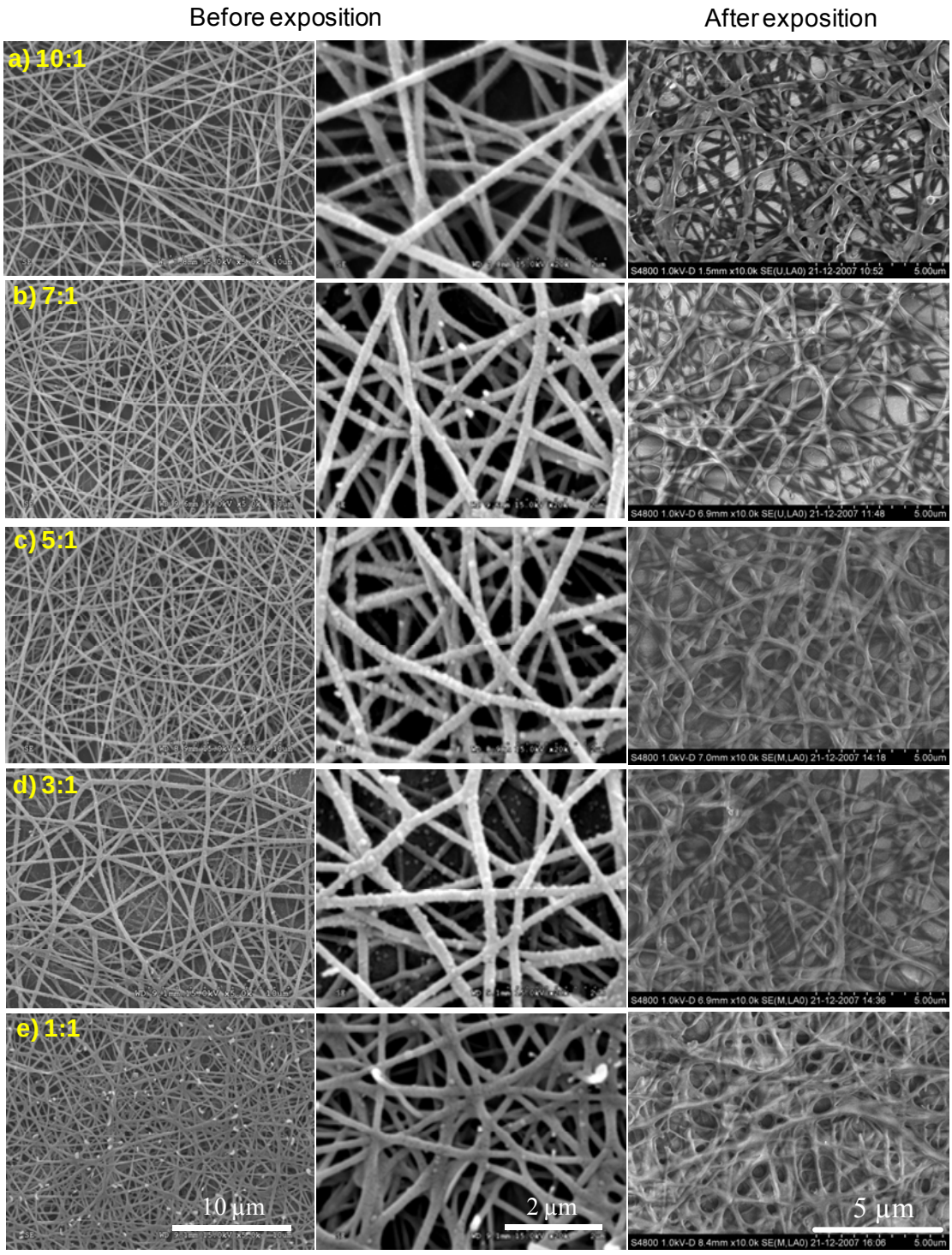

Figure 4. SEM images of PVAm/PAE crosslinked electrospun fibers (before exposition) and their water stabilization (after exposition) (a) 10:1, (b) 7:1, (c) 5:1, (d) 3:1 and (e)1:1 (spinning condition : 20 kV, 20cm 0.5 ml/h).

From a practical viewpoint, it is very important to know the maximum time that can be waited in between preparation of the PVAm/PAE solution and the electrospinning. We have already discussed the gelation time determined by rheology study, which revealed crossover points about 15 hours before the polymer solutions of 10:1 and 5:1 began to gel and a viscoelastic exponent of 0.73 indicative of a critical gel was found after about 12 hours. Electrospining of PVAm/PAE (5:1) was performed after time 0h, 2h, 4h, 6h, 10h and 12h (Figure 5). Defined fiber morphologies were observed until 10 h after mixing providing constant diameter fibers. After 12 h, it is not easy to fabricate fine nanofibers due to the elastic behavior of the critical gel related to the start of gelation as also indicated in Figure 3. The above results indicate that the electrospinning processing should be performed within 10 hours after mixing, which is enough time for fabricating nanofiber webs.

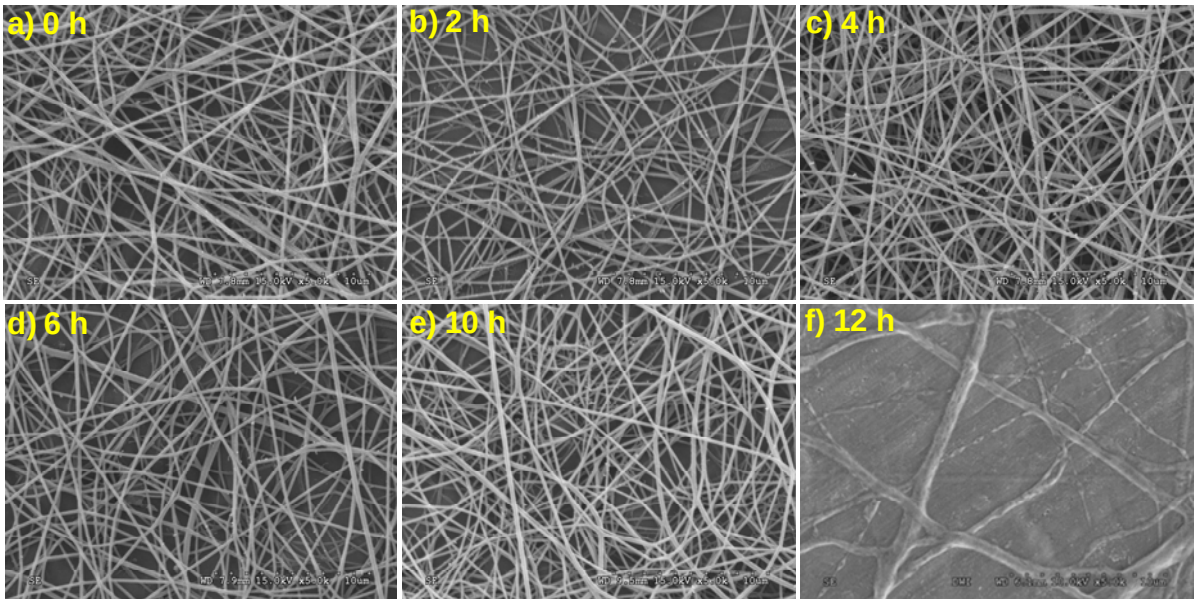

Figure 5. PVAm/PAE nanofiber morphologies of blend ratio (5:1) generated from aqueous gelating spinning solution dependence on reaction time of PVAm/PAE 0 h (a), 2 h (b), 4 h (c), 6 h (d), 10 h (e), and 12 h (f) respectively.

Water and moisture absorption behavior of polyeletrolyte crosslinked hydrogels

Water soluble polymers are able to form a water insoluble polymer network by crosslinking and such a polymer network is refered to as a hydrogel. Previously, we showed the swelling behavior of PVAm/PAE ultrathin hydrogel films on silicon surfaces prepared by layer-by-layer self-assembly.[40] Therefore, the resulting nanofibers are also expected to exhibit hydrogel properties i.e. that they absorb water into the crosslinked network of nanofibers.

The effect of crosslinking density on the swelling behavior of the crosslinked hydrogel films is shown in Figure 6. The kinetic graph in Figure 6 (a) illustrates the water absorption rate of the hydrogels in water. As the amount of PAE was increased, the absorption speed is decreased, which is due to the formation of a more dense network. The 1:1 and 5:1 blends almost reached the equilibrium water content but blend 10:1 did not reach a plateau within 24 hours and might be regarded as superabsorber. The amount of PAE in the mixtures governs the swelling behavior: less PAE results in a lower density network that can absorb a large amount of water, while, more PAE resulted in a dense network. Figure 6 (c) shows the pH responsive swelling behaviors of PVAm/PAE films revealing almost no pH dependency despite the presence of a large number of amines. Only at pH 3, the film with the 10:1 blend showed increased swelling due to protonation.

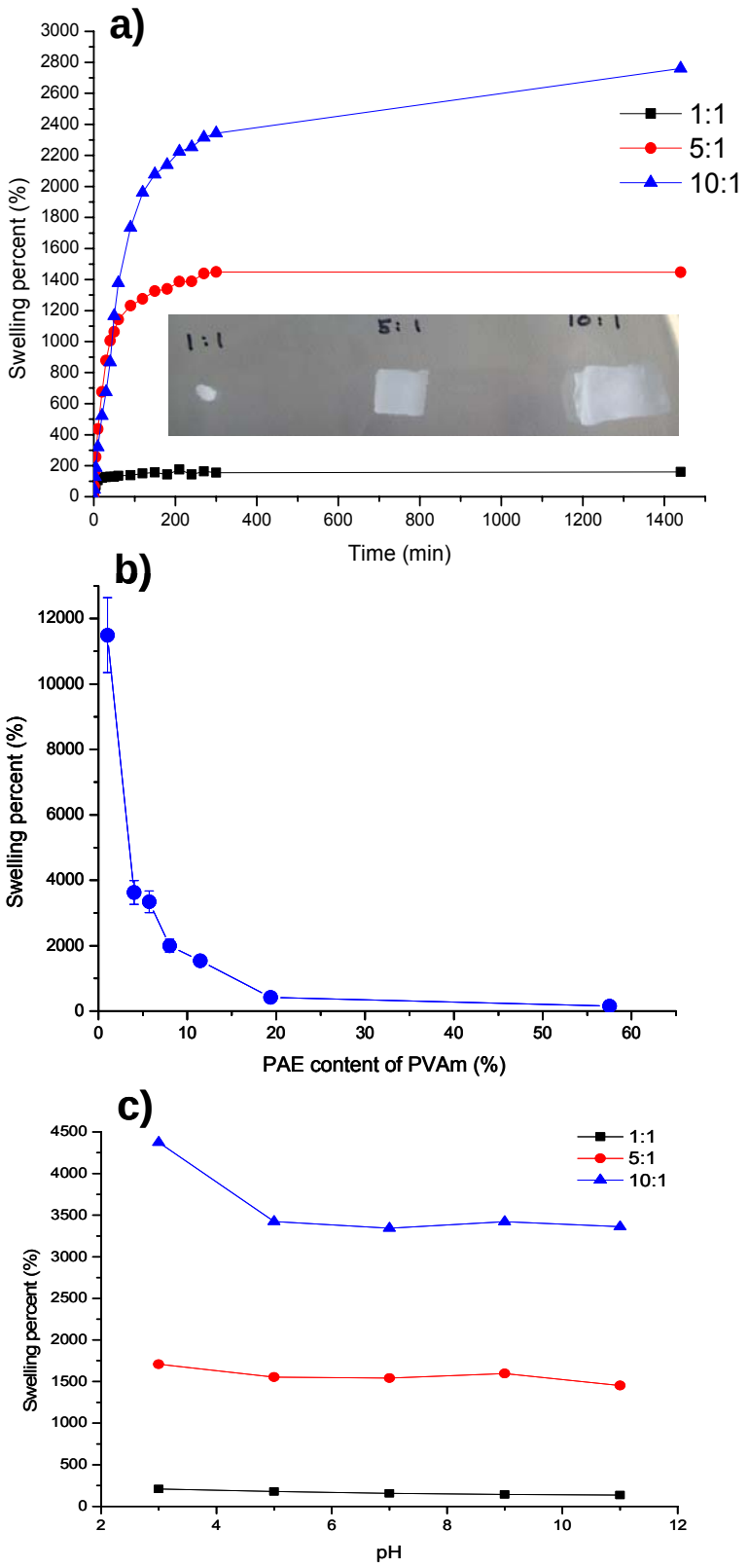

Figure 6. Hydrogel swelling behaviors of PVAm/PAE clicking crosslinked gel at different blend ratios: swelling kinetics and pictures of the swollen hydrogels (a), various amount of PAE (crosslinking density) (b), and pH response (c).

Subsequently, the water absorption of the hydrogel nanofibers was investigated. At first the moisture sorption of the nanofibers was studied by Istothermal gravimetric analysis (IGAsorp), i. e. the weight of the samples is monitored with increasing and decreasing relative humidity from 0 % to 95 %. As shown in Figure 7 (a) the PVAm/PAE 5:1 hydrogel fibres are able to absorb up to 250 % of moisture, which is 10 times more than native wool fibers. Nonetheless, the hydrogel nanofibers can even absorb a higher amount of moisture when RH keeps 95 % for a longer time. The systematic investigation of the sorption and desorption revealed some hysteresis whereby the absorption isotherm is lower than the desorption isotherm which can be related to the continued moisture sorption in between measuring the absorption and desorption isotherms in a higher starting point for the desorption measurement compared to the end point of the absorption measurement. SEM-images of the nanofibers before and after swelling are depicted in Figure 7 (b). The morphology of the nanofibers after water absorption were clearly swollen but preserved the fibrous topology. The swelling behavior of the hydrogel nanofibers in response to solution pH is shown in Figure 8 (c). Importantly, the swelling significantly increased from 450% to 800 % in acidic conditions and decreased from 450% to 250 % in basic conditions. Note that the hydrogel nanofibers did not dissolved at any pH. The increased water absorption at lower pH is due to protonation of the primary amine making the fibers more hydrophilic. The decreased swelling of the nanofibers in comparison to the bulk gels can be ascribed to the increased surface area of the fibers since the increased chain flexibility at the surface will lead to less water absorption compared to the bulk of the gels. The hydrogel fibers behave pH response and act as a smart material, in contrast to the hydrogel films where apparently protonation at the bulk of the material does not occur.

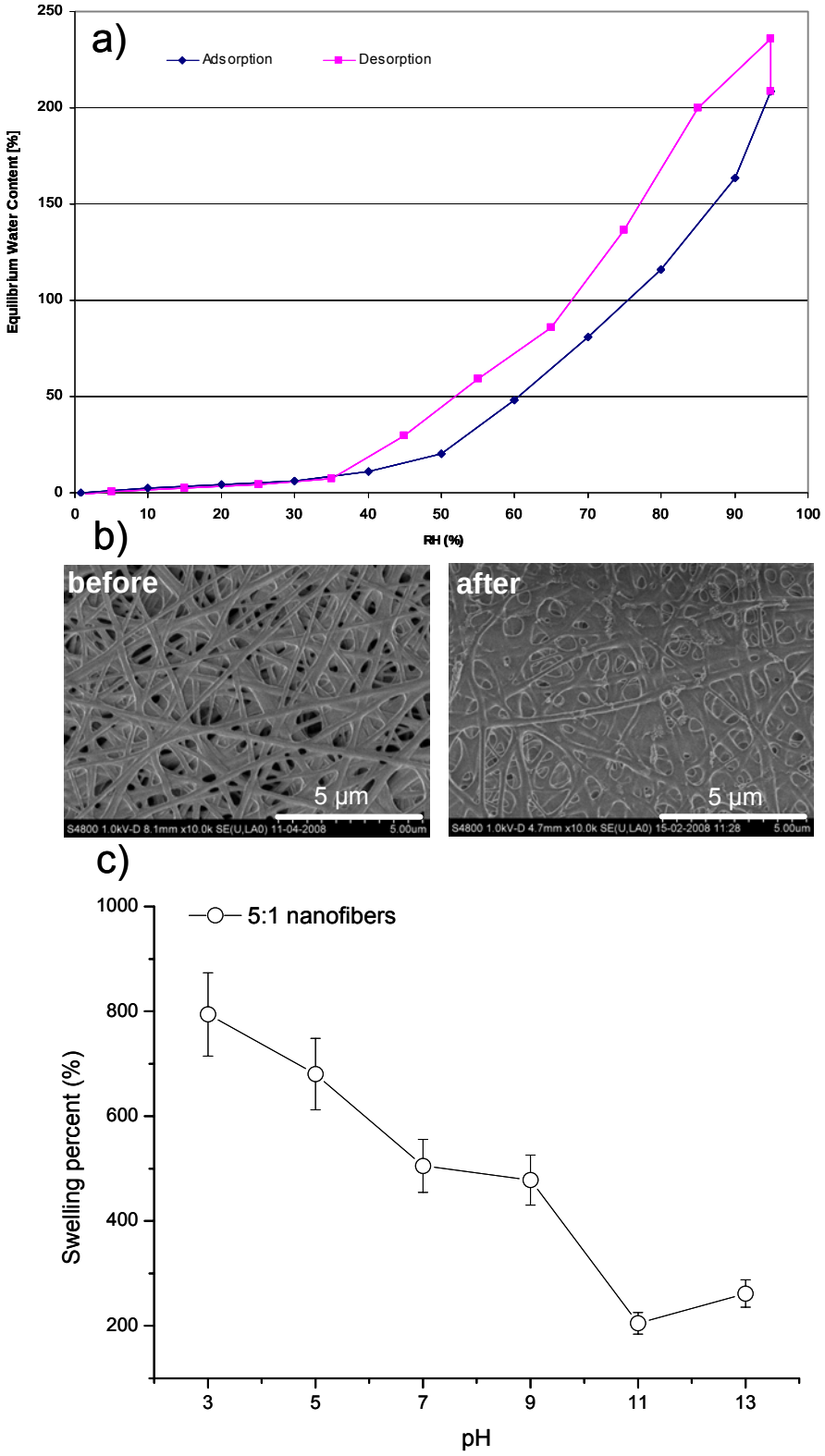

Figure 7. Moisture uptake of hydrogel nanofibers PVAm/PAE at varying relative humidity (RH) measured by Isothermal gravimetric analysis (IGAsorp) (a), SEM-images before and after moisture absorption (b), and influence of pH on the swelling behavior of the hydrogel nanofibers exposed to liquid water (c) (Error bar normalized 10 %).

Characterization of polyeletrolyte crosslinked hydrogels in bulk

Figure 8 shows the ^{13}C solid NMR MAS spectrum of PVAm/PAE crosslinked hydrogel. The broad signal of the PVAm backbone chain from CH and CH_2 groups is observed at about 47 ppm.[44] The signal is appeared all the sample blends 10:1, 5:1 and 1:1, especially blend 10:1 and 5:1show clear peak of PVAm main chain. An additional signal is observed at 165.3 ppm which is caused by the carbonyl carbons of formamide groups remaining from the parent PVFA.[42] The amide carbonyl carbons in PAE of appears at 171.9 ppm[45] and the signal in broad range of 29, 40, 44 and 45 ppm belongs to CH and CH_2 groups from PAE backbone. Obviously, less amount of PVAm decreases the peak of 47 and 171.9 ppm however, more amount of PAE shows intensity peak of 39 ppm.

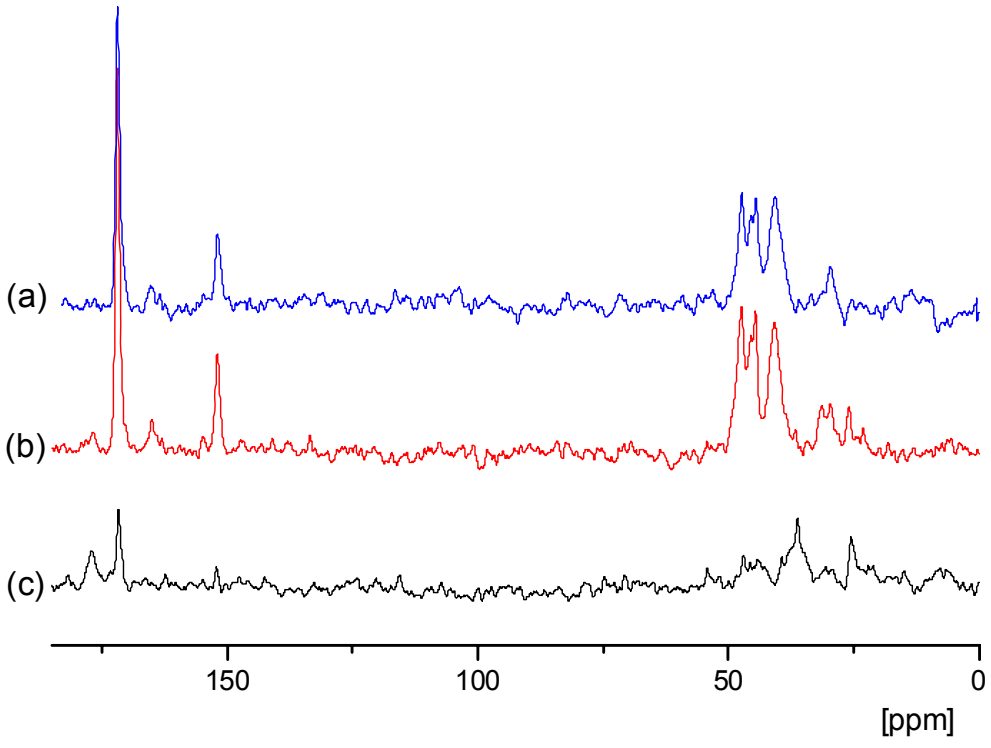

Figure 8. Solid-state ^{13}C cross-polarized magic-angle spinning (CPM-AS) NMR spectra of PVAm:PAE mixed hydrogels in volume ratio of (a) 10:1 (b) 5:1 and (c) 1:1 PVAm (Mw 340.000 g/mol, 21.5wt%), PAE (Mw 269.000 g/mol, 12.5 wt%)

Qualitative information on the crosslinking of PVAm/PAE was obtained from the FT-IR spectra, pure compounds of PVAm and PAE and after crosslinking of PVAm/PAE. Figure 9 (a) represents the FTIR spectra of PVAm and observed the signal at the ν(N–H) around 3250 cm^{-1} and δ(N–H) around 1700 cm^{-1} indicate the presence of amino groups in the PVAm. The spectra of PAE in Figure 9 (b) shows the amide bond around 3350 cm^{-1} and C=O (CONH) around 1640 and 1690 cm^{-1}. The major chemical structures pure and mixed compound are overlayed. However, the intensity of the peak at 3350cm^{-1} in Figure 9 (c) is evidently disappeared and the signal of 1700 cm^{-1} is decreased from lower than that of PVAm, suggesting a change of polymer structure after blending.

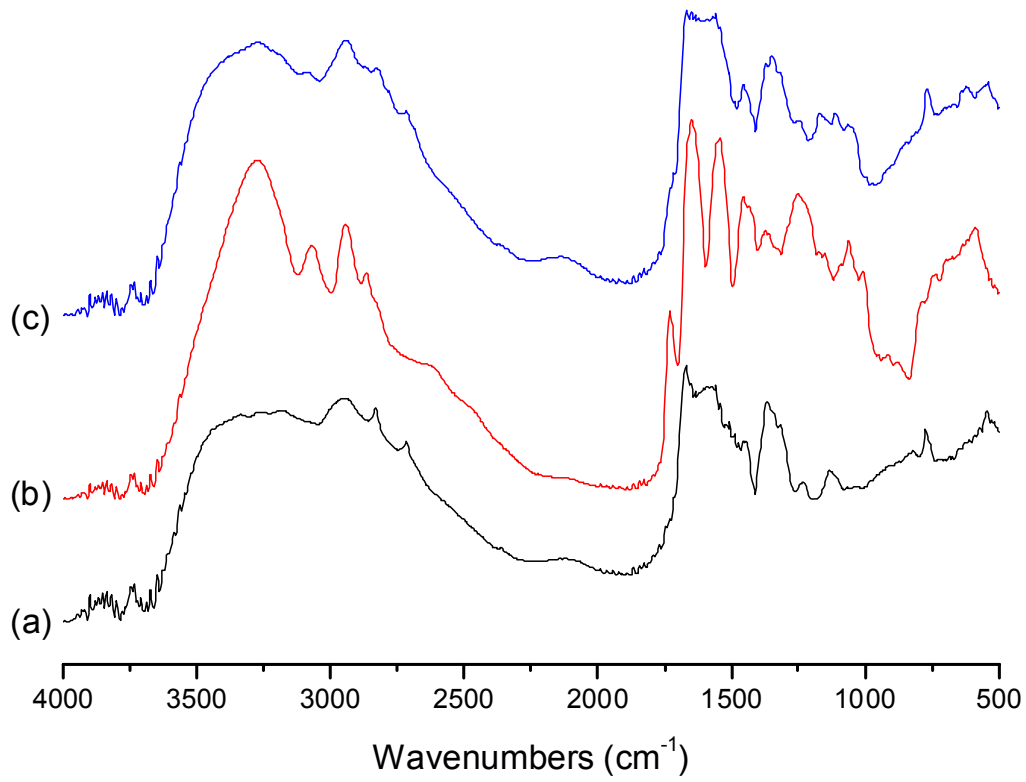

Figure 9. FT-IR spectras of (a) PVAm (Mw 340.000 g/mol), (b) PAE Mw (269.000 g/mol) and (c) crosslinked PVAm/PAE (10:1)

The TGA graph of the PVAm/PAE blend in Figure 10 shows only the decrease of sample weight by increasing temperature. The weight change of PVAm and PVAm/PAE blend suggest that PVAm/PAE blend appears slower the loss of weight at 125 ºC and shows slower thermal decomposition than pure PVAm due to crosslinking rigid. PVAm are highly crystalline , no apparent Tg was found in PVAm samples.[46] The first step corresponds to the loss of water and the water eliminated below 150°C. PVAm/PAE presents accelerating thermal decomposition behavior between 275 and 910 ºC.

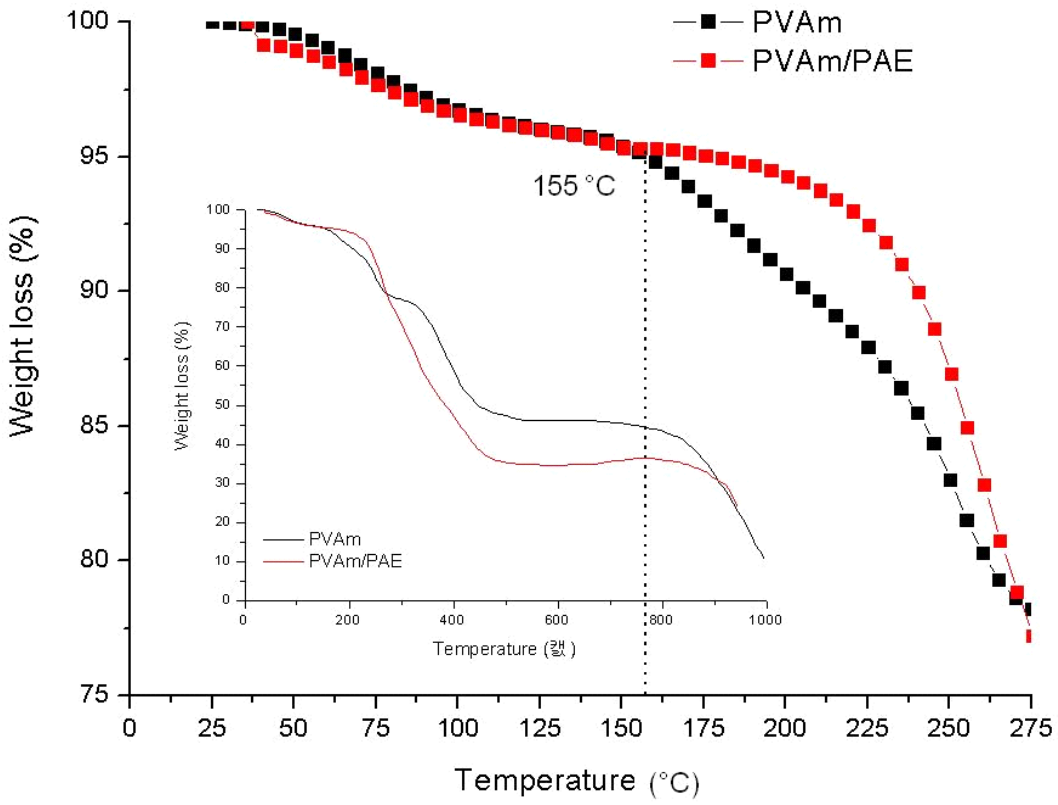

Figure 10. Weight loss of PVAm and crosslinked PVAm/PAE determined by TG analysis with heating rate 5 °C min^{-1}.

The inner-structure morphologies of frozen swollen hydrogel samples were observed by Cryo FE-SEM. Microscopic images revealed the different pore size in the network dependent on the blend ratio. Blend of 10:1 has obviously bigger pore size than blend 5:1 and 1:1 due to crosslinking density. Loose crosslinking density shows the lager pore size in Figure 11. Although the hydrogel of 10:1 was formed under ambient condition, their homogeneity was less regular than hydrogel 1:1 due to self assembly crosslinking.

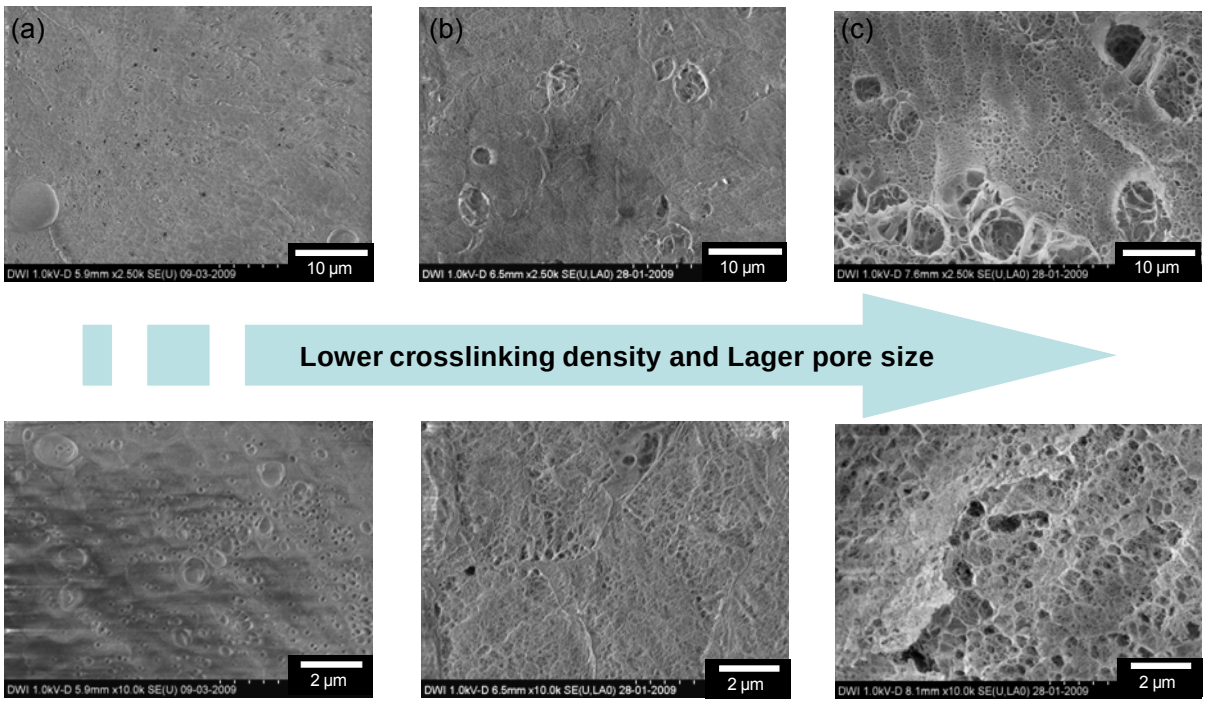

Figure 11. Cryo-FE SEM images of inner structure from different blend ratio of hydrogel (a) 1:1, (b) 5:1 and (c) 10:1 at the cross-section in bulk.

6.4 CONCLUSIONS

Crosslinked PVAm/PAE hydrogel nanofibers were prepared by an environmentally friendly aqueous electrospinning and could be performed with varying ratio of PVAm:PAE. SEM of the nanofibers showed an uniform morphology and average diameter of ~160 nm. We investigate the rheological properties of a PVAm/PAE polymer solution by examining dynamic frequency sweep to prove sol-gel transition as a function of reaction time. Blends of 10:1 and 5:1 need ~14 hours for gelation as determined by measuring the crossover point of the elastic modulus (G′) and viscous modulus (G″) curves, while the electrospinning process should be performed up to 10 hours after mixing for excellent spinnability.

The “amine-azetidinium” click reaction occurs in solutions of PVAm/PAE resulting in the formation of a crosslinked hydrogel as demonstrated by its stability upon immersion in water. As such, crosslinked electrospun hydrogel nanofibers could be prepared. The resulting nanofiber webs are swelling in water up to 800% at pH 3, up to 500% at pH 7and 250% at pH 13 demonstrating that it is a pH responsible smart materials with possible applications in wound dressing as well as superabsorbent material. In future work, we will evlauated the reactive and antimicrobial properties of PVAm/PAE hydrogel.

6.5 REFERENCES

M5 Reproduced with permission from Yu, M.; Hoogenboom, R.; Thomas, H.; Moeller, M. *manuscript in preparation.*

[1] Kolb, H. C.; Finn, M. G.; Sharpless, K. B. *Angwe. Chem. Int. Ed.* **2001**, 40, 2004.

[2] Kolb, H. C.; Sharpless, K. B. *Drug Discovery Today* **2003**, 8, 1128.

[3] Becer, C. R.; Hoogenboom, R.; Schubert, U. S. *Angew. Chem. Int. Ed.* **2009**, 48, 4900.

[4] Buck, M. E.; Zhang, J.; Lynn, D. M. *Adv. Mater.* **2007**, 19, 3951.

[5] Rostovtsev, V. V.; Green, L. G.; Fokin, V. V.; Sharpless, K. B. *Angew. Chem. Int. Ed.* **2002**, 41, 2596.

[6] Horne, W. S.; Yadav, M. K.; Stout, C. D.; Ghadiri, M. R. *J. Am. Chem. Soc.* **2004**, 126, 15366.

[7] O´Brien, P.; Phillips, D. W.; Towers, T.D. *Tetrahedron Lett.* **2002**, 43, 7333.

[8] Couty, F.; David, O.; Drouillat, B. *Tetrahedron Lett.* **2007**, 48, 1027.

[9] Bogaert, Y.; Goethals, E.; Schacht, E. *Makromol. Chem.* **1981**, 182, 2687.

[10] Guise, G. B.; Smith, G. C. *J. Appl. Polym. Sci.* **1985**, 30, 4099.

[11] Chuang, T.; Sharpless, K. B. *Org. Lett.* **1999**, 1, 1435.

[12] Kricheldorf, H. R. *J. Polym. Sci. Polym. Chem.* **1981**, 19, 2195.

[13] Obokata, T.; Isogai, A. *J. Appl. Polym. Sci.* **2004**, 92, 184.

[14] Obokata, T.; Yanagisawa, M.; Isogai, A. *J. Appl. Polym. Sci.* **2005**, 97, 2249.

[15] Asquith, R. S.; Gardner, K. L.; Mcgarel, W. S.; Otterburn, M. S. *J. Appl. Polym. Sci.* **1978**, 22, 3267.

[16] Fischer, S. A. *Tappi. J.* **1996**, 79, 179.

[17] Swerin, A.; Wågberg, L. Nordic. *Pulp Paper Res. J.* **1994**, 9, 18.

[18] Shenoy, S. L.; Bates, W. D.; Wnek, G. *Polymer* **2005**, 46, 8990.

[19] Raghavan, S. R.; Chen, L. A.; McDowell, C.; Khan, S. A. *Polymer* **1996**, 37, 5869.

[20] Pai, V. B.; Khan, S. A. *Carbohydrate Polymers* **2002**, 49, 207.

[21] S. Y. Kim, D. G Choi, S. M. Yang *Korean J. Chem, Eng.* **2002**, 19, 190.

[22] Yu, M.; Hoogenboom, R.; Thomas, H.; Moller, M. *Manuscript in preparation*, In chapter 5.

[23] Rivas, B. L.; Seguel, G. V.; Geckeler, K. E. *Die Angew. Makromol. Chem.* **1997**, 251, 97.

[24] Chen, X.; Wang, Y.; Pelton, R. *Langmuir* **2005**, 21, 11673.

[25] Roth, I.; Spange, S. *Macromol. Rapid Commun.* **2001**, 22, 1288.

[26] Mitchell, M.A.; Beihoffer, T. W.; Trzupek, L. L.; Darlington, J. W. USP 5,981,689 to Amcol. International Corporation, Nov. 9, **1999**.

[27] Hähnle, H.; Walter, M.; Tropsch, J.; Kremeskötter, J.; Schornick, G.; Anstock, T. EP0884993 to BASF AKTIENGESELLSCHAFT July. 31, **2002**.

[28] Miao, C.; Chen, X.; Pelton, R. *Ind. Eng. Chem. Res.* **2007**, 46, 6486.

[29] Xu, J.; Pelton, R. *Macromolecules* **2007**, 40, 1624.

[30] Chen, W.; Lu, C.; Pelton, R. *Biomacromolecules* **2006**, 7, 701.

[31] Diflavio, J.; Bertoia, R.; Pelton, R.; Leduc, M. *13th Fundamental research symposium*, Cambridge, **2005**, 1293.

[32] Badesso, R. J.; Nordquist, A. F.; Pinschmidt, R. U.; Sagl, D. J. *Adv. Chem. Ser.* **1996**, 248, 489.

[33] Fischer, T.; Heitz, W. *Macromol. Chem. Phys.* **1994**, 195, 679.

[34] McKee, M.G.; Wilkes, G. L.; Colby, R. H.; Long, T. E. *Macromolecules* **2004**, 37, 1760.

[35] McKee, M.G.; Hunley, M. T.; Layman, J. M.; Long, T. E. *Macromolecules* **2006**, 39, 575.

[36] McKee, M.G.; Elkins, C. L.; Long, T. E. *Polymer* **2004**, 45, 8705.

[37] Talwar, S.; Hinestroza, J.; Pourdeyhimi, B.; Khan, S. A. *Macromolecules* **2008**, 41, 4275.

[38] Yu, J. H.; Fridrikh, S. V.; Rutledge, G. C. *Polymer* **2006**, 47, 4789.

[39] Tung, C. Y. M.; Dynes, P. J. *J. Appl. Polm. Sci.* **1982**, 27, 569

[40] Yu, M.; Hoogenboom, R.; Thomas, H.; Moller, M. *Manuscript in preparation*, In chapter 3.

[41] Winter, H. H; Mours, M. *Adv. Polym. Sci.* **1997**, 134, 165.

[42] Richer, S.; Boyko, V.; Schröter, K. *Macromol. Rapid Commun.* **2004**, 25, 542.

[43] Richer, S. *Macromol. Chem. Phys.* **2007**, 208, 1495.

[44] Voigt, I.; Simon, F.; Jacobasch, H. J.; Spange, S. *Colloid Polym.Sci.* **2000**, 278, 48.

[45] Obokata, T.; Isogai, A. *J. Appl. Polym. Sci.* **2004**, 92, 1847.

[46] Deng, L.; Kim, T. J.; Hägg, M. *J. Membrane Sci*. **2009**, 340, 154.

CHAPTER 7

ANTIMICROBIAL HYDROGEL NANOFIBERS BASED ON CROSSLINKED POLY(VINYLAMINE) [M6]

ABSTRACT

Recently, we demonstrated a straightforward method for the preparation of well-defined cross-linked nanofibers by aqueous electrospinning of a solution of PVAm and poly(amide epichlorohydrin) (PAE). In the current work, the antimicrobial properties of these hydrogel nanofibers as well composite fibers with silver nanoparticles are reported. The latter were prepared by mixing of preformed silver nanoparticles with the nanofibers, whereby the primary amine groups of PVAm chelate the silver. We investigated the hydrogel and Ag-composite nanofibers on cell toxicity and cell viability by CytoTox-ONE™ and CellQuanti-Blue™. Based on these tests, the hydrogel nanofibers and films can be considered as cell toxicity free crosslinked materials. Furthermore, antimicrobial activity against gram-positive (*Bacillus subtilis*) and gram-negative (*Escherichia coli*) was evaluated by shake test and patch test. Both hydrogel nanofibers and Ag-composite nanofibers showed excellent antimicrobial activity. Thus, the hydrogel nanofibers are promising candidates for use in wound dressing.

7.1 INTRODUCTION

Microbial Microbial infestation is a continuous threat to daily living. Over the past decades, worldwide communications have reported the needs for antimicrobials and also raised increasing awareness of a hygienic life style. There are various compounds with antimicrobial properties and the high concern of infectious diseases has greatly stimulated research activities to develop new antimicrobial agents and polymers.[1-5] These substances are required to inhibit bacterial growth and to reduce the risk of infections in medical devices and healthcare-related hygiene goods. Typically, there are five major classes of antimicrobial compounds that are used in creating antimicrobial barriers: i) natural herbal compounds,[6] ii) quaternary ammonium compounds,[7-8] iii) chitosan and its derivatives,[9-10] iv) amphiphilic polycations as special class of quaternary ammonium ions,[1-3, 11-12] v) complexing metallic compounds based on silver.[13-23] Polymeric quaternary ammonium based antimicrobial materials can be synthesized from a polyamine based polymer such as poly(ethylene imine) (PEI) and poly(vinylamine) (PVAm). Pasquier *et al.* reported a new amphiphilic antimicrobial polymer based on a one-step multifunctionalization of PEI with functionalized cyclic carbonates and studied the antimicrobial effect of modified PEI by varying the hydrophilic/hydrophobic balance.[1-2] Westman *et al.* reported modified PVAm with hydrophobic C_6 and C_8 alkyl chain and evaluated the antimicrobial activity against gram-negative bacteria (*Escherichia coli*) and gram-positive bacteria (*Bacillus subtilis*).[3] Although these latter examples are based on PVAm containing secondary amines, these polymers will be protonated in aqueous solution resulting in antimicrobial activity.

Recently, we developed a method for the preparation of crosslinked hydrogel nanofibers from poly(vinylamine) (PVAm)/poly(amideamine-epichlorohydrin) (PAE) by electrospinning from aqueous solution.[25-26] For tissue engineering and medical materials the hydrophilic character and biocompatibility of the materials is very important. Moreover, the design of nanofiber scaffolds can mimic the native extracellular matrix (ECM), which is a three-dimensional

tissue consisting of fibrillar structures.[27-34] Therefore, electrospun fibrous membrane hydrogels are interesting materials as 3D scaffolds for cell growth and tissue engineering. Cross-linked hyaluronic acid (HA) hydrogel nanofibers prepared by dual-syringe electrospinning and were effectively absorbed fibronectin, which enable the cells to migrate into 3D scaffold matrix.[34] Amino group conjugated nanofiber scaffolds were investigated for surface covalent immobilization of fibronectin and hematopoietic stem/progenitor cell (HSPC) adhesion and proliferation.[31] To suppress undesired infections, the use of antimicrobial nanofibers would be preferable. Therefore, poly(ethylene glycol) (PEG) based multiblock thermoplastic polyurethanes incorporating polyhedral oligomeric silsequioxane (POSS) nanostructured hydrogel webs with or without $AgNO_3$ were reported to inhibit biofilm formation for 14 days.[19]

In this work, we investigated a simple and efficient way of generating PVAm based hydrogel nanofibers incorporating silver nanoparticle using ex situ method. Ag nanoparticles are absorbed into crosslinked PVAm nanofiber and films due to the presence of primary amine groups. The resulting Ag nanoparticle hybrid hydrogels were characterized by atomic absorption spectroscopy (AAS), energy dispersive X-ray (EDX) spectrum analysis and transmission electron microscopy (TEM). Furthermore, the reactivity of PVAm nanofibers is demonstrated by grafting 4-chloro-7-nitrobenzofurazan, which is important for further functionalization to promote cell adhesion. To evaluate the potential use of these hydrogel nanofibers, we validated the cell toxicity and viability with commercial fluorometric methods, namely CytoTox-ONE and CellQuanti-Blue. Furthermore, antimicrobial activity was examined against *Escherichia coli* (*E. coli*) and *Bacillus subtilis* (*B. sub*) by bacteria growth kinetic and diffusion test, which is important for future use of these hydrogel fibrous webs as wound dressing materials.

7.2 EXPERIMENTAL PART

Materials

All chemicals were used without further purification. Poly(vinylamine) (PVAm) technical product (Lupamin 9095) was kindly provided by BASF. The polymer was obtained as 21.5 wt% solution. The PVAm is produced by 90% hydrolysis of poly (N-vinylformamide) with a molecular weight of 340.000 g/mol. Poly(amideamine-epichlorohydrin) (PAE) was purchased from SI group and contained 12.5 wt% polymer in water. The average molecular weight of commercial PAE is 269.000 g/mol as measured by static light scattering. Silver nitrate ($AgNO_3$) and trisodium citrate ($NaC_6O_7H_5$) were purchased from Merck and the sodium borohydride ($NaBH_4$) reducing agent and 4-chloro-7-nitrobenzofurazan (NBF) were obtained from Aldrich. Ultrapure water was used as the solvent for silver nanoparticle seed solution (Milli-Q, 18.2MΩ).

Silver nanoparticle synthesis

Silver nanoparticles were prepared according to literature.[24] Ten milliliters of an aqueous silver ion solution (0.01M $AgNO_3$) was prepared and 0.5 ml of this silver ion solution was added to 19.5 ml sodium citrate (0.001M $NaC_6O_7H_5$). 0.5 ml sodium borohydride (0.001M $NaBH_4$) was added into the resulting aqueous silver ion solution and stirred for 5 min. To obtain the reduced silver nanoparticles, the reaction was stirred for 90 minutes. UV-VIS spectroscopy was used to observe plasmon resonance of the silver nanoparticles with a photometer (Varian Cary 100 Bio). The silver seed solution was filtered with a 0.2 μm aqueous membrane filter and scanned from 200 to 800 nm.

Electrospinning

Previous work on the fabrication and characterization of hydrogel nanofiber from PVAm/PAE blends has been reported in references 25 and 26. Simply mixing 5ml of poly(vinylamine) (21.5 wt% PVAm) and 1ml of poly(amideamine-epichlorohydrin) (12.5 wt% PAE) was

performed for 30 minutes before electrospinning. Triton X-100 (0.01 wt%) was added to reduce the surface tension of the aqueous electrospinning solution. Optimized electrospinning conditions were used with a voltage of 20 kV, a tip to collector distance of 20 cm and a feeding rate of 0.5 ml/h. In order to prove the reactivity of hydrogel nanofibers, 4-chloro-7-nitrobenzofurazan (NBF) was used as fluorescence dye to detect the amino-groups from PVAm/PAE nanofibers. The nanofiber webs were immersed into a solution of 0.02g of NBF in 10ml Ethanolabs for 10 min. After intensively rinsing with ethanol, the fibers were dried with a flow of nitrogen. The samples were measured by fluorescence microscopy (Axioplan Zeiss) with excitation at 467 nm and maximum emission at 528 nm.

Preparation silver/hydrogel materials

The silver/hydrogel nanofiber hybrid was prepared by simply dipping the fiber webs (0.0057g) and hydrogel films (0.0056g) into an 0.01M, silver seed solution 2ml for 5 minutes. The remaining silver seed solution was examined by UV-VIS spectroscopy and atomic absorption spectroscopy (AAS) in order to determine the silver content within the solutions. The hybrid hydrogel nanofibers were characterized by scanning electron microscopy (SEM, Carl Zeiss, S 360) and energy dispersive X-ray (EDX) spectrum analysis of silver. Furthermore, transmission electron microscope (TEM, Zeiss / Libra120) was performed to obtain images from hydrogel fibers with integrated Ag-nanoparticles.

Biological assays

CytoTox-ONE™ Homogeneous Membrane Intergrity Assay was performed following the manufacturer's protocol for cytotoxicity assay[35] and CellQuanti-Blue™ was applied as Cell viability assay kit.[36] The kits are fluorometric methods for estimating the number of non-viable cells present in 96-well plate and determining the release of Lactate dehydrogenase (LDH) from damaged cell membranes. The hydrogel nanofibers and films (0.0035g/2ml) were incubated with PBS buffer solution and culture medium for 24 hour at 37 ºC from 1 to 4

days. L929 cells were applied to control medium and incubated samples with CytoTox-ONE™ reagent incubated for 10 min and CellQuanti-Blue™ reagent incubated for 3 hours at 37 ºC. Then Cell toxicity and viability were measured by analyzing the fluorescent intensity on a fluorescence plate reader with excitation at 530-570 nm and emission at 580-620 nm.

Antimicrobial activity of the ultrathin films was performed by Schütteltest (shake test, DSMZ 347) with Gram-positive *Bacillus subtilis* (*B. sub*) and Gram-negative *Escherichia coli* (*E. coli*). The hydrogel nanofiber webs and hybrid nanofibers were sterilized at 120 ºC for 30 min and overlaid with 15 µL of a diluted suspension of bacteria in nutrient solution. After exposure, the nanofibers were incubated in a climate chamber at 25 ºC and 90 % relative humidity for 3 hours. Schütteltest was carried out with the incubated substrates shaking with 1 ml nutrient solution at 20 ºC and 150 rpm for 30 min. Afterwards, the extracted suspensions were transferred into a well plate and the optical density was measured each 30 min at 612 nm 37 ºC by using a microplate reader/incubator (GENIOS PRO, Tecan) and photometer Cary 100 (VARIAN). The bacteria growth curve was obtained by optical density by comparison with control substrate and individual monolayer polymer substrates. For supplementary antimicrobial activity, hydrogel nanofibers and Ag-nanoparticle hybrid nanofibers were tested using patch test with *E.coli* (DSMZ 498). The nanofibers were sterilized for 30 min at 110 °C and inoculated with *E.coli* for 3 h at 25 °C and 90 % relative humidity in a climate chamber. The bacteria inoculated samples were patched onto nutrient agar plates for 15 min and then removed. Afterward, the bacteria contacted agar plates were incubated overnight at 37 °C to observe the bacteria growth.

7.3 RESULTS AND DISCUSSION

Electrospinning of PVAm/PAE was performed from aqueous polymer solution at 20 kV voltage, 0.5 ml/h flow rate, and 20 cm tip-to-collector distance resulting in an average diameter of 160 nm and homogenous nanofibrous webs.[25-26] Subsequently, these nanofibers were transformed into silver hybrid nanofiers by immersion into a silver nanoparticle solution (Scheme 1).

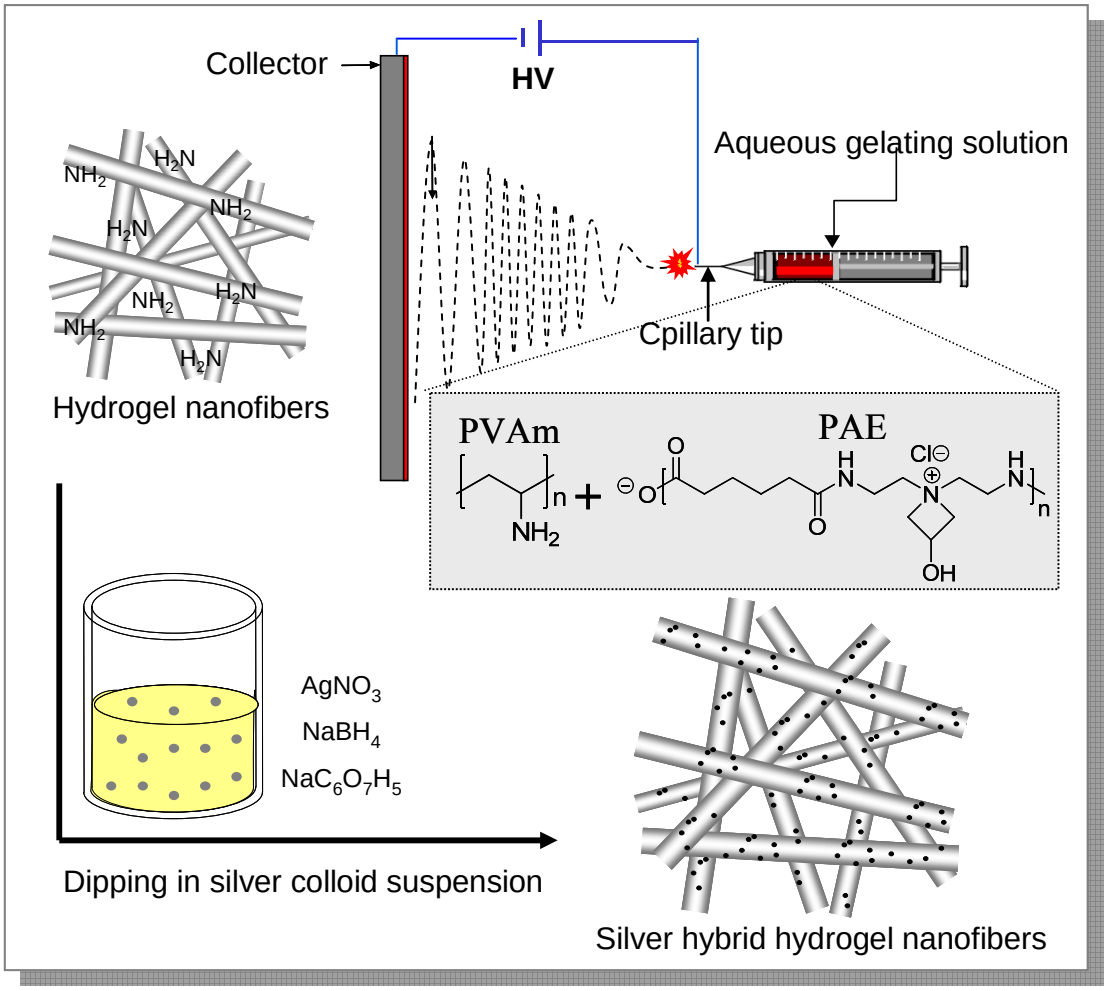

Scheme 1. Schematic representation of hydrogel nanofiber preparation by aqueous electrospinning and *ex situ* procedure for generating hydrogel nanofiber/silver NP composite.

The Ag nanoparticle suspension was prepared by the chemical reduction method, whereby an aqueous solution of citrate-protected silver nitrate (0.01M) was stirred and reduced with an aqueous solution containing 1 mM $NaBH_4$. The Ag nanoparticles had a mean diameter of 10 nm and appeared as a bright yellow colored aqueous solution as shown in Figure 1. Figure 1 also depicts a typical UV-vis spectrum of the silver colloid suspension in water, where the extinction band of the Ag nanoparticles appears at 420 nm corresponding to the plasmon resonance of small spherical silver particles.[24] The silver-hydrogel composites are prepared by 5 min dipping of the hydrogel nanofibers (0.0057g) and cast films (0.0056g) into the silver aqueous colloid solution. Comparison of the color of the solutions after dipping reveals (a) bright yellow (silver colloid suspension), (b) water-like transparent (after dipping of the nanofibers), and (c) slightly light brown (after dipping of the hydrogel films) solutions indicating that the Ag nanoparticles of the (b) and (c) solutions were extracted into the hydrogel matrix. Therefore, the UV-vis spectrum of the (b) solution was measured revealing that the signal of Ag nanoparticles disappeared. As such, by a simple dipping method, it is possible to obtain the silver-hydrogel hybrid nanofiber webs and films. Furthermore, we have measured the atomic absorption spectroscopy (AAS) to quantitatively evaluate the concentration of the silver seed solution. Figure 2 shows the silver concentration of (a) silver seed solution of 18.28 mg/l, (b) hydrogel nanofibers dipped solution of 0.0001 mg/l, and (c) hydrogel film dipped solution of 0.04 mg/l. When comparing the silver content of the (a) solution to the (b) and the (c) solutions it can be concluded that more than 99.8 % of the silver nanoparticles is embedded into the hydrogel matrix. In addition, the higher specific area of the nanofibers shows better absorption of silver nanoparticles than cast film. The resulting hybrid materials were collected and washed with distilled water to remove the residual reagent.

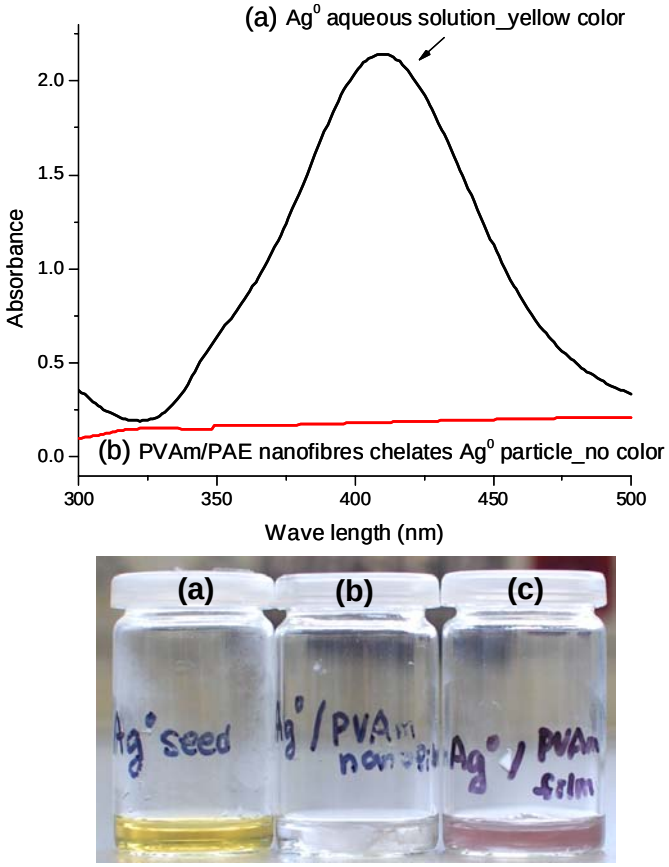

Figure 1. UV-Vis spectra of silver nanoparticle solution (a) and silver extracted solution by dipping reactive hydrogel nanofibers (b) as well as a picture of the corresponding solutions (bottom) (a) silver seed solution, (b) hydrogel nanofiber, and (c) hydrogel cast films.

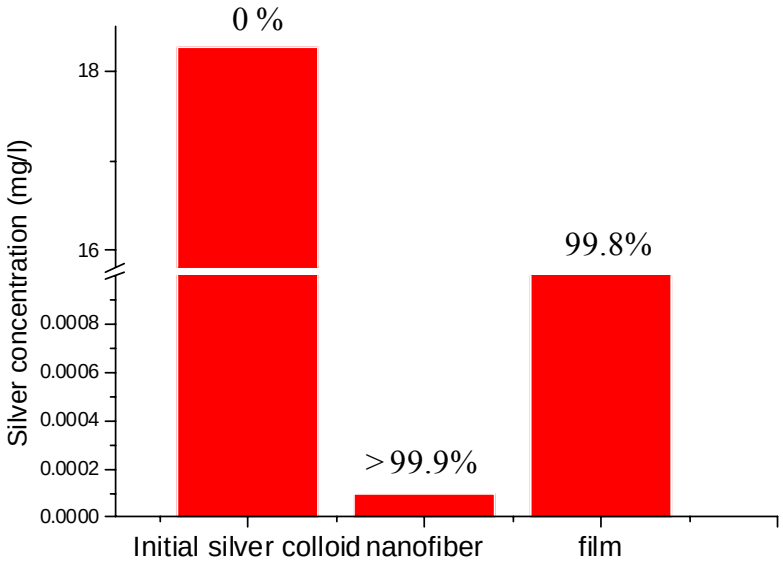

Figure 2. AAS data of Ag adsorption capacity of PVAm/PAE nanofiber webs and films.

The Ag-hydrogel hybrid webs and films were coated on silicon oxide to allow gold sputtering for measurement of SEM-EDX. The SEM images of hybrid nanofibers and cast film are shown in Figure 3 (a) and (c). In order to stimulate the emission of silver elemental from hydrogel composites, a high energy beam of X-ray is focused into the samples to produce the Ag mappings in yellow color in Figure 3 (b) and (d). The Ag mapping images demonstrate that the silver was evenly embedded on the surface of the fibers and film. EDX spectra display peaks corresponding to the energy level of specific elements. Thus, the peaks were identified for carbon, nitrogen, oxygen, silicon and silver. The presence of silver in the hybrid hydrogel was confirmed by the appearance of a peak at 3 keV. TEM micrographs of PVAm/PAE hydrogel and Ag-hydrogel composite are shown in Figure 4. Ag nanoparticles are observed as dark spherical spots and aggregates dispersed on the surface of hydrogel nanofiber. Image analysis software determined that the diameter of nanofiber and Ag-composite are 160 nm and 167 nm. The detected fine spots and the aggregates of Ag nanoparticles have an average size of 5 nm and 27 nm. Herein, we demonstrate that the PVAm/PAE hydrogel nanofibers form composites with silver nanoparticles by a simple dipping method, primary amine groups of PVAm. As such, the reactive nanofibers have the potential to form many types of metallic hybrid materials. In addition, the reactive amine groups on the surface of nanofibers can be further modified with targeting molecules drugs or markers.

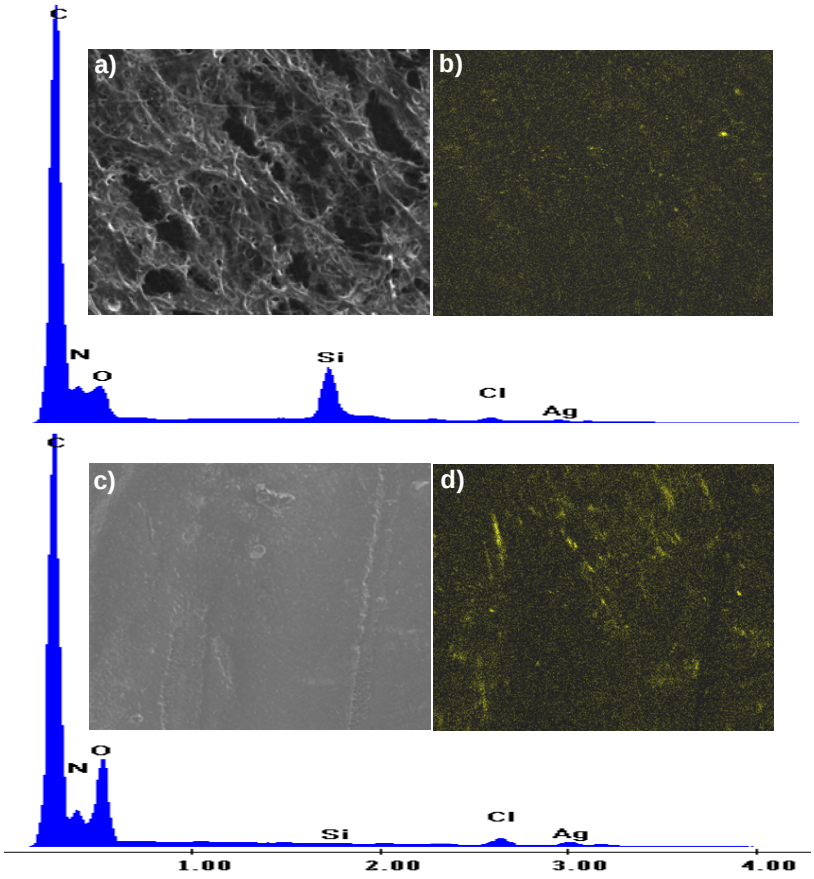

Figure 3. SEM images of the hydrogel (a) nanofibers web and (c) cast film after silver complexation and EDX mappings of (b) Ag of silver complexed nanofiber and (d) Ag of silver complexed cast film.

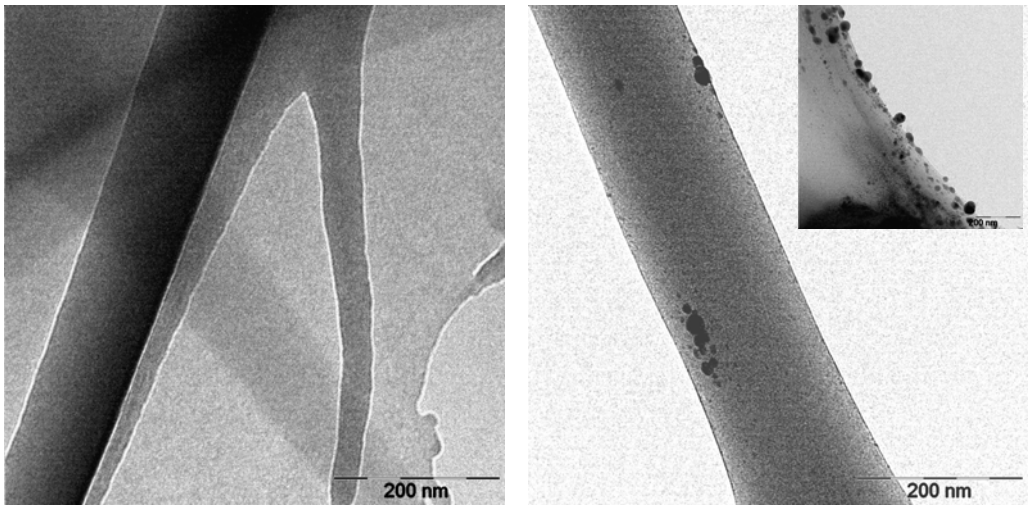

(a) (b)

Figure 4. TEM images of hydrogel nanofibers (a) and hydrogel nanofibers with incorporated silver nanoparticles.

To demonstrate the possibility of further functionalization of the PVAm/PAE nanofibers, we have investigated modification of the free amino groups in the cross-linked nanofibers network with a fluorescent derivative. The reaction of primary and secondary amines with 4-chloro-7-nitrobenzofrazan (NBF) is used to the covalent attachment and yellow fluorescence upon excitation at 467 nm with a maximum emission at 528 nm. Fluorescence images demonstrate the increase in fluorescence intensity after thorough rinsing to remove unreacted NBF, indicating the reaction of free amino groups with NBF (Figure 5).

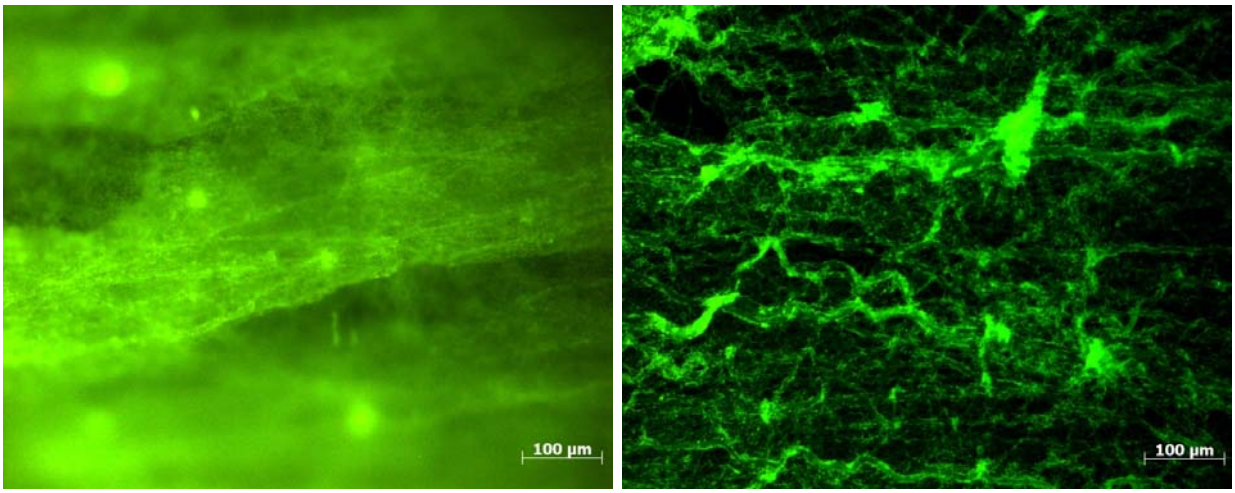

(a) (b)

Figure 5. Fluorescence microscopy images of crosslinked PVAm/PAE nanofibers (a) without and (b) with NBF to indicate the presence of reactive amino groups.

Cell cytotoxicity and viability in the presence of the PVAm/PAE nanofibers were investigated by commercial fluorometric methods that assess cell membrane integrity. Lactate dehydrogenase (LDH) is released from damaged cells and is measured by an enzymatic assay within 10 min.[35] The methods determine relative numbers of live and dead cells compared to the control cell population. Cell toxicity and cell vitality were examined using L929 mouse fibroblasts for the hydrogel nanofibers and films directly after PVAm/PAE electrospinning

and casting after 1 to 4 days (Figure 6). The results from cell toxicity show that the first day assay of nanofibers and films revealed some cell toxicity most likely due to unreacted water-soluble sol phase of hydrogel. However, the hydrogel can be considered as a purified crosslinked hydrogel after 1 day extraction of hydrogel in cell culture medium (buffer solution or water). From 2 days to 4 days, the LDH activities of hydrogel remain constant indicating that the hydrogels do not affect cell growth. Furthermore, cell vitality was evaluated using CellQuanti Blue reagent, which is a resazurin-based assay such as the Alamar Blue.[36] The redox dye resazurin is not fluorescent, but reduction by metabolically active cell makes it fluorescent. Thus, the healthy living cell reduces the reagent and the fluorescence intensity is increasing, which can be monitored by fluorescence spectroscopy. As also observed by the cell toxicity results, the cells were not very active the first day, but after the second day the fluorescence intensity was retrieved demonstrating that the cells are active and living. Mohammadi *et al.* reported the cell of PVAm nanoparticles viability using MTS test with human umbilical cord vacular endothelial cell (HUVEC), revealing an IC50 ~ 0.1 mg/ml.[37] In our study, we demonstrated that the crosslinked PVAm/PAE hydrogel nanofibers and film have relatively low cytotoxicity. Difficult to compare our results with ref 37 due to concentration. These properties may motivate the use of PVAm hydrogel as a potential biomedical material.

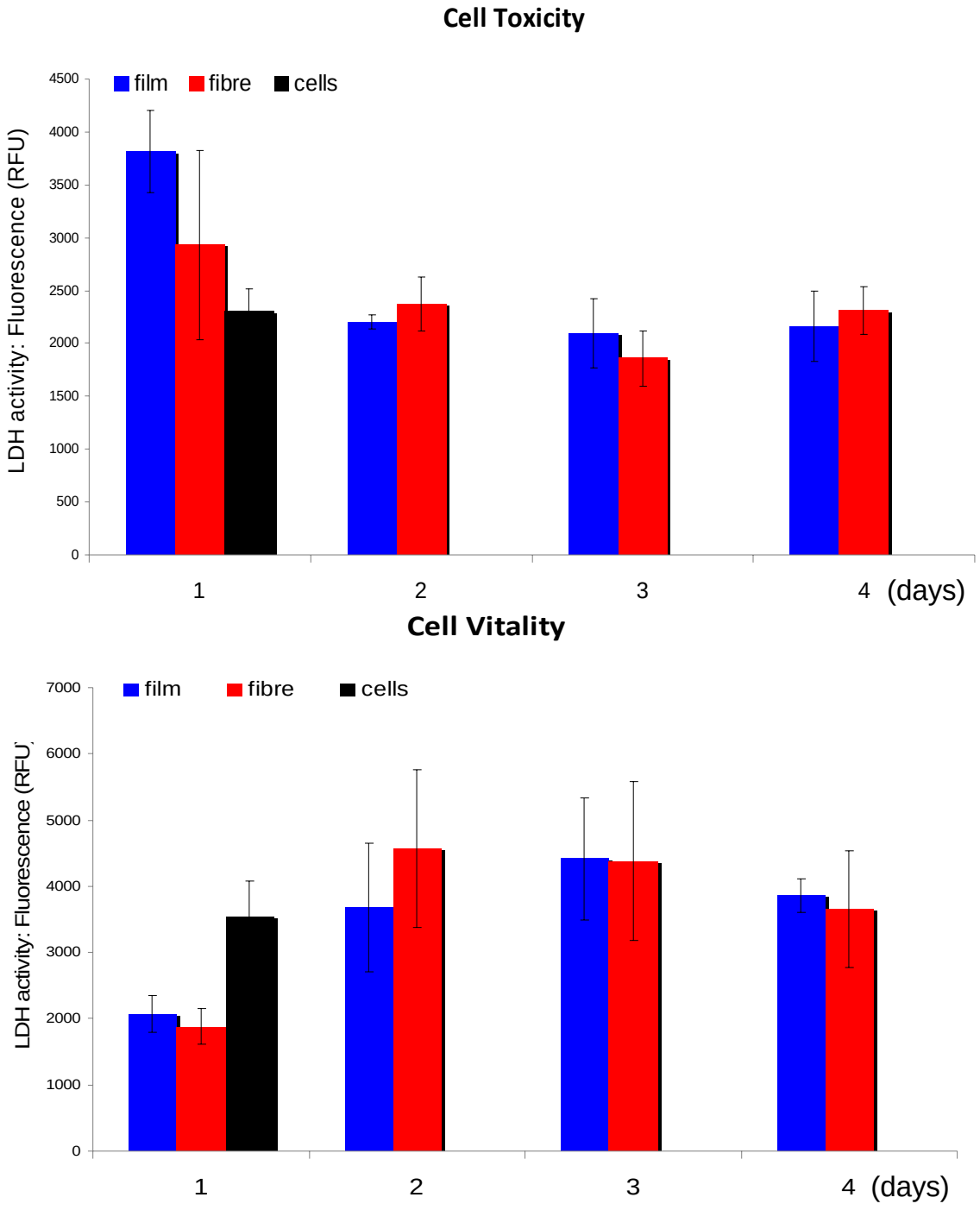

Figure 6. Cell toxicity (top) and vitality (bottom) of reactive hydrogel nanofibers studied with L292 cell for 4 days.

The antimicrobial activities of PVAm/PAE hydrogel and Ag-PVAm/PAE hybrid hydrogel were tested against *E. coli* and *B.sub* according to the shake test (Figure 7) and patch method (Figure 8). Since the nanofibers showed some cytotoxicity in the first day, the samples were washed in distilled water before measuring antimicrobial test. The kinetics of bacteria growth of a negative control (without bacteria), positive control (with bacteria), hydrogel and Ag-hydrogel showed a complete bacteria growth inhibition on the positive control, hydrogel and Ag-hydrogel against gram positive and negative bacteria. The photos in Figure 8 represent the antimicrobial activity from a patch test against gram positive bacteria *E. coli* and demonstrate the bacteria growth inhibiting effect of the hydrogel and Ag-hydrogel nanofibres. After the bacteria were in contact with the hydrogel nanofibers with or without silver, the bacterial colony was almost completely inhibited. It is well-known that silver is an antimicrobial agent already since ancient Greece and Rome. The silver ions have high activities to interact to intracellular proteins and nucleic acids of both of gram positive and negative bacteria, leading to destruction of the bacteria cell membranes.[19] Also, silver-polymer nanofibers have provided the antimicrobial efficacy with a sustained release of silver. Therefore, silver impregnated polymer materials have been interesting in the field of antimicrobial agents, biomaterials, and medical devices.[13-23] However, the complete bacteria growth inhibition for both bacteria of the unmodified PVAm/PAE hydrogels is less straightforward. Even though PVAm modified with hydrophobic alkyl chain C_6 and C_8, PVAm-C_6 was effective against *E. coli* and PVAm-C_8 was more active against *B. subtilis*,[3] unmodified PVAm showed only antimicrobial activity against *B. subtilis* ascribed to positively charged primary amines. The increased antimicrobial activity of PVAm/PAE crosslinked nanofibers in comparison to PVAm is most likely related to a combination of factors including the presence of both secondary and tertiary amines next to the primary amines as well as the presence of relatively hydrophobic moieties in the PAE. The higher amines are more basic and thus will lead to a higher charge density compared to PVAm.

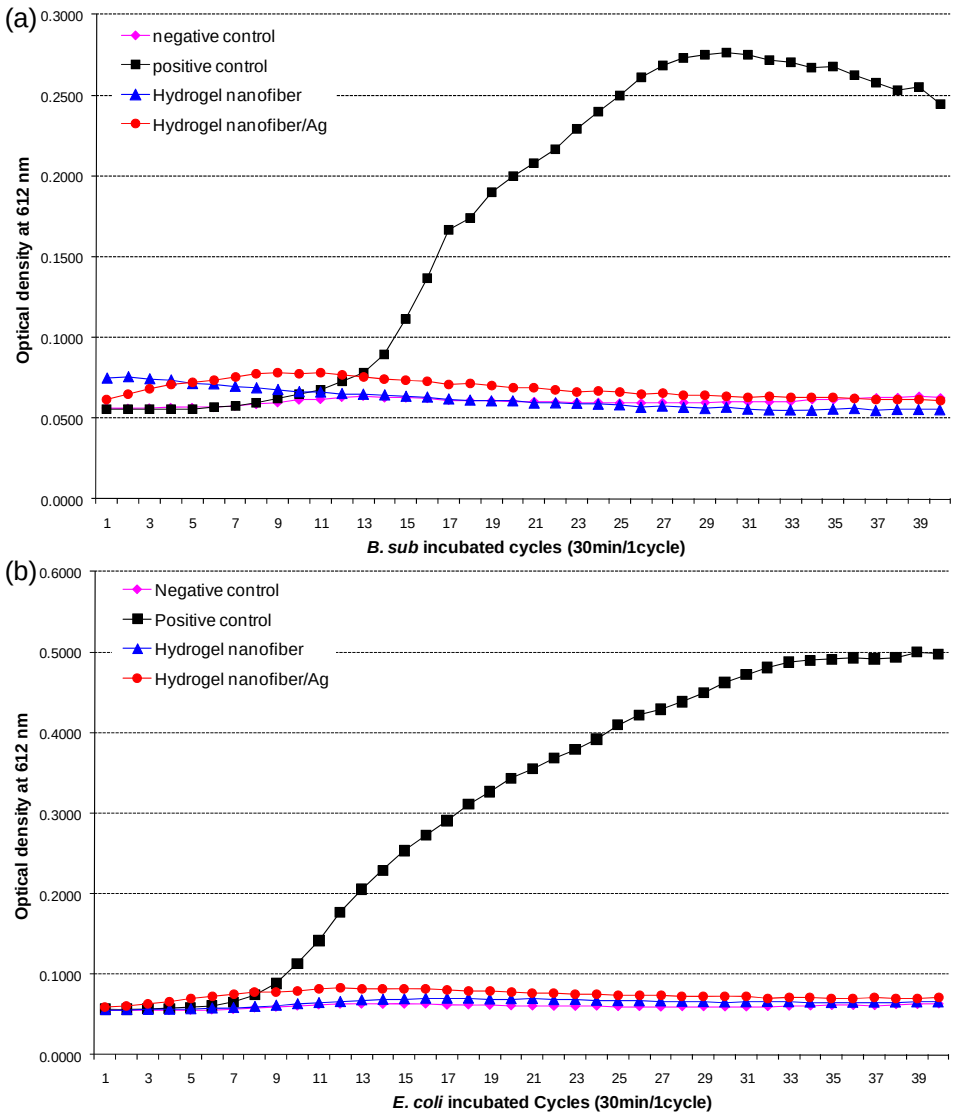

Figure 7. Antimicrobial activities of hydrogel nanofibers and silver nanoparticles functionalized nanofibers recorded on (a) *B. sub* and (b) *E. coli* growth for 20 hours.

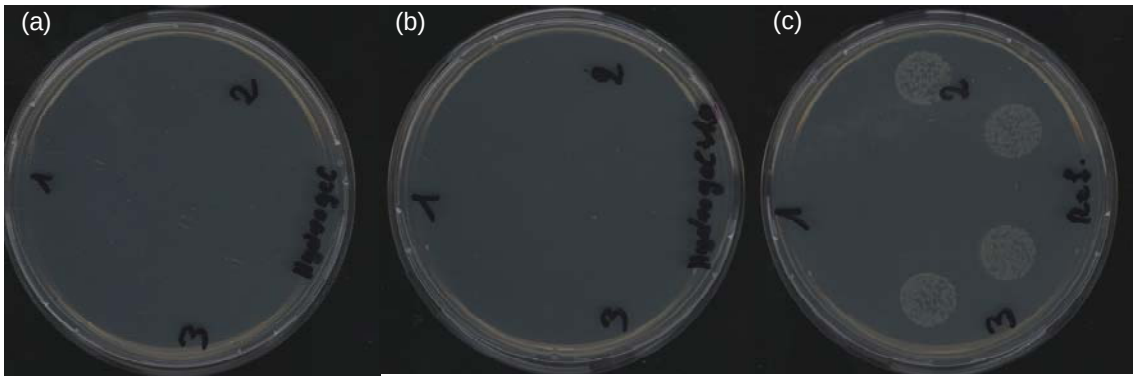

Figure 8. Antimicrobial test photographs from patch tests of the growth of *E.coli* after direct contact inoculated (a) nanofibers, (b) Ag/nanofibers, and (c) control for 20 hours.

7.4 CONCLUSIONS

We have fabricated a new class of hydrogel electrospun nanofibers exhibiting excellent antimicrobial properties and relatively low cell toxicity. The hydrogel hybrid materials with silver nanoparticles were prepared by simple dipping of the fibers or films into an aqueous silver seed solution, which consisted of silver nanoparticles with an average size of 10 nm. Antimicrobial hydrogel nanofibers composed of PVAm/PAE and Ag/PVAm/PAE inhibited bacteria growth against two different types of bacteria *E.coli* and *B. subtilis*. Furthermore, we have demonstrated that the hydrogel fiber retains reactive amino groups at the surface by reaction with 4-chloro-7-nitrobenzofurazan. It is proposed that the positively charged free primary amine groups as well as the more basic secondary and tertiary amines resulting from the crosslinking reaction between PVAm and PAE together with the relatively hydrophobic spacers of PAE provide effective resistance against bacteria growth. Therefore, the hydrogels with and without Ag nanoparticles reported in this study are valuable and useful antimicrobial biomaterials for application in wound dressings and tissue engineering.

7.5 REFERENCES

M6 Reproduced with permission from Yu, M.; Hoogenboom, R.; Thomas, H.; Moeller, M. *manuscript in preparation.*

[1] Pasquier, N.; Keul, H.; Heine, E.; Moeller, M. *Biomacomolecules* **2007**, 8, 2874.

[2] Pasquier, N.; Keul, H.; Heine, E.; Moeller, M.; Angelov, B.; Linser, S.; Willumeit, R. *Macrol. Biosci.* **2008**, 8, 903.

[3] Westman, E.; Ek, M.; Enarsson, L.; Wågberg, L. *Biomacomolecules* **2009**, 10, 1478.

[4] Tashiro, T. *Macromol. Mater. Eng.* **2001**, 286, 63.

[5] Park, D.; Wang, J.; Klibanov, A. M. *Biotechnol. Prog.* **2006**, 22, 584.

[6] Gamboea, R. W.; Chaveza, P.; Bakerb, W. P. *J. Arizona-Nevada Acad. Sci*. **2008**, 40, 165.

[7] Huang, J.; Koepsel, R. R.; Murata, H.; Wu, W.; Lee, S. B.; Kowalewski, T.; Russell, A. J.; Matyjaszewski, K. *Langmuir* **2008**, 24, 6785.

[8] Thorsteinsson, T.; Masson, M.; Kristinsson, K. G.; Hjalmarsdottir, M. A.; Hilmarsson, H.; Loftsson, T. *J. Med. Chem.* **2003**, 46, 4173.

[9] Rabea, E. I.; Badawy, M. E.T.; Steven, C. V.; Smagghe, G.; Steurbaut, W. *Biomacromolecules*, **2003**, 4, 1457.

[10] Kumar, M. N. V. R.; Muzzarelli, R. A. A.; Muzzarelli, C.; Sashiwa, H.; Domb, A. J. *Chem. Rev.* **2004**, 104, 6017.

[11] Tiller, J. C.; Liao, C. J.; Lewis, K.; Klibanov, A. M. *Proc. Natl. Acad. Sci. U.S.A.* **2001**, 98, 5981.

[12] Lin, J.; Tiller, J. C.; Lee, S. B.; Lewis, K.; Klibanov, A. M. *Biotechnol. Lett.* **2002**, 24, 801.

[13] Hong, K.H.; Kang, T. J. *J. Appl. Polym. Sci.* **2000**, 100, 167.

[14] Kong, H.; Jang, J. *Chem. Commun.* **2006**, 3010.

[15] Jin, W.; Lee, H. K.; Jeong, E. H.; Park, W. H.; Youk, J. H. *Macromol. Rapid Commun.* **2005**, 26, 1903.

[16] Son, W. K.; Youk, J. H.; Lee, T. S.; Park, W. H. *Macromo. Rapid Commun.* **2004**, 25, 1632.

[17] Lala, N. L.; Ramaseshan, R.; Bojun, L.; Sundarrajan, S.; Barhate, R. S.; Ying-jun, L.; Ramakrishna, S. *Biotechnol. Bioeng.* **2007**, 97, 1357.

[18] Barakat, N. A. M.; Woo, K.D.; Kanjwal, M. A.; Choi, K. E.; Khil, M. S.; Kim, H. Y. *Langmuir* **2008**, 24, 11982.

[19] Wu, J.; Hou, S.; Ren, D.; Mather, P. T. *Biomacomolecules* **2009**, 29, 1216.

[20] Bose, P. P.; Drew, M. G. B.; Banerjee, A. *Org. Lett.* **2007**, 9, 2489.

[21] Kuroyanagi, Y.; Kim, E.; Kenmochi, M.; Ul, K.; Kageyama, H.; Nakamura, M.; Takeda, A.; Shioya, N. *J. Appl. Biomater.* **1992**, 3, 153.

[22] Voigt, W.; Thomas, H.; Heine, E.; Moeller, M. "Electrospinning and stabilisation of Poly(vinyl alcohol) nanofibre webs with antimicrobial activity", in "Textiles for Sustainable Development", Anandjiwala, R.; Hunter, L.; Kozlowski, R.; Zaikov, G. (Eds.), Nova Publishers, New York, **2007**.

[23] Saquing, C. D.; Manasco, J. L.; Khan, S. A. *Small*, **2009**, 5, 944.

[24] Ung, T.; Liz-Marzán, L. M.; Mulvaney, P. *J. Phys. Chem. B* **1999**, 103, 6770.

[25] Yu, M.; Hoogenboom, R.; Thomas, H.; Moeller, M. *Manuscript in preparation*, In chapter 5.

[26] Yu, M.; Hoogenboom, R.; Thomas, H.; Moeller, M. *Manuscript in preparation*, In chapter 6.

[27] Kim, G.; Son, J.; Park, S.; Kim, W. *Macromol. Rapid Commun.* **2008**, 29, 1577.

[28] Tibbitt, M. W.; Anseth, K. S. *Biotech. Bioeng.* **2009**, 103, 655.

[29] Nain, A. S.; Phillippi, J. A.; Sitti, M.; Mackrell, J.; Campbell, P. G.; Amon, C. *Small.* **2008**, 4, 1153.

[30] Hoffmann, A. S. *Adv. Drug Delivery Rev.* **2002**, 43, 3.

[31] Chua, K. N.; Chai, C.; Lee, P.; Ramakrishna, S.; Leong, K. W.; Mao, H. *Exp. Hematol.* **2007**, 35, 771.

[32] Grafahrend, D.; Calvet, J. L.; Salber, J.; Dalton, P. D.; Moeller, M. *J. Mater. Sci. Mater. Med.* **2008**, 19, 1479

[33] Nisbet, D. R.; Forsythe, J. S.; Shen, W.; Finkelstein, D. I.; Horne, M. K. *J. Biomater. Appl.* **2009**, 24, 7.

[34] Ji, Y.; Ghosh, K.; Li, B.; Sokolov, J. C.; Clark, R. A.; Rafailovich, M. H. *Macromol. Biosci.* **2006**, 6, 811.

[35] www.promega.com (last accessed 21 January 2010)

[36] www.bioassaysys.com (last accessed 21 January 2010)

[37] Mohammadi, Z.; Cole, A.; Berkland, C. J. *J. Phys. Chem. C* **2009**, 113, 7652.

CHAPTER 8

SYNTHESIS OF WATER SWELLABLE HYBRID NANOGELS FUNCTIONALIZED BY SILVER NANOPARTICLES [M7]

ABSTRACT

In this work a simple one-pot preparation method for hybrid nanogels in aqueous solution is presented. Therefore, we describe the formation and characterization of croslinked polyamine nanogels as well as corresponding hybrid nanogels functionalized by silver nanoparticles. The nanogels are based on linear polyamine, poly(vinylamine) (PVAm) or branched polyamine, poly(ethyleneimine) (PEI) crosslinked with poly(amideamine-epichlorohydrin) (PAE). The nucleophilic amine groups of PVAm and PEI react with the polymeric azetidinium group leading to covalent crosslinking resulting in hydrophilic nanogels. In addition, the polyamine based nanogel enables the adsorption of silver nanoparticles. This unique straight forward preparation method for hybrid nanogels leads to a stable dispersed colloidal system. The colloids are stabilized by crosslinking and do not further agglomerate due to electrostatic repulsion of the positively charged nanoparticle surfaces.

In order to investigate the colloidal systems, dynamic light scattering (DLS) was carried out resulting particle diameters from 200 nm for to 360 nm. The hydrodynamic diameters are in good correspondence with the particle diameters observed by Cryo-FE SEM. Furthermore, in dry state the particles collapsed and TEM revealed particles with a diameter in the range of 30 nm.

8.1 INTRODUCTION

Micro/nanogels represent crosslinked polymeric particles which can be considered as hydrogels if they are composed of water soluble polymer chains.[1,2] Hydrogels are three-dimentional polymeric networks entrapping large amounts of water. This fact is among others responsible for the fact that hydrogel based materials have shown excellent properties in biomedical applications.[3] Depending on the chemical composition of micro/nanogels, they are tunable materials, which can offer biodegradability or stimuli responsive character making them useful for several applications, e.g. coating,[4] cosmetics,[5] tissue engineering,[6] biomedical implants or drug delivery.[7-9]

For a number of applications, e.g. antimicrobial coatings and contrast agents, hybrid nanogel particles containing metal nanoparticles have shown great potential.[10] In particular, the use of micro/nanogel particles as nanocarriers for the incorporation of metal nanoparticles such as gold nanoparticles,[11] silver nanoparticles,[12] and magnetic iron nanoparticles[13,14] was investigated by several goups. Pich *et al.* presented the preparation and characterization of hybrid microgels consisting of *N*-vinylcaprolactam/ acetoacetoxyethyl methacrylate/AgNP.[12] An increase of AgNP contents resulted in a decrease of the microgel size and stable colloid formation. These silver nanoparticles (AgNP) functionalized nanogels can be also employed as antimicrobial agent for hygienic surface coating. AgNP is the most well-known material for inhibiting 16 dangerous species of bacteria.[15] Aymonier *et al.* found that AgNP functionalized highly branched polyethyleneimines could be used as effective antimicrobial coatings for polar substrates.[16]

During the last decades there has been intensive research in the preparation of micro/nanogels by, e.g. controlled free radical polymerization in heterogenous media, precipitation and inverse emulsion.[1] A promising method to prepare polymeric nanoparticles is the inverse (mini) emulsion method. However, the remaining organic solvent and the surfactant are impurities, which will strongly influence the nanogel properties and thus, a workup procedure

is mandatory to purify the systems. In contrast, covalent chemical crosslinking can be also used for the preparation of polymeric nanoparticles in water.[1] In this approach the use of organic solvents and surfactances can be avoided. Bodnar *et al.* reported the synthesis of nanosized particles based on the biopolymer chitosan with natural di- and tricarboxylic acids[17] and a poly(ethylene glycol) dicarboxylic acid oligomer[18] using covalent cross-linking in aqueous media at room temperature. The condensation reaction of amino groups of chitosan and carboxylic groups was carried out using a water soluble carbodiimide coupling agent. This method prevents the use of organic solvents and surfactants, although the use of a coupling reagent is also not optimal.

Herein, we present the preparation of polyamine nanogels applying the azetidinium-amine coupling reaction in aqueous medium. Therefore, different polyamines, namely poly(vinylamine) (PVAm) and poly(ethyleneimine) (PEI), were used to undergo the nucleophilic ring opening reaction with the azetidinium groups of poly(amideamine epichlorohydrin) (PAE). Poly(vinylamine) (PVAm) is one of the simplest cationic polyelectrolyte having primary amine groups. It is commercially available and water soluble.[19,20] Polyethyleneimine (PEI) is a highly branched cationic polyelectrolyte with about 25% primary, 50% secondary and 25% tertiary amine groups.[21] Both types of water soluble polyamines act as weak cationic polyelectrolytes, but additionally they contain a number of accessible and reactive primary amino groups that can be used for nucleophilic crosslinking reactions with the azetidinium groups of commercially available PAE. Thus, micro/nanogels can be easily formed and stabilized in aqueous media.

Quiet a few publications concerning the preparation of macro/micro/nanogels from linear polyamines, are known in literature. Suh *et al.* have synthesized macrogels from PVAm by casting a polymer solution and crosslinking with bis-epoxides.[22] Yamamoto *et al.* reported thermo- and pH- responsive hydrogels from copolymers of *N*-vinylformamide and *N*-vinylisobutyramide.[23] Miao *et al.* prepared PVAm microgels crosslinked by 1,3-

divinylimidazolid-2-one to enhance wet adhesion on cellulose membranes.[24] Feng *et al.* described the swelling behavior of the polyelectrolyte complex of PVAm and carboxymethyl cellulose (CMC) as a function of polymer composition, pH and salt concentration.[25] Furthermore, hydrogels composed of PVAm have been utilized in the fields of drug delivery,[26] protein release[27] and magnetic resonance contrast enhancement.[28] Berkland *et al.* studied pH-sensitive cationic PVAm micro/nanocapsules crosslinked with 2-bis[2,2'-di(*N*-vinylformamido)ethoxy]poropane (BDEP)[26] and showed the encapsulation of lysozyme as a model for protein therapeutics.[27] Besides, iron oxide nanoparticles hybrid PVAm nanoparticles were synthesized with 100 nm diameter and a narrow size distribution.[28]

In the present work, water swellable nanoparticles were prepared by crosslinking applying azetidinium-amine coupling. The nanogel particles are based on two different polyamines, linear poly(vinylamine) (PVAm) and branched poly(ethyleneimine) (PEI), and the reactive poly(amideamine-epichlorohydrin) (PAE). In this cross-linking reaction the primary and secondary amine groups of the polyamines react with the azetidinium groups of PAE in aqueous medium. Apart from developing a simple preparation method for generating uniform nanogels in aqueous medium, the work presents the influence of molecular weight and polymer structure on the shape and size of the resulting particles. Furthermore, the synthesis of AgNP containing hybrid nanogels is presented. Stable and uniform collodial nanogels bearing AgNP could be prepared as demonstrated by DLS, electron microscopy and atomic force microscopy.

8.2 EXPERIMENTAL PART

Materials

Polyvinylamine (PVAm) technical products (Lupamin 5095, 9095) were kindly provided by BASF. The polymers were obtained from 90% hydrolysis of poly (N-vinylformamide) with a weight molecular weight of 45.000 g/mol and 340.000 g/mol and were used as received. Poly(ethyleneimine) (PEI) with an average molecular weight of 2.000 g/mol and 25.000 g/mol were obtained from Aldrich and were used as received. The poly(amideamine-epichlorohydrin) (PAE) (SI group) was purchased and has a weight average molecular weight of 269.000 g/mol determined by static light scattering. Silver nitrate ($AgNO_3$) and trisodium citrate ($NaC_6O_7H_5$) were purchased from Merck and the reducing agent sodium borohydride ($NaBH_4$) was received from Aldrich. MiliQ water was used solvent for all experiments (Milli-Q, 18.2MΩ).

Synthesis of water swellable nanogels and hybrids with Ag nanoparticles

The formation of nanogels was performed using a high speed homogenizer (11.000 rpm) to generate a homogeneous solution of water soluble polyamine (0.1 M,10 mM,1 mM, 10 ml) in continuous aqueous medium followed by crosslinking with water soluble PAE (1 g/l, 10 ml) for 10 min. To adjust the swelling behavior of the resulting nanogels, different concentrations of PAE were used.

Silver nanoparticles were prepared as a colloidal solution. 10 ml of an aqueous silver ion solution (0.01M $AgNO_3$) was prepared. In a next step, 0.5 ml of this silver ion solution was added to 19.5 ml sodium citrate (0.001M $NaC_6O_7H_5$). Subsequently, 0.5 ml sodium borohydride (0.001M $NaBH_4$) was added and the solution was stirred for 5 min. To obtain the reduced silver nanoparticles, the reaction was stirred for 90 minutes.

The synthessis of silver nanoparticles/polyamine hybrid nanogel nanostructures was performed by an *ex situ* method, i. e. first silver NP formation, followed by adsorption onto

polyamine nanogels and by an *in situ* method which involves the generation of hybrid nanogels by reduction of $AgNO_3$ in the presence of the polyamine nanogels.

Characterization of the polyamine nanogels

Z-average and intensity size distribution of the polyamine nanogels were examined by dynamic light scattering with a He-Ne laser (λ_0 = 633 nm) (DLS, Malvern Instruments: Zetasizer Nano). The DLS autocorrelation function of scattered intensity was measured in back-scattered light at the angle of 173º. All the measurements were performed at 25 ºC. The samples were filtered with 0.45 μm disposable filter. The measured data was analyzed by Cumulant approach for Z-average and hydrodynamic ratio (Rh).

UV-vis spectroscopy was used to observe plasmon resonance of the silver nanoparticles with a photometer (Varian Cary 100 Bio). The silver seed solution was filtered with a 0.2 μm aqueous membrane filter and scanned from 200 to 800 nm.

Cryo field-emission scanning electron microscopy (Cryo FE-SEM) was performed using HITACHI S-4800 instrument in a cryo-chamber with the cryo-transfer system Alto 2500 (GATAN). The nanogels were dropped into a sample holder and were quickly frozen with liquid nitrogen. The frozen sample was placed in the cryo chamber and was fractured. To avoid artefacts, the microscope images were taken from the inner-structure of frozen nanogels. Cryo FE-SEM was measured below -120 ºC.

For AFM, the polyamine nanogels were spin-coated on mica at the rotation speed of 2000 rpm for 1 min. The topology of the nanogels was studied by atomic force microscopy (AFM, Digital Instrument: Nanoscope III) using tapping mode imaging with standard silicon cantilevers (Nano world, NCH-W point probe). The force constant and resonant frequency was reported by the manufacturer as 42 N/m and 320 kHz, respectively.

Furthermore, the morphology of swollen and dried nanogels was investigated by transmission electron microscopy (TEM, Zeiss: Libra120). The polyamine nanogels were placed on 200 mesh copper grids and analyzed in the TEM immediately (swollen condition) and 24 hours later (dried condition).

8.3 Results and Discussion

The polyamine nanogels were prepared by chemical crosslinking of PVAm or PEI with PAE in aqueous medium followed by functionalization with AgNP to obtain hybrid nanogels (Scheme 1). Previously, we reported the preparation of an ultrathin hydrogel coating composed of PVAm and PAE on a silicon oxide surface by a novel type of click reaction, namely azetidinium ring-opening by reaction with amines.[29] In this work, we extend this approach to the preparation of polyamine nanopgels by azetidinium-amine coupling as "click" method in aqueous medium without surfactant and organic solvent.

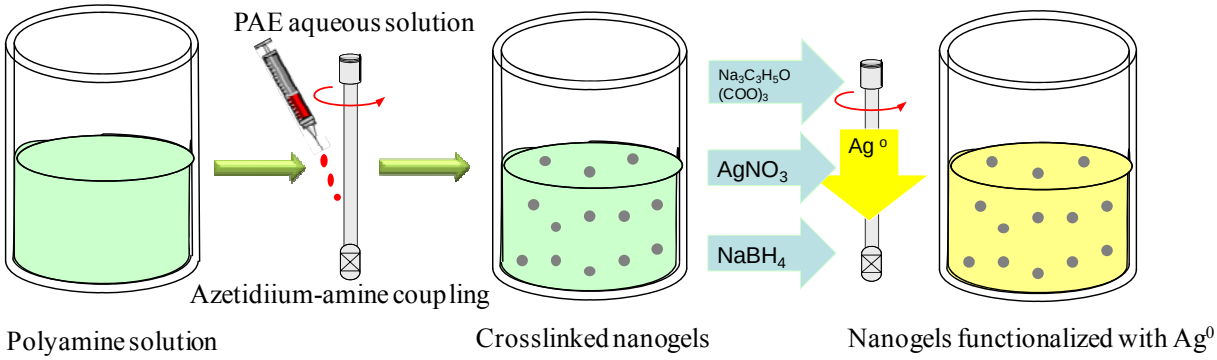

Scheme 1. Schematic representation of formation of polyamine nanogels and functionalized nanogels with silver nanoparticles (AgNP).

The Z-average size and size distribution of the starting polymers and polymeric nanogels in aqueous solution were determined by dynamic light scattering (DLS). Dynamic properties of

polymer chains in solution are complicated due to extensive chain motions as well polymer-water and polymer-polymer interactions. DLS measurements can help to understand dilute polymer solutions in terms of internal motions of the polymer coil by determining a correlation curve. Z-average size and polydispersity index (PDI) can be derived from a Cumulants analysis of the measured correlation curve. By suitable computer software an intensity-time correlation function $G_2(t)$ is calculated.[30,31]

$$G_2(\tau) = [I(t) \cdot I(t+\tau)] = A[1 + B_{exp}(-2\Gamma\tau)]$$

$$\Gamma = Dq^2, \qquad q = \frac{4\pi n}{\lambda_0}\sin\left(\frac{\theta}{2}\right), \qquad D = \frac{kT}{6\pi\eta R_h}$$

where I is the scattering intensity, t is the initial time, τ is the delay time, A is the amplitude or intercept of the correlation function, B is the baseline, D is the diffusion coefficient, q is the scattering vector, λ_0 is the vacuum laser wavelength, n is the medium refractive index, q is the scattering angle, k is the Boltzmann constant, T is the absolute temperature, η is the viscosity of the medium, and R_h is the hydrodynamic radius.

In the Cumulants approach, the exponential fitting function is extended to account for polydisperse small particles $G_2(t)$ is given by:

$$G_2(\tau) = A[1 + B_{exp}(-2\Gamma\tau + \mu_2\tau^2)]$$

Then, a multi-exponential account of $G_2(t)$ is linearized and fitted with data by applying a cumulants fit to the logarithmic correlation function:

$$y(\tau) = \frac{1}{2}\ln[G_2(\tau) - A] = \frac{1}{2}\ln\left[AB_{exp}(-2\Gamma\tau + \mu_2\tau^2)\right] \cong \frac{1}{2}\ln[AB] - (\Gamma)\tau + \frac{\mu^2}{2}\tau^2 = a_0 - a_1\tau + a_1\tau^2$$

$$Z_D = \frac{1}{a_1}\frac{kT}{3\pi\eta}\left[\frac{4\pi n}{\lambda_0}\sin(\frac{\theta}{2})\right]^2, PDI = \frac{2a_2}{a_1^2}$$

where a_1 is used to calculate the z-average size and a_2 is used to determine the polydispersity index (PDI)

In a first step, we studied the individual polymer dynamics as function of the polymer solution concentration. Figure 1 (a), (b) and (c) indicate the typical dynamics of polyelectrolyte chains.

When the interaction between polyelectrolyte chains is weak, the flexible chains are stretched in highly diluted solution. In contrast, the polyelectrolyte chains are globalized at higher concentration due to strong repulsive interactions. Thus, Z-average size is larger when the solution concentration is low and smaller when the solution concentration is high. Interestingly, the covalent crosslinked PEI/PAE nanogels revealed an increase in Z-average with increasing concentration Figure 1 (d).

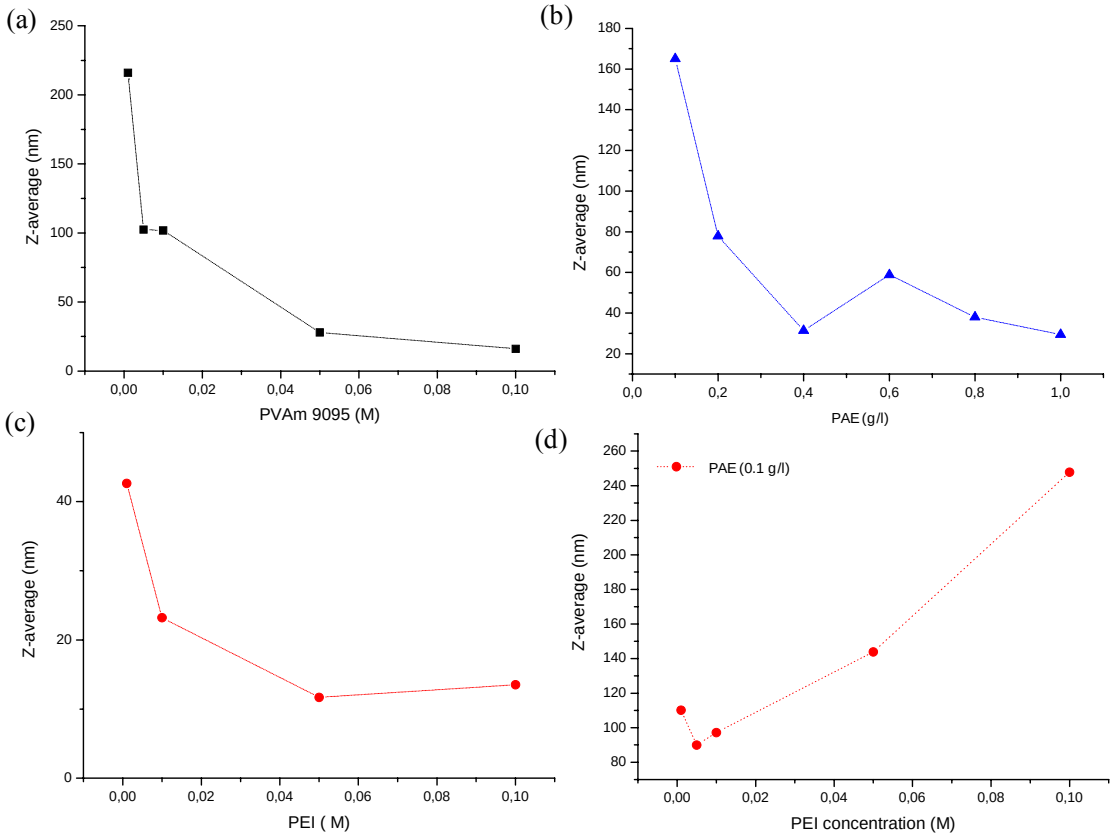

Figure 1. Z-average size of individual (a) PVAm solution (340.000 g/mol), (b) PAE solution (269.000 g/mol), (c) PEI solution (25.000 g/mol) and (d) Polyamine nanogels consisted of PEI (25.000 g/mol, 10ml) and PAE (0.1 g/L, 10ml) as function of the concentrations determined by DLS (cumulant analysis) at 25 °C in aqueous solution.

Figure 2 shows the hydrodynaminc radius of PVAm before and after high speed mechanical stirring. Before applying high speed rotation in PVAm solution, two distributions are

observed (R_h=167 and 4913 nm) most likely corresponding to individual polymer chains and aggregates. However, after high-speed mechanical stirring a narrow single distribution (R_h= 481 nm, PDI=0.399) of aggregated chanis is observed. Figure 2 (d) represents the PVAm nanogels with a narrow size distribution (R_h=350, PDI=0.243) obtained by high speed stirring and covalent crosslinking with PAE clearly indicating the successful formation of polyamine nanogels.

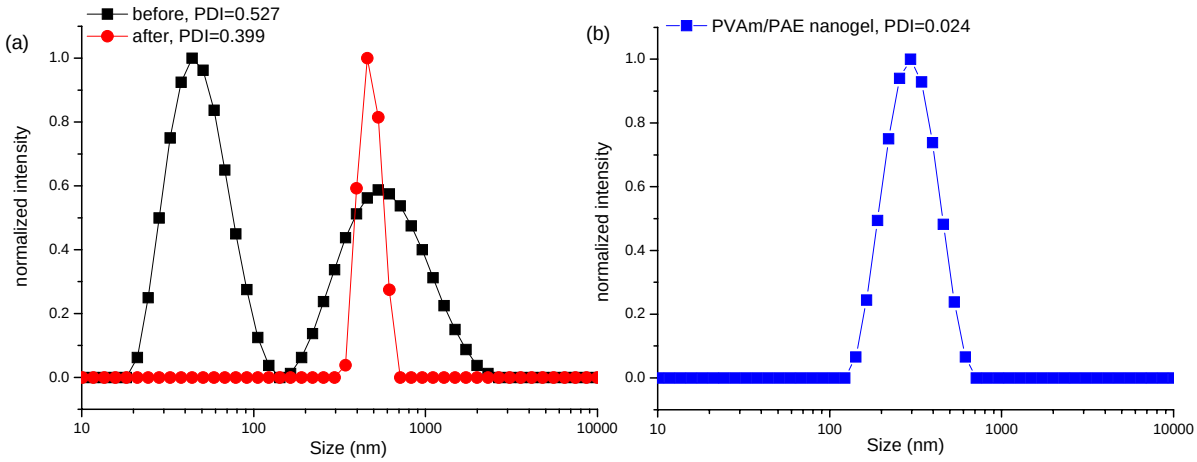

Figure 2. Z-average size of PVAm aqueous solutions (45.000 g/mol, 10ml) (a) 0.01 M before and after applying high-speed mechanical stirring at 11.000 rpm for 10 min and (b) PVAm nanogels consisting of PVAm (0.01M, 10ml) and PAE (0.1 g/L, 10ml) prepared after high speed stirring determined by DLS (CONTIN analysis) at 25 °C in aqueous solution.

The polyamine nanogels prepared by chemical crosslinking in aqueous medium show well-dispersed shape with a narrow size distribution as detected by DLS (Figure 3, 4). Regarding the influence on the molecular weight of polymer, we have studied the nanogel formation with PVAm Mw 45.000 g/mol and 340.000 g/mol and PEI Mw 2.000 g/mol and 25.000 g/mol as shown in Figure 3. Comparison of the hydrodynamic radius of the PVAm nanogel reveals that the lower molecular weight PVAm (45.000 g/mol) results in nanogels with a Z-average

size of 156 nm (PDI=0.244) and the higher molecular weight PVAm (340.000 g/mol) generates nanogels with a Z-average size of 311 nm (PDI=0.538). The size of the naogels of PVAm with 45.000 g/mol nicely corresponds to the size of the PVAm aggregates after high speed mechanical stirring (Figure 2) indicating that these aggregates template the size of the cross-linked nanogels. PVAm nanogels resulting from the lower molecular weight (45.000 g/mol) show narrower size distribution than PVAm nanogels from the higher molecular weight (340.000 g/mol). The same phenomenon was observed for PEI nanogels from PEI Mw 2.000 g/mol and PEI Mw 25.000 g/mol. The PEI nanogels of Mw 2.000 g/mol and 25.000 g/mol generate nanogels with a Z-average size of 139 nm (PDI=0.225) and 246 nm (PDI=0.400). Thus, the formation of polymeric nanoparticles is highly affected by polymer molecular weight, whereby higher molecular weight polymers tend to form larger sized particles than lower molecular weight polymers.

In addition, the influence of crosslinking density on the formation of nanogels was investigated. The ratios of PVAm or PEI with PAE were varied from 4:1 and 1:1 (Figure 4) to control the cross-linking density. The hydrodynamic radius of less dense crosslinked nanogels (mass ratio PVAm/crosslinker: 4:1) was observed to be larger than denser crosslinked gels (mass ratio PVAm/crosslinker: 1:1). Figure 4 (a) shows the Z-average sizes of 311 nm (PDI=0.538) and 177 nm (PDI=0.511) prepared from 4:1 and 1:1 of PVAm:PAE and Figure 4 (b) reveals Z-average sizes of 233 nm (PDI=0.440) and 139 nm (PDI=0.211) for nanogels prepared from 4:1 and 1:1 of PEI:PAE.

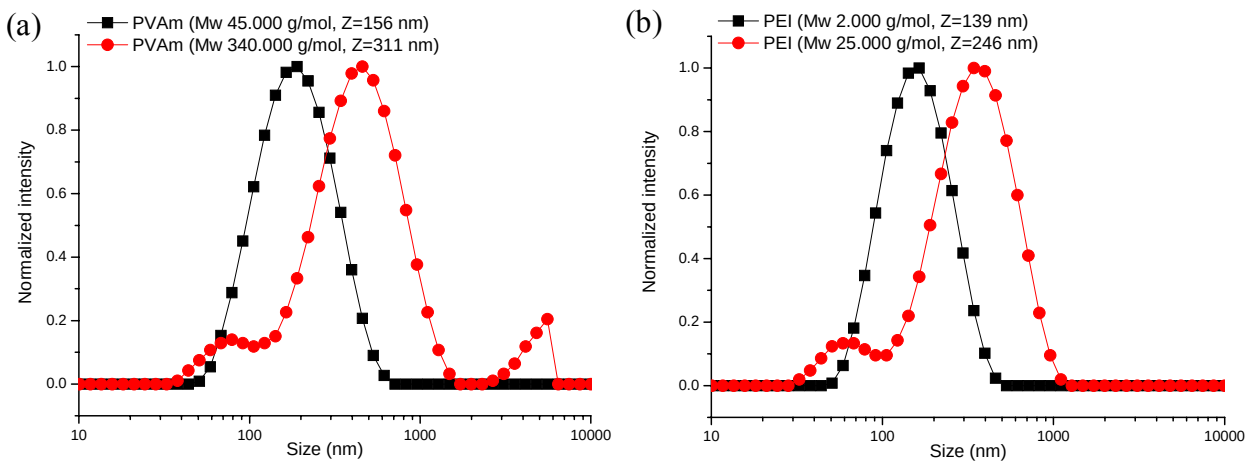

Figure 3. Z-average size of the polyamine/PAE nanogels as function of the molecular weight of polyamine; (a) linear PVAm 45.000 g/mol and 340.000 g/mol and (b) branched PEI 2000 g/mol and 25.000 g/mol prepared (CONTIN analysis) at 11.000 rpm for 10 min determined by DLS at 25 °C in aqueous solution.

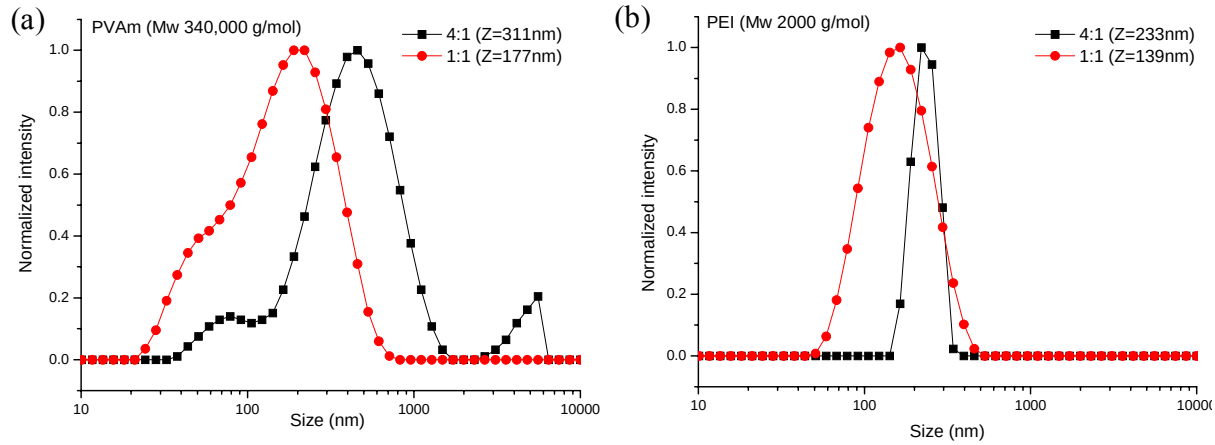

Figure 4. Z-average size of the polyamine/PAE nanogels as function of the ratio of polyamine and PAE; (a) 4:1, 1:1 (PVAm Mw 340.000 g/mol, 0.01M) and (b) 4:1, 1:1 (PEI Mw 2000 g/mol, 0.01M) prepared at 11.000 rpm for 10 min determined by DLS (CONTIN analysis) at 25 °C in aqueous solution.

The effect of crosslinking density was investigated in detail by systematically varying the PVAm:PAE ratio as shown in Table 1 and Figure 5. By increasing the PAE content, the size of the polymeric nanogels decrease from 344 nm to 237 nm, indicating the formation of denser and less swollen particles. In contrast, the PDI of sample 6 is broader compared to sample 1, which may be due to the presence of unreacted polymer chains resulting from the larger amount of PAE. By varying the ratio of PVAm and PAE, the size of particles can be controlled for specific applications.

Table 1. Conditions for the preparation of PVAm (Mw 45.000 g/mol)/PAE (Mw 269.000 g/mol) nanogels and the z-average and the polydispersity index (PDI) from DLS.

Sample	PVAm aqueous solution		PAE aqueous solution		Mixing speed (rpm)	Mixing time (min)	Z-average (nm)	PDI
	PVAm (mg)	Water (ml)	PAE (mg)	Water (ml)				
1	43	10	1	1	11000	10	344	0.12
2	43	10	2	2	11000	10	340	0.16
3	43	10	4	4	11000	10	311	0.16
4	43	10	6	6	11000	10	303	0.21
5	43	10	8	8	11000	10	272	0.27
6	43	10	10	10	11000	10	237	0.31

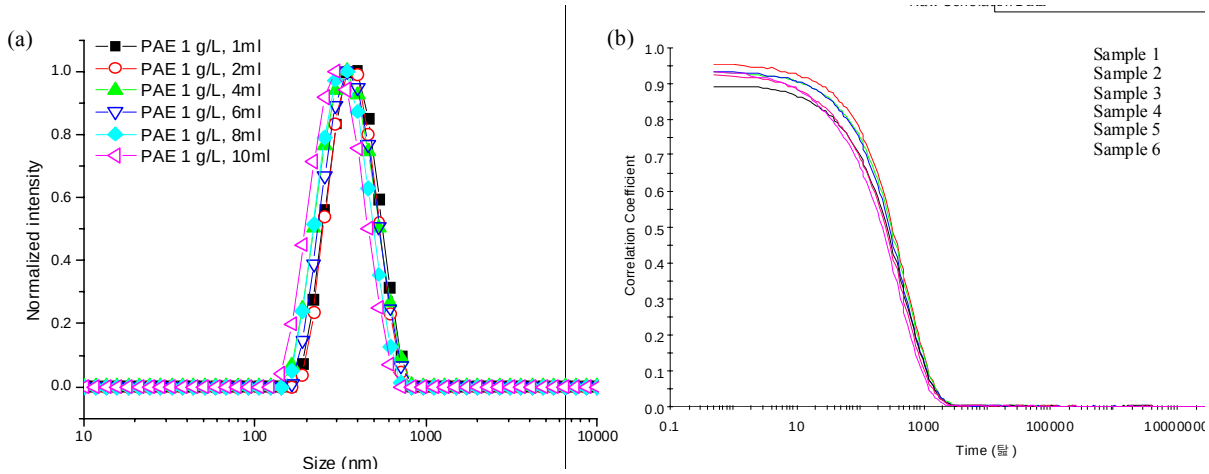

Figure 5. (a) Hydrodynamic radius (CONTIN analysis) and (b) Cumulants fit of the PVAm/PAE nanogels as function of the reacted mass ratio of PVAm (0.1M, 10ml, Mw 45.000 g/mol) and PAE (1 g/L, 1-10 ml, Mw 269.000 g/mol) prepared at 11.000 rpm for 10 min determined by DLS at 25 °C in aqueous solution.

Furthermore, different concentrations of PVAm solution with constant amount of PAE were investigated (Table 2 and Figure 6). The most-defined nanogels were obtained with sample 2 (0.05 M PVAm) and 3(0.01 M PVAm) with PAE (1 g/L, 5 ml). The resulting particles have a Z-average size of 179nm and 163 nm with a PDI of 0.29 and 0.28. The excess amount of PVAm in sample 1 or excess of PAE in samples 4 and 5 result in broad polydispersity, which emphasizes the importance of the reaction ratio.

Table 2. Conditions for preparation of PVAm (Mw 45.000 g/mol) /PAE (Mw 269.000 g/mol) nanogels and the z-average and the polydispersity index (PDI) from DLS.

Sample	PVAm aqueous solution		PAE aqueous solution		Mixing speed (rpm)	Mixing time (min)	Particles size (nm)	PDI
	PVAm (mg)	Water (ml)	PAE (mg)	Water (ml)				
1	43	10	0.5	5	11000	10	101	0.68
2	21.5	10	0.5	5	11000	10	179	0.29
3	4.3	10	0.5	5	11000	10	163	0.28
4	2.15	10	0.5	5	11000	10	160	0.42
5	0.43	10	0.5	5	11000	10	135	0.48

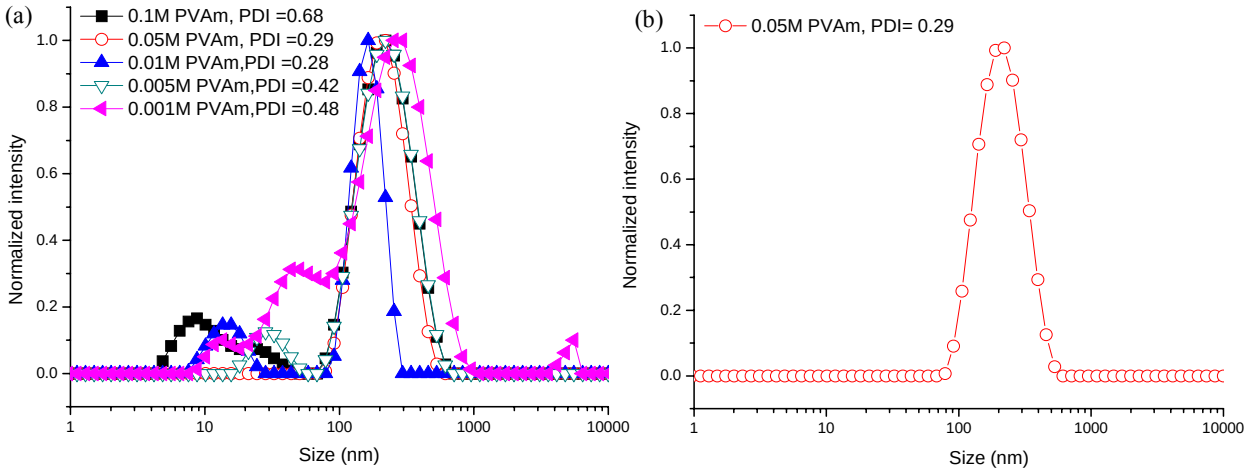

Figure 6. (a) Hydrodynamic radius of PVAm/PAE nanogels as function of the ratio of PVAm (0.1M- 0.001M, 10ml, Mw 45.000 g/mol) and PAE (1 g/L, 5 ml, Mw 269.000 g/mol) and (b) narrow size distribution of nanogel consisting of PVAm (0.5M, 10ml, Mw 45.000 g/mol)/PAE (1 g/L, 5 ml, Mw 269.000 g/mol) prepared at 11.000 rpm for 10 min determined by DLS (COTIN anaylsis) at 25 °C in aqueous solution.

For the preparation of PEI nanogels, the ratio of PEI and PAE revealed a similar influence as was found for PVAm/PAE, the ratio of the polymers is important to obtain defined nanogels. Table 3 and Figure 7 summarize the reaction conditions as well as the obtained particle size and PDI. Sample 4 with 0.005 M PEI yielded the most-defined nanogel with a PDI of 0.32 and a Z-average size of 105 nm.

Table 3. Conditions for preparation of PEI (Mw 2.000 g/mol) /PAE (Mw 269.000 g/mol) nanogels and the z-average and the polydispersity index (PDI) from DLS.

Sample	PEI aqueous solution		PAE aqueous solution		Mixing speed (rpm)	Mixing time (min)	Particles size (nm)	PDI
	PVAm (mg)	Water (ml)	PAE (mg)	Water (ml)				
1	43	10	0.5	5	11000	10	97	0.46
2	21.5	10	0.5	5	11000	10	118	0.57
3	4.3	10	0.5	5	11000	10	115	0.52
4	2.15	10	0.5	5	11000	10	105	0.32
5	0.43	10	0.5	5	11000	10	92	0.50

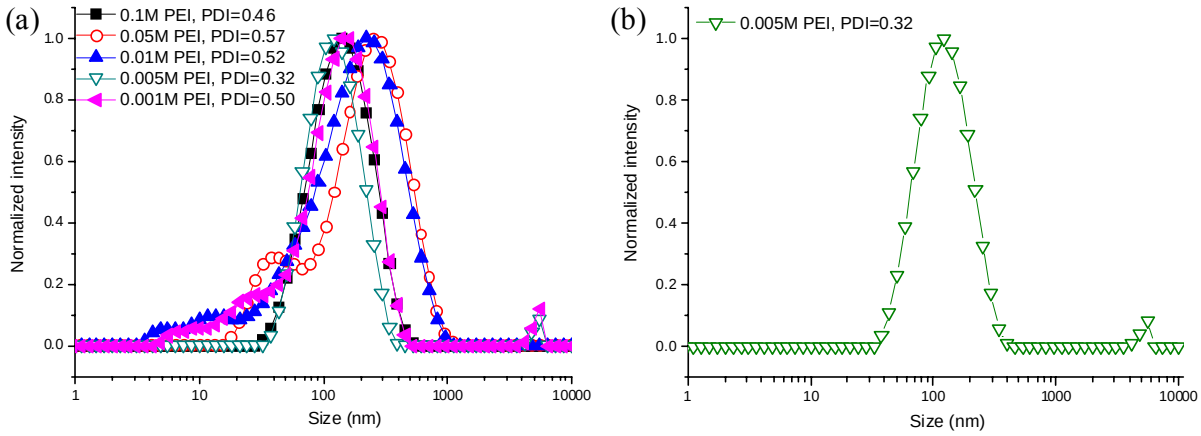

Figure 7. (a) Hydrodynamic radius of PEI/PAE nanogels as function of the ratio of PEI (0.1M- 0.001M, 10ml, Mw 2.000 g/mol) and PAE (1 g/L, 5 ml, Mw 269.000 g/mol) and (b) narrow size distribution of nanogel consisting of PEI (0.005M, 10ml, Mw 2.000 g/mol)/PAE (1 g/L, 5 ml, Mw 269.000 g/mol) prepared at 11.000 rpm for 10 min determined by DLS (CONTIN analysis)at 25 °C in aqueous solution.

Microscopic techniques are powerful tools to investigate the morphology of nanogels. Electron microscopy includes diffraction, reflection, and refraction of electron beam interacting with the matter, following by the subsequent collection of the scattered radiation to build up the image. We have chosen different microscopic techniques to study the morphology of polyamine nanogels in swollen and dried conditions using cryo field emission scanning electron microscopy (cryo FE-SEM), transmission electron microscopy (TEM) and atomic force microscopy (AFM). To visualize the nanogels in the swollen condition, cryo FE-SEM was employed by evaluating the frozen samples. Figure 8 (a) and (c) show the PVAm nanogels, which was measured from a frozen colloid solution (a) or dip coated on mica (c). The nanogels were observed as spherical particles with a diameter up to 400 nm in Figure 10 (a) and as homogenous distribution of spherical nanoparticles with an average size of 140 nm in Figure 8 (c). The larger size observed in the frozen liquid is not a statistical size since only a few particles could be captured. We could observe the formation of some aggregates but mainly individual particles. Furthermore, PEI nanogels are shown in Figure 8 (b) and (d). Similar to the morphology of PVAm nanogels, the SEM images depict spherical particles, although more aggregates are presented compared to PVAm nanogels. These SEM results clearly demonstrate the successful formation of hydrogel nanoparticles based on PVAm and PEI by the azetidinium-amine coupling as crosslinking reaction.

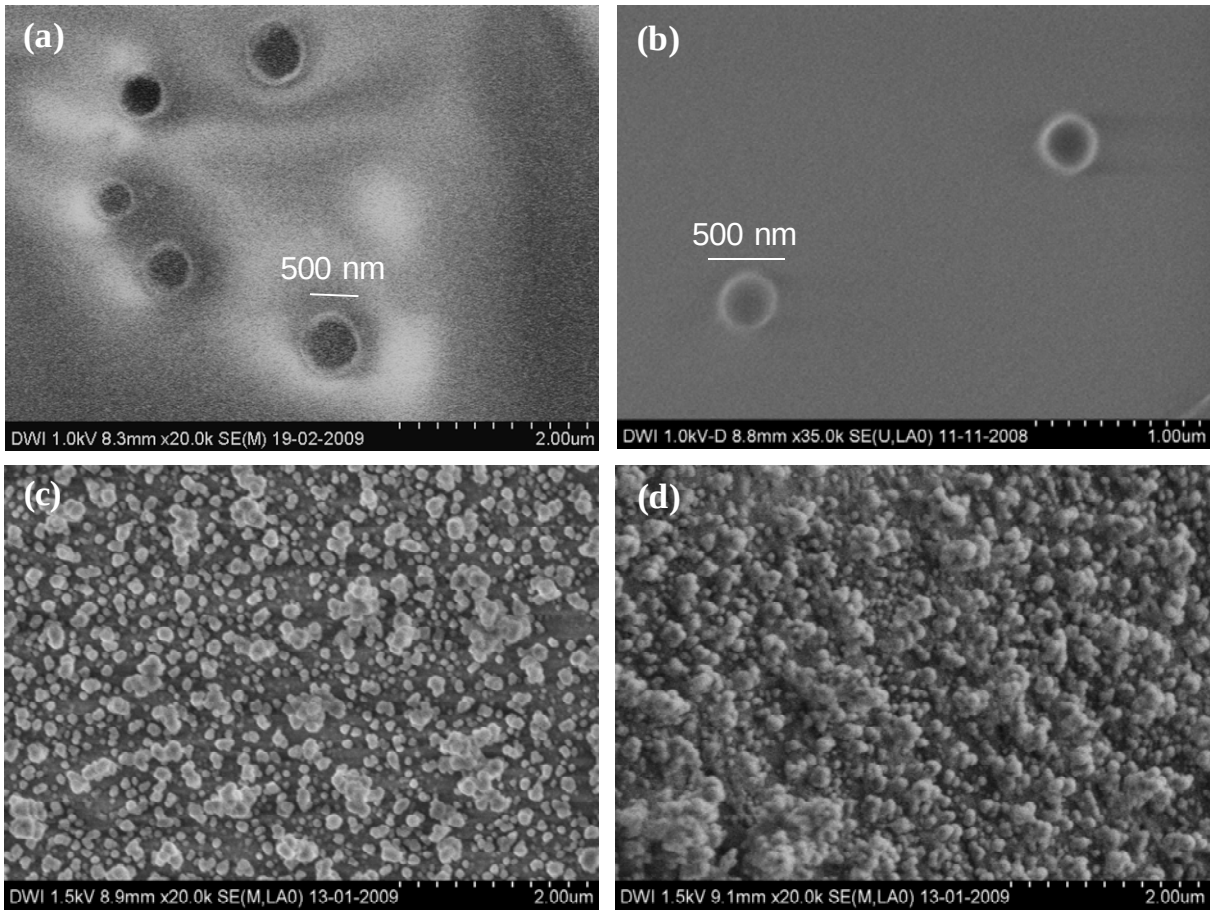

Figure 8. Cryo FE-SEM images of (a) and (c) PVAm nanogels composed of PVAm (0.01M, 10ml, Mw 45.000 g/mol) and PAE (1 g/L, 10 ml, Mw 269.000 g/mol), (b) and (d) PEI nanogels based on PEI (0.01M, 10ml, Mw 2.000 g/mol) and PAE (1 g/L, 10 ml, Mw 269.000 g/mol) prepared by freezing the solution (a+b) or a dip-coated sample on mica (c+d) in liquid nitrogen.

Transmission electron microscopy (TEM) also provided the morphology of polyamine nanoparticles. The PVAm nanogels were synthesized by mechanical stirring of PVAm (0.1M, 10 ml, Mw 45,000g/mol) followed by dropping PAE (1g/L, 10 ml, Mw 269,000g/mol) for 10 min. The TEM sample was prepared on a copper grid by dropping of PVAm nanogel colloids and kept in air for 10 min to evaporate the solvent. TEM images in Figure 11 clearly show PVAm nanogels. PVAm hydrogel nanoparticles were measured directly after sample

preparation representing the swollen state with an average diameter of 150 nm in aqueous medium (Figure 9 (a)). The exactly same sample was measured by TEM 2 days later and we observed collapsed of nanogels with an average diameter of 30 nm (Figure 9(b)).

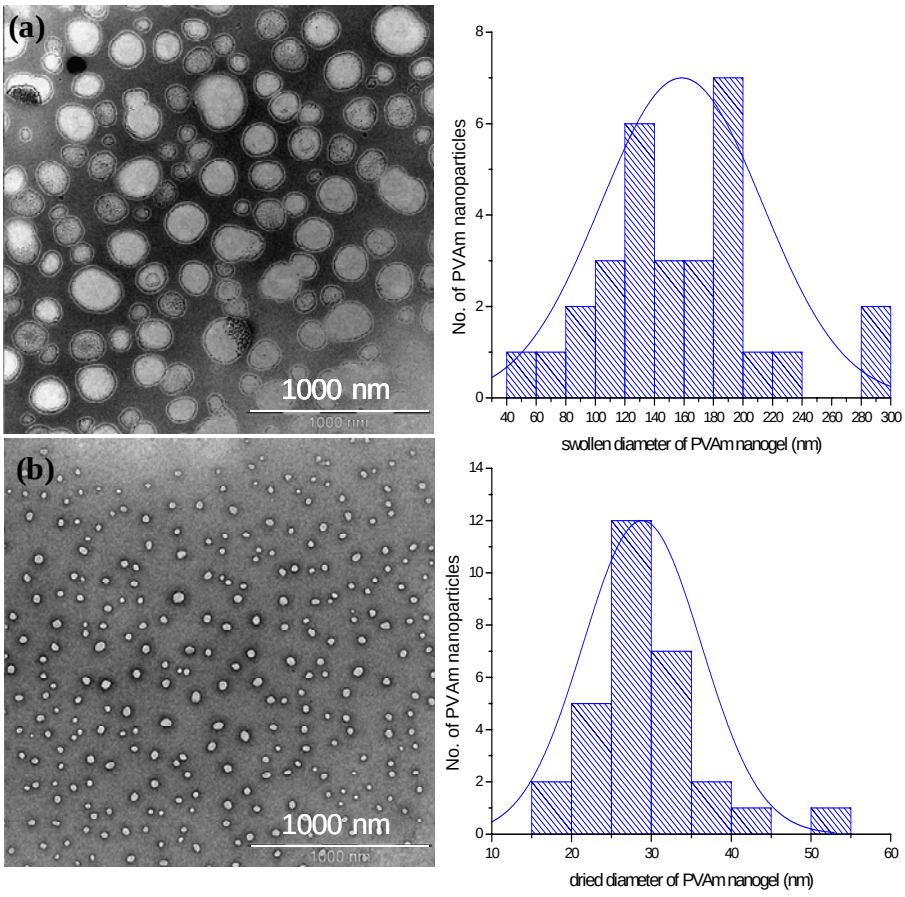

Figure 9. TEM images of (a) swollen PVAm nanogels composed of PVAm (0.01M, 10ml, Mw 45.000 g/mol) and PAE (1 g/L, 10 ml, Mw 269.000 g/mol) with an average size of 150nm and (b) deswollen PVAm nanogels with an average size of 30nm.

Furthermore, atomic force microscopy (AFM) was used to determine the nanogel morphology as function of the molecular weight of PVAm. In Figure 10 (a) and (b), PVAm nanogels were prepared from Mw 45.000 g/mol and Mw 340.000 g/mol. We observed significantly larger nanoparticles with higher molecular weight as was also found by DLS.

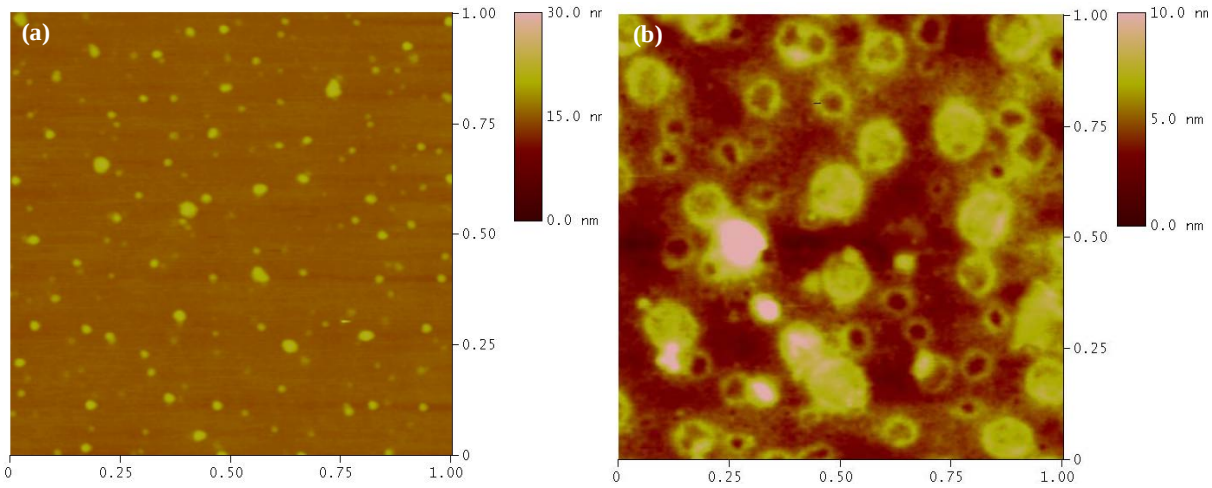

Figure 10. AFM images of (a) PVAm nanogels (Mw 45.000 g/mol) and (b) PVAm nanogels (Mw 340.000 g/mol) spin-coated on the mica at the rotation speed of 2000 rpm for 1 min.

The preparation of AgNP colloids was performed by chemical reduction of $AgNO_3$ using $NaBH_4$ and $Na_3C_3H_5O(COO)_3$ as stabilizer in aqueous solution for *ex situ* AgNP hybrid nanogel preparation and direct reduction of $AgNO_3$ in polyamine nanogel as *in situ* approach. Silver nanoparticles were synthesized by the chemical reduction method: an aqueous solution of citrate-protected silver nitrate (0.01M) is reduced by addition of an aqueous solution of 1 mM $NaBH_4$ as a reductant. AgNP/PEI nanogels were first synthesized by *in situ* method, which is a two-step procedure to prepare the hybrid nanogels. In the first step, PEI nanogels based on PEI (0.01M, 10ml, Mw 2.000 g/mol) and PAE (1 g/l, 10ml, Mw 269.000 g/mol) were prepared. In the second step, AgNP/PEI hybrid particles were formed in the PEI nanogel by chemical reduction of silver nitrate in the presence of the nanogel that chelates the silver ions. Figure 11 shows a typical extinction band of Ag nanoparticles at 420 nm corresponding to plasmon resonance of AgNP/PEI nanogels measured by UV-vis spectra.[32] The Ag seed colloids appear as a bright yellow colored aqueous solution and AgNP/PEI nanogels have a slightly yellowish color. In contrast, PEI nanogels appear as colorless aqueous solution. This result demonstrates the efficient capping of AgNP into polyamine nanogels.

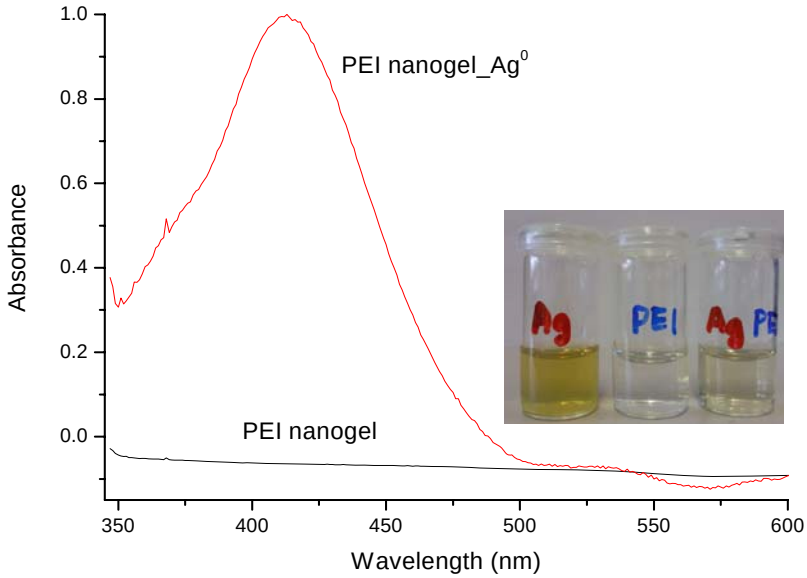

Figure 11. UV-Vis spectra of PEI nanogels composed of PEI (0.01M, 10ml, Mw 2.000 g/mol)/ PAE (1 g/l, 10ml, Mw 269.000 g/mol) and AgNP/PEI hybrid particles synthesized by *in situ* method with citrate- stabilized AgNP in PEI nanogel colloid.

In addition, the AgNP/PVAm nanogels and AgNP/PEI nanogels were synthesized by an *ex situ* method by adsorption of performed AgNP onto polyamine nanogles. The Z-average size of polyamine hybrid nanogels with AgNP incorporation was detemined by dynamic light scattering shown in Figure 12. Incorporation of AgNP into polyamine nanogels results in a decrease in particle size compared to pure polyamine nanogels. In Figure 12 (a) and (b), the Z-average of pure PVAm nanogels is 172 nm with PDI of 0.275 and the Z-average of AgNP/PVAm nanogels is 150 nm with PDI of 0.229. The primary amine groups of PVAm nanoparticles are enable to chelate the heavy metal.[14] As a result binding of the silver nanoparticles inside the polymeric nanogels results in contraction of the polymieric matrix and thus a decrease in particle size. In the case of PEI nanogels functionalized with AgNP, the Z-average size of the nanogels is also reduced by binding of silver nanoparticles from 150 nm (PDI=0.225) to 123 nm (PDI=0.169). This result shows that incorporation of AgNP provides

the reduction of nanogels size and the similar phenomenon was reported on the hybrid nanogels with AuNP,[11] AgNP[12] and iron nanoparticles.[14] Especially, the hydrodynamic radius of *N*-vinylcaprolactam/ acetoacetoxyethyl methacrylate nanogel was continuously decreased from 280 nm to 130nm with increasing AgNP amount from 0 % to 50 %.[12]

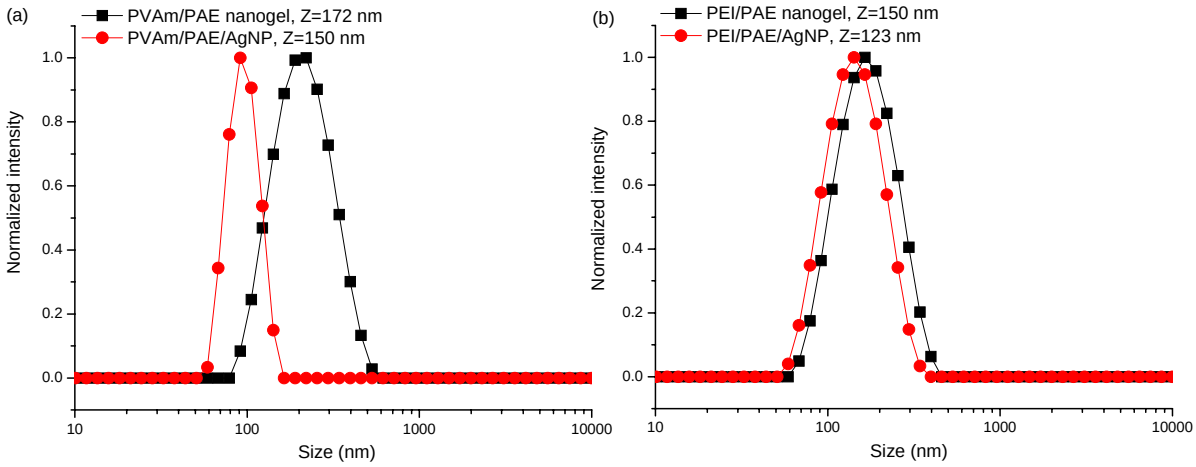

Figure 12. Hydrodynamic radius of (a) PVAm (0.01M, 10ml, Mw 45.000 g/mol)/PAE (1 g/L, 10 ml, Mw 269.000 g/mol), AgNP(0.01M, 500 µl)/PVAm (0.01M, 10ml, Mw 45.000 g/mol)/PAE (1 g/L, 10 ml, Mw 269.000 g/mol), and (b)PEI (0.01M, 10ml, Mw 25.000 g/mol)/PAE (1 g/L, 10 ml, Mw 269.000 g/mol), AgNP(0.01M, 500 µl)/PEI (0.01M, 10ml, Mw 25.000 g/mol)/PAE (1 g/L, 10 ml, Mw 269.000 g/mol) prepared at 11.000 rpm for 10 min determined by DLS (CONTIN analysis) at 25 °C in aqueous solution.

Morphology images of PEI nanogels and AgNP within PEI nanogels were measured with TEM which provides a high contrast of polymeric nanogels and inorganic nanoparticles (Figure 13). The effect of incorporating AgNP into PEI nanogels appears the different darkness due to transmission of silver nanoparticles. Therefore, it can be concluded that the polyamine nanogels are absorbed silver particles by chelating of silver with free amino groups.

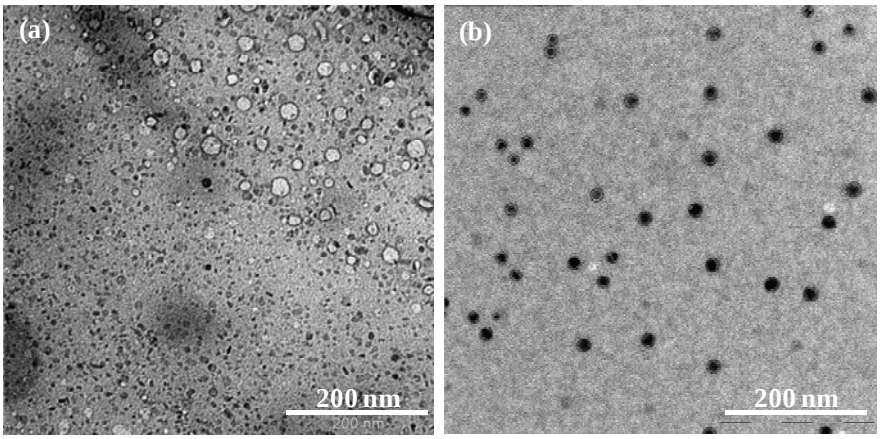

Figure 13. TEM images of (a) PEI nanogels composed of PEI (0.01M, 10ml, Mw 2.000 g/mol) and PAE (1 g/L, 10 ml, Mw 269.000 g/mol) and (b) PEI nanogels functionalized silver nanoparticles

PEI nanogels and its hybrid with AgNP are shown in Figure 14 (a) and (b). An average particle size of PEI nanogels is calculated by image J software and to be 70 nm. AFM reveals smaller nanogels after AgNP incoporation with an average diameter of 40 nm compared to pure PEI nanoparticles confirming the DLS results.

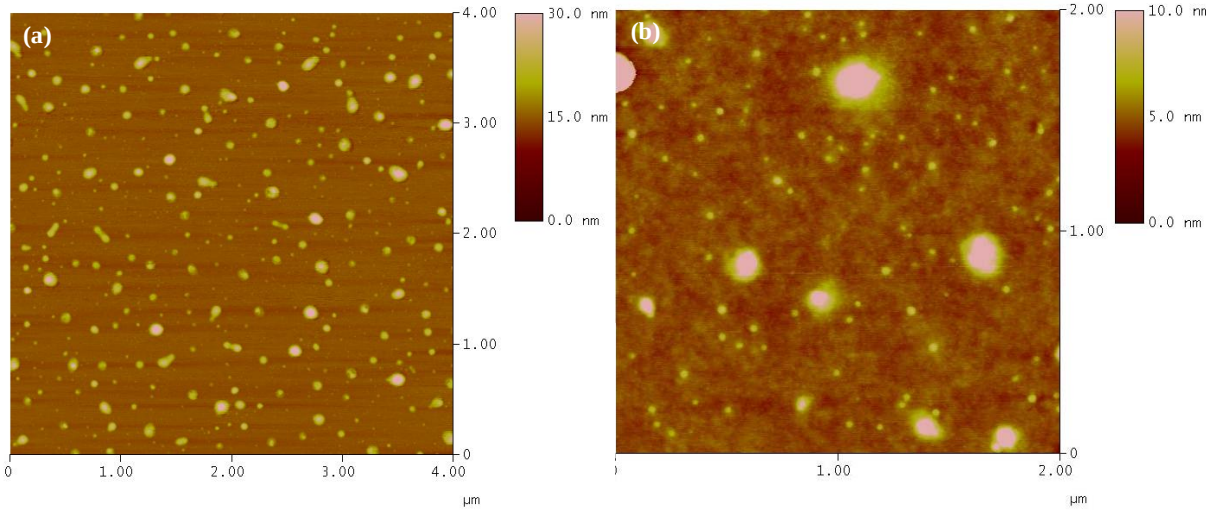

Figure 13 AFM images of (a) PEI nanogels (Mw 2.000 g/mol) and (b) PEI nanogels functionalized with silver particles (Mw 2.000 g/mol) spin-coated on the mica at the rotation speed of 2000 rpm for 1 min.

8.4 CONCLUSIONS

We have introduced a successful simple covalent chemical crosslinking of PVAm as well as PEI by click reaction of azetidinium-amine coupling from primary and secondary amine groups of polyamine and azetidinium ions of poly(amideamine-epichlorohydrin) (PAE) in aqueous medium. Our system offers a new type of hydro-nanogel based on readily crosslinked polyamine, which is of both fundamental academic interest and potential commercial utility. The hydrodynamic radius of resulting nanoparticles was determined by dynamic light scattering. Well-defined polymeric nanogels were obtained with a z-average size of 160 nm with polydispersity of 0.24 from PVAm of Mw 45.000 g/mol and a z-average size of 140nm with polydispersity of 0.21 from PEI of Mw 2.000 g/mol. We studied the morphology of swollen PVAm and PEI nanoparticles with cryo FE-SEM and deswollen nanogel with TEM and AFM. The chelating characteristics of primary and secondary amine groups in PVAm and PEI nanoparticles could be used to incorporate silver nanoparticles. Future work will focus on the polyamine nanogels with AgNP as an universal antimicrobial coating for textile.

8.5 REFERENCES

M7 Reproduced with permission from Yu, M.; Hoogenboom, R.; Thomas, H.; Moeller, M. *J. manuscript in preparation.*

[1] Oha, J.K.; Drumright, Siegwartb, D.J., Matyjaszewsk, K. *Prog. Polym. Sci.* **2008**, 33, 448.

[2] Saunders, B.R, Laajam, N, Daly, E. Teow, S, Hu, X., Stepto, R., *Adv. Colloid Interface Sci.* **2009**,147-148, 251.

[3] Vinogradov, S. V.; Bronich, T. K.; Kabanov, A. V. *Adv. Drug Delivery Rev*. **2002**, 54, 135.

[4] Singh, A.; Mukherjee, M. *Macromolecules* **2003**, 36, 8728.

[5] Kaneda, I.; Sogabe, A.; Nakajima, H. *Int. J. Cosmetic Sci.* **2006**, 28, 151.

[6] Wang, Q.; Wang, L.; Detamore, M. S.; Berkland, C. *Adv. Mater.* **2008**, 20, 236.

[7] Kaggwa, G. B.; Carey, M. J.; Such, C.; Saunders, B. R. *J. Colloid Interface Sci.* **2003**, 257, 392.

[8] Yu, L.; Ding, J. *Chem. Soc. Rev.* **2008**, 37, 1473.

[9] Das, M.; Zhang, H.; Kumacheva, E. *Annu. Rev. Mater. Res.* **2006**, 36, 117

[10] Antonietti, M. *Adv. Mater.* **1998**, 12, 1743.

[11] Oishi, M.; Hayashi, H.; Uno, T.; Ishii, T.; Iijima, M.; Nagasaki, Y. *Macromol. Chem. Phys.* **2007**, 208, 1176.

[12] Pich, A.; Karak, A.; Lu, Y.; Ghosh, A. K.; Adler, H. P. *Macromol. Rapid Commun.* **2006**, 27, 344.

[13] Ma, Z. Y.; Dosev, D.; Nichkova, M.; Geer, S. J.; Hammock, B. D.; Kennedy, I. M. *J. Mater. Chem.* **2009**, 19, 4696.

[14] Mohammadi, Z.; Cole, A.; Berkland, C. J. *J. Phys. Chem. C* **2009**, 113, 7652.

[15] Sondi, I.; Salopek-Sondi, B. *J. Colloid Interface Sci.* **2004**, 275, 177.

[16] Aymonier, C.; Schlotterbeck, U.; Antonietti, L.; Zacharias, P.; Thomann, R.; Tiller, J. C. Mecking ,S. *Chem. Commun.* **2002**, 24, 3018.

[17] Bodnar, M.; Hartmann, J. F.; Borbely, J. *Biomacromolecules* **2005**, 6, 2521.

[18] Bodnar, M.; Hartmann, J. F.; Borbely, J. *Biomacromolecules* **2006**, 7, 3030.

[19] Pinschmidt, R.K.; Renz, W. L.; Caroll, W.E.; Yacouth, K.; Drescher, J.; Nordquist, A. F.; Chen, N. *J. Macromol. Sci. Pure Appl. Chem. A* **1997**, 34, 1885.

[20] Sumaru, K.; Matsuoka, H.; Yamaoka, H. *J. Phys. Chem.* **1996**, 100, 9000.

[21] Pasquier, N.; Keul, H.; Heine, E.; Moeller, M. *Biomacromolecules* **2007**, 8, 2874.

[22] Shu, K.D.; Bae, Y.C.; Kim, J.W.; Kobayashi,S., *J. Macromol. Sci.* **1999**, A36, 507.

[23] Yamamoto, K., Seriza, T., Muraoka, Y., Akashi, M., *Macromolecules* **2001**, 34, 8014.

[24] Miao, C.; Chen, X.; Pelton, R. *Ind. Eng. Chem. Res.* **2007**, 46, 6486.

[25] Feng, X.; Pelton, R. *Macromolecules* **2007**, 40, 1624.

[26] Shi, L.; Berkland, C. *Macromolecules* **2007**, 40, 4635.

[27] Shi, L.; Khondee, S.; Linz, T. H.; Berkland, C. *Macromolecules* **2008**, 41, 6546.

[28] Mohammadi, Z.; Cole, A.; Berkland, C. *J. Phys. Chem.* **2009**, 1113, 7652.

[29] Yu, M.; Hoogenboom, R.; Thomas, H.; Moller, M. *manuscript in preparation.*.

[30] http://www.malvern.com/labeng/products/zetasizer/zetasizer.htm

[31] Koetz, J.; Kosmella, S. *Polyelectrolytes and Nanoparticles* : Springer, Berlin **2007**.

[32] Ung, T.; Liz-Marzán, L. M.; Mulvaney, P. *J. Phys. Chem. B* **1999**, 103, 6770.

CHAPTER 9

ANTIMICROBIAL SURFACE MODIFICATION ONTO FABRICS USING POLYAMINE NANOGELS FUNCTIONALIZED BY SILVER NANOPARTICLES

ABSTRACT

Polyamine nanogels based on azetidinium-amine coupling as crosslinking reaction and their hybrid nanogels with silver nanoparticles were incorporated onto cotton and polyester fabrics. The nanogel treated fabrics were prepared by a pad-dry process in aqueous nanogel solution for 60 min, pre-drying at 80 ºC and finish-dry at 100 ºC. The presence of amine groups in the functionalized fabrics was determined by XPS, zeta potential measurements, and cryo-FESEM. It was confirmed by XPS that a peak of N 1s from poly(vinylamine) (PVAm) and poly(ethyleneimine) (PEI) was present in the nanogel coated fabrics. In addition, the silver nanoparticles from the polyamine hybrid nanogels treated fabric showed a signal of Ag $3d_{5/2}$ at 368.27 eV. The morphology of nanogel on the coated fabrics was revealed binding of the spherical nanogel particles onto the fabrics. Regarding the reactivity of the polyamine nanogel coated fabrics, zeta potential surface characterization demonstrated a positive charge after nanogels deposition and fluorescence imaging after labeling with 4-chloro-7-nitrobenzofurazan (NBF) proved the presence of reactive amine groups at the fabric surfaces. The most important property of polyamine hybrid nanogels coated fabrics was found to be thier excellent antibacterial activity against gram positive and negative bacteria. Such as, these readily prepared polyamine nanogels may be a new type of sustainable antimicrobial coating for hygiene goods for medical applications.

9.1 INTRODUCTION

A growing concern of emerging microbial infestation has intensively stimulated research activities in the field of medical devices, health care, and hygiene goods.[1-3] More importantly, intelligent and smart textiles research was driven to comply with stringent textile requirement for medical uses.[4-7] Therefore, the prevention of microbial expose on textiles and wearers is very important for medicine consumers and intelligent textile suppliers. Conventional classes of antimicrobial agents for textile finish include quaternary ammonium salts,[8-9] zirconium-based organo-metallics,[10] silver compounds[11-13] and chitosan.[14-16] Silver ions and silver compounds form irreversible complexes in bacteria resulting in antimicrobial effects; due to denaturation of structural proteins and inhibition of oxygen transport, nutrient uptake, and excretion.[13] In addition, silver treatment has been extended to commercial scale by Nanohorizon Inc. (SmartSilver®) and was applied to wool for fabric and garment treatment.[17] Nanotechnology is a hot issue and is covering a broad range of material engineering including textile chemistry. It was demonstrated to improve textile properites, such as fabric softness, durability, breathability, water repellency, fire retardancy, and antimicrobial properties.[4, 18] In a previous study, we have reported the preparation and characterization of poy(vinylamine) (PVAm) and poly(ethyleneimine) (PEI) nanogels using azetidinium-amine coupling as crosslinking reaction as well as their hybrid nanogels with silver nanoparticles using chelation in aqueous medium.[19] Furthermore, we developed most-defined cross-linked nanofibers from PVAm/PAE (poly(amideamine epichlorohydrin) with/without silver nanoparticles which demonstrated excellent antimicrobial activity against gram positive bacteria (*Bacillus subtilis*) and gram negative bacteria (*Escherichia coli*).[20] As such, the same compositions of the nanogels are anticipated to have similar antimicrobial activity as the nanofibers.

Other examples of PVAm and PEI micro/nanogel system or polymer modification have been already reported. Pelton *et al.* reported the preparation of the PVAm microgels crosslinked by 1, 3-divinylimidazolid-2-one, which were deposited on a regenerated cellulose membrane to

enhence the wet adhesion properties.[21-22] Berland *et al.* developed PVAm nanogel capsules crosslinked by 2-bis[2, 2'-di(N-vinylformamido)ethoxy]propane onto silica particles[23]. These crosslinked nanogels were to release lysozyme dependent on the pH solution.[24] Moreover, they reported the synthesis of iron oxide within PVAm nanoparticles and demonstrated the relatively low cytotoxicity for potential biomedical applications.[25] Biodegradable colloidal gels consisting of (D,L-lactic-co-glycolic acid) (PLGA)/PVAm or poly(ethylene-co-maleic acid) (PEMA) were demonstrated as moldable or injectable tissue scaffolds.[26] Early work within the field of antimicrobial coatings reported the antimicrobial activity of glass slides functionalized with pure PVAm and PVAm derivatives, modified with C_6 and C_8 chains.[27-28] This work showed that PVAm C_6 was most potent against *E. coli* while PVAm C_8 was more active against *B. subtilis*. In addition, PEI modified with quaternary ammonium groups, alkyl chain, allylic and benzylic groups was synthesized revealing 99.9% efficiency against *E. coli* and *B. subtilis*.[29-30]

In this study, crosslinked PVAm and PEI nanogels as well their hybrids with silver nanoparticles were applied onto cotton and polyester fabrics using a simple dip-coating method. The chemical compositions of the modified fabrics were evaluated by XPS and the surface charge of the fabrics was determined with zeta potential measurements. Further functionalization of the nanogel modified fabrics was proven by grafting 4-chloro-7-nitrobenzofurazan (NBF) followed by extensive rinsing and fluorescence microscopy. Antimicrobial activities of the nanogel modified fabrics were assessed against *B. subtilis* and *E. coli* using shake test and patch test. Thus, this present work demonstrates a platform towards antimicrobial coatings for potential use for biomedical textile finishing.

9.2 EXPERIMENTAL PART

Materials

Polyvinylamine (PVAm) technical products (Lupamin 5095, 9095) were kindly provided by BASF. The polymers were obtained from 90% hydrolysis of poly (N-vinylformamide) with a weight molecular weight of 45.000 g/mol and 340.000 g/mol and were used as received. Poly(ethyleneimine) (PEI) with an average molecular weight of 2.000 g/mol and 25.000 g/mol were obtained from Aldrich and was used as received. The polyamideamine-epichlorohydrin (PAE) (SI group) was purchased and has a weight molecular weight of 269.000 g/mol determined by static light scattering. Silver nitrate ($AgNO_3$) and trisodium citrate ($NaC_6O_7H_5$) were purchased from Merck and reducing agent sodium borohydride ($NaBH_4$) was received from Aldrich. 4-chloro-7-nitrobenzofurazan (NBF) was also received from Aldrich. Cotton fabrics (102 g/m^2) and polyester (PET) (126 g/m^2) were purchased from Testex Prüftextilen. MiliQ water was used solvent for all experiments (Milli-Q, 18.2MΩ).

Fabric finishing process

In order to prepare the polyamine nanogels, PVAm or PEI (43 mg, 10 mmol) was dissolved in distilled water (10 mL), and PAE (10 mg) was dissolved in distilled water (10 mL). The crosslinked nanogels were applied as coating by dipping method. Scheme 1 shows the process of the fabric surface modification with polyamine nanogels and AgNP hybrid nanogels in detail. The cutted fabrics were immersed in a nanogels solution of 10 ml for 30 min at room temperature. The nanogel coated fabrics were pre-dried at 80°C for 60 min, and intensively rinsed in distill water, and cured at 100°C for 60 min. In order to confirm the primary amine reactivity, fluorescent dye NBF labeling was performed bz dipcoating in 2 ml of immersing solution for 10 min. Subsequently, the fabrics were washed with distilled water and nitrogen-dried. The samples were kept in a dark container before further examination.

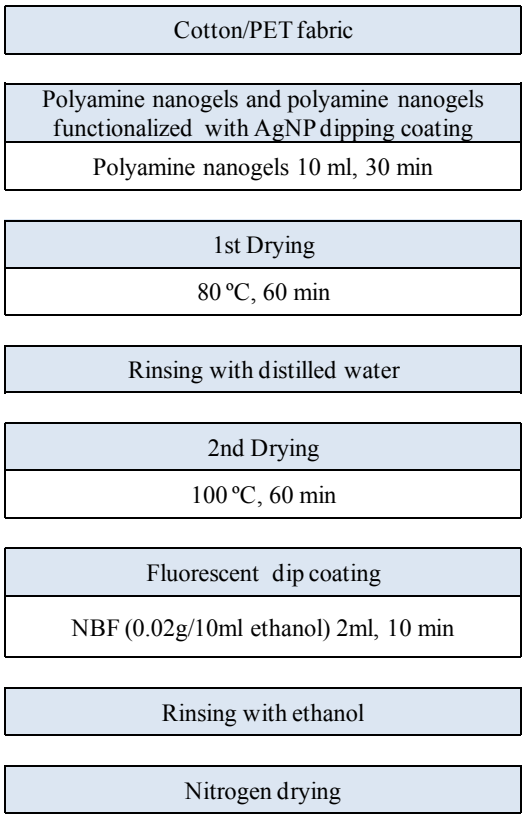

Scheme 1. Fabric finishing process of polyamine nanogels and AgNP hybrid nanogels surface modification on cotton and polyester fabrics.

Characterization

X-ray photoelectron spectroscopy (XPS) analysis of polyamine nanogel coated fabrics was carried out using an Ultra AxisTM Spectrometer from Kratos analytical (UK). The elements on the substrate were excited with monoenergetic Aluminium K1,2 irradiation with an energy of 1486.6 eV and a power of 150 W. The analysed sample area was 600 x 800 μm² with an information depth of around 10 nm. All spectra were adjusted to the hydrocarbon reference peak C 1s at 285.00 eV. Zeta potential of polyamine nanogel coated fabrics was measured with ELS Z series (Photal OTSUKA ELECTRONICS). Cryo field-emission scanning electron microscopy (Cryo FE-SEM) was performed using a HITACHI S-4800 instrument in a cryo-chamber with the cryo-transfer system Alto 2500 (GATAN). The nanogel coated fabrics were dropped into liquid nitrogen and the frozen sample was placed in the cryo chamber. 4-chloro-

7-nitrobenzofurazon (NBF) was used as fluorescent labeling to detect amino-groups from PVAm/PAE nanogels treated fabics. The reattivity of the fabrics was observed by fluorescence microscopy (Axioplan Zeiss) at an absorption maximum of 467 nm and an emission maximum of 528 nm. Antimicrobial activities of the nanogel coated fabrics were performed by shake test (DSMZ 347) with Gram-positive *Bacillus subtilis* (*B. sub*) and Gram-negative *Escherichia coli* (*E. coli*) and patch test. The fabrics were sterilized at 120 ºC for 30 min and covered with 15 µL of a diluted suspension of bacteria in nutrient solution. After exposure, the fabrics were incubated in a climate chamber at 25 ºC and 90 % relative humidity for 3 hours. Shake test was performed with an incubated substrates shaking with 1 ml nutrient solution at 20 ºC 150 rpm for 30 min. Afterwards extracted suspensions were transferred into a well plate and the optical density was measured at 612 nm and 37 ºC each 30 min by using a microplate reader/incubator (GENIOS PRO, Tecan) and photometer Cary 100 (VARIAN). The bacteria growth curve was obtained by comparison of the optical density with a control substrate and individual monolayer polymer substrates. For supplementary antimicrobial activity, the fabrics were tested using patch test with *E.coli* and *B. sub* (DSMZ 498). In order to prove the coating adhesive property, washing tests were carried out using the standard machinary washing process (DINEN ISO 105-C06), which involves twice intensive shaking and washing at 60°C for 30 min, and a last step at 40°C for 10 min with 1g of fabric into 20ml washing media. Then, the color difference was measured with CIE lab to obtain the whiteness as Δ W-CIE.

9.3 RESULTS AND DISCUSSION

A simple process for textile finishing with polyamine nanogels composed of PVAm or PEI nanogels using azetidinium-amine coupling as crosslinking reaction has been developed in an aqueous medium (Scheme 2). The nanogels were functionalized with silver nanoparticles and applied onto fabric to enhance the antimicrobial coating. The reactive amino groups coated fabrics can be directly coated onto negatively charged fabrics, cotton and polyester. Especially, PVAm can be adsorbed onto cellulose fibers in a dilute aqueous solution, which is induced by hydrogen bonding attraction between hydroxyl groups and primary amine groups.

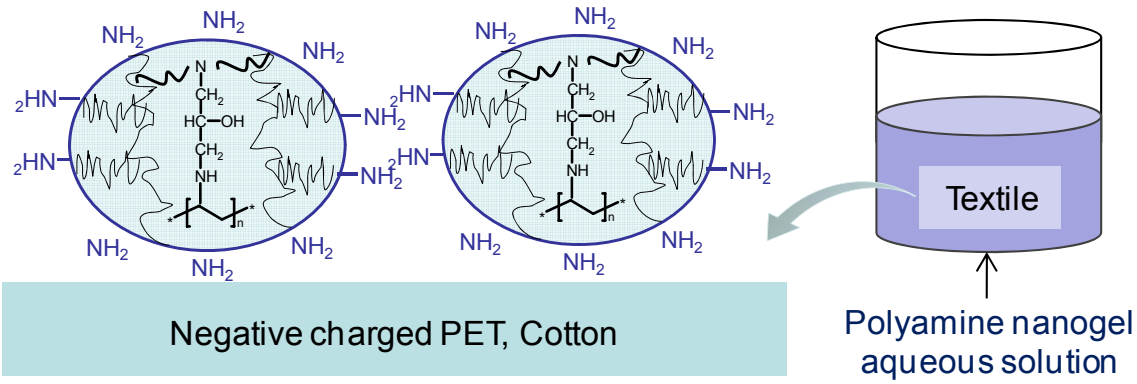

Scheme 2. Schematic representation for the surface modification of fabrics with polyamine nanogel aqueous solution.

A laboratory dipping procedure was used to coat the nanogels onto cotton and polyester fabrics and the wet pickup of coated samples was described, as shown in Table 1, 2. The adsorption indicates the degree of polymer coverage onto fabrics. The adsorption of polyamine nanogels was measured by a weighing method based on the weight changes of the fabric before and after treatment. Linear PVAm nanogel shows better adhesive coating effect than branch PEI nanogel onto cotton and polyester (Table 1). Note that there was no pretreatment or oxidation process for the coating prepared with polyamine nanogels. Nevertheless, PVAm nanogels were coated on the cotton with an adsorption of 3.7 % and on

the polyester with an adsorption of 4.2%. In addition, the coating with PVAm nanogels functionalized with silver nanoparticles resulted in an increase of adsorption from 2.7% to 3.4% onto cotton and from 3.9% to 4.0% onto polyester. These results demonstrate effective adhesion of hybrid nanogels onto fabrics. Adsorption values were calculated as follows:

$$\text{Adsorption}(\%) = \frac{W_1 \quad W_0}{W_0} \times 100$$

W_0 : The weight before polyamine nanogel coating, W_1 : Theweight after polyamine nanogel coating

Table 1. Surface modification of cotton and polyester with polyamine nanogels.

Samples	W_0 (mg)	W_1 (mg)	Adsorption (%)
Control cotton	45		
PVAm_cotton	46.5	48.2	3.7
PEI_cotton	43.1	43.4	0.7
Control PET	55.5		
PVAm_PET	54.8	57.1	4.2
PEI_PET	55.4	55.9	0.9

Table 2. Surface modification of cotton and polyester with polyamine nanogels functionalized silver nanoparticles.

Samples	W_0 (g)	W_1 (g)	Adsorption (%)
Control cotton	127.3		
PVAm_cotton	123.7	127.1	2.7
Ag_PVAm_cotton	118.4	122.4	3.4
Control PET	124		
PVAm_PET	129.4	134.4	3.9
Ag_PVAm_PET	117.1	121.8	4.0

The chemical compositions of PVAm nanogels, PEI nanogels, and their functionalization with silver nanoparticles treated cotton and polyester fabrics were investigated by X-ray photoelectron spectroscopy (XPS), as shown in Figure 1 and 2. A peak of nitrogen (N_{1s}) binding energy at 400 eV clearly appeared for the PVAm nanogels (Figure 1, 2 (b)) and PEI nanogel (Figure 1, 2 (d)) modified cotton and polyester surfaces. The XPS survey fitting of Ag_{3d} presents the silver functionalized surface modification of the cotton and polyester fabrics, which are widely used as medical textiles.[1, 6-7] In addition, the intensity of the XPS survey peak (C_{1s} at 285.5 eV) increases after PVAm nanogel (see Figure 1 (a), (b) and Figure 2 (a), (b)) and PEI nanogel (see Figure 1 (a), (d) and Figure 2 (a), (d)) adsorption due to the presence of polymer backbone.

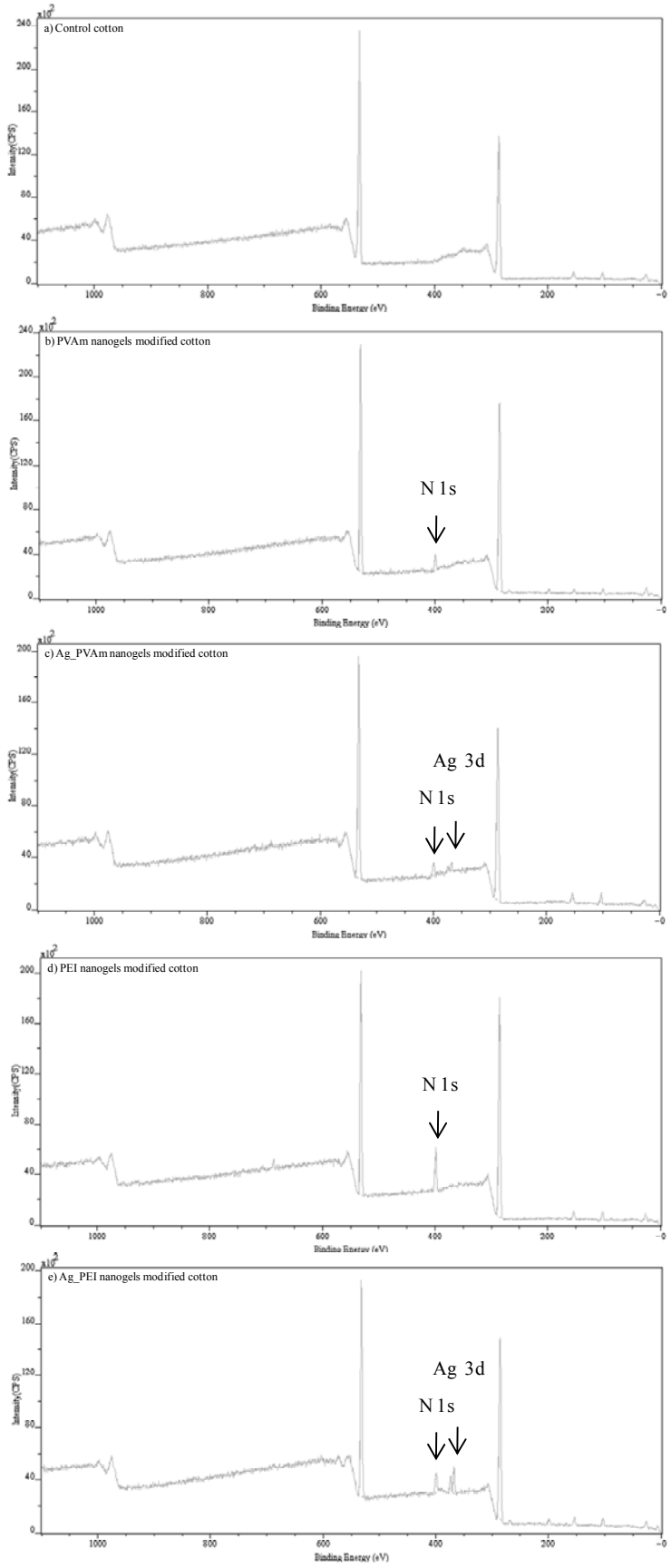

Figure 1. XPS analysis of (a) control, (b) PVAm nanogels, (c) Ag_PVAm nanogels, (d) PEI nanogels and (e) Ag_PEI nanogels modified cotton samples.

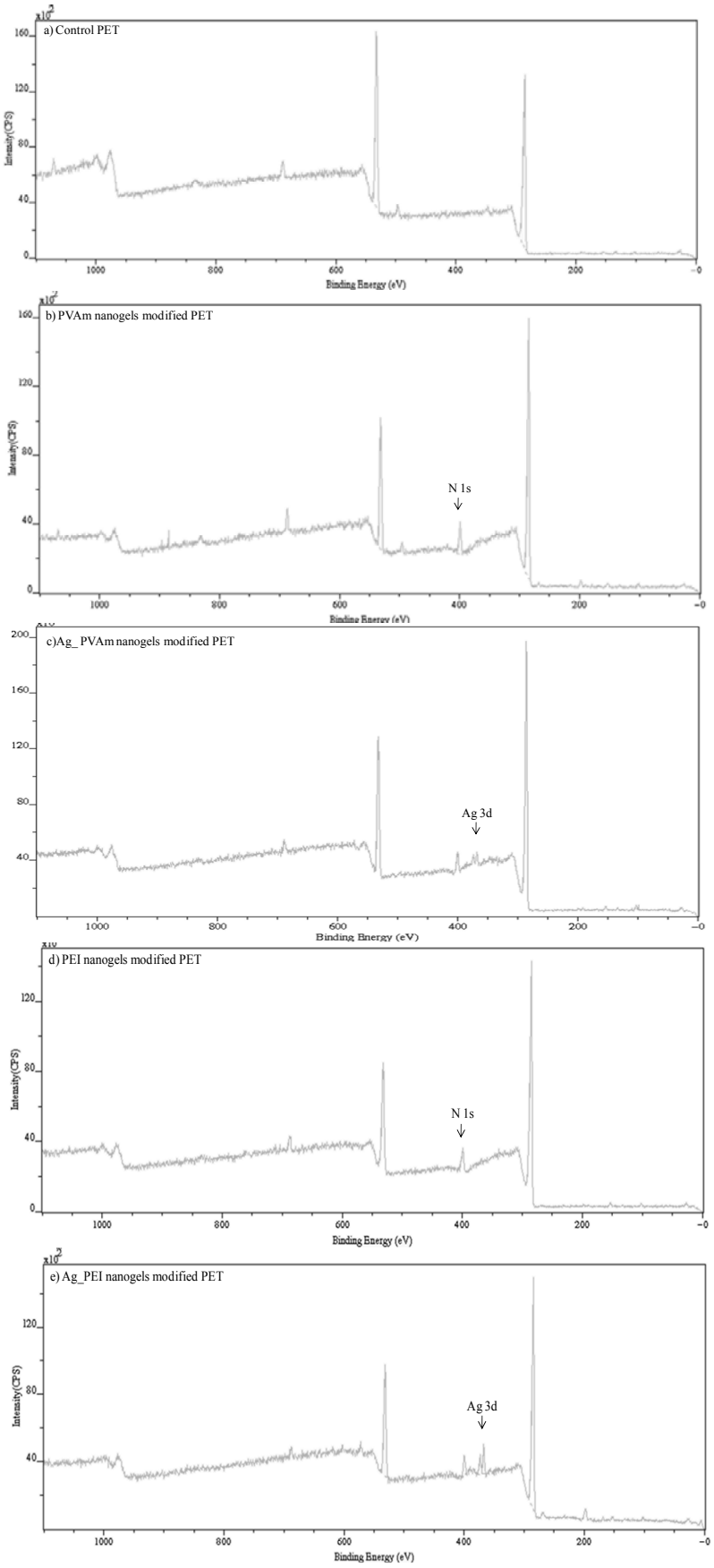

Figure 2. XPS analysis of (a) control, (b) PVAm nanogels, (c) Ag_PVAm nanogels, (d) PEI nanogels and (e) Ag_PEI nanogels modified polyester samples.

The zeta potential graphs were obtained by zeta potential measurements of unmodified and polyamine nanogel modified fabric surfaces (Figure 3). The zeta potential of the unmodified fabric surfaces shows mainly negative values at higher pH as well as their negatively charged surface at neutral pH, which is required for grafting with positively charged nanoparticles by electrostatic interaction in an aqueous medium. The surface charge of the nanogel modified cotton (Figure 3a) was not influence on pH solution indicating successful modification and charge compensation. The nanogel modified polyester (Figure 3b) revealed a significant decrease in zeta potential when the pH is increased. The positive zeta potential results from both the nanogel coating and the PET while the negative charges of rhe PET at higher pH are screened by the polyamine nanogel coating.

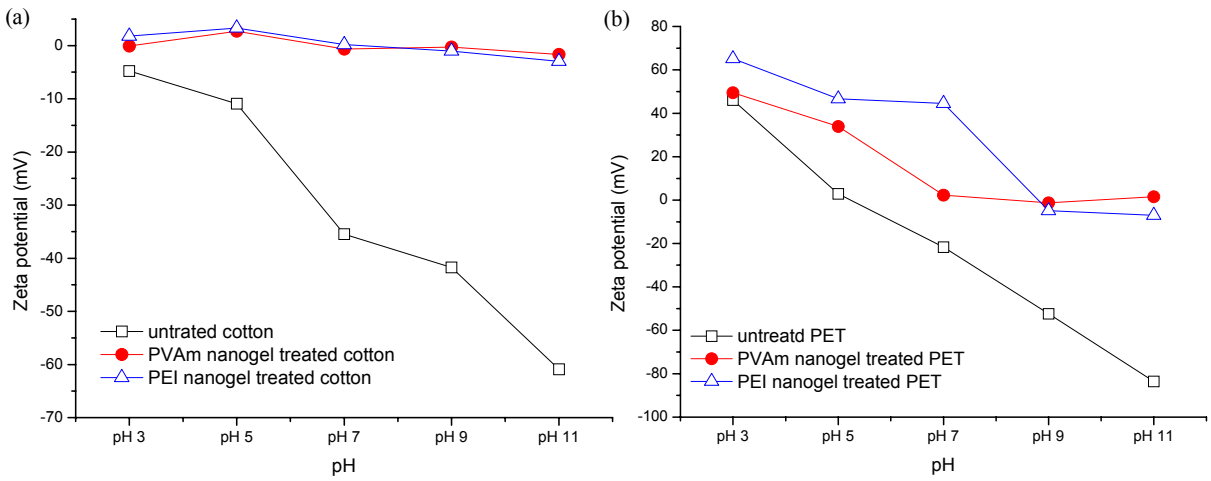

Figure 3. Zeta potential of polyamine nanogels modified (a) cotton and (b) polyester.

The nanogel coated cotton and polyester were also investigated with cryo-FESEM as shown in Figure 4. The unmodified fabric surface is smooth, while the surface treated with nanogel is rough with embossing nubs-like particles. However, PEI nanogel coated fabrics of (c) and (f) seem that the particles were not uniformly well-dispersed comparing to PVAm nanogel treated fabrics of (b) and (e). It indicates that the PVAm nanogel is the good adhesive modifier for textile surface functionalization. Especially, the SEM image of PVAm nanogel

has treated cotton on the high magnification depicts the homogenous coating all over surface in Figure 5 (b) and (c). Figure 5 (a) shows the particle on the surface, which occurs from freezing ice particles. Comparing of cotton and polyester modified with PVAm nanogel, PVAm nanogel shows better surface modification with well-dispersed coating.

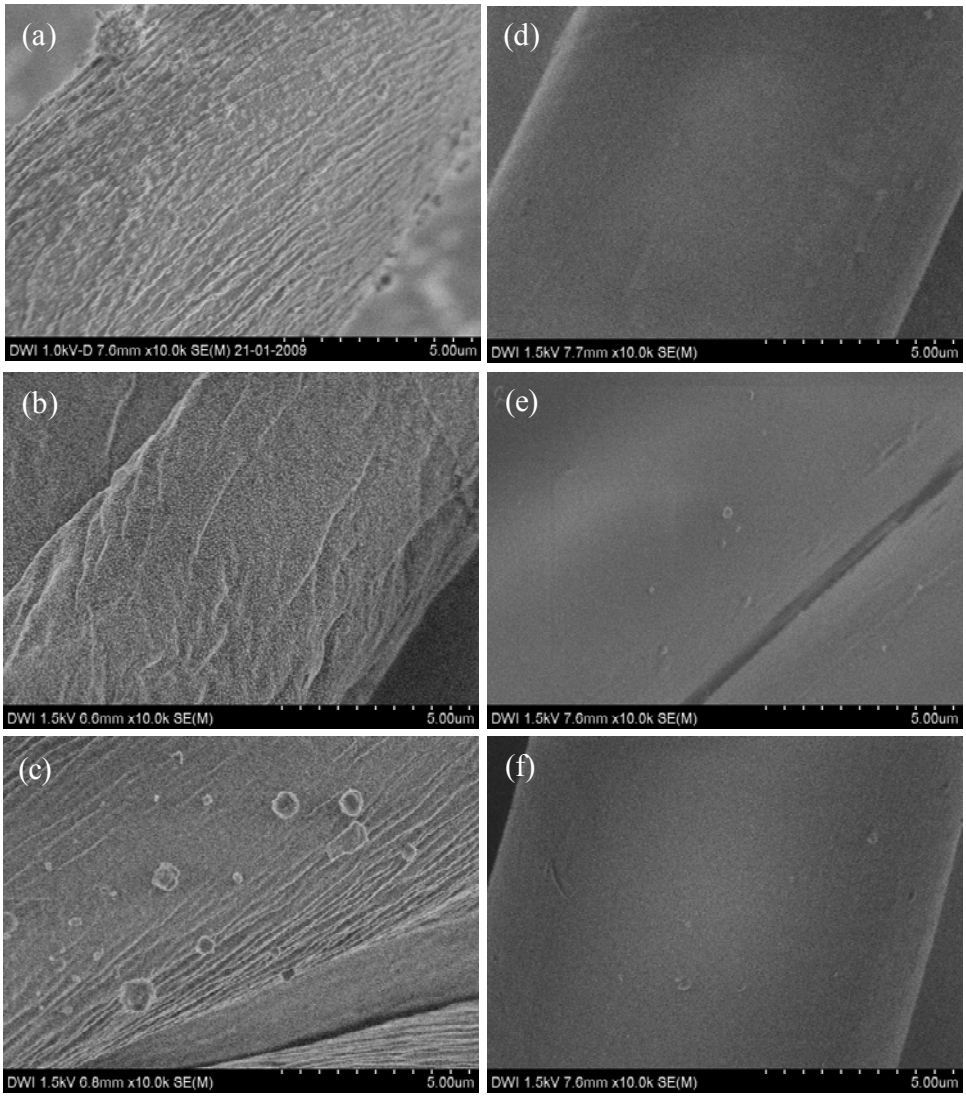

Figure 4. Cryo FE-SEM images of (a) control cotton, (b) PVAm nanogels modified cotton, (c) PEI nanogels modified cotton, (d) control polyester, (e) PVAm nanogels modified polyester and (f) PEI nanogels modified polyester.

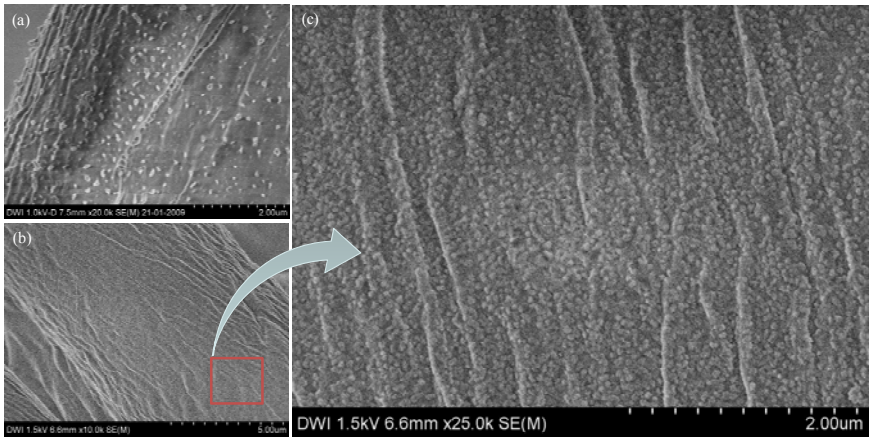

Figure 5. Cryo FE-SEM images of (a) ice particles from control cotton surface, (b) cotton modified with PVAm nanogels on the magnification 10 k and (c) cotton modified with PVAm nanogels on the magnification 25 k.

To demonstrate potential post-functionalization of the nanogel modified fabrics, we have carried out fluorescence dye labeling with 4-chloro-7-nitrobenzofurazan (NBF) by dip-coating. The mass increase indicates successful NBF grafting on the nanogel treated fabrics in Table 3 and, thus, the presence of reactive amine groups. Figure 6 shows the fluorescence microscopy images of unmodified and nanogel modified fabrics also demonstrating that NBF can react with primary and secondary amines in the coating. Thus, PVAm and PEI nanogel treated fabrics could be further modified with functional units making them suitable for a wide range of applications.

Table 3. Surface modification of cotton and polyester with polyamine nanogel following NBF.

Samples	W_0 (g)	W_1 (g)	Adsorption (%)
Control cotton	0.04501		
NBF_PVAm_cotton	0.04305	0.1254	191
NBF_PEI_cotton	0.04207	0.1198	185
Control PET	0.05551		
NBF_PVAm_PET	0.05513	0.1104	100
NBF_PEI_PET	0.0603	0.1388	130

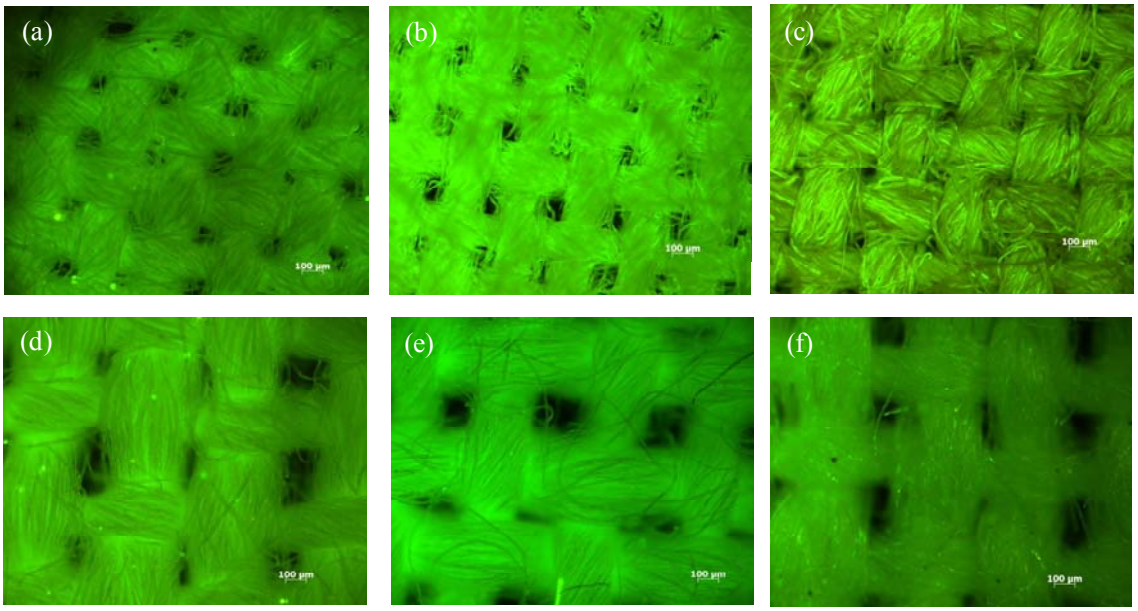

Figure 6. Fluorescence images of (a) control cotton, (b) PVAm nanogels coated cotton, (c) PEI nanogels coated cotton, (d) control polyester, (e) PVAm nanogels coated polyester and (f) PEI nanogels coated polyester is shown the reactive surface modification.

The antimicrobial activities of PVAm nanogel and silver hybrid nanogel modified cotton and polyester were evaluated against *E. coli* and *B.sub* according to the shake test (Figure 7, Figure 8) and were tested against *E. coli* by patch method (Figure 9). The bacteria growth of negative control (without bacteria), positive control (with bacteria), nanogel and hybrid nanogel treated fabrics showed a complete bacteria growth inhibition on the positive control, nanogel and hybrid nanogel treated fabrics against gram positive and negative bacteria. The photos in Figure 9 represent the antimicrobial activity from a patch test against gram positive bacteria *E. coli* and demonstrate the bacteria growth inhibiting effect. After the *E. coli* were in contact to pure nanogel or nanogel silver hybrid modified fabrics, the bacterial colony from patched inoculated fabric surfaces was almost completely inhibited. It is well-known that the silver ions have high activities to interact to intracellular proteins and nucleic acids of both gram positive and negative bacteria leading to destruction of the bacteria cell membranes.[5] Interestingly, the antimicrobial activity of the pure PVAm nanogel also shows complete

bacteria growth inhibition for both bacteria, which is similar to the result from PVAm nanofibers in our previous work.[20] It may be concluded that the antimicrobial activity of pure PVAm nanogel modified fabric is most likely related to a combination of factors including a weak polyelectrolyte with a positive charged surface as well the presence of both secondary and tertiary amines next to the primary amines. Especially, it is important to consider the charge of polyelectrolyte material in the pH of the solution due to direct influence of antimicrobial activity.[27]

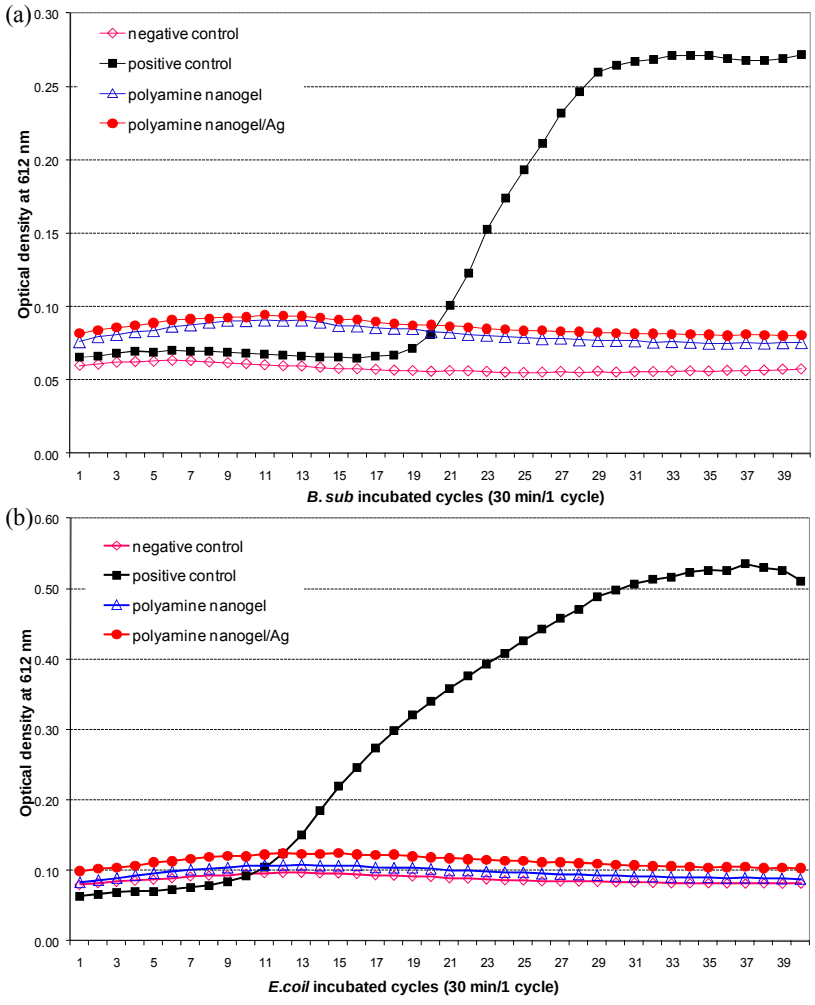

Figure 7. Antimicrobial activity of polyamine nanogels and silver nanoparticles functionalized polyamine nanogel modified cotton against (a) gram-positive bacteria (*B.sub*) and (b) gram-negative bacteria (*E.coli*).

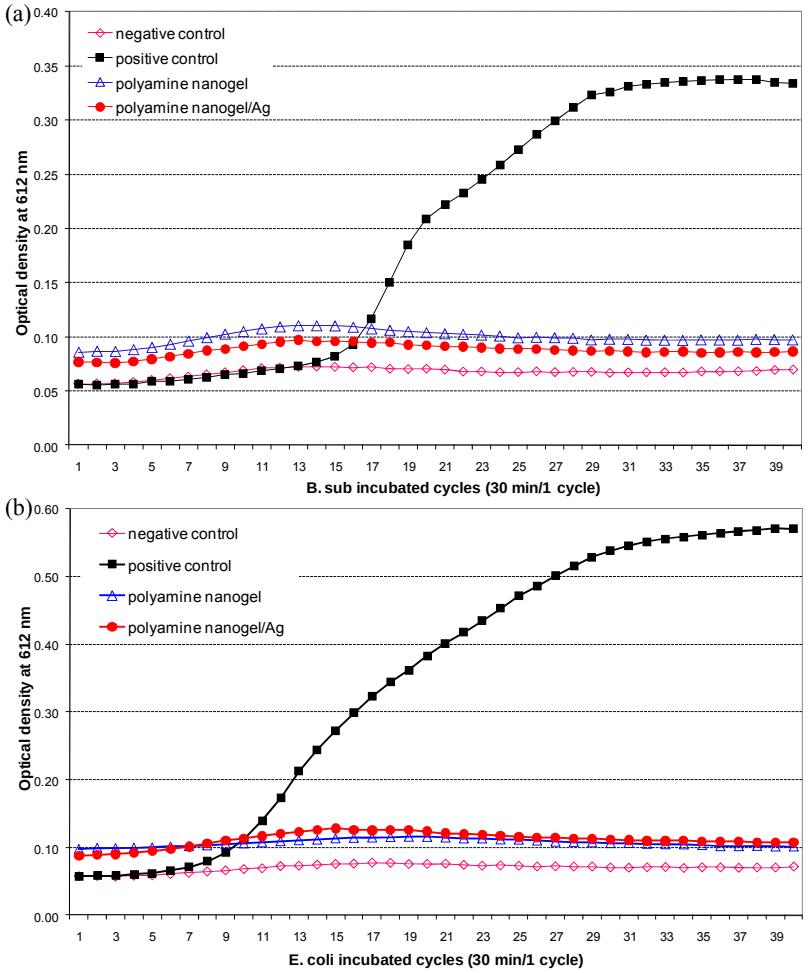

Figure 8. Antimicrobial activity of polyamine nanogels and Ag hybrid nanogel modified polyester against (a) gram-positive bacteria (*B.sub*) and (b) gram-negative bacteria (*E.coli*).

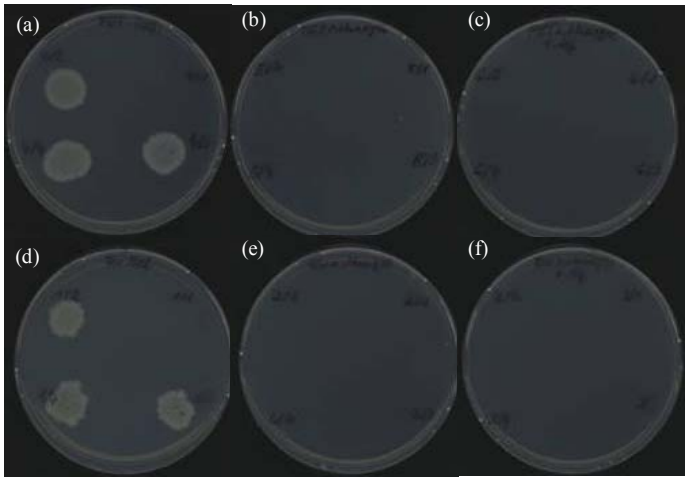

Figure 9. Antimicrobial test photographs from patch test against growth of *E.coli* after direct contact with the (a) control cotton, (b) PVAm nanogels modified cotton, (c) Ag_PVAm nanogels modified cotton, (d) control polyester, (e) PVAm nanogels modified polyester and (f) Ag_PVAm nanogels modified polyester.

Coating stability and washing fastness of the pure and silver hybrid nanogel treated fabrics were evaluated with color difference of whiteness (Δ W-CIE) before and after an intensive washing process. The Δ W-CIE of samples was measured with standard method of CIE whiteness, which may give a different impression of the relative whiteness of two samples relative to what human eyes would recognize.[31] Figure 10 shows the reduction of whiteness with the unmodified and modified fabrics after the three consecutive washing processes. The value of Δ W-CIE is below 1.5, which indicates a slightly a faded color and represents apparently a preferred washing fastness. Moreover, we investigated the microscopic images of nanogel treated fabrics after washing process (Figure 11). Clearly, the nanoparticles observe on the fabric surfaces and the morphology is comparable with Figure 4 before washing. It is apparent that they are effectively crosslinked on the fabric surfaces and are achieved the suitable coating stability.

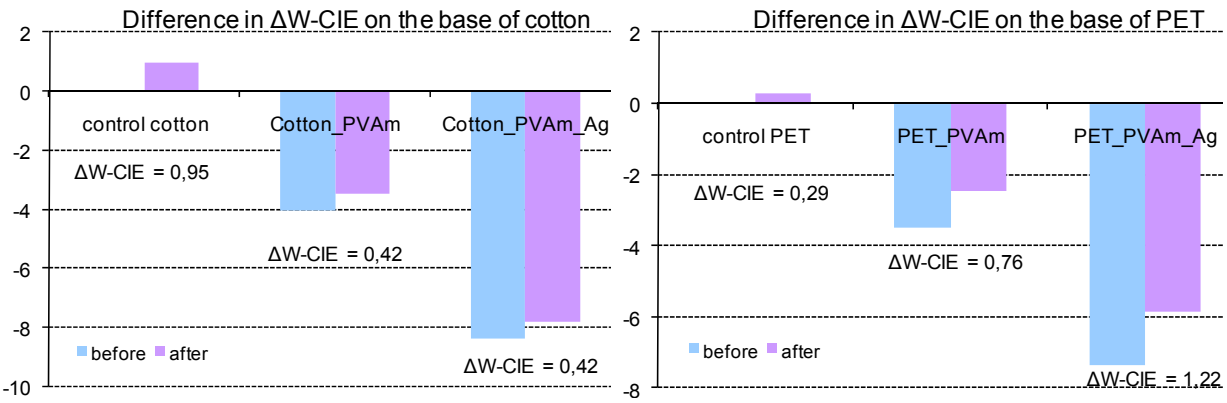

Figure 10. Colorimetric data of PVAm and hybrid nanogels modified cotton and polyester measured by CIE lab system.

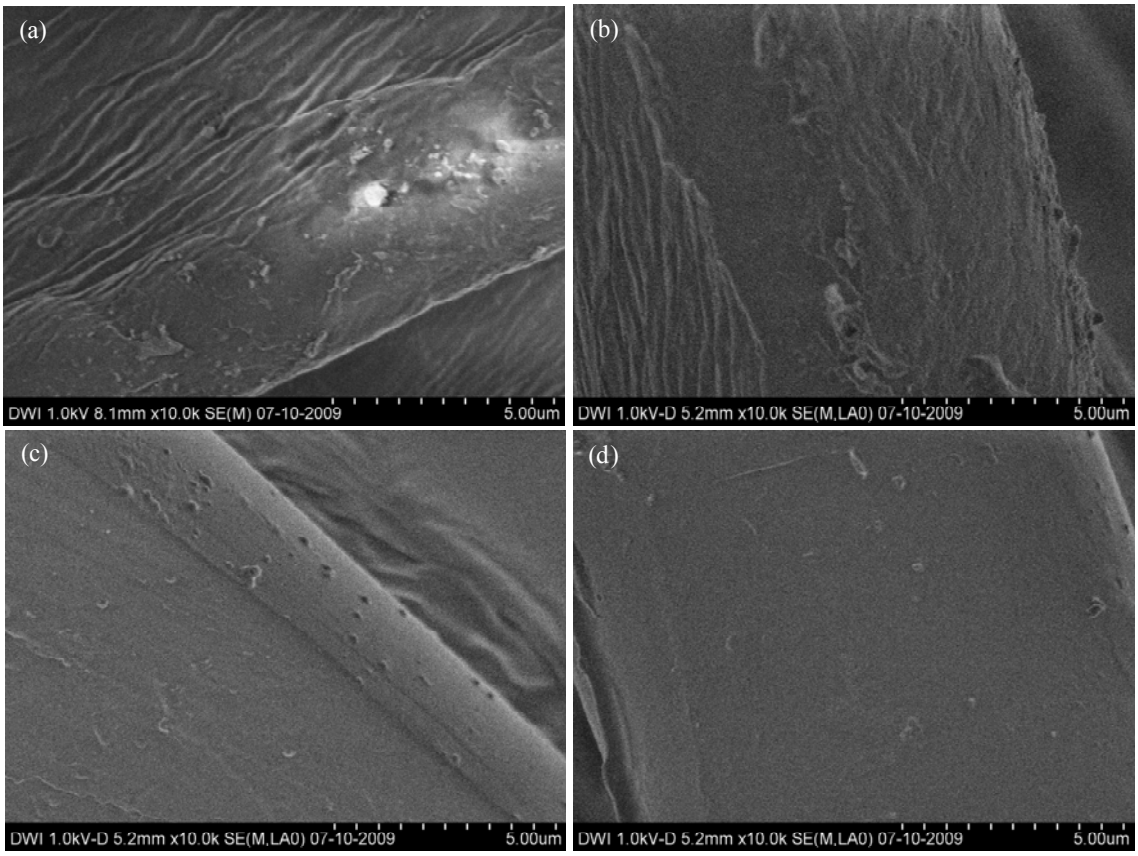

Figure 11. Cryo FE-SEM images after washing test of (a) cotton modified with PVAm nanogels, (b) cotton modified with Ag_PVAm nanogels, (c) polyester modified with PVAm nanogels, and (d) polyester modified with Ag_PVAm nanogels.

9.4 CONCLUSIONS

We demonstrated that the crosslinked polyamine nanogels and silver-hybrid nanogels could be successfully coated onto non-activated cotton and polyester fabrics by a simple dip-coating procedure. The pure and hybrid nanogels depositions achieved by dip-coating on cotton and polyester completely inhibit the microbial growth of gram positive (*B.sub*) and gram negative bacteria (*E. coli.*) for 20 hours. The possible reason of antimicrobial activity of pure polyamine nanogel deposition on the fabrics may be influence on the combination of a weak polyelectrolyte with a positive charged surface as well the presence of both secondary and tertiary amines next to the primary amines. The positive surface charge of the nanogel modified fabrics was indicating to be reactive surface for further post-modification. The stability of nanogel modification on the fabrics was demonstrated by intensive washing and colorimetric test. Especially, the PVAm crosslinked nanogel applied on the cotton shows a good stability as well homogeneous deposition. Therefore, this work, following previous research of antimicrobial nanofibers,[20] can be adapted to the textile finishing industry for the growing needs related to health and hygiene goods.

9.5 REFERENCES

[1] Mucha, H.; Hoter, D.; Swerev, M. "Antimicrobial finishes and modifications" Melliand International, **2002**, 8, 148.

[2] Kenawy, E. R.; Abdel-Hay, F. I.;Abouel-Magd, A. *J. Bioactive Compatible Polymers* **2005**, 20, 95.

[3] Daoud, W. A.; Xin, J. H.; Zhang, Y *Surface Sci.* **2005**, 599, 69.

[4] Sawhney, A.P.S.; Condon, B.; Singh, K.V.; Pang, S.S.; Li, G.; Hui, D. *Textile Research J.* **2008**, 78, 731.

[5] Gao, Y.; Cranston, R. *Textile Research J.* **2008**, 78, 60.

[6] Schindler, W. D.; Hauser, P. J. "Chemical finishing of textiles" Woodhead publishing limited, Washington DC, **2004**.

[7] Langenhove, L. V. "Smart textiles for medicine and healthcare" Woodhead publishing limited, Washington DC, **2007**.

[8] Kim, Y. H.; Choi, H. M.; Yoon, J. H. *Textile Research J.* **1998**, 68, 428.

[9] McDonnell, G.; Russell, A. D. *Antiseptics and Disinfectants:Activity, Action, and Resistance, Clin. Microbiol. Rev.***1999**, 12, 147.

[10] Conner, C. J.; Danna, G.S.; Cooper, A.S.; Reeves, W.A. *Textile Research J.* **1966**, 36, 359.

[11] Parikh, D. V.; Fink, T.; Rajasekharan, K.; Sachinvala, N. D.; Sawhney, A. P.S.; Calamari, T. A. Parikh, A. D. *Textile Research J.* **2005**, 75, 134.

[12] Gorensek, M.; Gorjanc, M.; Bukosek, V.; Kovac, J.; Jovancic, P.; Mihailovic, D. *Textile Research J.* **2010**, 80, 253.

[13] Sondi, I.; Salopek-Sondi, B. *J. Colloid Interface Sci.* **2004**, 275, 177.

[14] Seong, H. S.; Kim, J. P.; Ko, S. W. *Textile Research J.* **1999**, 69, 483.

[15] Lim, S. H.; Hudson, S. M. *J. Macromol. Sci. Polym. Rev.* **2003**, 43, 223.

[16] Lim, S. H.; Hudson, S. M. *Carbohydrate Res.* **2004**, 339, 313.

[17] http://www.smartsilver.com/ (accessed January 25, 2010).

[18] Mahltig, B.; Textor, T. "Nanosols and Textiles" World Scientific Pub Co, Singapore, **2008**.

[19] Yu, M.; Hoogenboom, R.; Thomas, H.; Moller, M. *Manuscript in preparation*, In chapter 8.

[20] Yu, M.; Hoogenboom, R.; Thomas, H.; Moller, M. *Manuscript in preparation*, In chapter 7.

[21] Li, X.; Pelton, R. *Ind. Eng. Chem. Res.* **2005**, 44, 7398.

[22] Miao, C.; Chen, X.; Pelton, R. *Ind. Eng. Chem. Res.* **2007**, 46, 6486.

[23] Shi, L.; Berland, C. *Macromolecules*, **2007**, 40, 4635.

[24] Shi, L.; Khondee, S.; Linz, T. H.; Berkland, C. *Macromolecules* **2008**, 41, 6546.

[25] Mohammadi, Z.; Cole, A.; Berland, C. *J. Phys. Chem.* **2009**, 1113, 7652.

[26] Wang, Q.; Wang, L.; Detamore, M. S.; Berkland, C. *Adv. Mater.* **2008**, 20, 236.

[27] Westman, E.; Ek, M.; Enarsson, L.; Wågberg, L. *Biomacomolecules* **2009**, 10, 1478.

[28] Westman, E.; Ek, M.; Enarsson, L.; Wågberg, L. *Holzforschung* **2009**, 63, 33.

[29] Pasquier, N.; Keul, H.; Heine, E.; Moeller, M. *Biomacomolecules* **2007**, 8, 2874.

[30] Pasquier, N.; Keul, H.; Heine, E.; Moeller, M.; Angelov, B.; Linser, S.; Willumeit, R. *Macromol. Biosci.* **2008**, 8, 903.

[31] Burak Aksoy, Margaret K. Joyce and Paul D. Fleming, TAPPI Spring Technical Conf. & Trade Fair, (Academic, Chicago, May 12-15,2003).

CURRICULUM VITAE

NAME	Miran Yu
DATE OF BIRTH	January 14, 1980
PLACE OF BIRTH	Nonsan, Republic of Korea
CITIZENSHIP	Republic of Korea (ROK)

1986.03 – 1993.02	Jung Ang elementary school, Kangkyeng, Korea
1993.03 – 1996.02	Kangkyeng women middle school, Kangkyeng, Korea
1996.03 – 1998.02	Kangkyeng high school, Kangkyeng, Korea
1998.03 – 2003.02	**B.S.** in department of Textile Engineering, Soong-Sil University, Seoul, Korea *Thesis*: Research and development of electrospinning technology *Advisor*: Prof. HyenJu Shim
2002.12 – 2003.10	Specialist for producing textile and trading in JEFFTEX Ltd, Korea
2004.03 – 2006.02	**M.Sc.** in school of Materials Science and Engineering, Seoul National University, Seoul, Korea *Thesis*: Energy absorption behavior of fumed silica suspension /Kevlar Composite *Advisor*: Prof. TaeJin Kang
2006.02 – 2006.08	Development and Research in HYOSUNG CORPORATION, Korea
2007.03 – 2010.03	**PhD** in DWI an der RWTH Aachen e.V. Textile Chemistry and Macromolecular Chemistry of RWTH, Aachen, Germany *Thesis*: Clicking polyelectrolyte to form a crosslinked hydrogel; their use for surface modification, electrospinning and preparation of nanoparticles *Advisor*: Prof. Martin Moeller
2010.04 – present	Global Polymer Research at BASF SE, Ludwigshafen, Germany
18. 02. 2011	Oral PhD examination

Ludwighafen, February 2011

LIST OF PUBLICATIONS

Parts of this thesis are published, submitted to be published, or presented at conferences:

POSTER PRESENTATIONS

1. "Stabilisation strategies for nanofibres derived from aqueous polymer solutions"
W. Voigt, M. Bozukov, M. Yu, H. Thomas, M. Möller
1st Aachen-Dresden International Textile Conference, 29/30 November **2007**, Aachen (Germany)

2. "Fabrication of polyelectrolyte poly(vinlyamine) nanofiber by electrospining from aqueous solutions"
M. Yu, M. Bozukov, H. Thomas, M. Möller
Synthetic fibre talks, Designing properties-A promise of nanotechnology, 8/9 May **2008**, Vaalsbroek (Netherlands)

3. "Selective surface modification with linear and branched polyelectrolytes and their derivatives"
V. Goel, M. Yu, M. Bozukov, H. Thomas, M. Möller, U. Beginn
Bio&Polymer, New polymer technologies with water, 28-30 September **2008**, Aachen (Germany)

4. "Amine terminated selective surface modification with linear poly(vinylamine) and branched poly(ethyleneimine)"
M. Yu, V. Goel, M. Bozukov, H. Thomas, M. Möller
2nd Aachen-Dresden International Textile Conference, 4/5 December **2008**, Dresden (Germany)

5. "Generation and stabilization of polyelectrolytes nanofibres by aqueous electrospinning"
M. Yu, M. Bozukov, H. Thomas, M. Möller
2nd Aachen-Dresden International Textile Conference, 4/5 December **2008**, Dresden (Germany)

6. "Fabrication of polyelectrolytes complex hydrogel nanofibre by aqueous solution electrospinning"
M. Yu, M. Bozukov, H. Thomas, M. Möller
Nano for the 3rd millennium–Nano for Life, 11/12 March **2009**, Prague (Czech Republic)

7. "Ultra-thin coating of surfaces with quarternary ammonium groups containing polyamines via polyelectrolyte complex formation and generation of electrospun polyelectrolyte nanofibres"
A. Körner, N. Fricker, A. Mendrek, M. Yu, M. Bozukov, H. Thomas, H. Keul, M. Möller
European Coatings CONGRESS, 30 March - 1 April **2009**, Nürnberg (Germany)

8. "Preparation and characterization of polyamine nanogels in aqueous medium"
M. Yu, H. Thomas, M. Möller
ACS National Meeting & Exposition, 16-20 August **2009**, Washington DC (USA)

PUBLICATIONS

1. "EKC2008 Proceedings of the EU-Korea Conference on Science and Technology"
M. Yu, M. Bozukov, W. Voigt, H. Thomas, M. Moeller
Springer Proceedings in Physics, Springer Berlin Heidelberg, **2008**, 124, 525-530

2. "Preparation and Characterization of Polyamine Nanogels in Aqueous Medium"
M. Yu, H. Thomas, M. Moeller
PMSE preprints, **2009**, 101, 1526

3. "Crosslinked self-assembled Poly (vinylamine) / Poly (amideamine-epichlorohydrin) hydrogel films for silicon oxide surface modificiation"
M. Yu, H. R. Hoogenboom, Thomas, M. Moeller
Manuscript in preparation

4. "Azetidinium-amine coupling as "click" method for the preparation of ultrathin hydrogel films on silicon oxide"
M. Yu, R. Hoogenboom, H. Thomas, M. Moeller
Manuscript in preparation

5. "Aqueous electrospinning and stabilisation of poly(vinylamine) based ultrathin nanofibers"
M. Yu, M. Bozukov, R. Hoogenboom, H. Thomas, M. Moeller
Manuscript in preparation

6. "Polyelectrolyte crosslinked hydrogel nanofibers by azetidinium-amine click reaction from aqueous gelation solution"
M. Yu, R. Hoogenboom, H. Thomas, M. Moeller
Manuscript in preparation

7. "Antimicrobial hydrogel nanofibers based on poly(vinylamine)"
M. Yu, R. Hoogenboom, H. Thomas, M. Moeller
Manuscript in preparation

8. "Synthesis of water swellable hybrid nanogels functionalized with silver nanoparticles"
M. Yu, R. Hoogenboom, H. Thomas, M. Moeller
Manuscript in preparation

9. "Ultrathin hydrogel coating to enhance the shrinkproofing of corona treated wool"
M. Yu, H. Thomas, M. Moeller
Manuscript in preparation

Aachen, February. 2011

Miran Yu

ACKNOWLEGDGMENT

"The greatest discovery of my generation is that man can alter his life simply by altering his attitude of mind." - Willim James

In 2007, I was standing in the midst of a huge surging change in my life from the land of the morning calm, Korea to the multiculturalism and pragmatism, Germany. It is great challenge as well as the solution of the questions about the purpose and goal of my own life. Herein, I would like to present the appreciation to all the people who are scientifically and warmly supporting to obtain this dissertation at the DWI e.V. and Institute of Technical and Macromolecular Chemistry (ITMC), RWTH Aachen, Germany.

I would like to thank my supervisor, Prof. Martin Möller, for his continuous encouragement, support and scientific guidance throughout the perfection of this thesis.

I appreciate Dr. Helga Thomas for providing the chance to come to Germany and motivating to accomplish the phD thesis from the topics of BMBF and AiF projects.

I would also love to appreciate Dr. Richard Hoogenboom for reviewing all the manuscripts and for helping to improve the scientific writing skills.

There are many technical supports and I wish to give them all the best and appreciation for helping the arrangement of experiment; Dr. Helmut Keul and Jörg Meyer are helping to figure out the model reaction of azetidinium-amine coupling. Prof. Demco is helping to evaluate hydrogels with solid NMR. Dr. Kim-Hô Phan and Stephan Rütten are the experts to operate and evaluate the micro/nano structure of materials and introducing the measuring skills of SEM, FE-SEM, Cryo-FE SEM, and TEM. Dr. Elisabeth Heine and Rita Gartzen are helping to obtain the antimicrobial results of hydrogel nanofibers and nanogel coated textiles. Dr. Jürgen Groll and Meike Beer are responsible of cell biology and allow performing the cell toxicity and vitality. Dr. Robert Kaufmann and Michaela Hoffmann are operating the XPS and helping the analysis of the XPS software. Dr. Petra Mela is giving the introduction of

AFM measurement. Dr. Artur Henke provides the great help to measure static light scattering to know the molecular weight of PAE. Renate Jansen and Birgit Mohr are supporting the work relative to the surface modification of wool fibers. Yesmin Yazici is helping the experimental to prepare the nanogels. Ewgeni Stab is printing all the posters and solving the network problem. I would like to thank all colleagues at DWI for cooperation.

I would like to acknowledge Jung-gun Nam (Seoul National University) for helping with the rheological characterization and Eun-mi Noh (Photal Otsuka electronics) for helping with the zeta potential measurement.

There is also heartening aid since I have lived in Aachen and I would like to tell them the special thanks; Wiebke Voigt and Michaela Hoffmann are helping the arrangement to register at RWTH and show the beautiful smiling and the kindness. Christina Klaus and Konstantina Dyankova are the personal consultants of the learning of the overall culture and society in Germany and good friends to discuss a lot of things. Jörg Meyer, Marc Hans, Dragos Popescu, Cristian Vaida, Mar Díez, Markus Kettel, Thomas Weyand, Metodi Bozukov, Yingchun He and Wiktor Steinhauer are the great people to share the nice time in Aachen.

I am grateful to the Verein Koreanischer Naturwissenschaftler und Ingenieure in der BRD e.V.(VeKNI) and Korean Student Association of Aachen University of Technology (KSV) for providing the close network with Korean scientists and students in Germany.

In the end, I would love to dedicate the last glowing honor to my parent, sisters, brother, brothers-in-law and my cute nephews and nieces. I am happy to share the glory with my husband, Matthias Barz and Family Barz. Vielen Dank!

사랑하는 아빠, 엄마, 지우네 가족, 정대네 가족, 은숙언니, 크리스찬네 가족 그리고 순종!!! 항상 지켜봐 주고 응원해 주어서 너무 고맙습니다. 모든 영광을 함께 나눌 수 있어서 정말 행복합니다. 앞으로도 모든 일에 최선을 다하는 모습 보여드리겠습니다. 사랑합니다. 그리고 고맙습니다!!